Shakil Mahmud • Research Monograph

SHAKIL MAHMUD EDITORIAL & RESEARCH MONOGRAPHS

The Evolutionary Odyssey

From prebiotic thermodynamics at deep-sea hydrothermal vents through the Cambrian explosion and dinosaur dominance to the speciation of Homo sapiens.

SHAKIL MAHMUD

Independent Scholar & Systems Researcher

SHAKIL MAHMUD EDITORIAL & RESEARCH SERIES

First Collected Edition • Dhaka & Singapore • 2026

The Evolutionary Odyssey

From prebiotic thermodynamics at deep-sea hydrothermal vents through the Cambrian explosion and dinosaur dominance to the speciation of Homo sapiens.

LIBRARY & CATALOGING-IN-PUBLICATION DATA

Title: The Evolutionary Odyssey
Author: Shakil Mahmud
Series: Shakil Mahmud Editorial & Research Series (Monograph Collection)
Subjects: Science -- History -- Philosophy -- Mathematics -- Civilization
Published: Dhaka & Singapore, 2026
Format: Digital Monograph Offprint (PDF) • Complete 20-Part Collected Edition
Permanent URI: https://shakilmahmud.com/series/evolution/

Suggested Academic Citation:
Mahmud, Shakil. (2026). *The Evolutionary Odyssey: The Complete 20-Part Collected Monograph*. Shakil Mahmud Research Series. https://shakilmahmud.com/series/evolution/

Open Scholarly Access: This collected monograph is published under Open Scholarly Access for personal study, academic citation, university pedagogy, and non-commercial research.

© 2026 Shakil Mahmud. All rights reserved. Typeset and published at Dhaka and Singapore.

Shakil Mahmud • Research Monograph

EDITORIAL PREFACE

Preface: The Scaffolding of Reality

Four billion years ago, in the alkaline thermodynamic gradients of prebiotic hydrothermal vents, geochemical energy organized into the first self-replicating molecular catalysts. Across twenty rigorous chapters, this monograph traces the grand narrative of biological complexity: the RNA world, endosymbiosis, the Cambrian explosion, the conquest of land, the rise and fall of the dinosaurs, and the emergence of human consciousness.

The purpose of this collected monograph is not merely didactic exposition, but the systematic synthesis of conceptual revolutions. Each chapter examines an intellectual threshold where old paradigms faltered and new mathematical or physical insight illuminated deeper structures of reality.

— Shakil Mahmud
Dhaka & Singapore, 2026

INDEX OF PARTS

Table of Contents

PHASE I: ANCIENT & CLASSICAL FOUNDATIONS

PART I	**The Spark of Abiogenesis — Prebiotic Thermodynamics, Alkaline Vents, and the RNA World** *The Spark of Abiogenesis — Prebiotic Thermodynamics, Alkaline Vents, and the RNA World*	1,555 words
PART II	**The Last Universal Common Ancestor (LUCA) and the Divergence of Domains** *The Last Universal Common Ancestor (LUCA) and the Divergence of Domains*	1,418 words
PART III	**The Solar Energy Revolution — Phototrophy, Water-Splitting, and the Great Oxidation Catastrophe** *The Solar Energy Revolution — Phototrophy, Water-Splitting, and the Great Oxidation Catastrophe*	1,397 words
PART IV	**The Eukaryotic Leap — The Asgard Archaea, Mitochondriogenesis, and the Complex Cell** *The Eukaryotic Leap — The Asgard Archaea, Mitochondriogenesis, and the Complex Cell*	1,531 words
PART V	**The Dawn of Multicellularity — Cell Adhesion, Morphogenesis, and the Ediacaran Garden** *The Dawn of Multicellularity — Cell Adhesion, Morphogenesis, and the Ediacaran Garden*	1,404 words

PHASE II: MEDIEVAL TRANSFORMATIONS

PART VI	**The Cambrian Explosion — Hox Gene Toolkits, Hard Skeletons, and Predatory Arms Races** *The Cambrian Explosion — Hox Gene Toolkits, Hard Skeletons, and Predatory Arms Races*	1,497 words
PART VII	**The Chordate Dawn — The Origin of the Backbone, Notochord, and Cranial Brain** *The Chordate Dawn — The Origin of the Backbone, Notochord, and Cranial Brain*	1,477 words
PART VIII	**The Conquest of the Depths — The Origin of Jaws and the Age of Armored Placoderms** *The Conquest of the Depths — The Origin of Jaws and the Age of Armored Placoderms*	1,492 words
PART IX	**The Water-to-Land Transition — The Anatomy of Sarcopterygian Tetrapodomorphs** *The Water-to-Land Transition — The Anatomy of Sarcopterygian Tetrapodomorphs*	1,369 words
PART X	**The Carboniferous Amphibian World & The Cleidoic Amniotic Breakthrough** *The Carboniferous Amphibian World & The Cleidoic Amniotic Breakthrough*	1,395 words

PHASE III: THE MODERN SCIENTIFIC REVOLUTION

PART XI	**The Synapsid Hegemony & The Permian-Triassic Great Dying** *The Synapsid Hegemony & The Permian-Triassic Great Dying*	1,411 words
PART XII	**The Archosaur Empire — Dinosaurs, Pterosaurs, and the Avian Transition** *The Archosaur Empire — Dinosaurs, Pterosaurs, and the Avian Transition*	1,468 words
PART XIII	**The Nocturnal Mammalian Bottleneck & The K-Pg Asteroid Crucible** *The Nocturnal Mammalian Bottleneck & The K-Pg Asteroid Crucible*	1,484 words
PART XIV	**The Paleogene Mammalian Explosion & Primate Origins** *The Paleogene Mammalian Explosion & Primate Origins*	1,520 words
PART XV	**The Catarrhine Split, Trichromatic Vision & The Miocene Ape Radiations** *The Catarrhine Split, Trichromatic Vision & The Miocene Ape Radiations*	1,580 words

PHASE IV: CONTEMPORARY HORIZONS & SYNTHESIS

PART XVI	**The Great Ape Split & The Biomechanics of Habitual Bipedalism** *The Great Ape Split & The Biomechanics of Habitual Bipedalism*	1,633 words
PART XVII	**Australopithecus, The Laetoli Tracks & Robust Paranthropus** *Australopithecus, The Laetoli Tracks & Robust Paranthropus*	1,560 words
PART XVIII	**The Dawn of Genus Homo & Oldowan Lithic Technology** *The Dawn of Genus Homo & Oldowan Lithic Technology*	1,616 words
PART XIX	**Homo erectus, Fire & The Global Diaspora** *Homo erectus, Fire & The Global Diaspora*	2,136 words

Shakil Mahmud • Research Monograph

PART XX **The Archaic Mosaic & The Dawn of Modern Humanity** 2,061 words

The Archaic Mosaic & The Dawn of Modern Humanity

SHAKIL MAHMUD RESEARCH MONOGRAPHS • PART I

The Spark of Abiogenesis — Prebiotic Thermodynamics, Alkaline Vents, and the RNA World

The Spark of Abiogenesis — Prebiotic Thermodynamics, Alkaline Vents, and the RNA World

1,555 words • November 1, 2026 • Permanent URI



Plate I: *Figure: Deep-sea alkaline hydrothermal vent chimneys at the primordial ocean floor (~4.0 Ga), providing the proton gradients, catalytic iron-sulfur minerals, and micro-compartments that sparked prebiotic abiogenesis and the origin of cellular life.*

Four billion years ago, on a tumultuous, ocean-engulfed Earth under the faint young Sun, the most improbable transition in cosmic history occurred: non-living geochemical reactions crossed the threshold into self-sustaining, replicating biochemistry. Far from being an accidental stroke of lightning in a static primordial soup, the origin of life was an inevitable thermodynamic consequence of a planet striving to dissipate electrochemical disequilibrium across the porous labyrinth of deep-sea alkaline hydrothermal vents.

I. Far-From-Equilibrium Thermodynamics and the Dissipation of Planetary Potential

In classical thermodynamic equilibrium, physical systems inexorably decay toward maximum entropy, as dictated by the Second Law of Thermodynamics: $dS \geq \frac{dQ}{T}$. Life, however, is a quintessential non-equilibrium dissipative structure. As physicist Erwin Schrödinger famously postulated in 1944, a living organism avoids decay into thermodynamic equilibrium by continually drawing negative entropy (\Delta S < 0) from its surroundings, sustaining an internal state of low entropy and high molecular organization.

The primordial Hadean Earth was an immense geochemical electrochemical battery. The planet's mantle and crust were rich in reduced iron, molecular hydrogen (H_2), and methane, while the ocean and atmosphere were heavily oxidized with volcanic carbon dioxide (CO_2) and sulfur dioxide (SO_2). The reduction of carbon dioxide by hydrogen gas to form methane and organic carboxylic acids is thermodynamically favored:

$$CO_2 + 4H_2 \rightarrow CH_4 + 2H_2O \quad (\Delta G^\circ = -131\ \text{kJ/mol})$$

However, despite the immense thermodynamic driving force (\Delta G < 0), this reaction faces an imposing kinetic activation barrier. Without specialized catalysts, dissolved carbon dioxide and dissolved hydrogen remain inert in ambient water. To bridge this barrier, nature required a sustained, continuous physical reactor possessing both transition-metal catalysts and a continuous flow of electrochemical energy.

Shakil Mahmud • Research Monograph

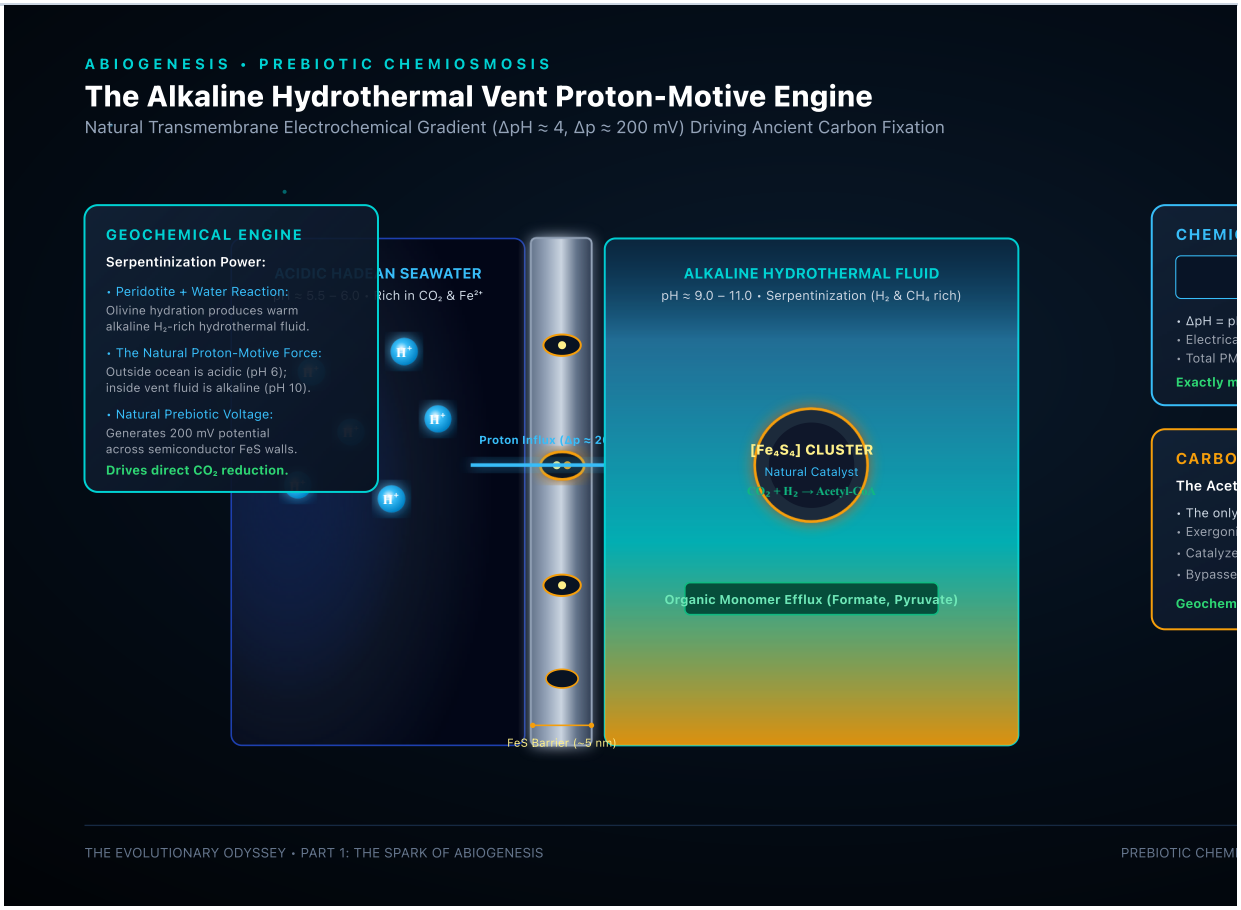


Figure 1.1: The Prebiotic Proton-Motive Reactor. Thin inorganic mackinawite (FeS) chimney micropores separating alkaline hydrothermal fluid (\text{pH } 9\text{–}11) from mildly acidic Hadean ocean water (\text{pH } 5.5\text{–}6.0), generating a natural chemiosmotic electrochemical potential ($\Delta p \approx 200\ \mathrm{mV}$) driving early carbon reduction ($E_h \approx -600\ \mathrm{mV}$).

2. Alkaline Hydrothermal Vents: The Geochemical Engine of Life

In the late 1980s, geochemist Michael Russell proposed a revolutionary paradigm: life did not originate in aerial tide pools or superheated volcanic black smokers, but within moderate-temperature submarine alkaline hydrothermal vents, analogous to the modern Lost City hydrothermal field discovered on the Mid-Atlantic Ridge.

These vents arise through serpentinization, an exothermic geochemical reaction in which ultramafic mantle rock (peridotite, rich in olivine) reacts with seawater at moderate temperatures (100\text{–}150^\circ\text{C}):

$$(\mathrm{Mg,Fe})_2\mathrm{SiO_4} + \mathrm{H_2O} + \mathrm{CO_2} \rightarrow \mathrm{Mg_3Si_2O_5(OH)_4} + \mathrm{Mg(OH)_2} + \mathrm{Fe_3O_4} + \mathrm{H_2}$$

Serpentinization charges the effluent fluid with immense quantities of molecular hydrogen ($\mathrm{H_2}$) and creates a warm, highly alkaline solution (\text{pH } 9\text{–}11). When this alkaline hydrothermal fluid percolated upward into the ancient Hadean ocean—which was saturated with dissolved volcanic $\mathrm{CO_2}$ rendering it mildly acidic (\text{pH } 5.5\text{–}6.0) and devoid of oxygen—an extraordinary precipitation reaction occurred. Dissolved ferrous iron ($\mathrm{Fe^{2+}}$) in the ocean reacted with sulfide ($\mathrm{HS^-}$) in the fluid to precipitate porous inorganic towers made of mackinawite (FeS) and greigite ($\mathrm{Fe_3S_4}$).

These microporous chimney walls acted as natural, semi-conducting inorganic membranes only a few nanometers thick. On the alkaline interior, the hydroxide ion concentration was high; on the oceanic exterior, the hydronium ion concentration ($\mathrm{H_3O^+}$) was hundreds of times greater. Across this mineral barrier spanned a natural proton concentration gradient of approximately 4 to 5 pH units:

$$\Delta p = \Delta \Psi \text{–} \frac{2.303\ R\ T}{F} \Delta \text{pH} \approx 180\text{–}220\text{ mV}$$

This natural proton-motive force (Δp) is strikingly identical in magnitude and sign to the chemiosmotic electrochemical gradient used by every living cell on Earth today to synthesize adenosine triphosphate (ATP) via ATP synthase. Before biological enzymes or genetic coding existed, the geology of the Hadean Earth provided a ready-made proton-gradient engine.

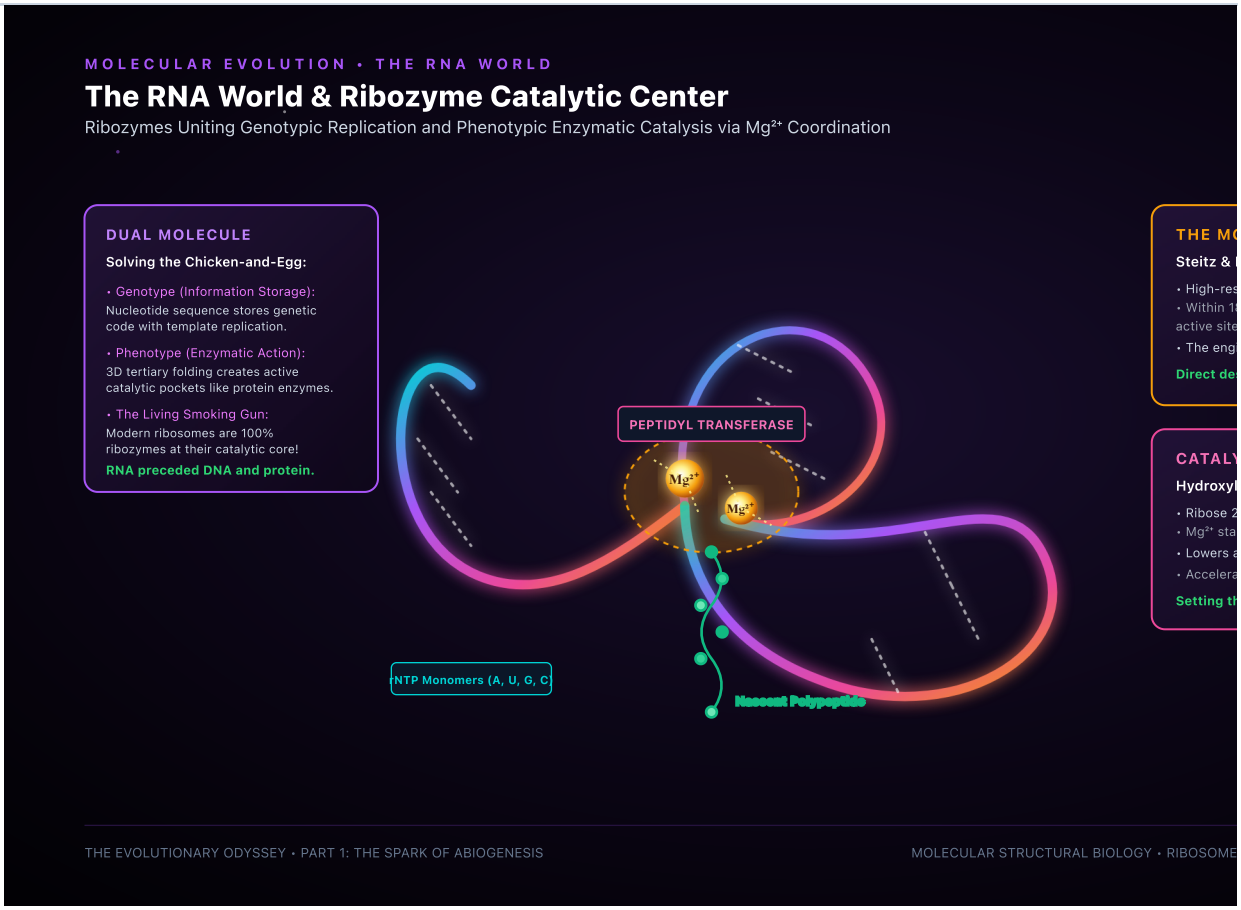


Figure 1.2: The RNA World Ribozyme Architecture. Catalytic secondary structures featuring stem-loops, pseudoknots, and coordinated divalent magnesium ions (Mg^{2+}) facilitating nucleophilic phosphodiester bond formation and peptidyl transferase activity prior to the evolution of encoded protein enzymes.

3. The RNA World: Bridging the Genotype-Phenotype Divide

A classic chicken-and-egg paradox long haunted origin-of-life biology: modern cells require nucleic acids (DNA) to store genetic instructions for synthesizing proteins, yet they require protein enzymes to replicate DNA. How could either emerge without the other?

The resolution came with the discovery of **ribozymes**—RNA molecules possessing enzymatic catalytic capabilities—by Thomas Cech and Sidney Altman in the early 1980s, which earned them the 1989 Nobel Prize in Chemistry. Because ribonucleic acid (RNA) can simultaneously serve as an informational sequence (genotype) and fold into complex tertiary conformations capable of catalyzing chemical reactions (phenotype), it is universally accepted that an ancient *RNA World* preceded modern DNA-and-protein biochemistry.

The definitive molecular fossil confirming this epoch lies at the very heart of the contemporary ribosome. High-resolution X-ray crystallography of the large 50S ribosomal subunit revealed that the peptidyl transferase center—the universal engine that forms peptide bonds between amino acids—is composed entirely of catalytic ribosomal RNA (rRNA), with not a single amino acid residue within $18\ \text{Å}$ of the active site. The ribosome is, at its foundational core, a ribozyme.

In the presence of divalent cations such as magnesium (Mg^{2+}), RNA folds into precise catalytic clefts. Nucleophilic attack by a 3’\text{-hydroxyl} group on the activated α-phosphate of a complementary ribonucleotide allows RNA to self-assemble phosphodiester linkages, polymerizing functional chains without external protein machinery.

Shakil Mahmud • Research Monograph

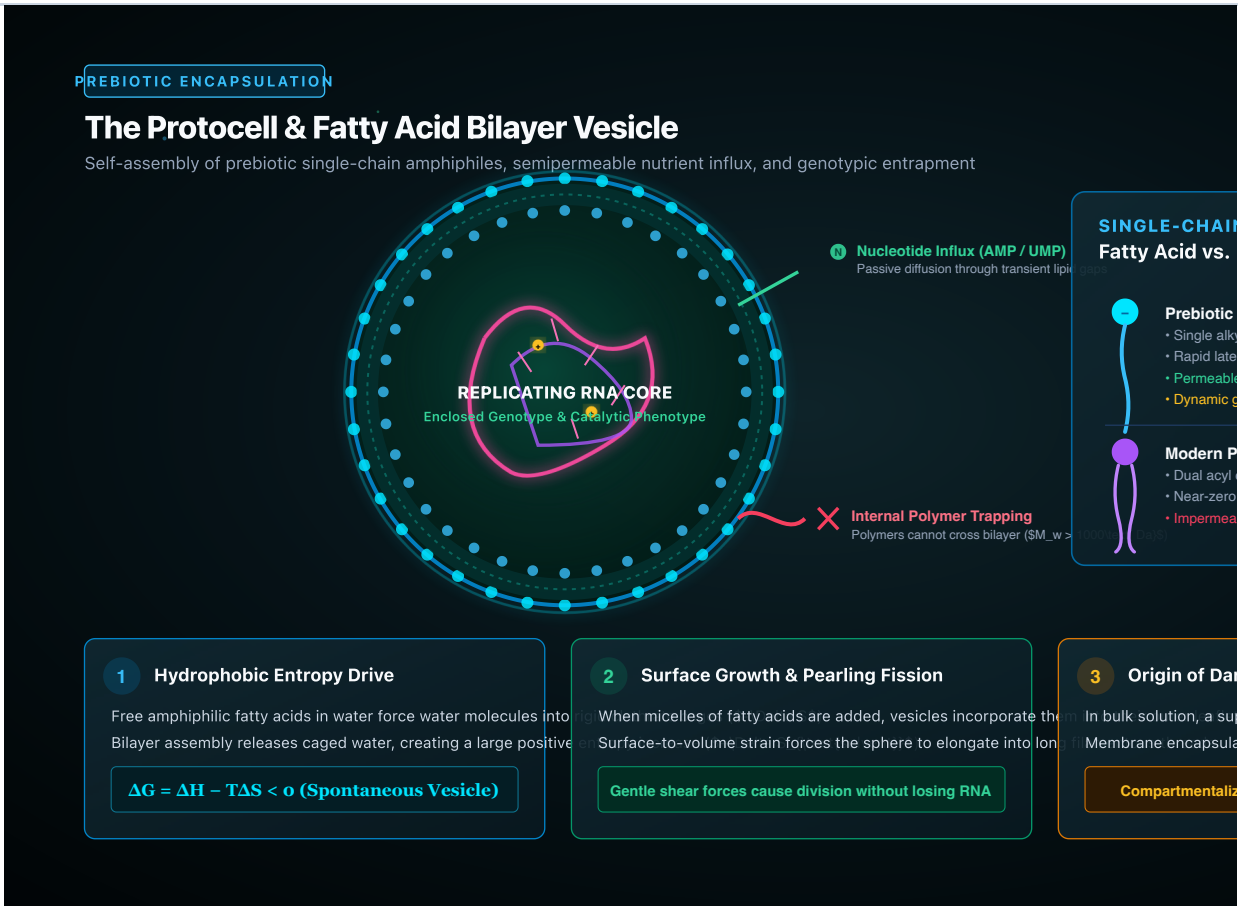


Figure 1.3: Prebiotic Compartmentalization and Protocell Dynamics. Single-chain fatty acid amphiphiles spontaneously assemble into bilayer vesicles driven by hydrophobic entropy (\Delta G = \Delta H – T\Delta S < 0). Dynamic lipid flip-flop permits monomer nucleotide influx while permanently trapping replicating RNA ribozymes, initiating Darwinian selection.

4. Prebiotic Encapsulation: The Genesis of the Protocell

While catalytic ribozymes could replicate inside hydrothermal rock pores, open water presented an insurmountable evolutionary dilemma: diffusion. In an unconstrained aqueous medium, newly replicated RNA molecules and their metabolic products would disperse instantly. Furthermore, a superior catalytic ribozyme would inadvertently share its metabolic advantage with parasitic, non-functional mutant RNA strands ("molecular parasites").

To initiate genuine Darwinian natural selection, life required encapsulation—a semipermeable barrier linking an organism's genotype to its own phenotype. The solution was the self-assembly of **fatty acid protocells**.

Unlike modern cellular membranes composed of complex diacyl phospholipids with near-zero spontaneous permeability, prebiotic membranes consisted of simple single-chain amphiphiles, such as oleic, lauric, and myristic acids. When fatty acids are suspended in water above their critical vesicle concentration (CVC) at neutral or slightly alkaline pH, they spontaneously aggregate into closed spherical bilayer vesicles. This self-assembly is driven by the *hydrophobic effect*: water molecules surrounding exposed nonpolar hydrocarbon tails are forced into highly ordered, hydrogen-bonded "clathrate cages" of low entropy ($-\Delta S$). Aggregation of the hydrocarbon tails into an interior membrane core releases these caged water molecules back into bulk solution, generating a massive gain in solvent entropy ($+\Delta S_{\text{solvent}}$):

$$\Delta G_{\text{assembly}} = \Delta H – T \Delta S < 0$$

Crucially, single-chain fatty acid bilayers possess dynamic physical properties absent in modern membranes. Their high rate of lateral lipid flip-flop (>100\text{ s}^{-1}) creates transient structural defects, granting selective permeability. Small uncharged molecules and hydrophilic monomer precursors—such as ribose, amino acids, and activated nucleotide monophosphates—diffuse freely across the membrane into the protocell interior. In contrast, once inside, when ribozymes polymerize these monomers into long polyanionic RNA chains (M_w > 1000\text{ Da}), their bulky size and multiple negative charges prevent them from leaking out.

When additional fatty acid micelles are added to a solution of protocells, the vesicles incorporate the new lipids into their outer leaflet faster than their internal volume can expand through osmotic water influx. The resulting surface-to-volume mechanical tension forces the spherical protocell to distort into an elongated, thread-like tubular structure. Under gentle hydrodynamic agitation—such as ocean surf or vent currents—these pearling filaments spontaneously pinch off into daughter vesicles, dividing without any complex protein machinery while retaining their internal genetic payload.

Conclusion: The Threshold of Life

By **3.8 billion years ago**, all essential components of the prebiotic toolkit had coalesced. Deep within the electrochemical hearths of alkaline hydrothermal vents, inorganic iron-sulfur minerals catalyzed the reduction of carbon dioxide into primitive organics. Chemiosmotic proton gradients drove continuous thermodynamic disequilibrium. RNA ribozymes achieved both informational storage and catalytic polymer synthesis. And fatty acid protocells provided the physical boundary required for individual identity and natural selection.

The stage was set for the emergence of the single most pivotal organism in planetary history: the Last Universal Common Ancestor (LUCA). In Part 2, we will explore how phylogenomic archaeology reconstructs LUCA's 355-gene minimal genome and decrypts the momentous divergence that split the tree of life into Bacteria and Archaea.

Key Academic Citations

- Russell, M. J., & Hall, A. J. (1997). The emergence of life from iron monosulphide bubbles at a submarine hydrothermal redox and pH front. *Journal of the Geological Society*, 154(3), 377–402.
- Martin, W., & Russell, M. J. (2003). On the origins of cells: a hypothesis for the evolutionary transitions from abiotic geochemistry to chemoautotrophic prokaryotes, and from prokaryotes to nucleated cells. *Philosophical Transactions of the Royal Society of London. Series B: Biological Sciences*, 358(1429), 59–85.
- Cech, T. R. (1986). A model for the RNA-catalyzed replication of RNA. *Proceedings of the National Academy of Sciences*, 83(12), 4360–4363.
- Szostak, J. W., Bartel, D. P., & Luisi, P. L. (2001). Synthesizing life. *Nature*, 409(6818), 387–390.
- Lane, N. (2015). *The Vital Question: Why Is Life the Way It Is?* Profile Books / W. W. Norton.

Citation: Mahmud, S. (2026). "The Spark of Abiogenesis — Prebiotic Thermodynamics, Alkaline Vents, and the RNA World." In The Evolutionary Odyssey, Part 1. https://shakilmahmud.com/evolutionary-odyssey-part-1-the-spark-of-abiogenesis/

Shakil Mahmud • Research Monograph

SHAKIL MAHMUD RESEARCH MONOGRAPHS • PART II

The Last Universal Common Ancestor (LUCA) and the Divergence of Domains

The Last Universal Common Ancestor (LUCA) and the Divergence of Domains

1,418 words • November 1, 2026 • Permanent URI



Plate II: *Figure: Microscopic visualization of LUCA (Last Universal Common Ancestor, ~3.8 Ga), showcasing its primordial lipid membrane, circular DNA chromosome, universal ribosomal translation machinery, and membrane-bound chemiosmotic ATP synthases.*

Deep in the warm, anoxic gloom of the Paleoarchean seafloor, approximately 3.8 billion years ago, lived a microscopic entity from which every bacterium in the soil, every archaeon in boiling volcanic springs, every blade of grass, and every human thought is directly descended: the Last Universal Common Ancestor (LUCA). Neither a single freak individual nor a free-swimming modern bacterium, LUCA was a communal population of half-born cells inhabiting the labyrinthine mineral micropores of deep-sea hydrothermal vents, balanced on the thermodynamic knife-edge where geochemical energy became biological heredity.

1. Phylogenomic Archaeology: Reconstructing LUCA's Molecular Anatomy

Because soft-bodied microbial cells from four billion years ago leave negligible macroscopic fossils, modern evolutionary biologists turn to *phylogenomic archaeology*. By comparing the complete genomic sequences of tens of thousands of contemporary bacterial and archaeal species across hundreds of distinct phyla, computational algorithms can calculate the evolutionary divergence time and trace genes back to their point of coalescence.

In a milestone 2016 study published in *Nature*, William Martin, Madeline Weiss, and their colleagues analyzed 6.1 million protein-coding genes across 1,847 bacterial and 134 archaeal genomes. By filtering out horizontal gene transfer (HGT) events and identifying only those gene families exhibiting ancient, un-split orthology present in both primary domains, they reconstructed a high-confidence minimal core genome for LUCA consisting of exactly **355 protein-coding genes**.

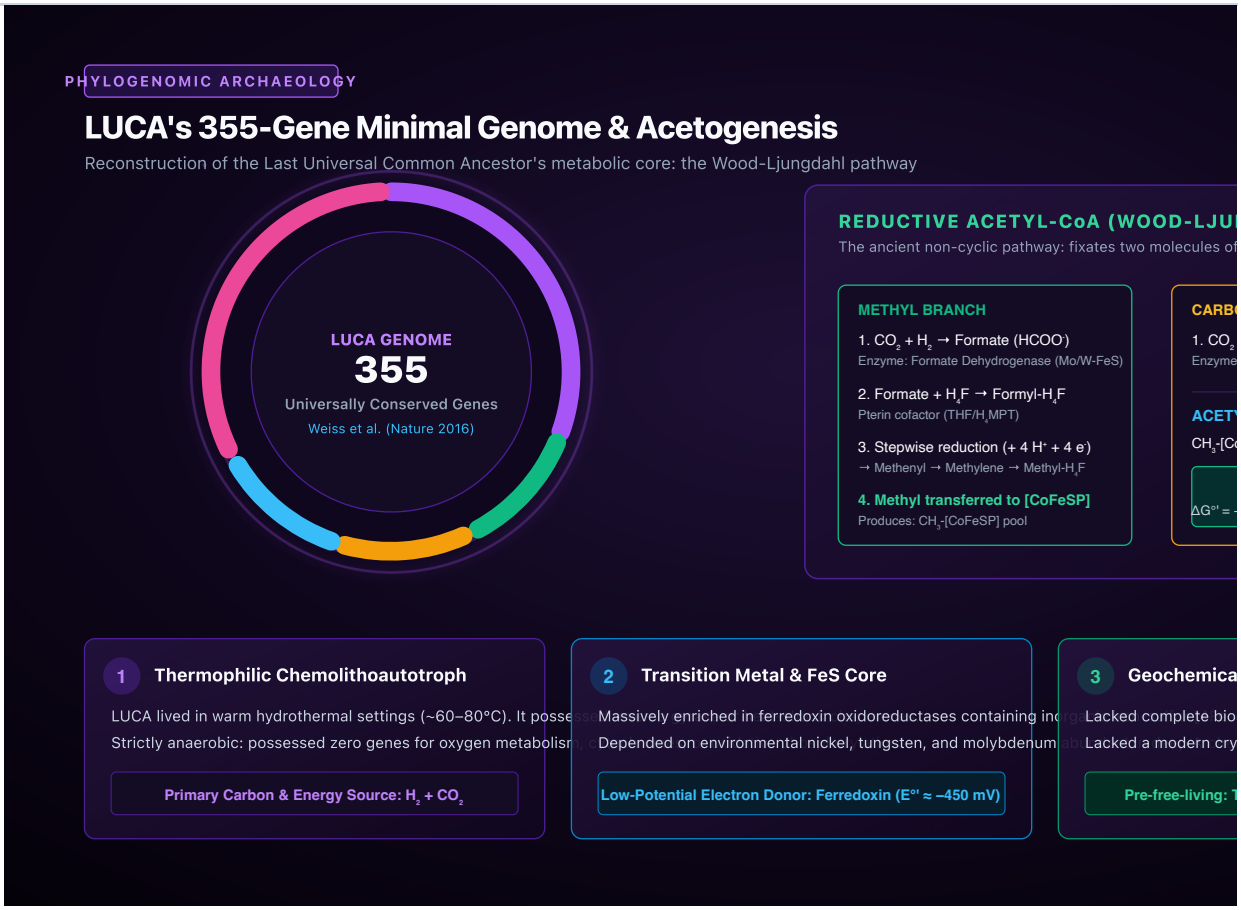


Figure 2.1: LUCA's Conserved Genomic Core. Circular distribution of the 355 universally conserved protein-coding genes identified by Weiss et al. (2016), highlighting the dominance of the non-cyclic Wood-Ljungdahl (reductive acetyl-CoA) carbon-fixation pathway powered by inorganic [4Fe-4S] ferredoxins ($E^\circ \approx -450\ \mathrm{mV}$) and nickel-iron carbon monoxide dehydrogenases.

The metabolic profile encoded by these 355 genes paint an unmistakable portrait of LUCA's physiology:

- **Anaerobic Chemolithoautotroph:** LUCA possessed zero genes requiring molecular oxygen ($\mathrm{O_2}$). It contained no cytochromes, no quinones, and no capacity for aerobic respiration or oxidative phosphorylation.
- **Hyperthermophile / Thermophile:** LUCA possessed reverse gyrase and heat-shock chaperones, indicating an optimal living temperature between $60^\circ\mathrm{C}$ and $80^\circ\mathrm{C}$, matching the hydrothermal vent environment.
- **The Wood-Ljungdahl Pathway:** LUCA fixated inorganic carbon using the linear reductive acetyl-CoA pathway—the only carbon-fixation pathway found in both Bacteria and Archaea that generates net ATP rather than consuming it.

The overall bioenergetic reaction of the Wood-Ljungdahl pathway is exergonic, allowing LUCA to synthesize biomass while releasing metabolic energy:

$$2\mathrm{CO_2} + 4\mathrm{H_2} + \mathrm{HS\text{-}CoA} \rightarrow \mathrm{CH_3CO\text{-}S\text{-}CoA} + 3\mathrm{H_2O} \quad (\Delta G^{\circ\prime} = -37.4\ \mathrm{kJ/mol})$$

Remarkably, LUCA lacked complete biosynthetic pathways for many basic amino acids and nucleotides, as well as the modern crystallized rotor enzymes of ATP synthase ($\mathbf{F_1F}_o$). This implies that LUCA was not yet a fully autonomous, free-living organism; it was a "half-born" creature mechanically confined to the catalytic iron-sulfur chambers of alkaline hydrothermal vents, feeding directly on geochemically supplied hydrogen, carbon dioxide, and mineral proton gradients.

Shakil Mahmud • Research Monograph

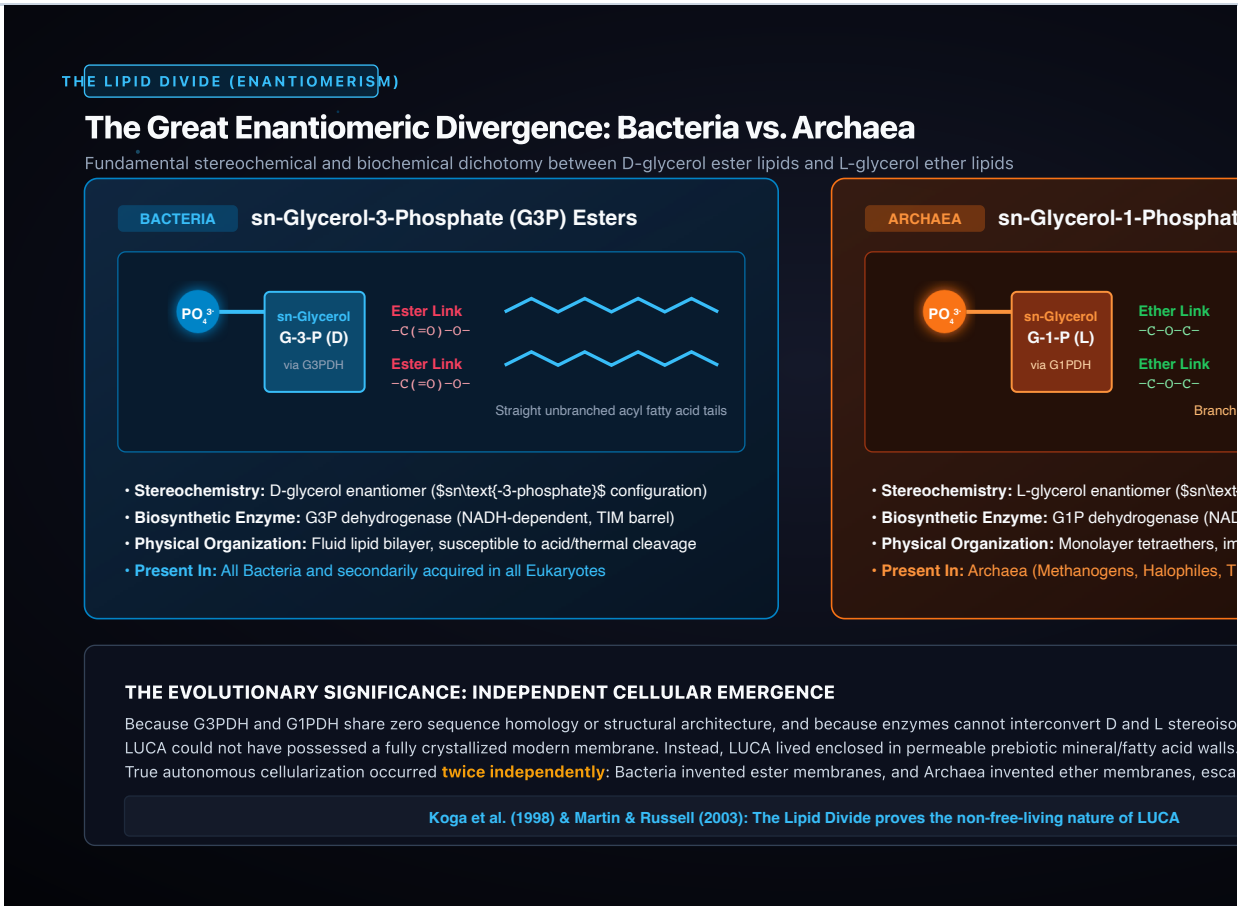


Figure 2.2: The Great Enantiomeric Membrane Divergence. The stereochemical dichotomy between Bacterial G3P fatty acid esters (synthesized by G3PDH) and Archaeal G1P branched isoprenoid ethers (synthesized by G1PDH). Because the enzymes share zero homology and cannot interconvert enantiomers, true cellular membranes evolved twice independently.

2. The Lipid Divide: Why Life Split Into Two Primary Domains

If LUCA represents the universal common ancestor, why did the root of the tree of life split irrevocably into two starkly distinct domains—**Bacteria** and **Archaea**—long before eukaryotes emerged?

The definitive biochemical answer is known as the *Lipid Divide*. Every cellular organism requires a hydrophobic membrane to prevent cellular components from dissipating and to sustain a chemiosmotic electrochemical gradient. Yet when we compare the cell membranes of Bacteria and Archaea, we find a fundamental, irreconcilable chemical chasm:

1. **Glycerol Stereochemistry:** Bacterial lipids are constructed from ***sn*-glycerol-3-phosphate** (G3P), synthesized by the enzyme G3P dehydrogenase (G3PDH). In contrast, archaeal lipids are constructed from the enantiomeric mirror-image, ***sn*-glycerol-1-phosphate** (G1P), synthesized by G1P dehydrogenase (G1PDH). These two enzymes belong to completely unrelated protein superfamilies and share zero phylogenetic homology.
2. **Chemical Linkage:** Bacteria link their hydrocarbon tails to the glycerol backbone via *ester bonds* (-C(=O)-O-). Archaea link their hydrocarbon chains via *ether bonds* (-C-O-C-), which are significantly more resistant to oxidation, acidic hydrolysis, and thermal breakdown.
3. **Hydrocarbon Chains:** Bacterial membranes consist of unbranched, straight-chain fatty acids synthesized through the fatty acid synthase (FAS) pathway. Archaeal membranes consist of branched isoprenoid chains (repeating 5-carbon phytanyl units) derived from the mevalonate pathway. In extreme thermophiles, archaeal lipids fuse into a single covalent *biphytanyl tetraether monolayer* that remains completely intact at temperatures exceeding 100°C and at $\text{pH}\ 0$.

Because the stereocenters of G1P and G3P are enantiomers, an organism cannot gradually mutate from one to the other without destabilizing the packing geometry of its lipid bilayer. As demonstrated by Koga et al. (1998) and Martin & Russell (2003), this chemical divergence proves that LUCA itself lacked a modern, enzymatically synthesized phospholipid membrane. LUCA utilized fragile, leaky prebiotic fatty acid membranes. When independent lineages evolved the enzymatic machinery to synthesize tight, impermeable membranes, they did so via two distinct biochemical pathways—one producing the bacterial ester lineage, the other producing the archaeal ether lineage. Armed with robust, self-sealing envelopes, Bacteria and Archaea independently broke free from their hydrothermal nursery to conquer the primordial oceans.

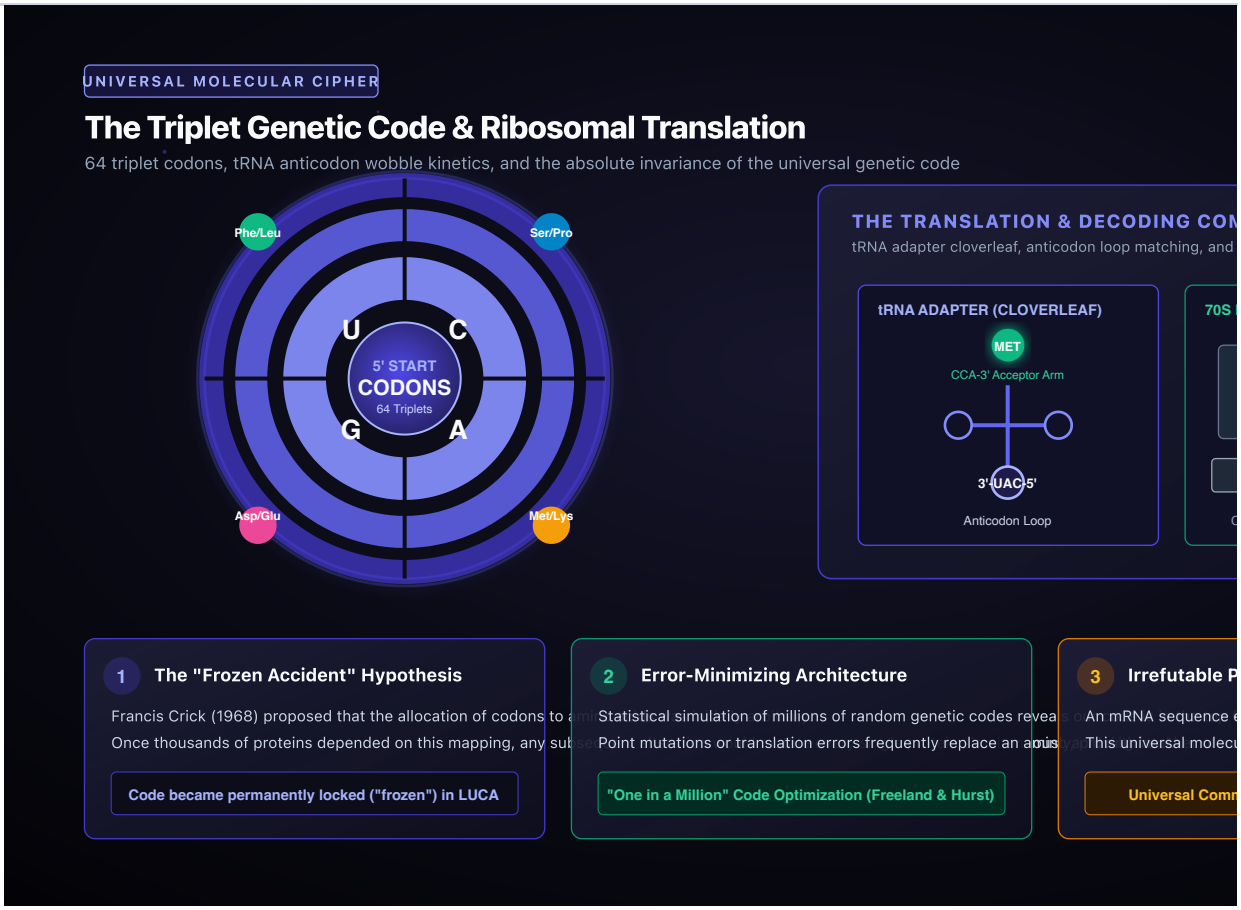


Figure 2.3: The Universal Genetic Code and Decoding Kinetics. The 64 triplet codons mapped onto the universal translation machinery: transfer RNA (tRNA) cloverleaf adapters with CCA-3′ acceptor stems, the universal 70S ribosome decoding center (A, P, and E sites), and Crick's wobble pairing at the third codon position.

3. The Universality of the Genetic Code: The Frozen Accident of LUCA

While the lipid membranes of Bacteria and Archaea diverged completely, their interior molecular machinery is virtually identical. Both domains utilize the exact same **universal genetic code**: a sequence of 64 triplet nucleotide codons specifying the exact same 20 standard L-amino acids (plus stop codons).

Francis Crick famously coined the term *The Frozen Accident* in 1968 to describe this universal mapping. While the initial association between a given triplet codon (such as \text{5′-AUG-3′} for Methionine) and an amino acid may have possessed chemical or stereochemical affinities in the prebiotic era, once an ancestral organism had evolved thousands of interdependent protein-coding genes, any global reassignment of a codon would simultaneously alter hundreds of vital proteins, resulting in immediate lethality. The code became permanently "frozen" before LUCA diverged.

Furthermore, quantitative bioinformatic analyses by Freeland and Hurst demonstrate that the standard genetic code is not a purely arbitrary random choice: it is an extraordinary "one-in-a-million" error-minimizing masterpiece. Codons differing by only a single nucleotide point mutation typically code for either the identical amino acid (synonymous mutation) or an amino acid with near-identical hydrophobicity and steric volume. For instance, replacing a purine with another purine at the wobble position rarely causes any functional disruption to protein folding:

$$\omega = \frac{K_a}{K_s} \ll 1 \quad \text{(Purifying Selection Dominance)}$$

This universal invariance is why human insulin can be cloned into a bacterial plasmid and synthesized flawlessly by *Escherichia coli* cells. The statistical probability of two independent origins of life arriving at the identical 64-codon mapping by pure chance is less than $1 \text{ in } 10^{2,860}$. The genetic code is living mathematical proof that all life on Earth is monophyletic—a single, unbroken family tree extending back to a shared Paleoarchean ancestor.

Conclusion: The Great Departure

By **3.5 billion years ago**, the two primordial domains had separated forever. Bacteria radiated across shallow marine sediments, developing robust peptidoglycan cell walls, rotary flagella, and vast metabolic repertoires. Archaea populated the planetary extremes: boiling hydrothermal abysses, hyper-saline basins, and deep crustal sediments, pioneering methanogenesis through their unique ether-lipid armor.

Shakil Mahmud • Research Monograph

For more than half a billion years, life remained exclusively microscopic and predominantly anoxic. But in the sunlight-drenched surface waters of the ocean, a group of photosynthetic bacteria was preparing to execute the most audaciously destructive and creative geochemical coup in planetary history: the oxidation of water and the Great Oxidation Event. In Part 3, we will witness the Solar Energy Revolution.

Key Academic Citations

- Weiss, M. C., et al. (2016). The physiology and habitat of the last universal common ancestor. *Nature Microbiology*, 1(9), 16116.
- Woese, C. R., & Fox, G. E. (1977). Phylogenetic structure of the prokaryotic domain: the primary kingdoms. *Proceedings of the National Academy of Sciences*, 74(11), 5088–5090.
- Koga, Y., et al. (1998). Did the last common ancestor have a membrane of lipids with ether or ester linkages? *Journal of Molecular Evolution*, 46(2), 125–134.
- Crick, F. H. (1968). The origin of the genetic code. *Journal of Molecular Biology*, 38(3), 367–379.
- Freeland, S. J., & Hurst, L. D. (1998). The genetic code is one in a million. *Journal of Molecular Evolution*, 47(3), 238–248.

Citation: Mahmud, S. (2026). "The Last Universal Common Ancestor (LUCA) and the Divergence of Domains." In The Evolutionary Odyssey, Part 2. https://shakilmahmud.com/evolutionary-odyssey-part-2-the-luca-and-domain-divergence/

SHAKIL MAHMUD RESEARCH MONOGRAPHS • PART III

The Solar Energy Revolution — Phototrophy, Water-Splitting, and the Great Oxidation Catastrophe

The Solar Energy Revolution — Phototrophy, Water-Splitting, and the Great Oxidation Catastrophe

1,397 words • November 1, 2026 • Permanent URI

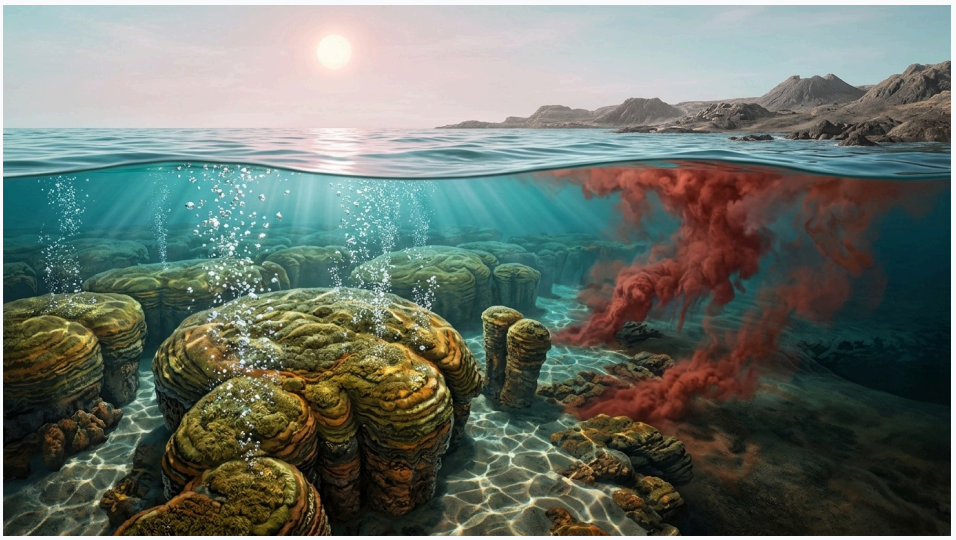


Plate III: *Figure: Shallow Archean coastal marine environment showing mounded cyanobacterial stromatolites releasing oxygen bubbles through water-splitting phototrophy, triggering the Great Oxidation Event and banded iron formations ~2.4 Ga.*

Three billion years ago, life on Earth faced a hard planetary energetic boundary. Confined to dark hydrothermal seafloors or shallow volcanic mudflats, primitive microbes fed on geochemical trickles of dissolved hydrogen and volcanic hydrogen sulfide. In the sunlit surface waters of the ocean, however, an audacious evolutionary revolution was underway. Cyanobacteria engineered an inorganic manganese-calcium cubane cluster capable of performing the most thermodynamically demanding biochemical feat in nature: cracking the covalent bonds of ambient water to harvest electrons, unleashing molecular oxygen as a byproduct and permanently transforming the geochemistry of the Earth.

1. The Thermodynamics of Water Oxidation: The Mn_4CaO_5 Cluster

Early photosynthetic bacteria were strictly anoxygenic. Purple sulfur and green sulfur bacteria utilized simple photosystems to extract electrons from dissolved hydrogen sulfide (H_2S) or ferrous iron (Fe^{2+}). While thermodynamically facile due to the low redox potential of hydrogen sulfide ($E^{\circ\prime} \approx -0.25\ \text{V}$), this ecology was fundamentally localized: life was tethered to volcanic sulfur springs and mineral seeps.

To liberate itself and colonize the open oceans, life needed an electron donor that was ubiquitous. That donor was water (H_2O). However, oxidising water to release oxygen is a monumental energetic challenge. Water is an exceptionally stable molecule with an extraordinarily high standard reduction potential:

$$2H_2O \rightarrow O_2 + 4H^+ + 4e^- \quad (E^{\circ\prime} = +0.815\ \text{V at pH 7})$$

To pull electrons away from water, nature had to create an oxidizing chemical species even more electronegative than oxygen itself. In Photosystem II (PSII), the light-harvesting reaction center chlorophyll pair, **P680**, achieves an excited-state oxidation potential of $+1.25\ \text{V}$—making P680* the most powerful biological oxidizing agent known.

Shakil Mahmud • Research Monograph

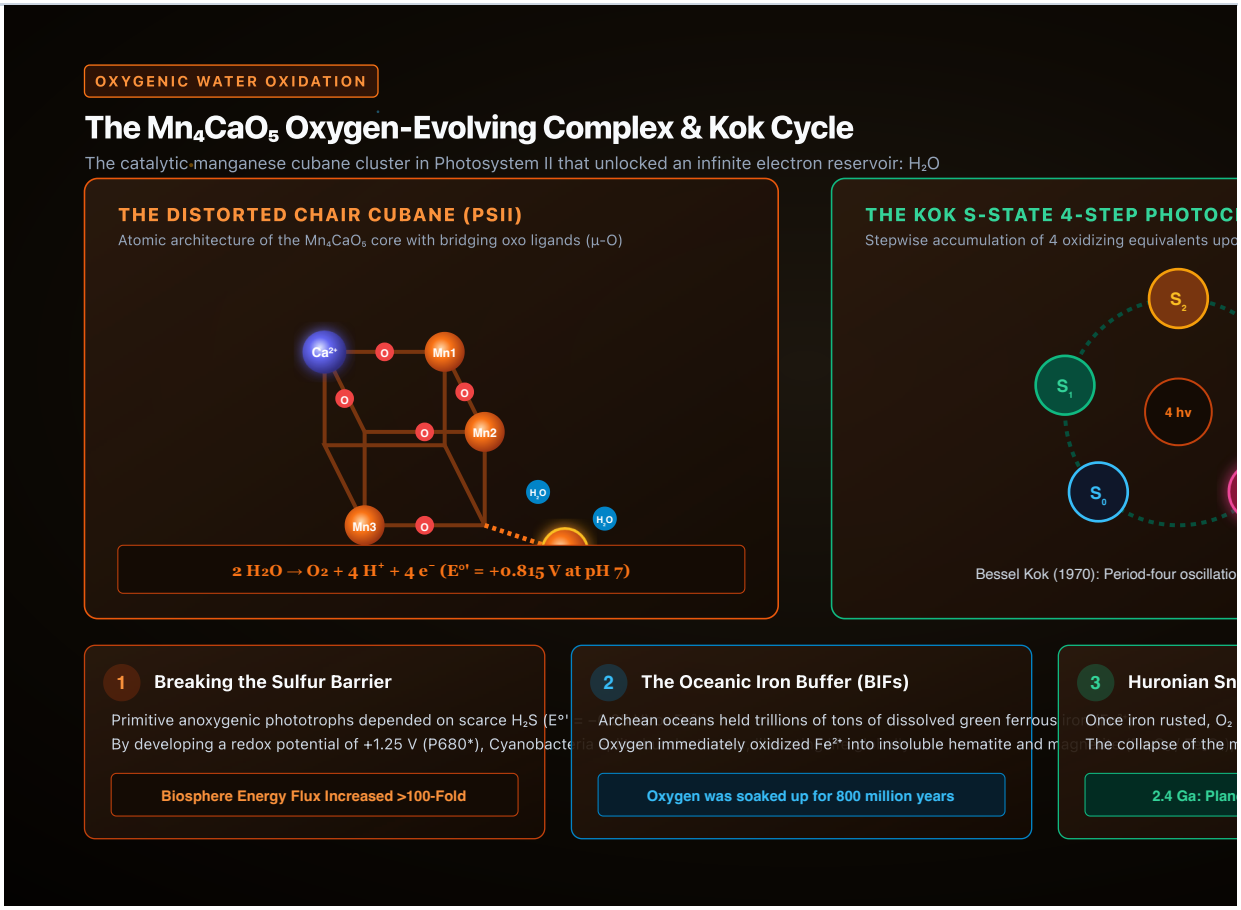


Figure 3.1: The Catalytic Core of Oxygenic Photosynthesis. The distorted chair cubane architecture of the Mn_4CaO_5 Oxygen-Evolving Complex (OEC) in Photosystem II. Coordinated water molecules undergo stepwise oxidation across Bessel Kok's period-four S-state clock ($S_0 \rightarrow S_4$), accumulating 4 oxidizing equivalents upon absorbing 4 photons ($h\nu$) before releasing a molecule of diatomic oxygen (O_2).

The molecular catalytic engine that manages this four-electron oxidation is the **Oxygen-Evolving Complex (OEC)**, an asymmetric distorted chair cubane composed of four manganese atoms, one calcium atom, and five bridging oxygen ligands: Mn_4CaO_5.

Because water oxidation requires removing four electrons simultaneously to avoid producing lethal single-electron reactive oxygen intermediates (such as hydroxyl radicals $\cdot OH$), Bessel Kok demonstrated in 1970 that the OEC functions as a chemical capacitor. Known as the *Kok S-state cycle* ($S_0 \rightarrow S_1 \rightarrow S_2 \rightarrow S_3 \rightarrow [S_4] \rightarrow S_0$), the manganese cluster absorbs one photon of light at a time, stepping through progressively higher oxidation states until four oxidizing equivalents have accumulated. At state S_4, it spontaneously coordinates two substrate water molecules, forms an $O{=}O$ bond, ejects one molecule of O_2 and four protons (H^+), and resets back to S_0.

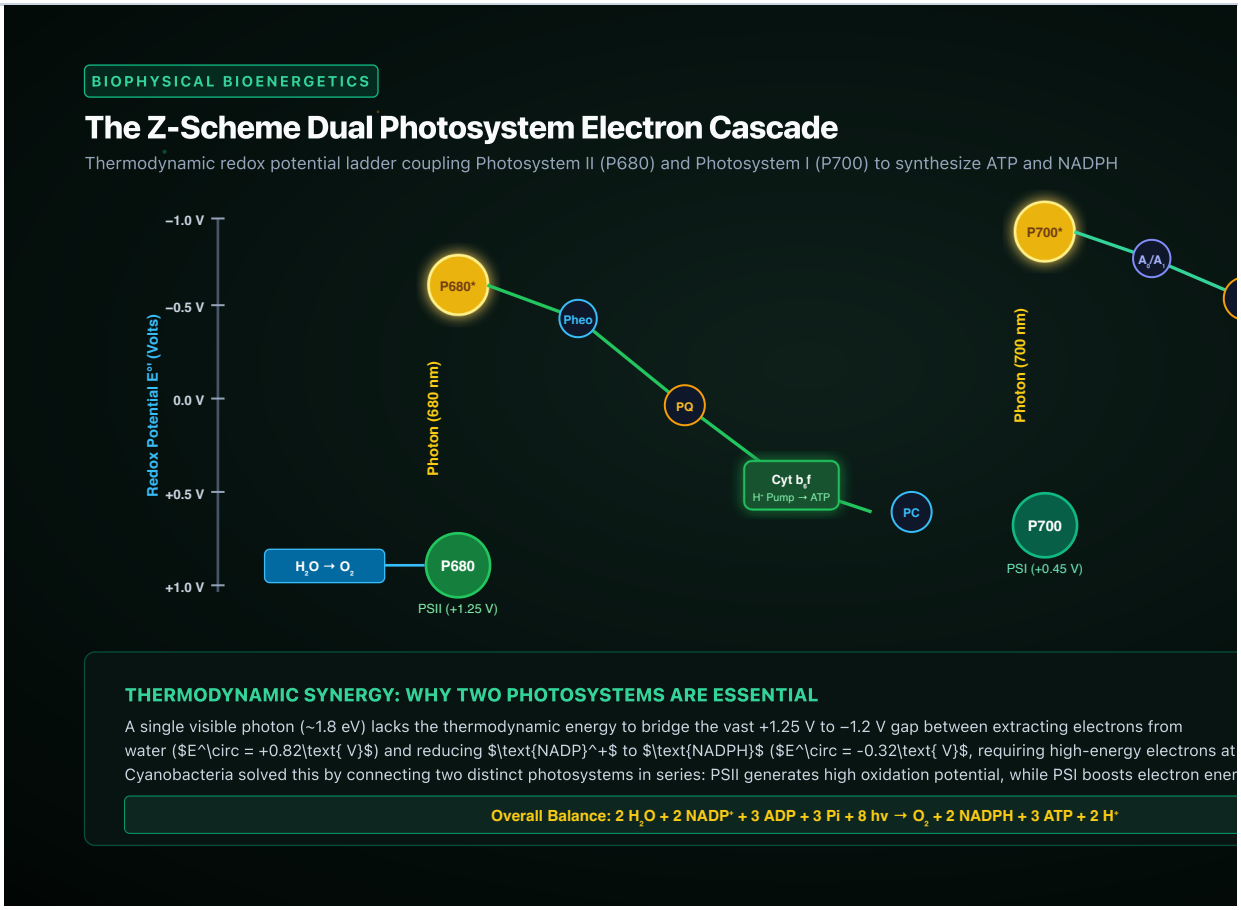


Figure 3.2: The Biophysical Z-Scheme. Two photosystems wired in series bridge the thermodynamic gap between extracting electrons from water ($+0.82\text{ V}$) and reducing NADP^+ to NADPH (-0.32 V). Downhill electron transport through the cytochrome b_6f complex pumps protons into the thylakoid lumen, driving rotary ATP synthesis.

2. The Z-Scheme: Coupling Two Photochemical Engines

A single photon of visible light ($\sim 1.8\text{ eV}$) does not possess sufficient thermodynamic energy to both rip an electron from water ($+0.82\text{ V}$) and elevate it to the low-potential state required to reduce NADP^+ to NADPH (-0.32 V, via ferredoxin at -0.45 V).

Cyanobacteria solved this thermodynamic shortfall through a stroke of biophysical brilliance: the **Z-Scheme**. By wiring two distinct photosystems—Photosystem II (PSII) and Photosystem I (PSI)—in series, electrons receive two sequential optical boosts:

1. **First Photochemical Boost (PSII):** Light absorption at P680 promotes an electron to an excited state (-0.6 V). The electron cascades exergonically through pheophytin, plastoquinone (Q_A, Q_B), and the cytochrome b_6f complex. As it moves downhill, cytochrome b_6f translocates protons across the thylakoid membrane, generating a chemiosmotic gradient that synthesizes ATP.
2. **Inter-Photosystem Shuttle:** The mobile copper-containing protein plastocyanin (PC) delivers the electron to the reaction center of Photosystem I (P700).
3. **Second Photochemical Boost (PSI):** Light absorption at P700 excites the electron again to a hyper-reducing potential of -1.2 V. From this peak, the electron cascades through iron-sulfur centers to ferredoxin, and finally to Ferredoxin-NADP^+ Reductase (FNR), generating the biochemical reducing power: NADPH.

The net outcome is a self-sustaining bioenergetic engine powered purely by water and sunlight:

$$2\text{H}_2\text{O} + 2\text{NADP}^+ + 3\text{ADP} + 3\text{P}_i + 8h\nu \rightarrow \text{O}_2 + 2\text{NADPH} + 3\text{ATP} + 2\text{H}^+$$

With unlimited access to oceanic water and sunlight, the biosphere's primary productivity exploded by over a hundredfold. Massive cyanobacterial colonies formed undulating coastal microbial reefs known as **stromatolites**, preserved today in the 3.48-billion-year-old Dresser Formation of Western Australia.

Shakil Mahmud • Research Monograph

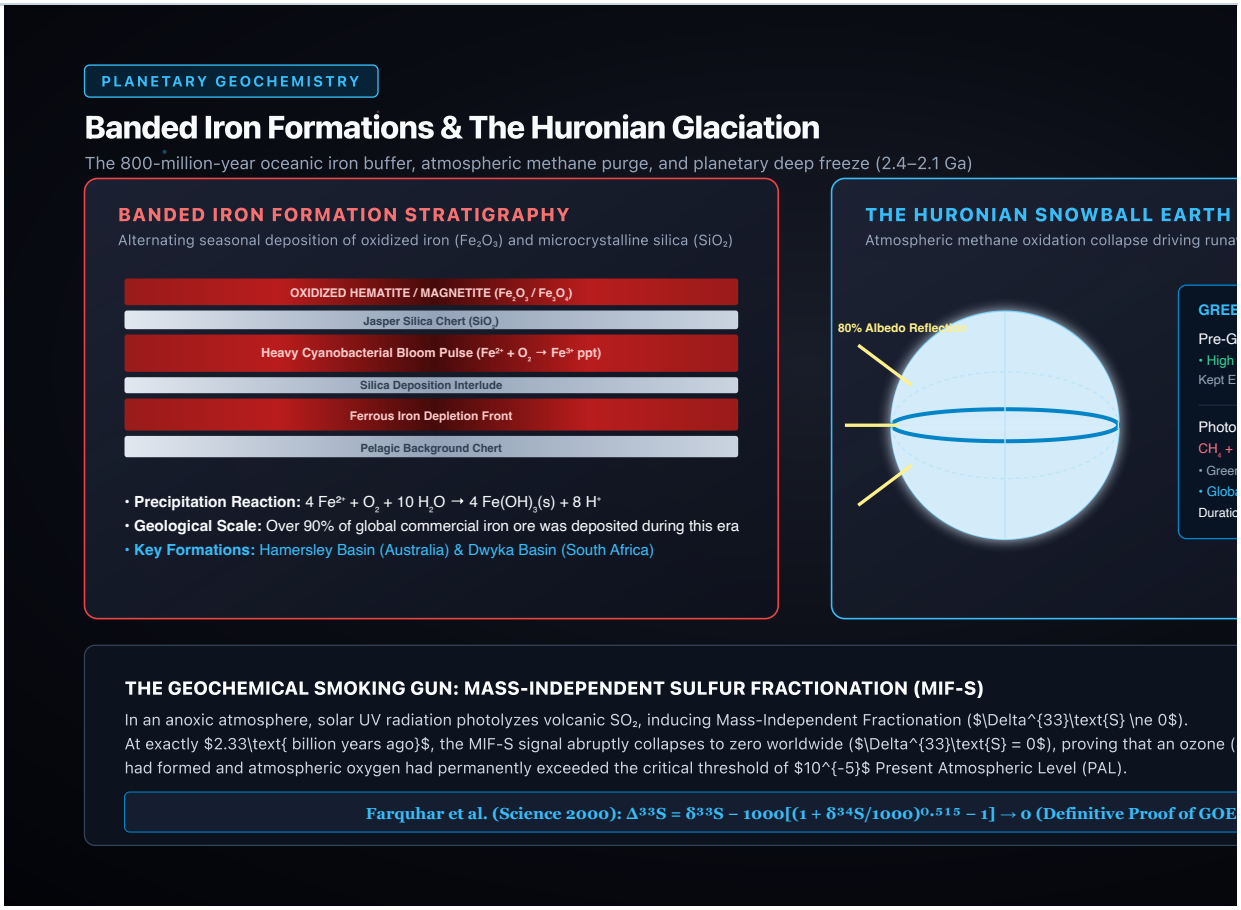


Figure 3.3: The Global Geochemical Catastrophe. Left: Alternating seasonal bands of oxidized hematite/magnetite (Fe_2O_3/Fe_3O_4) and silica chert in Banded Iron Formations, documenting the oceanic iron buffer. Right: Runaway ice-albedo feedback during the Huronian Snowball Earth (2.4–2.1 Ga) precipitated by the photochemical oxidation and collapse of atmospheric methane.

3. The Great Oxidation Catastrophe and the Huronian Snowball Earth

While oxygen was the ultimate metabolic fuel for future complex organisms, to the ancient Archean biosphere it was a lethal poison. Molecular oxygen and its reactive free radicals ($O_2^{\cdot-}, H_2O_2, \cdot OH$) violently oxidized exposed iron-sulfur enzyme clusters, denatured anaerobic proteins, and shredded naked DNA.

For roughly 800 million years (3.2\text{–}2.4\text{ Ga}), the planet remained shielded from free atmospheric oxygen by an enormous geochemical buffer: the Archean oceans were saturated with trillions of tons of dissolved green ferrous iron (Fe^{2+}) leached from basaltic seafloors. As cyanobacteria released oxygen, it reacted instantaneously with dissolved iron, precipitating insoluble rust particles onto the seabed:

$$4Fe^{2+} + O_2 + 10H_2O \rightarrow 4Fe(OH)_3(s) + 8H^+$$

This colossal oceanic filtration precipitated the planet's vast **Banded Iron Formations (BIFs)**—millions of square kilometers of alternating red jasper chert and silver-black hematite, which comprise over 90% of all iron ore mined on Earth today.

Around 2.4 billion years ago, the ocean's iron sponge was finally exhausted. Dissolved iron dropped to near-zero, and free oxygen began leaking into the atmosphere in what geologists term the **Great Oxidation Event (GOE)**.

The definitive geochemical proof of this transition was discovered by James Farquhar in 2000: prior to 2.33 Ga, sedimentary sulfides exhibit anomalous *Mass-Independent Fractionation of sulfur isotopes* ($\Delta^{33}S \neq 0$), caused by unfiltered solar UV radiation photolyzing volcanic SO_2. Exactly at 2.33 Ga, the $\Delta^{33}S$ signal abruptly vanishes worldwide to zero, proving that atmospheric oxygen had exceeded 10^{-5} Present Atmospheric Level, creating an ozone (O_3) shield.

The atmospheric injection of oxygen had catastrophic climatic consequences. Under the Faint Young Sun (which shone with 20–25% less luminosity than today), the Earth had remained warm due to a potent atmospheric blanket of biogenic methane (CH_4). Atmospheric oxygen reacted with methane, converting it to far weaker greenhouse gases:

$$CH_4 + 2O_2 \rightarrow CO_2 + 2H_2O$$

The greenhouse blanket collapsed. Global temperatures plummeted by tens of degrees. Polar ice sheets expanded across the continents, reflecting incoming solar radiation back into space. This positive ice-albedo feedback triggered the **Huronian Glaciation** (2.4\text{–}2.1\text{ Ga})—a 300-million-year global deep freeze during which glaciers reached the equator, encasing the entire planet in an icy shell kilometers thick.

Conclusion: The Crucible of Aerobic Life

The Great Oxidation Event was history's first planetary-scale ecological crisis and the greatest mass extinction of anaerobic life. Yet within the frozen slush and hydrothermal refugia of Snowball Earth, the survivors evolved antioxidant defense mechanisms: superoxide dismutase, catalase, and peroxiredoxins.

More importantly, the stage was set for an energetic leap of staggering proportions. Anaerobic fermentation yielded only 2 ATP molecules per glucose; aerobic respiration using oxygen as the terminal electron acceptor would yield 36 to 38 ATP molecules—an 18-fold increase in bioenergetic efficiency. In Part 4, we will examine how this oxygen-fueled energy bonanza facilitated the most transformative symbiosis in history: the Eukaryotic Leap.

Key Academic Citations

- Kok, B., Forbush, B., & McGloin, M. (1970). Cooperation of charges in photosynthetic O2 evolution–I. A linear four step mechanism. *Photochemistry and Photobiology*, 11(6), 457–475.
- Barber, J. (2006). Photosystem II: an enzyme of global significance. *Biochemical Society Transactions*, 34(5), 619–625.
- Farquhar, J., Bao, H., & Thiemens, M. (2000). Atmospheric influence of Earth's earliest sulfur cycle. *Science*, 289(5480), 756–758.
- Lyons, T. W., Reinhard, C. T., & Planavsky, N. J. (2014). The rise of oxygen in Earth's early ocean and atmosphere. *Nature*, 506(7488), 307–315.
- Fischer, W. W., Hemp, J., & Johnson, J. E. (2016). Evolution of oxygenic photosynthesis. *Annual Review of Earth and Planetary Sciences*, 44, 647–672.

Citation: Mahmud, S. (2026). "The Solar Energy Revolution — Phototrophy, Water-Splitting, and the Great Oxidation Catastrophe." In The Evolutionary Odyssey, Part 3. https://shakilmahmud.com/evolutionary-odyssey-part-3-the-solar-energy-revolution/

Shakil Mahmud • Research Monograph

SHAKIL MAHMUD RESEARCH MONOGRAPHS • PART IV

The Eukaryotic Leap — The Asgard Archaea, Mitochondriogenesis, and the Complex Cell

The Eukaryotic Leap — The Asgard Archaea, Mitochondriogenesis, and the Complex Cell

1,531 words • November 1, 2026 • Permanent URI

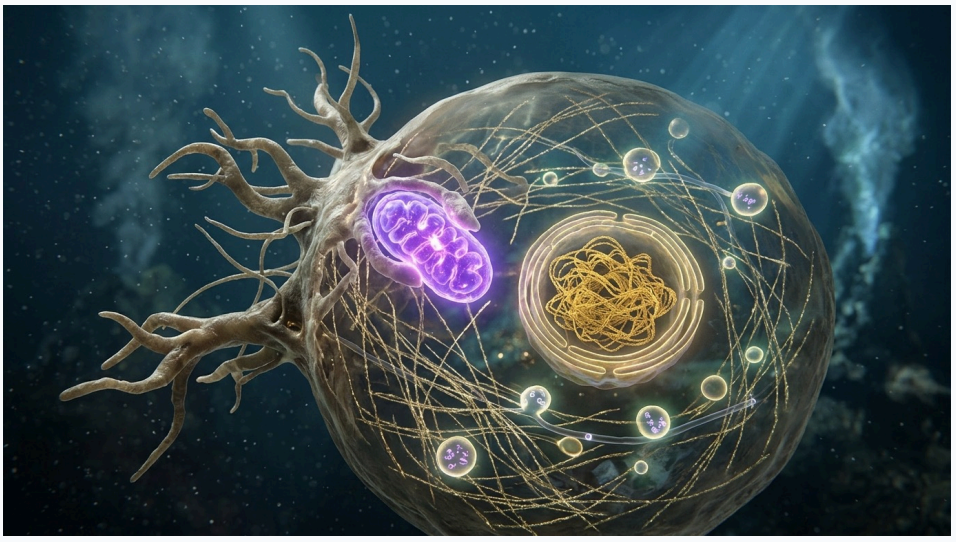


Plate IV: *Figure: Cellular endosymbiosis in the Mesoproterozoic (~1.8 Ga): an Asgard archaean host cell engulfs an alphaproteobacterium ancestor, giving rise to the mitochondrion, complex endomembrane system, and the first eukaryotic cells.*

For the first two billion years of planetary history, life on Earth remained stubbornly microscopic. Bacteria and archaea radiated into every conceivable thermodynamic niche, mastering photosynthesis, nitrogen fixation, and methanogenesis, yet structurally they never transcended the basic prokaryotic body plan: tiny, wall-bound sacks of biochemistry. Then, around 1.8 billion years ago, an unprecedented endosymbiotic union occurred between two utterly divergent microbes—an event so biologically singular that it happened only once in four billion years, dissolving the bioenergetic ceiling of the prokaryotic cell and giving birth to every amoeba, redwood, mushroom, and human being on Earth.

1. The Asgard Archaea: Discovering Our True Ancestral Roots

For decades following Carl Woese's classic ribosomal RNA phylogenies in 1977, biology taught the "Three-Domain Tree of Life": Bacteria, Archaea, and Eukaryota diverging as three co-equal primary lineages from LUCA. However, this model left the morphological origin of eukaryotes an unresolved mystery—complex cells possess an internal cytoskeleton, endomembrane networks, and vesicular trafficking systems completely absent in typical bacteria and archaea.

In 2015, a revolutionary metagenomic discovery off the coast of Svalbard, Norway, shattered the three-domain dogma. A team led by Thijs Ettema recovered environmental DNA from deep hydrothermal sediment at Loki's Castle and assembled the genome of an uncultivated organism named **Lokiarchaeum**. Subsequent expeditions identified an entire deep-branching superphylum: the **Asgard Archaea** (including Thor, Odin, and Heimdallarchaeota).

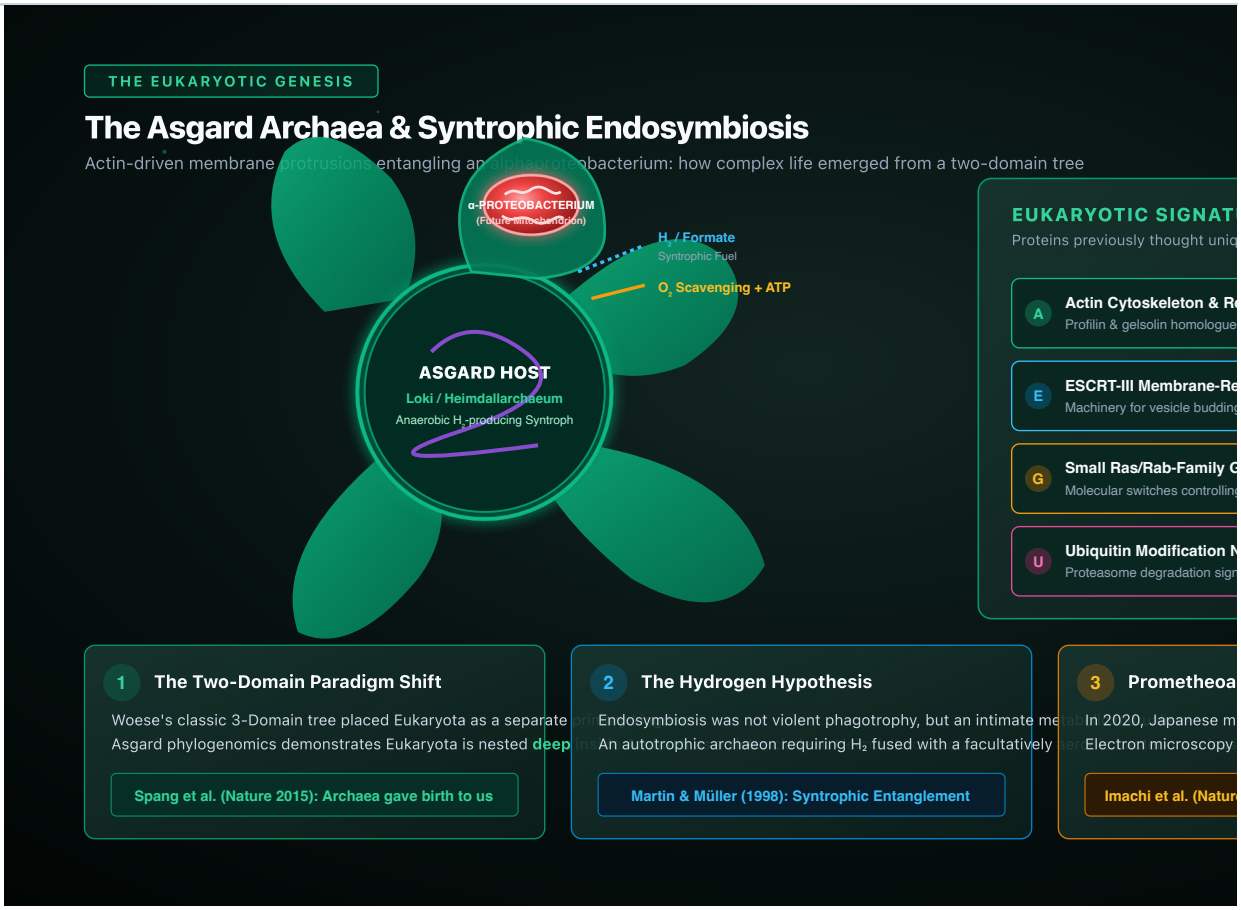


Figure 4.1: The Archaeal Cradle of Eukaryotes. An Asgard archaeon (e.g., *Prometheoarchaeum syntrophicum*) extending actin-rich membrane protrusions to cradle an α-proteobacterium. Metagenomic analysis reveals that Asgard genomes encode an astonishing repertoire of Eukaryotic Signature Proteins (ESPs), including profilin, gelsolin, small Ras-family GTPases, and ESCRT-III membrane-remodeling complexes.

The Asgard genomes stunned the biological community. Embedded inside these archaea were dozens of genes previously believed to be unique to eukaryotes: **Eukaryotic Signature Proteins (ESPs)**. They encoded authentic actin cytoskeletons, actin-binding regulators (profilin and gelsolin), small Ras-family GTPases for intracellular trafficking, and the entire ESCRT-III protein machinery responsible for vesicle budding and membrane remodeling.

Phylogenomic trees constructed with hundreds of conserved proteins confirmed that Eukaryotes do not form a third independent domain: *we are branch of Archaea*, emerging directly from within the Asgard superphylum as sister to Heimdallarchaeota.

In 2020, Japanese microbiologist Masaru Nobu and colleagues achieved what was thought impossible: after 12 years of painstaking laboratory cultivation, they successfully isolated and photographed the first live Asgard archaeon, *Prometheoarchaeum syntrophicum*. Cryo-electron tomography revealed that rather than engulfing prey through phagocytosis, the cell produces long, delicate, branching tentacles that physically entangle partner bacteria, confirming the **Hydrogen Hypothesis** of Martin and Müller (1998): endosymbiosis was an intimate metabolic syntrophy where an anaerobic archaeon feeding on hydrogen embraced a facultatively aerobic, hydrogen-excreting α-proteobacterium.

Shakil Mahmud • Research Monograph

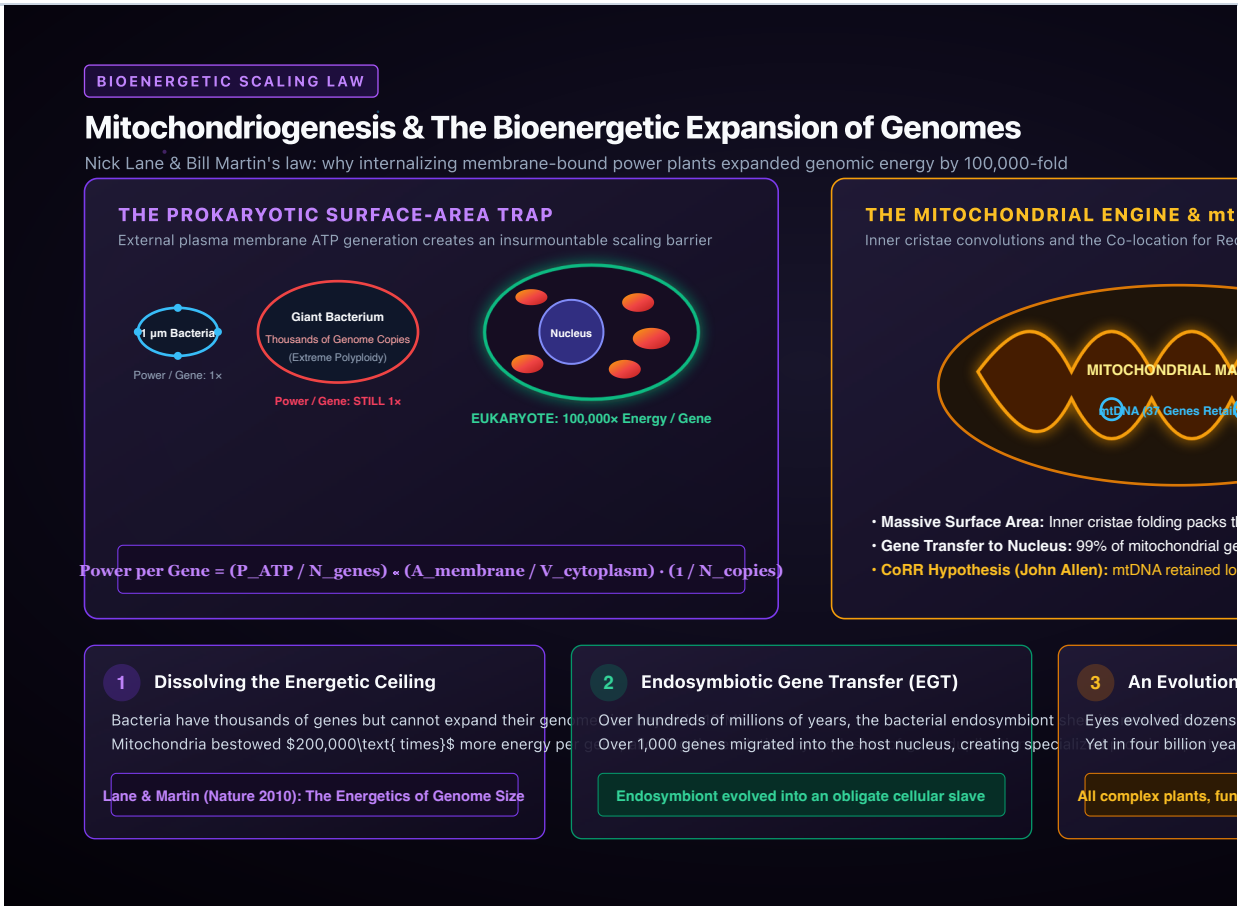


Figure 4.2: Dissolving the Bioenergetic Ceiling. Nick Lane & Bill Martin's bioenergetic scaling law. Left: Prokaryotes generate ATP across their external plasma membrane, causing power per gene to collapse as cell volume expands. Middle: Giant bacteria survive only through extreme polyploidy, failing to expand genomic energy. Right: By internalizing hundreds of cristae-dense mitochondria, eukaryotes expanded bioenergetic power per gene by over $100,000$-fold.

2. Mitochondriogenesis and the Bioenergetic Scaling Law

Why did complex life never evolve in bacteria? Why did bacteria remain small and morphologically simple despite experiencing four billion years of continuous natural selection and possessing immense biochemical diversity?

The answer, formulated by biochemist Nick Lane and evolutionary biologist William Martin in their groundbreaking 2010 *Nature* paper, is purely physical: **bioenergetic scaling constraints**.

Every bacterium generates its chemiosmotic proton gradient across its outer boundary: the plasma membrane. As a spherical or rod-shaped cell grows larger, its surface area expands with the square of its radius ($A \propto r^2$), while its internal cytoplasmic volume expands with the cube of its radius ($V \propto r^3$). Because synthesizing proteins to support a larger volume requires thousands of active ribosomes and continuous transcription, a large prokaryote faces an acute energy crisis:

$$\text{Power per Gene} = \frac{P_{\text{ATP}}}{N_{\text{genes}}} \propto \frac{A_{\text{membrane}}}{V_{\text{cytoplasm}}} \cdot \frac{1}{N_{\text{genome copies}}}$$

When rare "giant bacteria" evolve—such as the 600-μm surgeonfish gut symbiont *Epulopiscium fishelsoni* or the sulfur pearl *Thiomargarita magnifica*—they cannot support this volume with a single enlarged genome. Instead, they must maintain up to **tens of thousands of identical copies of their complete circular chromosome** plastered against their outer membrane to control local respiration. Consequently, the energy available per individual gene copy in a giant bacterium is completely unchanged compared to a microscopic 1-μm *E. coli*.

The acquisition of the mitochondrion dissolved this energetic straitjacket forever. By internalizing the respiration-competent α-proteobacterium, the host cell transformed its energy generation from a two-dimensional surface boundary into a three-dimensional internal network. Each mitochondrion folded its inner membrane into thousands of convoluted **cristae**, packing astronomical densities of electron transport complexes and ATP synthases inside the cell without compromising the host's surface-to-volume ratio.

Furthermore, over hundreds of millions of years, the intracellular endosymbionts underwent massive genome reduction: non-essential genes were deleted or transferred to the host nucleus via Endosymbiotic Gene Transfer (EGT). Today, human mitochondria retain a tiny circular genome of only 37 genes. By delegating genetic administrative overhead to the central host nucleus while retaining miniature local genomes solely to control lethal electron redox leaks (the CoRR hypothesis of John Allen), the eukaryotic cell gained over $100,000$ to $200,000$ times **more ATP energy per gene** than any bacterium on Earth. This energetic windfall provided the genomic budget required to evolve thousands of new regulatory genes, gene duplicates, complex signal transduction cascades, and macroscopic multicellular bodies.

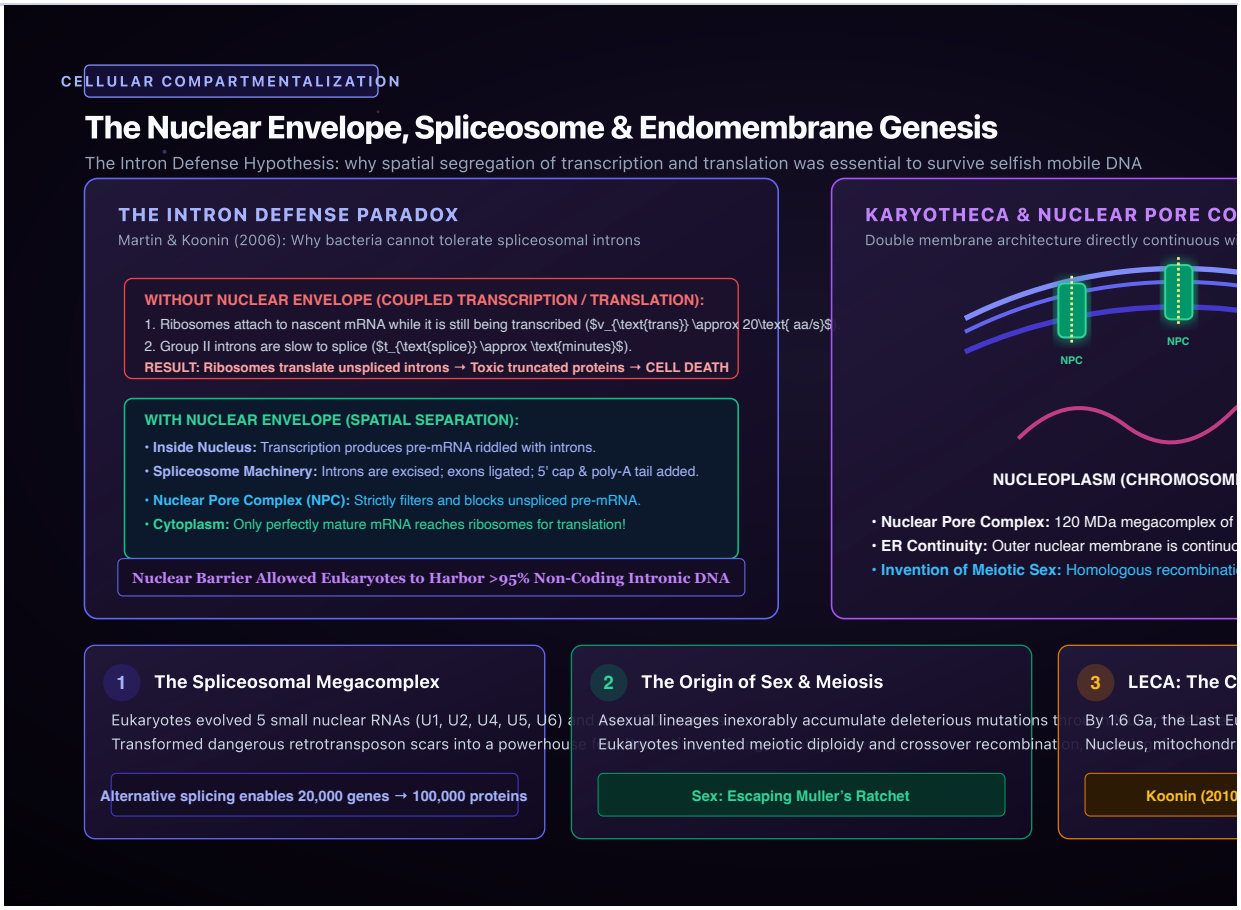


Figure 4.3: The Genesis of the Nucleus. The Intron Defense Hypothesis (Martin & Koonin, 2006). When bacterial endosymbionts lysed, selfish Group II self-splicing retrotransposons flooded the host genome. The evolution of the double-membrane nuclear envelope (karyotheca) and Nuclear Pore Complexes (NPCs) physically decoupled transcription from translation, ensuring ribosomes only translate fully spliced, mature mRNA.

3. The Genesis of the Nucleus and the Intron Defense Shield

While the mitochondrion solved the cell's energetic crisis, its initial acquisition triggered an existential genetic catastrophe: the invasion of selfish mobile genetic elements.

The ancestral α-proteobacterium harbored thousands of **Group II self-splicing introns**—selfish retrotransposons capable of reverse-transcribing and copying themselves randomly throughout genomes. When endosymbionts periodically lysed inside the archaeal host, fragments of bacterial DNA integrated into the host's chromosome, peppering vital archaeal genes with hundreds of parasitic mobile introns.

In prokaryotes, transcription and translation are obligatorily coupled: ribosomes physically attach to nascent mRNA while it is still being synthesized by RNA polymerase ($v_{\text{translation}} \approx 20$ amino acids/second). Splicing of an intron, however, is a slow catalytic process requiring minutes. In a coupled prokaryotic cytoplasm, ribosomes would inevitably read through unspliced introns before they could excise themselves, encountering in-frame stop codons and producing toxic truncated peptide fragments that would poison the cell.

To survive this genomic onslaught, the host cell evolved the single most defining morphological structure of our lineage: the **nuclear envelope (karyotheca)**.

By folding endomembranes into a double lipid bilayer perforated by giant 120-MDa **Nuclear Pore Complexes (NPCs)**, the cell created an absolute spatial and temporal barrier. Transcription and spliceosomal intron excision were confined exclusively to the interior of the nucleus. The nuclear pore complex acted as a strict molecular customs gate: only completely processed, spliced mRNA molecules bearing a 5’\text{-cap} and a 3’\text{-poly(A)} tail were permitted to exit into the cytoplasm for translation.

The evolutionary repurposing of this crisis was monumental: the host evolved the **spliceosome**—a massive RNA-protein machine composed of five small nuclear RNAs (U1, U2, U4, U5, U6) and over 150 proteins. Introns, once lethal genomic parasites, became the primary fuel for *alternative splicing*, allowing a single gene to encode dozens of distinct protein isoforms and conferring unparalleled proteomic flexibility on eukaryotic organisms.

Conclusion: The Emergence of LECA

By approximately 1.6 billion years ago, all these transformative innovations had coalesced into a single ancestral population: the **Last Eukaryotic Common Ancestor (LECA)**. LECA was not a primitive transition form; it was an extraordinarily sophisticated, fully modern eukaryotic cell equipped with:

- Mitochondria possessing functional cristae and ATP export mechanisms;
- A compartmentalized nucleus with nuclear pore complexes;

Shakil Mahmud • Research Monograph

- A dynamic endomembrane system (Endoplasmic Reticulum, Golgi apparatus, lysosomes);
- A flexible actin-tubulin cytoskeleton with motor proteins (kinesin, dynein, myosin);
- A 9+2 microtubule axoneme forming the eukaryotic cilium / flagellum;
- And regular **meiotic sex**—diploid homologous chromosome pairing and crossover recombination to purge accumulated deleterious mutations and escape Muller's ratchet.

From the crucible of LECA, the eukaryotic tree exploded into its major supergroups: Opisthokonta (animals and fungi), Archaeplastida (plants and red/green algae), SAR (stramenopiles, alveolates, rhizarians), and Amoebozoa. In Part 5, we will cross into Phase II and witness the momentous transition from solitary cells to cooperative multi-cellular organisms and the enigmatic macroscopic garden of the Ediacaran biota.

Key Academic Citations

- Spang, A., et al. (2015). Complex archaea that bridge the gap between prokaryotes and eukaryotes. *Nature*, 521(7551), 173–179.
- Imachi, H., et al. (2020). Isolation of an archaeon at the interface of the prokaryote–eukaryote divide. *Nature*, 577(7791), 519–525.
- Lane, N., & Martin, W. (2010). The energetics of genome complexity. *Nature*, 467(7318), 929–934.
- Martin, W., & Müller, M. (1998). The hydrogen hypothesis for the first eukaryote. *Nature*, 392(6671), 37–41.
- Martin, W., & Koonin, E. V. (2006). Introns and the origin of nucleus-cytosol compartmentalization. *Nature*, 440(7080), 41–45.
- Allen, J. F. (2003). Why chloroplasts and mitochondria contain genomes. *Comparative and Functional Genomics*, 4(1), 31–36.

Citation: Mahmud, S. (2026). "The Eukaryotic Leap — The Asgard Archaea, Mitochondriogenesis, and the Complex Cell." In The Evolutionary Odyssey, Part 4. https://shakilmahmud.com/evolutionary-odyssey-part-4-the-eukaryotic-leap/

SHAKIL MAHMUD RESEARCH MONOGRAPHS • PART V

The Dawn of Multicellularity — Cell Adhesion, Morphogenesis, and the Ediacaran Garden

The Dawn of Multicellularity — Cell Adhesion, Morphogenesis, and the Ediacaran Garden

1,404 words • November 1, 2026 • Permanent URI

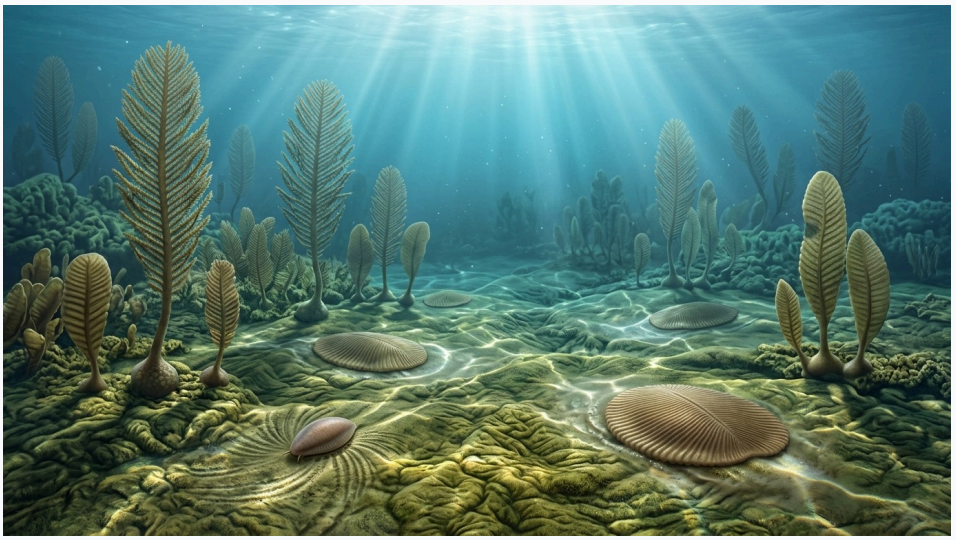


Plate V: *Figure: The late Neoproterozoic Ediacaran seafloor (~575–541 Ma), showing quilted, soft-bodied multicellular organisms including the disc-shaped Dickinsonia and frond-like Charnia anchored on microbial sediment mats.*

For over three billion years, the struggle for existence on Earth was waged exclusively at the single-cell frontier. Cells competed ruthlessly for nutrients, dividing as rapidly as their metabolic machinery permitted. Yet in the wake of the catastrophic Cryogenian Snowball Earth glaciations, around 600 million years ago, a radical biological pact was forged: individual cells surrendered their reproductive autonomy to unite into cooperative, specialized, macroscopic bodies. In the shallow, oxygen-rich Neoproterozoic seas, this transition spawned the serene, bizarre macroscopic world of the Ediacaran biota—the peaceful dawn of the animal kingdom.

1. The Genetic Toolkit of Multicellularity: Adhesion, Polarity, and Signaling

Multicellularity is not a singular invention; it evolved independently over 25 distinct times across fungi, slime molds, red algae, brown kelp, and green plants. However, the origin of complex, macroscopic **Metazoa (animals)** required a sophisticated, integrated molecular toolkit that went far beyond mere clonal aggregation.

To construct a viable animal body, cells required three foundational molecular capabilities:

1. **Intercellular Adhesion:** A physical mechanism to bind adjacent cells tightly together into tear-resistant sheets.
2. **Extracellular Matrix (ECM) Scaffolding:** A flexible, structural fibrous matrix providing mechanical support, shape, and tissue anchorage.
3. **Spatial Morphogenesis & Signaling:** Chemical communication networks allowing genetically identical cells to differentiate into distinct tissues (muscle, nerve, skin) based on their relative coordinates.

Shakil Mahmud • Research Monograph

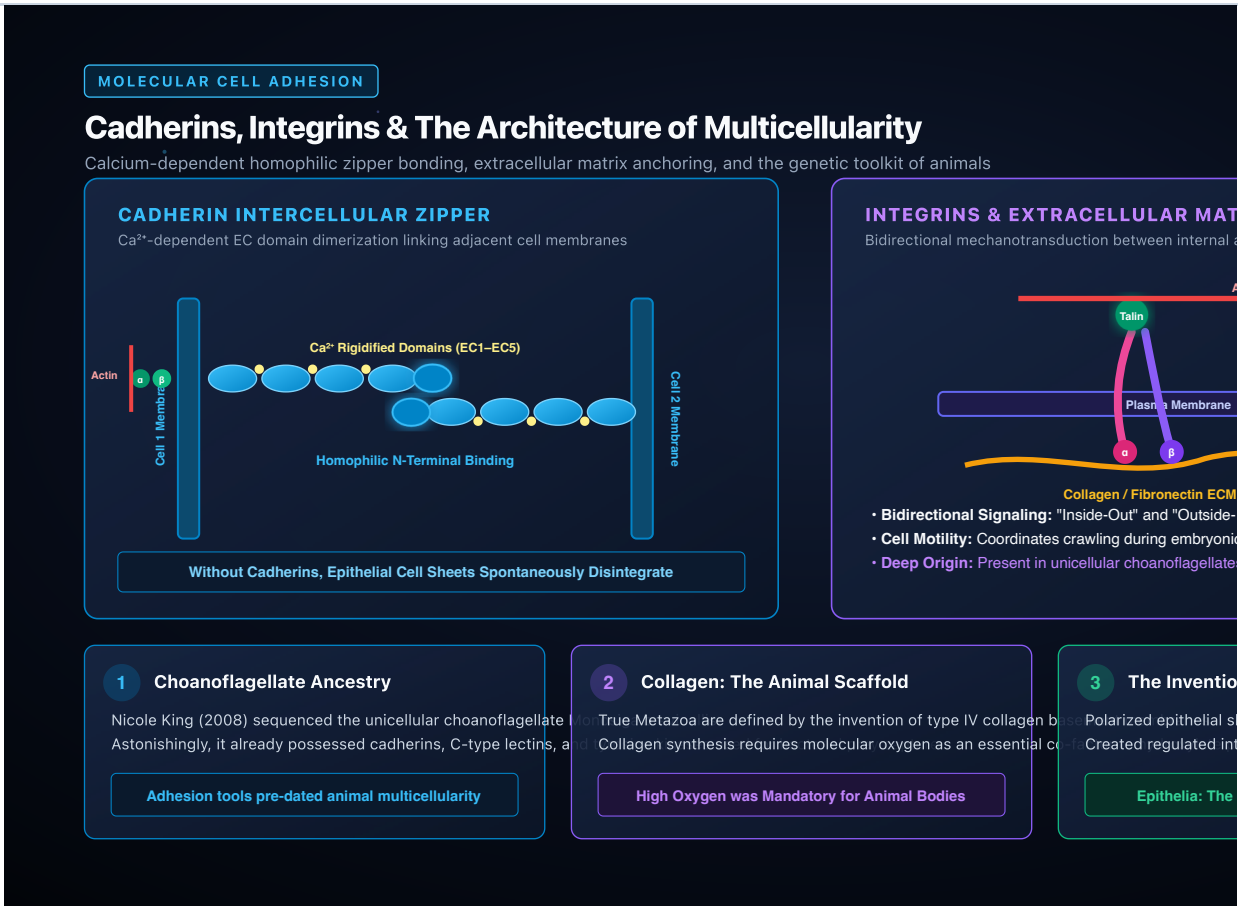


Figure 5.1: The Molecular Adhesion Complex of Metazoa. Left: Calcium-dependent cadherin homophilic zipper junctions linking adjacent cell membranes, anchored to the actin cytoskeleton via β-catenin and α-catenin. Right: Integrin heterodimers (α/β) spanning the plasma membrane to anchor internal actin stress filaments to the extracellular matrix (collagen and fibronectin), coordinating tissue morphogenesis.

In 2008, evolutionary biologist Nicole King and her team sequenced the genome of *Monosiga brevicollis*, a single-celled marine choanoflagellate representing the closest living unicellular relative of animals. The results yielded a profound evolutionary revelation: the molecular components for animal multicellularity existed long before true animals evolved.

Unicellular choanoflagellates already possessed classic **cadherins**, C-type lectins, and tyrosine kinase signaling networks. In solitary protists, these adhesion proteins functioned not to build tissues, but as sticky molecular tentacles deployed on external surfaces to capture bacterial prey. The transition to animal multicellularity was an exquisite evolutionary exaptation: rather than inventing entirely new proteins, natural selection repurposed existing prey-capture receptors to bind daughter cells together, creating the first polarized epithelial sheets.

Crucially, animal multicellularity depended on **Type IV collagen**, the foundational meshwork of basement membranes. Synthesizing stable triple-helical collagen fibers requires molecular oxygen as an obligate co-factor to hydroxylate proline and lysine amino acids. Without adequate environmental oxygen, cells cannot secrete collagen; without collagen, animals cannot build stable tissues. The expansion of animal bodies was chemically impossible until global oxygen levels crossed the Neoproterozoic threshold.



Figure 5.2: The Ediacaran Paradigm. Left: *Dickinsonia costata* exhibiting quilted isometric modular growth along an alternating glide-symmetry axis. Bobrovskiy et al. (2018) discovered 93% cholesteroids in fossil tissue, proving its true animal status. Right: *Charnia masoni* exhibiting 4th-order self-similar fractal branching, maximizing osmotic surface area for dissolved organic nutrient absorption without a digestive tract.

2. The Ediacaran Garden: Fractal Fronds and Quilted Mattresses

Between **575 and 541 million years ago**, in the quiet, undisturbed Neoproterozoic seas, there flourished the most enigmatic macroscopic ecosystem in Earth history: the **Ediacaran Biota**.

First discovered in the Ediacara Hills of South Australia by Reginald Sprigg in 1946, and later identified in Newfoundland and the White Sea of Russia, these fossils perplexed paleontologists for decades. Lacking mineralized shells, jaws, eyes, or limbs, they resembled quilted air mattresses, segmented discs, and undulating ferns anchored to the seafloor.

The dominant organisms of the early Ediacaran (the Avalon Assemblage, 575\text{–}560\text{ Ma}) were the **Rangeomorphs** (such as *Charnia masoni*). Rangeomorphs possessed an extraordinary body architecture completely absent in modern animals: **self-similar fractal branching**. A primary frond branched into secondary frondlets, which branched into tertiary sub-frondlets, which branched into fourth-order microscopic leaflets. This mathematical fractal growth maximized surface area, allowing rangeomorphs to practice *osmotrophy*—absorbing dissolved organic carbon and nutrients directly from seawater across their skin without requiring a mouth, gut, or circulatory system.

The most iconic Ediacaran fossil is **Dickinsonia costata**—a flat, ribbed, oval organism reaching over a meter in length. For decades, scientists fiercely debated whether *Dickinsonia* was a giant lichen, a marine fungus, an extinct protozoan, or a primitive animal. German paleontologist Adolf Seilacher proposed the radical hypothesis of *Vendobionta*: that Ediacaran organisms were an independent, extinct experiment in multicellularity built from inflated, quilted air-mattress chambers.

The debate was decisively settled in 2018 by Australian biogeochemist Ilya Bobrovskiy. By excavating exceptionally preserved *Dickinsonia* fossils from 100-meter-high cliffs along the White Sea of Russia, his team extracted organic molecules directly from the fossil tissue. Gas chromatography-mass spectrometry revealed that while surrounding sedimentary microbial mats were dominated by plant/algal stigmasterols, the *Dickinsonia* specimens contained **over 93% cholesteroids** (cholesterol and cholestane)—the definitive molecular hallmark of true animal physiology. *Dickinsonia* was an authentic metazoan.

Shakil Mahmud • Research Monograph

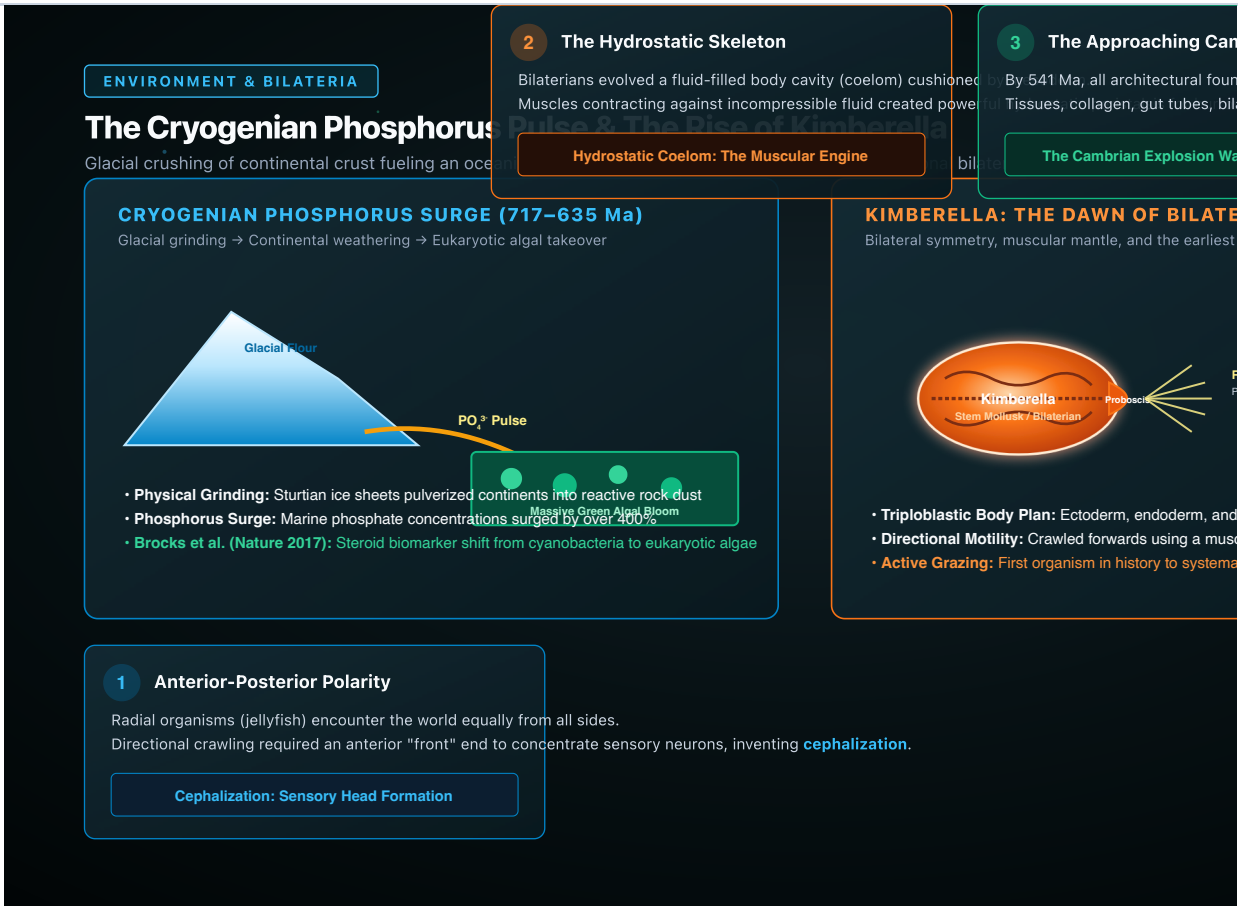


Figure 5.3: The Environmental Spark and Bilaterian Motility. Left: Sturtian and Marinoan Snowball Earth glaciers pulverized continental rocks, washing massive pulses of bioavailable phosphorus (PO_4^{3-}) into marine basins and fueling eukaryotic green algal blooms. Right: *Kimberella quadrata*, an early stem-bilaterian possessing a muscular foot, non-mineralized mantle, and a scratching radula that carved fan-shaped *Radulichnus* feeding traces into microbial mats.

3. The Environmental Spark and the Emergence of Bilateria

What environmental trigger unleashed this explosion of macroscopic animal life after billions of years of microbial stagnation?

The answer lies in the dramatic climatic convulsions of the preceding **Cryogenian Period** (720\text{–}635\text{ Ma}). During the Sturtian (717\text{–}660\text{ Ma}) and Marinoan (645\text{–}635\text{ Ma}) glaciations, continental ice sheets kilometers thick ground across global cratons like giant planetary rasp files. When the planet thawed in violent greenhouse super-warm spells, torrents of glacial meltwater washed thousands of cubic kilometers of pulverized mineral dust into shallow seas.

As demonstrated by Jochen Brocks and colleagues (2017), this continental weathering flushed a massive **Phosphorus Pulse** into the oceans. Bioavailable phosphate (PO_4^{3-}) is the primary limiting nutrient for marine primary productivity. The phosphorus deluge fueled an ecological revolution: ancient cyanobacteria were permanently supplanted by large, lipid-rich eukaryotic green algae. This massive expansion in primary productivity pumped atmospheric oxygen toward 10–20% of present levels, providing the metabolic fuel and collagen-synthesizing capacity demanded by macroscopic animal bodies.

In this enriched late Ediacaran ocean, the peaceful, immobile world of fractal fronds began to crack. Around **555 million years ago**, an extraordinary animal appeared: **Kimberella quadrata**.

Unlike immobile rangeomorphs, *Kimberella* was a committed **bilaterian**—an organism with clear anterior-posterior and dorsal-ventral axes. It possessed a tough, non-mineralized protective mantle, a muscular ventral foot for directional creeping, and an eversible snout equipped with paired tooth-like denticles. In fossil slabs, *Kimberella* is frequently preserved at the center of fan-shaped radiating scrape marks known as *Radulichnus*, created as it systematically rasped and harvested nutritious microbial mats.

Kimberella represents the evolutionary dawn of **triploblastic bilaterians**: organisms possessing three embryonic germ layers (ectoderm, mesoderm, endoderm), a hydrostatic coelom, and a nervous system concentrated at an anterior head (cephalization). The passive "Garden of Ediacara"—where life lay peacefully atop microbial slime—was drawing to a close.

Conclusion: The Agronomic Revolution and the Vanishing Garden

By **541 million years ago**, the tranquil Ediacaran world vanished in what paleontologists call the *Agronomic Revolution*. Newly evolved bilaterian worms began tunneling vertically into the seabed, burrowing through the sediment in search of buried organic matter.

This biological churning—**bioturbation**—shredded the impenetrable microbial mats that had stabilized seafloors for three billion years. As the mats disintegrated, the specialized anchorages and osmotrophic feeding mechanisms of the sessile Ediacaran fauna collapsed, precipitating their extinction.

In their place, mobile, burrowing, predatory bilaterians inherited the world. Armed with bilateral symmetry, through-guts, and Hox master developmental genes, they were on the brink of executing the most explosive evolutionary radiation in fossil history. In Part 6, we will enter the crucible of the Cambrian Explosion.

Key Academic Citations

- King, N., et al. (2008). The genome of the choanoflagellate *Monosiga brevicollis* and the origin of metazoans. *Nature*, 451(7180), 783–788.
- Bobrovskiy, I., et al. (2018). Ancient steroids establish the Ediacaran fossil *Dickinsonia* as one of the earliest animals. *Science*, 361(6408), 1246–1249.
- Narbonne, G. M. (2005). The Ediacara biota: Neoproterozoic origin of animals and their ecosystems. *Annual Review of Earth and Planetary Sciences*, 33, 421–442.
- Brocks, J. J., et al. (2017). The rise of algae in Cryogenian oceans and the emergence of animals. *Nature*, 548(7669), 578–581.
- Fedonkin, M. A., & Waggoner, B. M. (1997). The Late Precambrian fossil *Kimberella* is a mollusc-like bilaterian organism. *Nature*, 388(6645), 868–871.

Citation: Mahmud, S. (2026). "The Dawn of Multicellularity — Cell Adhesion, Morphogenesis, and the Ediacaran Garden." In The Evolutionary Odyssey, Part 5. https://shakilmahmud.com/evolutionary-odyssey-part-5-the-dawn-of-multicellularity/

Shakil Mahmud • Research Monograph

SHAKIL MAHMUD RESEARCH MONOGRAPHS • PART VI

The Cambrian Explosion — Hox Gene Toolkits, Hard Skeletons, and Predatory Arms Races

The Cambrian Explosion — Hox Gene Toolkits, Hard Skeletons, and Predatory Arms Races

1,497 words • November 1, 2026 • Permanent URI



Plate VI: *Figure: Apex predator Anomalocaris canadensis hunting in 508-million-year-old Cambrian Burgess Shale seas, propelled by undulating lateral lobes and grasping prey with spiny raptorial appendages alongside Olenoides trilobites.*

Fifty-four million years into the dawn of the Phanerozoic Eon, between 541 and 485 million years ago, the fossil record underwent an explosive transformation so sudden that it troubled Charles Darwin to the end of his life. In barely twenty million years—a fleeting heartbeat in geological time—virtually every major animal body plan (phylum) that inhabits modern Earth materialized out of apparent nowhere. From the deep-sea muds emerged armored trilobites viewing the world through stone lenses, segmented arthropods with crushing claws, swimming chordates with stiff notochords, and metre-long apex leviathans executing the first macroscopic predatory hunts in history.

1. The Evo-Devo Engine: Hox Genes and Spatial Colinearity

For more than a century after Darwin, paleontologists debated whether the Cambrian Explosion represented an explosion of life itself or merely an "explosion of fossils"—the sudden appearance of mineralized shells that preserved easily. The advent of evolutionary developmental biology (*Evo-Devo*) in the late 20th century provided the definitive genetic explanation: the Cambrian animals did not invent thousands of separate genetic blueprints; they inherited an ancient, pre-existing master operating system known as the **Homeobox (Hox) gene cluster**.

Hox genes encode master transcription factors equipped with a conserved 60-amino-acid DNA-binding domain called the *homeodomain*. The homeodomain's recognition α-helix inserts precisely into the major groove of target DNA, binding the core sequence \text{5′-TAAT-3′} to activate or repress batteries of hundreds of downstream structural genes.

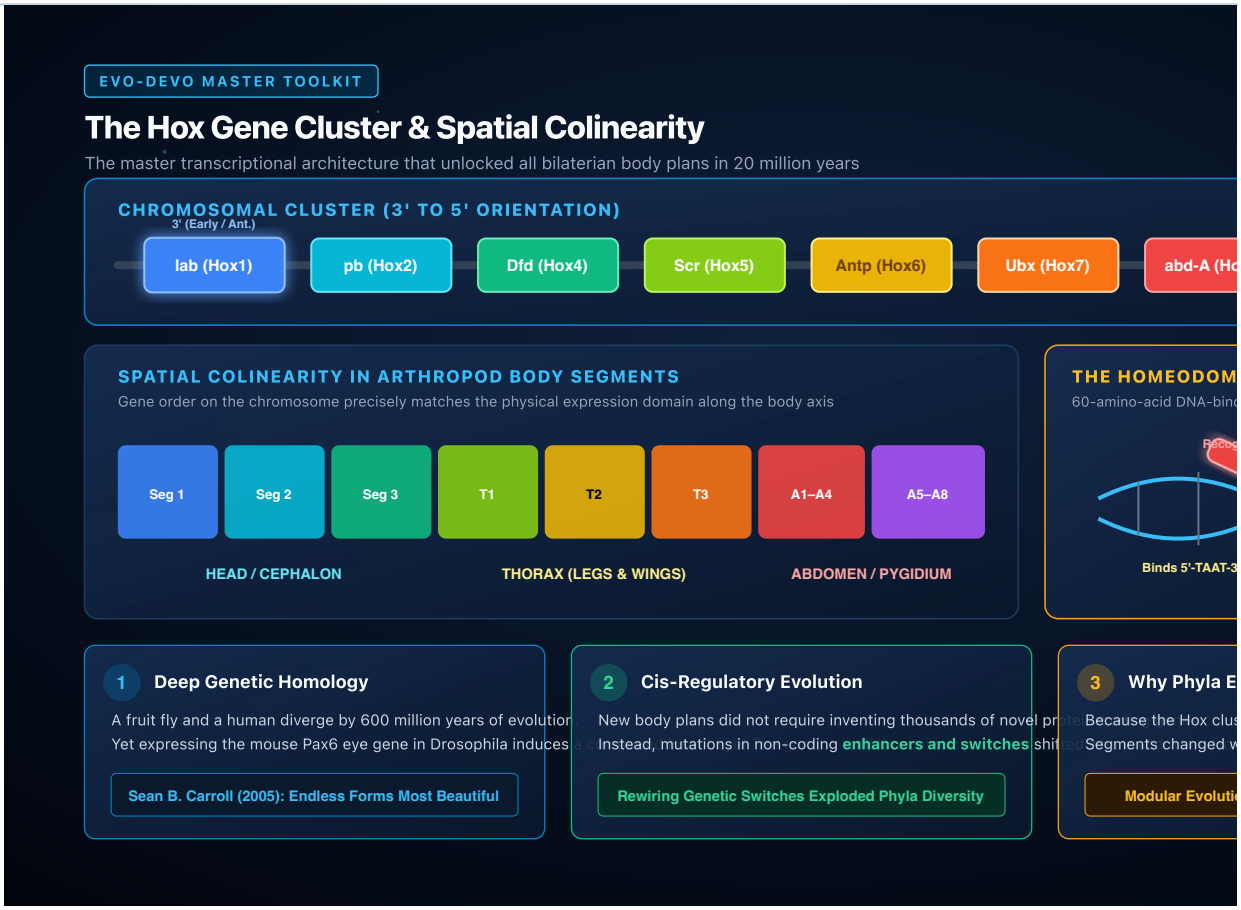


Figure 6.1: The Genomic Master Switchboard. Spatial and temporal colinearity of the bilaterian Hox cluster. The physical arrangement of genes on the chromosome (3′ \to 5’) precisely dictates their anterior-to-posterior expression domains along the developing embryo (head → thorax → abdomen). Inset: The 60-amino-acid homeodomain recognition helix inserting into the major groove of target DNA.

The organizing genius of the Hox cluster is the rule of **Spatial and Temporal Colinearity**, discovered by Edward B. Lewis (1995 Nobel Prize). The linear physical order of Hox genes along a chromosome directly mirrors their expression sequence along the animal's body axis:

- Genes at the 3’\text{-end} of the cluster (such as *labial* and *proboscipedia*) activate earliest in development and specify the anterior head structures.
- Genes in the middle of the cluster (*Deformed, Scr, Antennapedia, Ultrabithorax*) dictate the thoracic segments, directing the outgrowth of walking legs, claws, or antennae.
- Genes at the 5’\text{-end} (*abdominal-A, Abdominal-B*) turn on latest and establish the posterior abdominal segments and genital apparatus.

By dividing the bilaterian body into independent developmental compartments, the Hox cluster solved an insurmountable architectural problem. A mutation altering the limbs of a thoracic segment (such as transforming a walking leg into a grasping claw) could occur without causing fatal collateral disruptions to the adjacent head or digestive organs. This modularity enabled an exponential expansion into morphospace:

$$Y = aX^b \quad \Longrightarrow \quad \log Y = \log a + b \log X \quad \text{(Allometric Body Diversification)}$$

Natural selection did not need to invent new genes to create a crab, a millipede, or a chordate; it simply rewrote the non-coding cis-regulatory switches that controlled where and when these ancient Hox master genes turned on and off.

Shakil Mahmud • Research Monograph

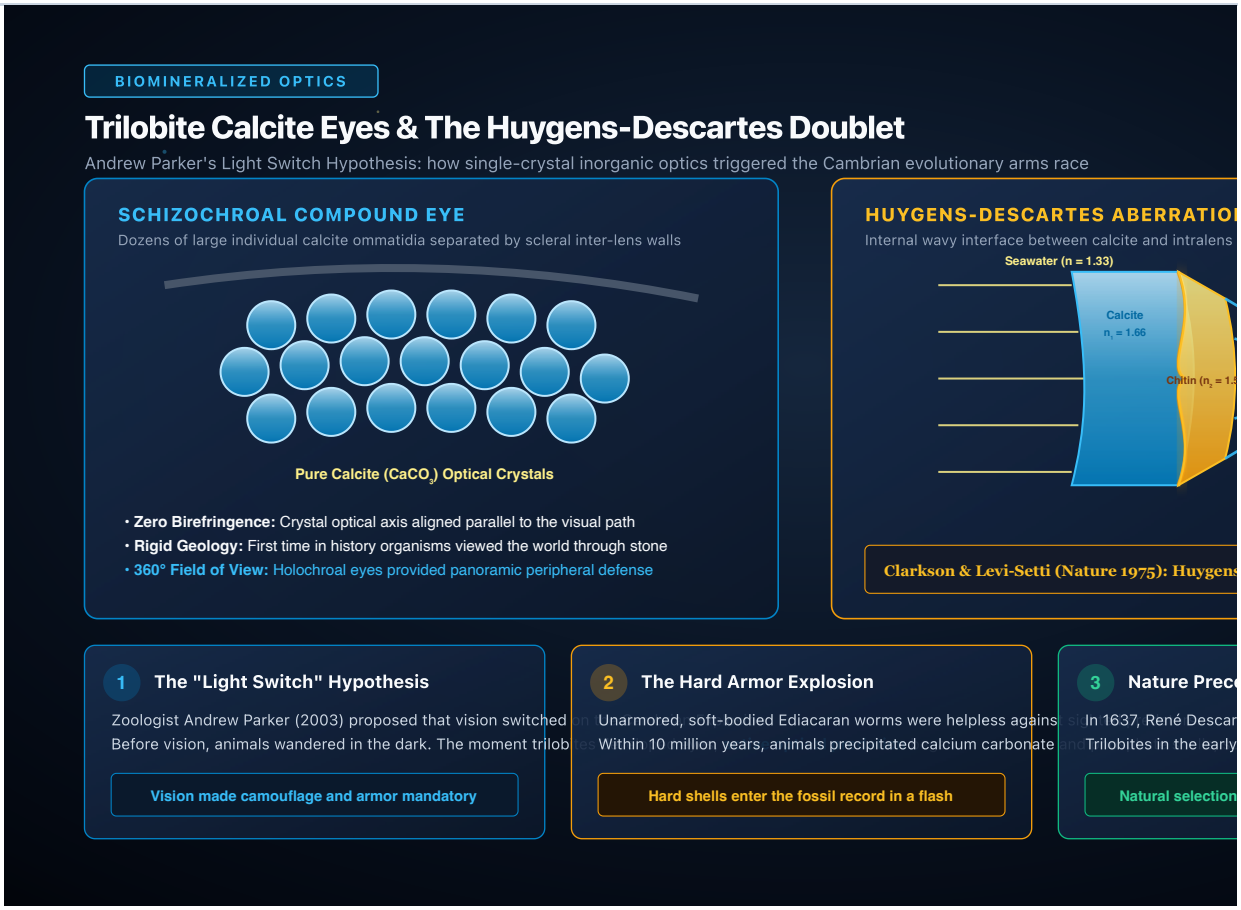


Figure 6.2: Biomineralized Optical Engineering. Left: Schizochroal compound eye of a phacopid trilobite consisting of individual rigid calcite ($CaCO_3$) crystal lenses. Right: Ray tracing through the Huygens-Descartes doublet lens. The wavy interface between upper calcite ($n_1 = 1.66$) and lower organic chitin ($n_2 = 1.53$) eliminates spherical aberration, focusing underwater light to a pinpoint focal point.

2. The Light Switch Hypothesis: Trilobites and Optical Calcite Lenses

While Hox genes provided the developmental engine, what provided the external ecological spark that ignited the explosion? In 2003, Oxford zoologist Andrew Parker proposed the **Light Switch Hypothesis**: the sudden emergence of the Cambrian fauna was triggered by the evolution of acute image-forming vision.

Before the Cambrian, the marine world was visually dark. Organisms possessed simple non-directional light-sensitive pigment spots, capable only of distinguishing day from night. Around **530 million years ago**, **Trilobites** achieved a biological and physical milestone: they evolved the first sophisticated compound eyes in animal history.

Because soft proteinaceous lenses decompose underwater, trilobites executed an unprecedented feat of biomineralization: their optical lenses were constructed from **pure, inorganic single-crystal calcite ($CaCO_3$)**. Calcite is an exceptionally rigid, clear mineral, but it possesses a severe optical flaw: *birefringence* (double refraction). Light entering an ordinary calcite crystal splits into two rays polarized at right angles, producing double, blurry ghost images. Trilobites eliminated this flaw with crystallographic precision: every single lens was grown with its optical axis oriented strictly parallel to the incoming light ray, reducing birefringence to zero!

Furthermore, early trilobite lenses suffered from *spherical aberration*: light entering the curved outer perimeter of a lens bends more sharply than light entering the center, blurring the image. In a classic 1975 *Nature* paper, Euan Clarkson and Riccardo Levi-Setti discovered that advanced phacopid trilobites solved this with a **Cartesian doublet lens**.

The upper lens was made of pure calcite ($n_1 = 1.66$); beneath it sat a lower lens of magnesium-rich chitinous material ($n_2 = 1.53$). The two layers met at a wavy, mathematically precise aspheric curve that exactly matched the optical equations derived by mathematicians René Descartes and Christiaan Huygens in the 17th century:

$$n_1 \sin \theta_1 = n_2 \sin \theta_2 \quad (\text{Snell’s Law of Refraction at the Cartesian Boundary})$$

Trilobites possessed 360-degree, aberration-free panoramic underwater vision 500 million years before humans invented calculus. The moment vision was switched on, darkness vanished. Predators could spot unarmored prey from meters away, and prey could spot approaching carnivores. Vision transformed the peaceful Ediacaran slime world into a lethal optical colosseum.

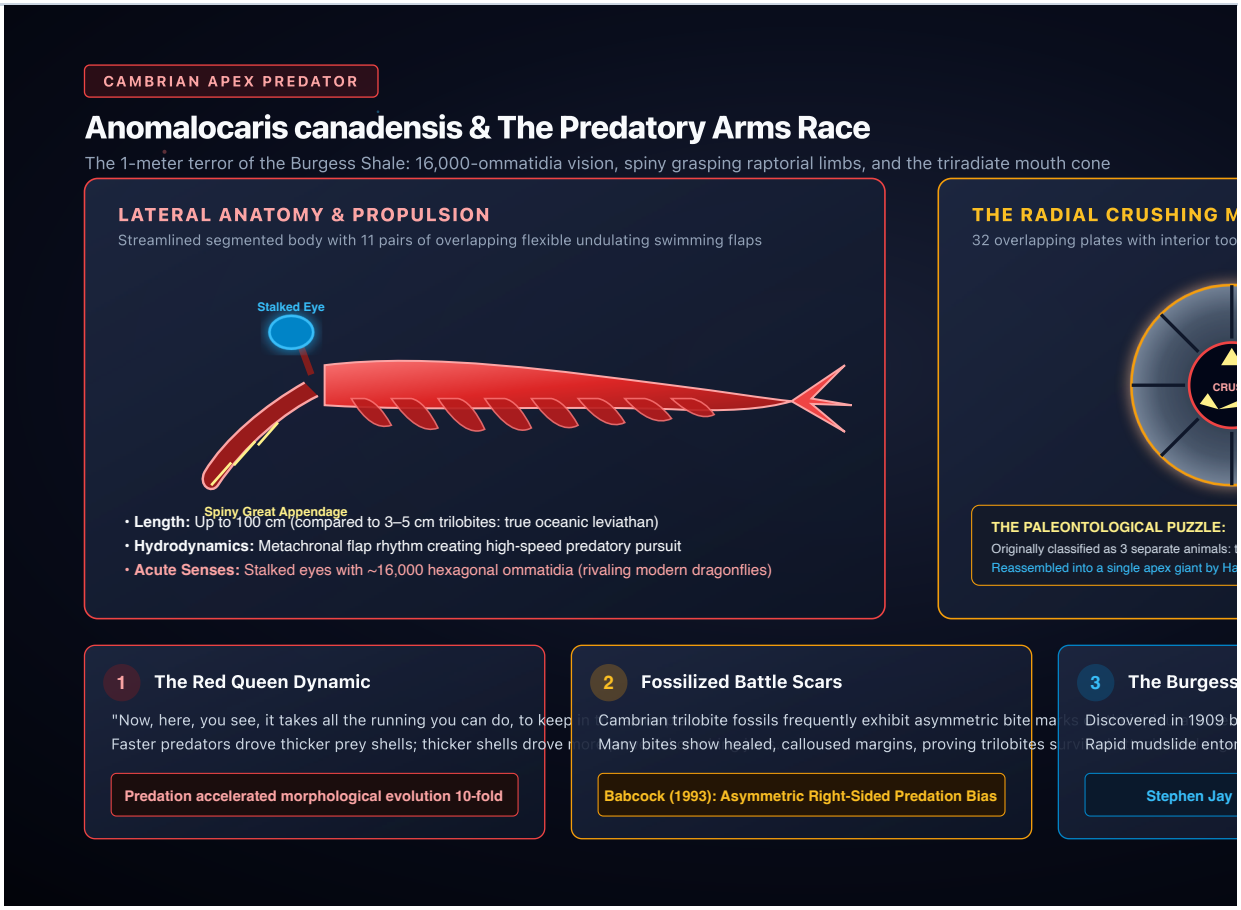


Figure 6.3: The Apex Terror of the Burgess Shale. *Anomalocaris canadensis*, a 1-meter stem-arthropod leviathan. Equipped with stalked compound eyes (16,000 ommatidia), flexible swimming lobes, and jointed spiny frontal appendages that shoved armored prey into its circular triradiate mouth cone composed of 32 crushing plates.

3. The Apex Predator and the Biomineralized Arms Race

Vision immediately ignited history's first **Red Queen predatory arms race**. The undisputed apex carnivore of the Cambrian seas was **Anomalocaris canadensis**, preserved with breathtaking soft-tissue fidelity in the 508-million-year-old Burgess Shale of British Columbia, Canada.

Reaching lengths of 60 to 100 cm, *Anomalocaris* was an oceanic titan in a world where typical creatures measured barely three centimeters. Its sleek, streamlined body was propelled by eleven pairs of overlapping lateral swimming flaps that undulated in metachronal waves. On its head perched two massive stalked compound eyes housing over **16,000 hexagonal ommatidia**—a visual resolution rivaling modern dragonflies.

To capture prey, *Anomalocaris* wielded a pair of segmented, spiny "great appendages" that could curl downward to seize skittering trilobites. It then shoved prey into its circular mouth cone—a radial nightmare composed of **32 overlapping chitinous plates** surrounding an inner ring of serrated teeth. By contracting these plates, *Anomalocaris* applied crushing, shearing mechanical forces that cracked defensive exoskeletons.

The fossilized evidence of this Cambrian arms race is etched directly into the rock. Paleontologist Loren Babcock (1993) documented extensive asymmetric bite scars on Cambrian trilobite fossils. Many trilobites show healed, calloused margins where their calcified carapaces were bitten through by an apex predator, survived the strike, and successfully molted and regenerated their mineral armor.

This predatory pressure unleashed an explosive cascade of natural selection:

1. **Hard Fortifications:** Soft-bodied organisms were systematically exterminated unless they armored themselves. In the span of a few million years, mollusks invented calcium carbonate shells, brachiopods secreted phosphatic valves, and arthropods developed hardened, jointed cuticles.
2. **Locomotive Breakthroughs:** Sluggish bottom-crawlers were replaced by streamlined swimming swimmers and deep-burrowing infaunal worms escaping into the sediment.
3. **Sensory Sophistication:** Antennae, chemical chemoreceptors, and statocysts (balance organs) evolved in rapid succession to detect predatory pressure waves.

Conclusion: The Architecture of the Modern Biosphere

By the close of the Cambrian Period at 485 million years ago, the foundations of the modern biosphere had been permanently established. The morphospace of animal architecture was fully staked out: Arthropoda, Mollusca, Annelida, Brachiopoda, Echinodermata, and Chordata all occupied distinct ecological niches.

Shakil Mahmud • Research Monograph

Yet swimming quietly in the shadows of the giant *Anomalocaris* was a tiny, translucent, five-centimeter creature that possessed no shell, no claws, and no mineralized armor: *Pikaia gracilens*. Inside its flexible body lay a simple, stiffened longitudinal rod—the notochord. In Part 7, we will follow this humble ribbon of flesh and witness the Chordate Dawn: the origin of the skull, the brain, and the human backbone.

Key Academic Citations

- Gould, S. J. (1989). *Wonderful Life: The Burgess Shale and the Nature of History*. W. W. Norton & Company.
- Parker, A. (2003). *In the Blink of an Eye: How Vision Sparked the Big Bang of Evolution*. Basic Books.
- Clarkson, E. N. K., & Levi-Setti, R. (1975). Trilobite eyes and the optics of Descartes and Huygens. *Nature*, 254(5502), 663–667.
- Whittington, H. B., & Briggs, D. E. (1985). The largest Cambrian animal, *Anomalocaris*, Burgess Shale, British Columbia. *Philosophical Transactions of the Royal Society B*, 309(1141), 569–609.
- Lewis, E. B. (1978). A gene complex controlling segmentation in Drosophila. *Nature*, 276(5688), 565–570.
- Carroll, S. B. (2005). *Endless Forms Most Beautiful: The New Science of Evo Devo*. W. W. Norton & Company.

Citation: Mahmud, S. (2026). "The Cambrian Explosion — Hox Gene Toolkits, Hard Skeletons, and Predatory Arms Races." In The Evolutionary Odyssey, Part 6. https://shakilmahmud.com/evolutionary-odyssey-part-6-the-cambrian-explosion/

SHAKIL MAHMUD RESEARCH MONOGRAPHS • PART VII

The Chordate Dawn — The Origin of the Backbone, Notochord, and Cranial Brain

The Chordate Dawn — The Origin of the Backbone, Notochord, and Cranial Brain

1,477 words • November 1, 2026 • Permanent URI



Plate VII: *Figure: The dawn of vertebrates: early Cambrian chordates Haikouichthys ercaicunensis and Pikaia gracilens swimming with a flexible dorsal notochord, V-shaped myomeres, and early cephalized eyes above ancient seafloor sponge fields.*

More than 525 million years ago, in the shadowed shallows of the Cambrian oceans, an unassuming ribbon of flesh scarcely longer than a human thumbnail embarked on one of the most consequential anatomical journeys in the history of life. Amidst a seabed dominated by armored arthropods and predatory priapulid worms, this creature possessed neither a mineral shell nor crushing jaws. Yet inside its body ran a flexible, fluid-filled rod of pressurized cells that would become the mechanical blueprint for every fish, amphibian, reptile, bird, and mammal that ever lived: the notochord. This is the story of Phylum Chordata and the developmental revolution that forged the vertebrate brain, face, and skeleton.

1. The Five Definitive Chordate Synapomorphies

To understand the evolutionary genesis of humanity, we must trace our lineage back to the deuterostome branch of bilaterian animals. While protostomes (such as arthropods, annelids, and mollusks) develop their mouth from the primary embryonic blastopore and position their main nerve cords ventrally along the belly, deuterostomes (chordates, hemichordates, and echinoderms) develop the blastopore into the anus, forming the mouth secondarily, and run their central nervous system along the dorsal spine.

Every member of our phylum—from the translucent marine lancelet (*Branchiostoma*) to modern *Homo sapiens*—is defined by five homologous anatomical innovations present at some stage of embryonic development:

Shakil Mahmud • Research Monograph

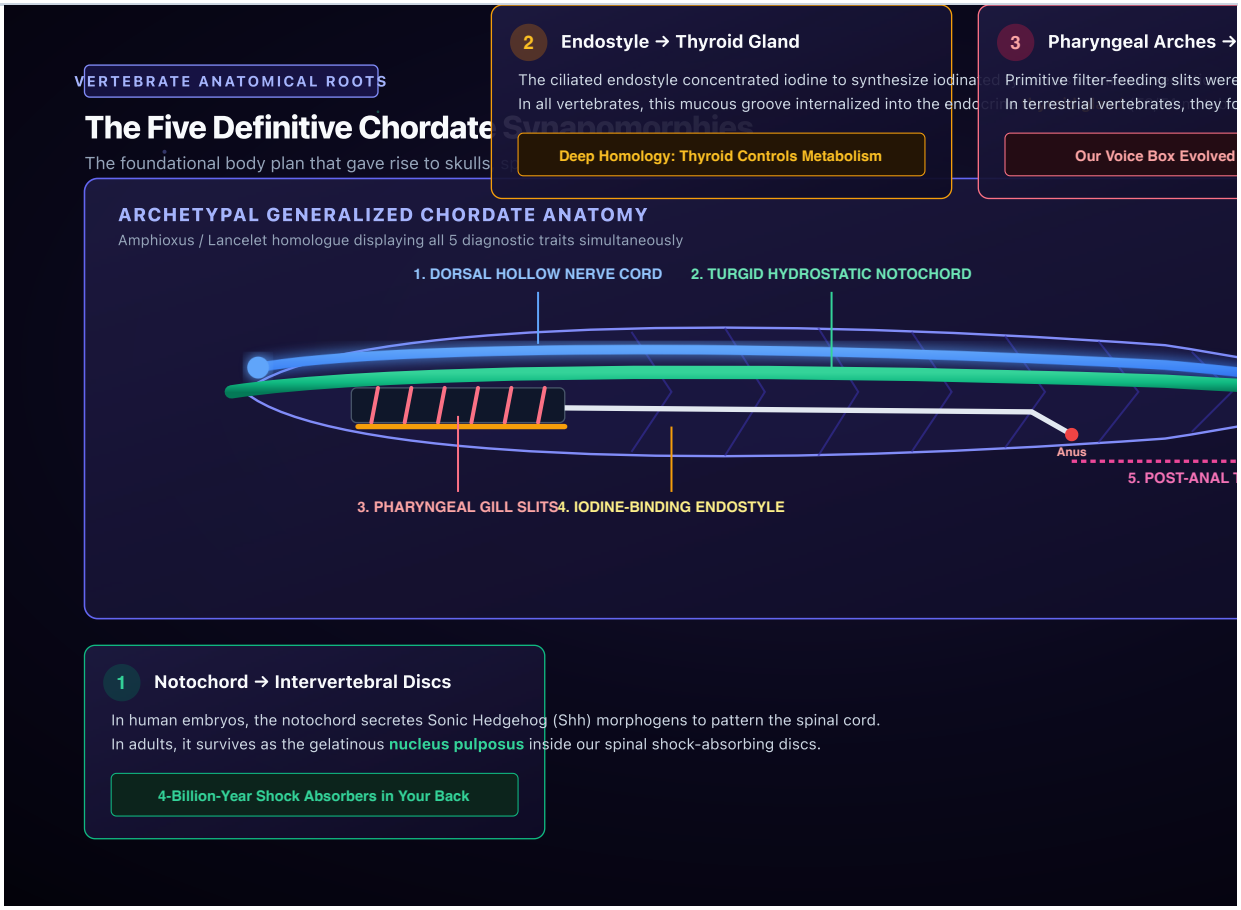


Figure 7.1: The Archetypal Chordate Body Plan. An anatomical cross-section demonstrating the five defining synapomorphies: (1) Dorsal hollow nerve cord, (2) Hydrostatic notochord, (3) Pharyngeal gill slits with internal branchial arches, (4) Iodine-concentrating endostyle (thyroid homologue), and (5) Muscular post-anal tail flanked by segmented V-shaped myomeres.

- **The Notochord:** A flexible, hydrostatic axial rod composed of vacuolated, glycoprotein-filled cells wrapped inside tightly woven collagenous sheaths. It prevents the body from shortening during lateral muscle contractions, translating lateral wave-like undulations into forward thrust. In adult humans, embryonic notochord remnants persist as the cushion-like *nucleus pulposus* within our intervertebral discs.
- **The Dorsal Hollow Nerve Cord:** Formed through primary neurulation by the invagination and folding of dorsal ectoderm. In non-chordate invertebrates, nerve cords are solid and ventral; in chordates, the dorsal cord envelops a fluid-filled neurocoel, which later enlarges anteriorly into the tripartite brain (prosencephalon, mesencephalon, and rhombencephalon).
- **Pharyngeal Slits / Clefts:** A series of bilateral lateral openings perforating the pharynx wall. Initially functioning as passive water-straining sieves for filter feeding, they transformed into gas-exchange gills in aquatic vertebrates and into Eustachian tubes, middle ear cavities, and parathyroid glands in land-dwelling tetrapods.
- **The Endostyle (Thyroid Precursor):** A ciliated, glandular groove along the ventral floor of the pharynx that secretes mucus to trap microscopic food particles. Critically, its cells concentrate environmental iodine to synthesize mono- and diiodotyrosine—marking it as the direct homologous evolutionary precursor to the vertebrate thyroid gland.
- **The Post-Anal Tail:** An active muscular elongation extending posterior to the digestive terminus (anus). Flanked by segmented, V-shaped or W-shaped myomeres, it transformed the posterior body into a dedicated locomotive hydrofoil.

2. Neural Crest Cells: The Developmental Miracle of the 'New Head'

While basal chordates like amphioxus possess the five foundational structures, they remain blind, brainless, and passive filter-feeders that lack a true skull, camera-style sensory eyes, or predatory teeth. What miraculous developmental leap converted sluggish mud-burrowers into active, hunting vertebrates?

In 1983, evolutionary morphologists Carl Gans and R. Glenn Northcutt formulated the groundbreaking **"New Head" Hypothesis**. They revealed that the vertebrate revolution was driven by the emergence of a transient, pluripotential population of migratory embryonic cells so unique they are universally recognized today as *the fourth germ layer*: the **Neural Crest Cells (NCCs)**.

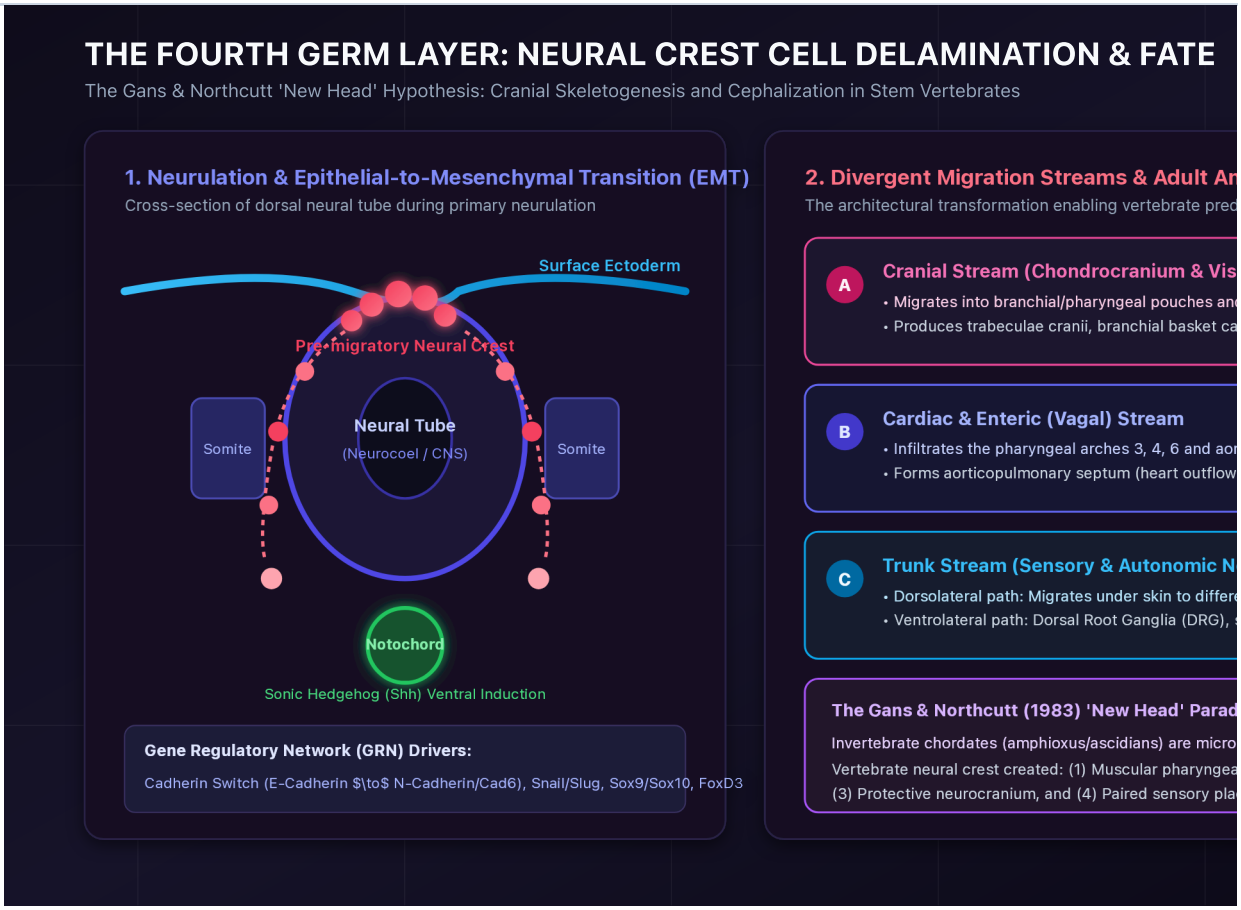


Figure 7.2: The Fourth Germ Layer. Left: Neurulation and Epithelial-to-Mesenchymal Transition (EMT) wherein dorsal neural fold cells lose cell adhesion (E-cadherin switch) and delaminate. Right: The three divergent migratory streams (cranial, cardiac, and trunk) generating the neurocranium, jaw precursors, aortic septum, sympathetic ganglia, and pigmentary melanocytes.

During early embryogenesis, as the neural plate folds to create the dorsal neural tube, cells at the neural plate border undergo an **Epithelial-to-Mesenchymal Transition (EMT)**. Governed by a conserved gene regulatory network—including transcription factors *Snail*, *Slug*, *Sox9*, *Sox10*, and *FoxD3*—these cells downregulate tight adhesion junctions (*E*-cadherin gives way to *N*-cadherin and cadherin-6), detach from the neuroepithelium, and embark on extensive migratory voyages throughout the embryo:

1. **Cranial Neural Crest:** Streams ventrally into the developing frontonasal prominence and pharyngeal arches. Unlike typical embryonic mesoderm, these cranial crest cells possess the remarkable capacity to form mineralized skeletal tissues—giving rise to the chondrocranium (cranial vault), trabeculae cranii, visceral jaw cartilages, sensory capsules around the eyes and ears, and dental odontoblasts that deposit dentine.
2. **Cardiac & Vagal Neural Crest:** Colonizes the pharyngeal pouches and the aortic outflow tract of the heart, orchestrating the formation of the spiral aorticopulmonary septum that divides arterial blood from venous return. It also seeds the entire enteric nervous system ("the second brain" within the gut wall).
3. **Trunk Neural Crest:** Migrates along two distinct routes:
    - *Dorsolateral pathway:* Infiltrates the epidermis to differentiate into melanocytes, granting vertebrates protective camouflage, sexual signaling, and UV shields.
    - *Ventrolateral pathway:* Penetrates through the anterior sclerotome to form the sensory Dorsal Root Ganglia (DRG), the sympathetic nervous chains, and the epinephrine-producing chromaffin cells of the adrenal medulla.

Without neural crest cells, vertebrates would have no skull to shield their expanding forebrain, no sensory capsules to focus stereoscopic vision and sound, no autonomic nervous system to orchestrate the flight-or-fight response, and no cartilaginous pharyngeal pump to replace sluggish cilia with high-volume, muscle-driven respiration.

3. The Fossil Record: Pikaia, Haikouichthys, and the Agnathans

The transition from invertebrate chordate to crown vertebrate is spectacularly documented across two of the world's most pristine Cambrian Lagerstätten: the 508-million-year-old Burgess Shale in British Columbia, Canada, and the 518-million-year-old Chengjiang Biota in Yunnan Province, China.

Shakil Mahmud • Research Monograph

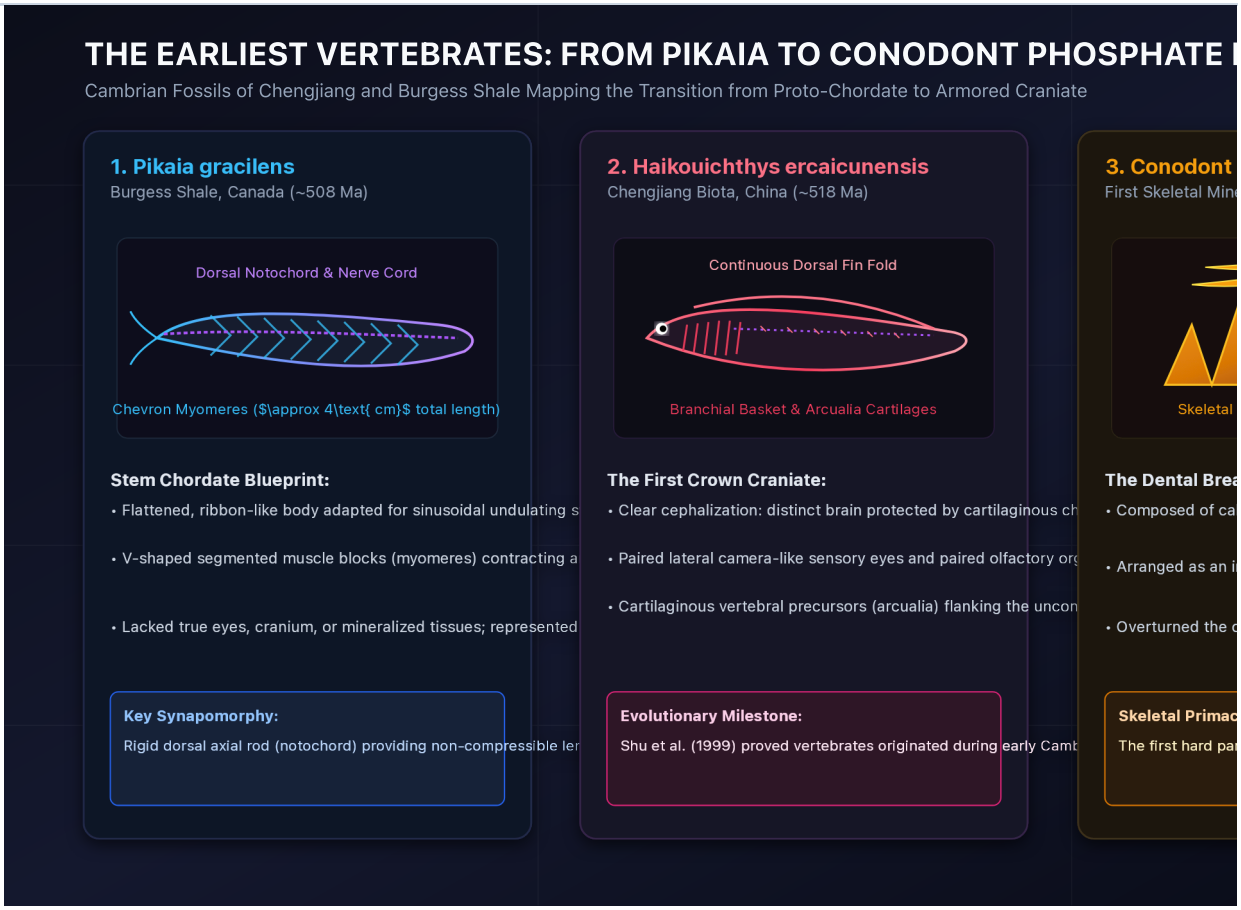


Figure 7.3: Deep Roots of the Vertebrate Lineage. Comparative anatomical profiles: (1) Pikaia gracilens showing primitive chevron myomeres and uncephalized head; (2) Haikouichthys ercaicunensis displaying true eyes, branchial basket, and cartilaginous proto-vertebrae (arcualia); (3) Conodont phosphatic feeding apparatus composed of hydroxyapatite, revealing the dental primacy of skeletal evolution.

Pikaia gracilens: The Proto-Chordate Prototype

Discovered by Charles Walcott in 1911 and re-analyzed in groundbreaking detail by Simon Conway Morris and Jean-Bernard Caron in 2012, *Pikaia gracilens* was a 4-centimetre-long, laterally flattened swimmer. It possessed a dorsal notochord extending almost to the anterior tip, approximately 100 distinct zigzagging muscle blocks (myomeres), and a dorsal blood vessel. However, *Pikaia* lacked a distinct head, eyes, and mineralized tissues, representing a stem chordate grade closely allied with living cephalochordates.

Haikouichthys ercaicunensis: The First True Craniate

Unearthed in the slightly older Chengjiang shales of Yunnan by Chinese paleontologist Shu Degan and colleagues in 1999, *Haikouichthys ercaicunensis* pushed the origin of true vertebrates back 518 million years—deep into the early Cambrian. Unlike *Pikaia*, *Haikouichthys* is an unambiguous craniate:

- It possessed a distinct cartilaginous head capsule housing a lobed anterior brain.
- It featured prominent paired lateral eyes and olfactory or otic sensory capsules.
- It displayed six to nine pairs of gill pouches supported by a branchial basket.
- Crucially, flanking its flexible notochord were microscopic repeated cartilaginous elements called **arcualia**—the evolutionary precursors to neural arches and vertebral segments.

Haikouichthys and its contemporary relative *Myllokunmingia* demonstrate that active, cephalized vertebrates armed with sensory optics and proto-vertebrae had already evolved alongside monstrous predators like *Anomalocaris*, playing an active locomotive role in the Cambrian explosion.

4. The Conodont Secret: Teeth Before Armor

For more than a century, an enduring dogma of vertebrate paleontology held that our internal mineralized skeleton evolved first as protective dermal armor—thick, bony plates encasing the exterior of jawless fish (ostracoderms) to shield them from giant predatory sea scorpions (eurypterids).

This "Armor First" hypothesis was decisively demolished by microscopic, amber-colored fossils known as **conodonts**. Ranging in size from 0.1 mm to several millimeters, conodont elements were discovered in vast quantities in marine strata from the Late Cambrian through the Triassic ($500\text{–}200\text{ Ma}$), but their biological identity remained an absolute enigma for over 130 years.

In 1983, a complete soft-bodied conodont animal was finally discovered in Carboniferous rocks near Edinburgh, Scotland. It was a slender, eel-like chordate equipped with a notochord, chevron myomeres, and giant camera eyes. At the front of its throat lay the famous conodont elements: an intricate, multi-component feeding apparatus consisting of delicate, needle-like grasping elements (S and M elements) and crushing, comb-like shearing plates (P elements).

High-resolution crystallographic and histological analysis revealed the stunning reality: conodont elements are composed of genuine biomineralized **calcium phosphate / hydroxyapatite**:

$$Ca_5(PO_4)_3(OH)$$

Their microstructure displays enamel-like crowns and cellular dentine-like bases, showing clear microscopic wear facets from grinding, grasping, and slicing soft-bodied prey.

The evolutionary implication is profound: **vertebrates invented biomineralized skeletal tissues not to defend themselves against predators, but to bite, slice, and hunt.** Dental tissue preceded skeletal bone armor. Armed with a flexible notochord, a neural-crest-derived sensory skull, and phosphate slicing tools, the stage was set for our aquatic ancestors to take over the world's oceans—setting the stage for the invention of the true, articulated jaw.

Citation: Mahmud, S. (2026). "The Chordate Dawn — The Origin of the Backbone, Notochord, and Cranial Brain." In The Evolutionary Odyssey, Part 7. https://shakilmahmud.com/evolutionary-odyssey-part-7-the-chordate-dawn/

Shakil Mahmud • Research Monograph

SHAKIL MAHMUD RESEARCH MONOGRAPHS • PART VIII

The Conquest of the Depths — The Origin of Jaws and the Age of Armored Placoderms

The Conquest of the Depths — The Origin of Jaws and the Age of Armored Placoderms

1,492 words • November 1, 2026 • Permanent URI

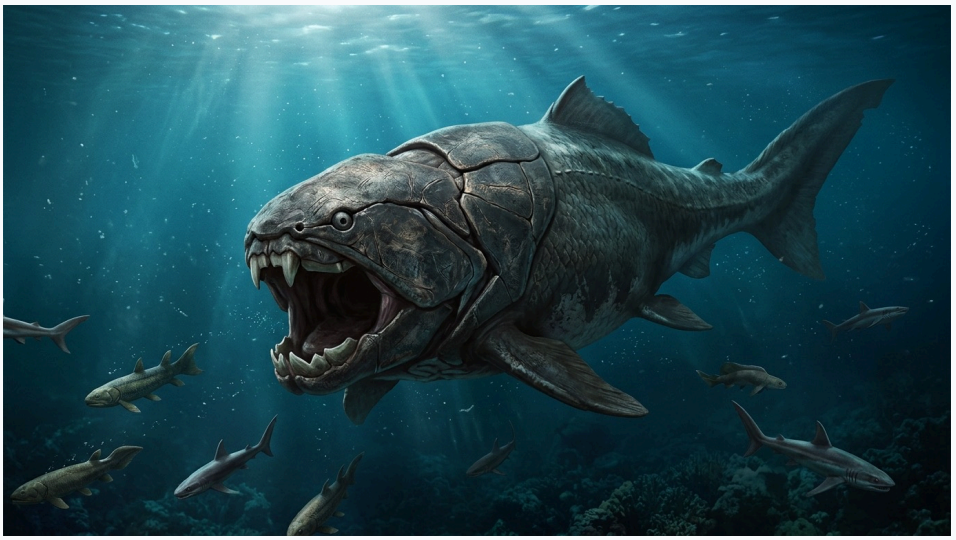


Plate VIII: *Figure: The apex Devonian placoderm predator Dunkleosteus terrelli (~380 Ma), lunging through the water column with its heavily armored cranial-thoracic shield and shearing gnathostome jaw blades.*

For more than one hundred million years after the first chordates undulated through Cambrian waters, vertebrates remained modest, bottom-dwelling mud-suckers confined to the lower tiers of the oceanic food pyramid. Giant sea scorpions (eurypterids) and shelled cephalopods ruled the Silurian seas. But between 440 and 380 million years ago, an astonishing morphological transformation re-engineered the front of the vertebrate gut into the most lethal anatomical weapon in biological history: the articulated jaw. With this single innovation, the Devonian Period exploded into the "Age of Fishes," unleashing nine-metre armored apex predators like *Dunkleosteus* and bifurcating our aquatic ancestors into ray-finned swimmers and the lobe-finned pioneers destined to walk upon land.

1. The Respiratory Origins of Jaws: Homology of Branchial Arches

For decades, popular imagination assumed that jaws arose directly through selection for biting and predation. However, comparative embryology and functional morphology revealed an even more elegant evolutionary truth: our jaws did not evolve for eating—they evolved for breathing.

In basal jawless fishes (agnathans), the pharynx is supported by a series of repeating, cartilaginous **visceral branchial arches** (labeled 1 through 7) that keep the gill slits open. As these animals developed higher metabolic rates, relying on passive water flow across the gills became insufficient. In 1996, anatomist John Mallatt demonstrated that the anterior-most branchial arch (Arch 1) underwent massive muscularization to act as a high-powered **ventilatory pump**, forcefully expanding and contracting to flush oxygenated water across the downstream gills.

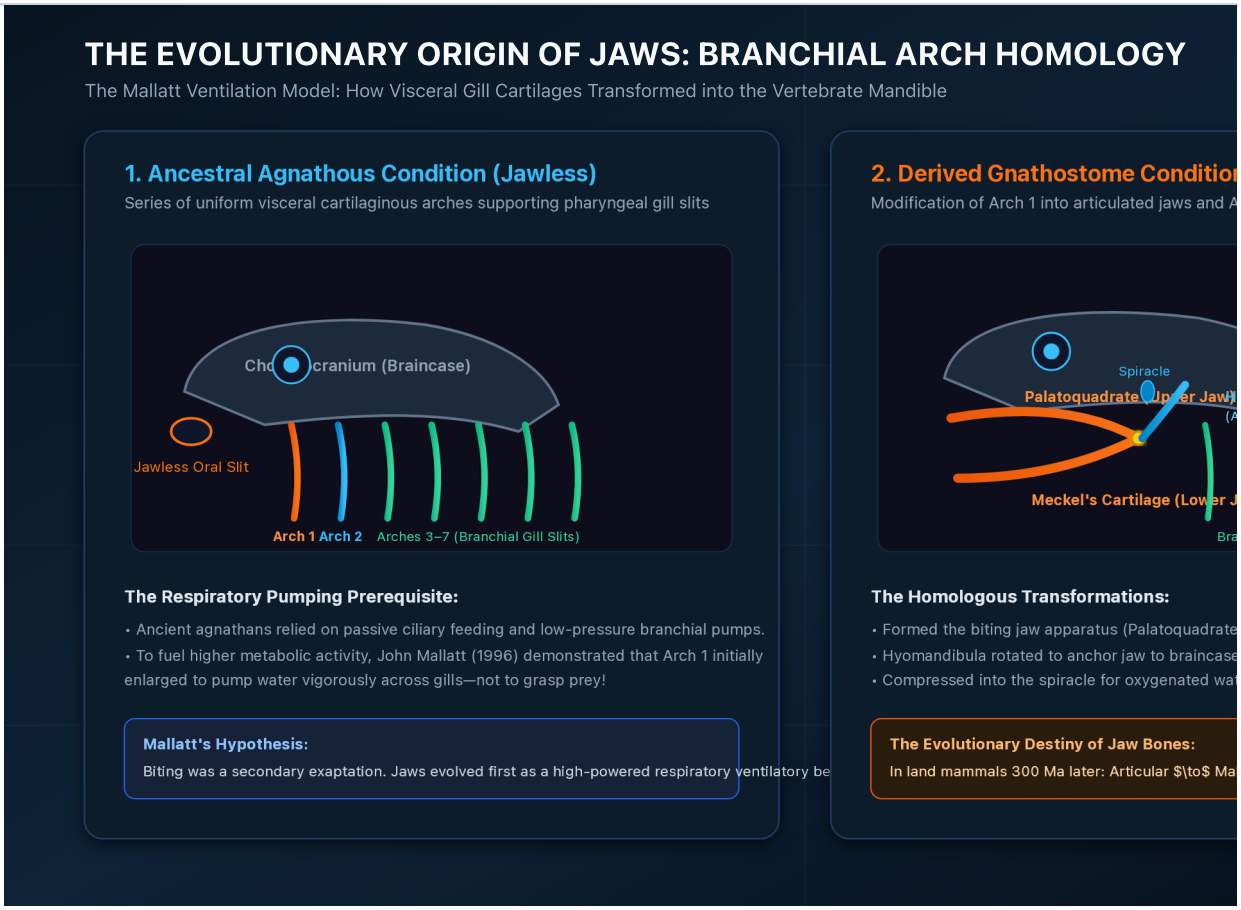


Figure 8.1: Homological Transformation of the Pharyngeal Skeleton. Left: The ancestral agnathan blueprint showing seven uniform visceral branchial arches. Right: The derived gnathostome condition, where Arch 1 bends to form the palatoquadrate (upper jaw) and Meckel's cartilage (lower jaw), Arch 2 forms the hyomandibula suspension strut, and Gill Slit 1 reduces into the spiracle.

Once this powerful muscular hinge existed for respiratory pumping, natural selection swiftly co-opted it for grasping prey—a classic evolutionary *exaptation*. The precise morphological remodeling unfolded in three distinct steps:

1. **The Mandibular Arch (Arch 1):** Folded forward and enlarged dramatically. Its dorsal half ossified into the **palatoquadrate cartilage** (the primary upper jaw, fusing to the neurocranium), while its ventral half formed **Meckel's cartilage** (the structural core of the lower jaw/mandible).
2. **The Hyoid Arch (Arch 2):** Rotated anteriorly to serve as an architectural anchor. Its dorsal element, the **hyomandibula**, functioned as an articulated brace wedged between the otic capsule of the braincase and the mandibular joint (a suspension mechanism known as *hyostyly*).
3. **Reduction to the Spiracle:** The original first pharyngeal gill slit between Arch 1 and Arch 2 was compressed into a dorsal accessory respiratory opening called the **spiracle** (still visible today behind the eyes of rays and sharks), allowing bottom-dwelling bottom-feeders to inhale clean water while buried in sediment.

> ***The Deep Homological Echo:*** *In one of evolution's most poetic transformations, when the synapsid ancestors of mammals remodeled their jaw joint 300 million years later, Meckel's articular bone transformed into our middle ear malleus (hammer), the palatoquadrate's quadrate bone became our incus (anvil), and the hyomandibula became our stapes (stirrup). Every time you hear music, you are listening through the repurposed gill arches of a Silurian fish!*

2. Biomechanics of Dunkleosteus: The Four-Bar Linkage Monster

Armed with jaws, gnathostomes radiated into diverse lineages during the Devonian Period, none more terrifying than the **Placoderms**—armored fishes encased in massive bony thoracic shields. The undisputed apex titan of this era was *Dunkleosteus terrelli*, a monstrous predator reaching up to 9 metres in length and weighing over 4 metric tons.

Unlike modern sharks or bony fishes, *Dunkleosteus* possessed no true teeth rooted in enamel. Instead, its jaws were armed with self-sharpening, serrated dermal bone plates: the upper *superognathal* and lower *inferognathal* bones. Histological cross-sections reveal that these gnathal plates constantly sheared past each other during closure, utilizing abrasive friction to hone their cutting edges into razor-sharp scythes.

Shakil Mahmud • Research Monograph

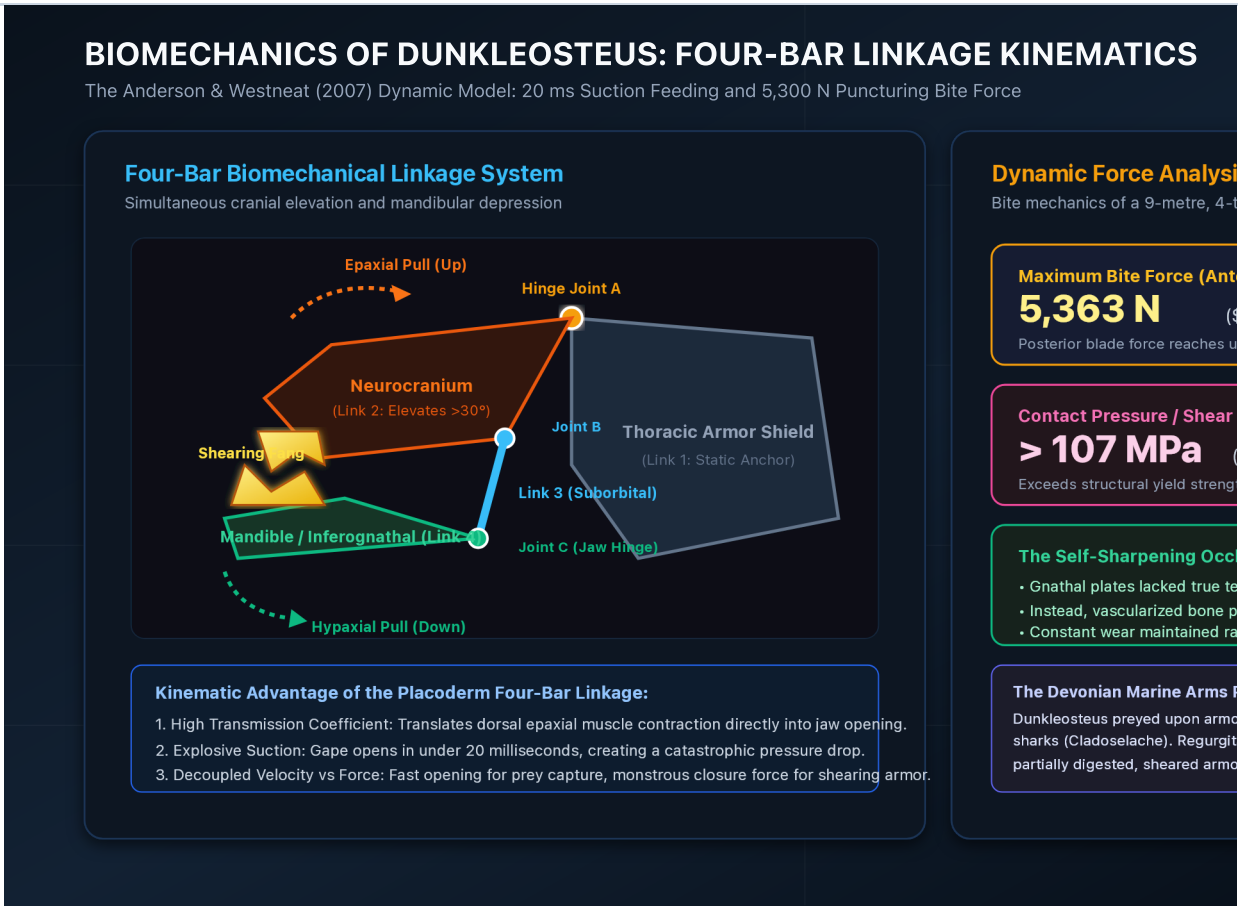


Figure 8.2: The Mechanical Engineering of Dunkleosteus terrelli. Left: The kinematic four-bar linkage model (Anderson & Westneat, 2007) showing how dorsal epaxial muscle contraction elevated the neurocranium while simultaneously depressing the lower jaw via the suborbital link. Right: Force metrics revealing a staggering 5,363 N puncturing force and contact stresses exceeding 107 MPa.

In 2007, biomechanical paleontologists Philip Anderson and Mark Westneat constructed a dynamic kinematic computer model of the *Dunkleosteus* skull, revealing that its jaw operated via a sophisticated **planar four-bar mechanical linkage**:

- **Link 1 (Fixed Base):** The massive dorsal thoracic armor shield.
- **Link 2 (Driver):** The neurocranium / head shield, hinged to the thoracic shield via bilateral ball-and-socket joints (Joint A). When massive dorsal epaxial muscles contracted, the entire head rotated upward by more than 30°.
- **Link 3 (Transmission):** The rigid suborbital plate connecting the skull to the lower jaw.
- **Link 4 (Output):** The inferognathal lower jaw, which depressed downward in synchronization with cranial elevation.

This four-bar linkage gave *Dunkleosteus* a dual mechanical superpower. In the opening phase, the system exhibited an extremely high velocity transmission coefficient: the monstrous mouth snapped open in less than **20 milliseconds** (0.02 seconds), generating a catastrophic suction vacuum that pulled large fish and cephalopods directly into its maw.

In the closing phase, the linkage converted the mechanical leverage of immense jaw adductor muscles into staggering crushing power:

$$F_{\text{bite}} \approx 5,363 \text{ N} \quad (\approx 1,200 \text{ lbs of force})$$

Because this monstrous force was concentrated upon the tiny contact area ($A \approx 0.5 \text{ cm}^2$) of the anterior fangs, the puncturing pressure reached astronomical levels:

$$P = \frac{F}{A} > 107\text{ MPa} \quad (\approx 15,500\text{ psi})$$

This contact pressure exceeded the structural yield strength of hardened steel and enabled *Dunkleosteus* to shatter through the thickest dermal bone plates of competing placoderms and primitive sharks like *Cladoselache* with effortless ease.

3. The Great Bifurcation: Ray-Fins (Actinopterygii) vs. Lobe-Fins (Sarcopterygii)

While placoderms dominated the open seas, another group of jawed vertebrates—the **Osteichthyes** (bony fishes)—underwent a fundamental phylogenetic divergence that would forever divide vertebrate destiny. Sometime in the Late Silurian, bony fishes split into two distinct subclasses based on the internal skeletal architecture of their fins:

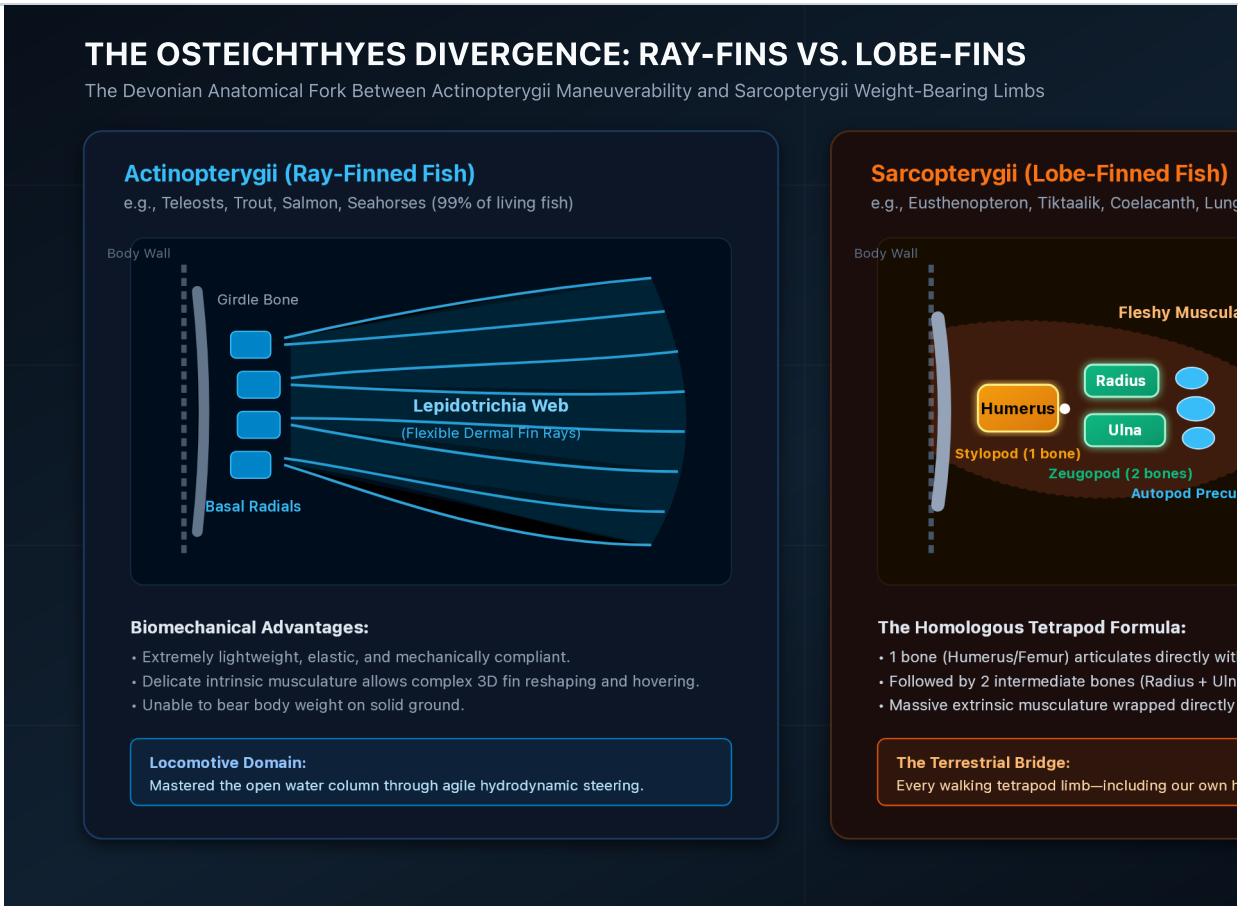


Figure 8.3: The Skeletal Crossroads of Osteichthyes. Left: Actinopterygian (ray-finned) architecture with internalized basal radials and a flexible fan of dermal lepidotrichia rays. Right: Sarcopterygian (lobe-finned) monobasic architecture with a fleshy muscular lobe wrapped around internal endochondral bones homologous to the tetrapod limb: humerus, radius, and ulna.

Subclass Actinopterygii: The Masters of Hydrodynamics

The ray-finned fishes confined their skeletal support bones (basal radials) entirely inside the body wall. The projecting fin itself is supported by an array of parallel, segmented, bony lepidotrichia (dermal fin rays) connected by delicate elastic webbing. This design is mechanically compliant, ultra-lightweight, and capable of undulating 3D curvature, granting ray-finned fishes unmatched maneuverability and acceleration. Today, Actinopterygii encompasses over 30,000 species—accounting for 99% of all living fish on Earth.

Subclass Sarcopterygii: The Architects of Walking

In contrast, the lobe-finned fishes adopted a radically different structural design. Instead of an internal fan of radials, their fin projected outward from the flank as a robust, fleshy muscular stalk supported by an internal, articulated chain of endochondral bones:

- **The Monobasic Articulation:** A single large proximal bone articulated directly with the pectoral girdle: the **Humerus** (or Femur in the pelvic fin).
- **The Intermediate Zeugopod:** The humerus articulated with two distal companion bones: the **Radius** and **Ulna** (or Tibia and Fibula).
- **Extrinsic Musculature:** Massive propulsive muscles wrapped directly around this axial bony core outside the main torso wall.

To an animal living in open pelagic water, a heavy, muscular lobe-fin was hydrodynamically inefficient compared to the feather-light ray-fin. But in the choked, weed-choked shallows of Devonian swamps and braided river deltas, the sarcopterygian lobe-fin was an extraordinary mechanical advantage. It allowed fish like *Eusthenopteron* and *Panderichthys* to prop themselves up on the riverbed, clamber over submerged logs, and crawl between evaporating pools.

4. The Lungs That Preceded Land: The Swim Bladder Story

A widespread misconception is that lungs evolved when vertebrates crawled onto land. In reality, molecular phylogenetics and paleontology prove the exact opposite: **lungs evolved in water millions of years before any vertebrate set foot on land.**

During the warm, sluggish Devonian greenhouse climate, stagnant freshwater riverbeds regularly experienced catastrophic oxygen depletion (hypoxia). Fish relying solely on gills suffocated. To survive, basal osteichthyans evolved vascularized outpocketings of the ventral esophagus. By gulping air at the water's surface, oxygen diffused directly into the rich capillary beds of these primitive ventral sacs—the ancestral **lungs**.

Later in evolution, when the ancestors of ray-finned fishes colonized deep, oxygen-rich marine waters, they no longer needed aerial respiration. Their ventral lungs shifted dorsally and lost their respiratory function, transforming into the hydrostatic **swim bladder**—a gas-filled buoyancy organ that allows fish to maintain neutral buoyancy at any depth without expending swimming energy.

Shakil Mahmud • Research Monograph

Meanwhile, our sarcopterygian ancestors retained their paired vascular lungs alongside their weight-bearing lobe-fins. By the end of the Devonian, armed with internal humerus-radius-ulna arm bones, sensory spiracles, and air-breathing lungs, a daring lineage of lobe-finned fish was mechanically pre-adapted to conquer the continents. The stage was set for the greatest invasion in Earth history: the water-to-land transition.

Citation: Mahmud, S. (2026). "The Conquest of the Depths — The Origin of Jaws and the Age of Armored Placoderms." In The Evolutionary Odyssey, Part 8. https://shakilmahmud.com/evolutionary-odyssey-part-8-the-age-of-fishes-and-jaw-evolution/

SHAKIL MAHMUD RESEARCH MONOGRAPHS • PART IX

The Water-to-Land Transition — The Anatomy of Sarcopterygian Tetrapodomorphs

The Water-to-Land Transition — The Anatomy of Sarcopterygian Tetrapodomorphs

1,369 words • November 1, 2026 • Permanent URI



Plate IX: *Figure: Transitional sarcopterygian tetrapodomorph Tiktaalik roseae (~375 Ma) hauling itself onto a muddy Late Devonian riverbank, showcasing weight-bearing wrist joints, upward-facing eyes, and a mobile neck distinct from ancestral fish.*

Three hundred and seventy-five million years ago, the edge of the world lay not in the deep open pelagic abyss, but along the sluggish, sun-baked margins of tropical floodplains and braided river deltas. Here, the boundary between water and land was an ambiguous tangle of mudbanks, decomposing vascular plants, and evaporating oxbow lakes. Fish that could only swim were trapped to die as water evaporated or became lethally anoxic. But one adventurous lineage of lobe-finned sarcopterygian fish—the tetrapodomorphs—underwent an anatomical transformation that would rewrite the destiny of vertebrate life: they transformed their fins into weight-bearing walking limbs, disconnected their skulls to invent the first flexible neck, and rewired their sensory systems to perceive the terrestrial realm.

1. The Homologous Tetrapod Limb Archetype: Stylopod, Zeugopod, and Autopod

Every four-limbed vertebrate alive today—from a leaping tree frog to a galloping cheetah, from a soaring hawk's wing to the human hand typing these words—shares an identical, deeply conserved architectural blueprint: the tripartite tetrapod limb.

Comparative anatomy and developmental genetics reveal that this formula was not invented from scratch on land. Instead, it represents the step-by-step modularization of the internal endochondral skeleton of Devonian lobe-finned fish, progressing through three sequential developmental zones along the proximodistal axis:

Shakil Mahmud • Research Monograph

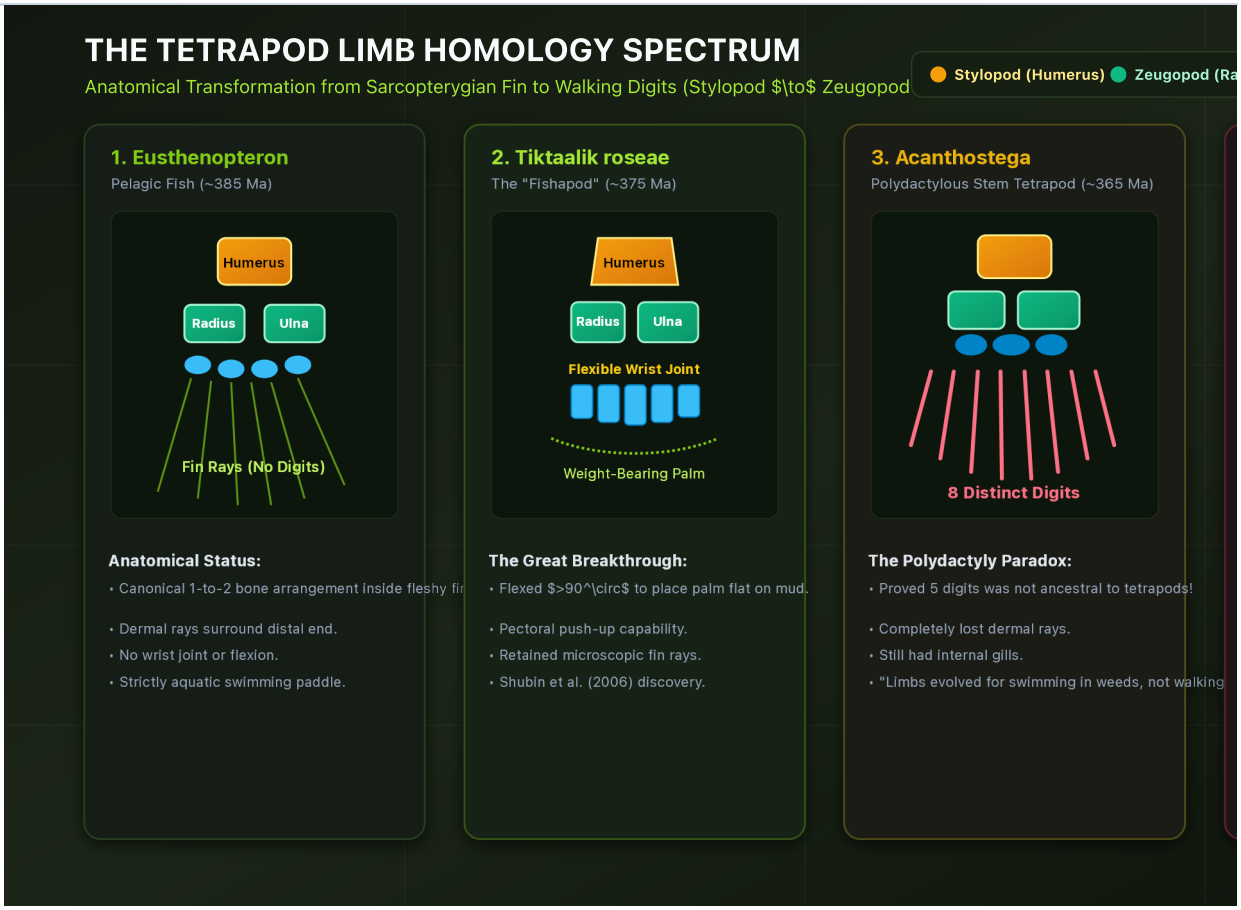


Figure 9.1: The Macroevolutionary Assembly of the Tetrapod Limb. The transition across four evolutionary stages: (1) Eusthenopteron showing internal humerus and paired radius/ulna flanked by dermal rays; (2) Tiktaalik roseae demonstrating the first flexing wrist joint and weight-bearing palm; (3) Acanthostega displaying true digits arranged in an ancestral 8-digit polydactylous paddle; (4) Crown Tetrapod stabilizing the canonical pentadactylous (5-digit) terrestrial limb.

1. **The Stylopod (One Bone):** The proximal segment consisting of a single massive endochondral bone that articulates directly with the shoulder or pelvic girdle: the **Humerus** in the forelimb, or the **Femur** in the hindlimb. In fish like *Eusthenopteron*, the humerus possessed massive ventral ridges and entepicondylar crests where powerful propulsive muscles anchored.
2. **The Zeugopod (Two Bones):** The intermediate segment articulating distally with the humerus: the **Radius** (axial) and **Ulna** (postaxial) in the forelimb, and the **Tibia** and **Fibula** in the hindlimb. This dual-bone arrangement provided rotational stability and mechanical resistance against torsional shearing stresses when propping the torso up on the ground.
3. **The Autopod (Many Bones):** The distal-most segment, encompassing the wrist/ankle bones (carpals/tarsals), palm/foot rods (metacarpals/metatarsals), and articulated finger/toe segments (phalanges). This region represents the most dramatic evolutionary novelty, governed by a secondary late-phase pulse of *HoxA* and *HoxD* gene expression that bent the main embryonic skeletal axis anteriorly to sprout walking digits.

2. The Tiktaalik roseae Breakthrough: The First Neck and Wrist

In 2004, on the desolate, frozen cliffs of Ellesmere Island in Nunavut, Canadian Arctic, paleontologists Neil Shubin, Edward Daeschler, and Farish Jenkins made one of the most celebrated fossil discoveries in the history of science: *Tiktaalik roseae* (popularly known as the "Fishapod"), dating precisely to 375 million years ago.

Tiktaalik sat exactly in the morphological gap between pelagic lobe-finned fish like *Panderichthys* and early four-limbed amphibians like *Acanthostega*. While it retained primitive fish traits—such as microscopic scales, swimming fin rays, and functional internal gills—it showcased two unprecedented anatomical breakthroughs that solved the mechanical challenges of living in shallows:

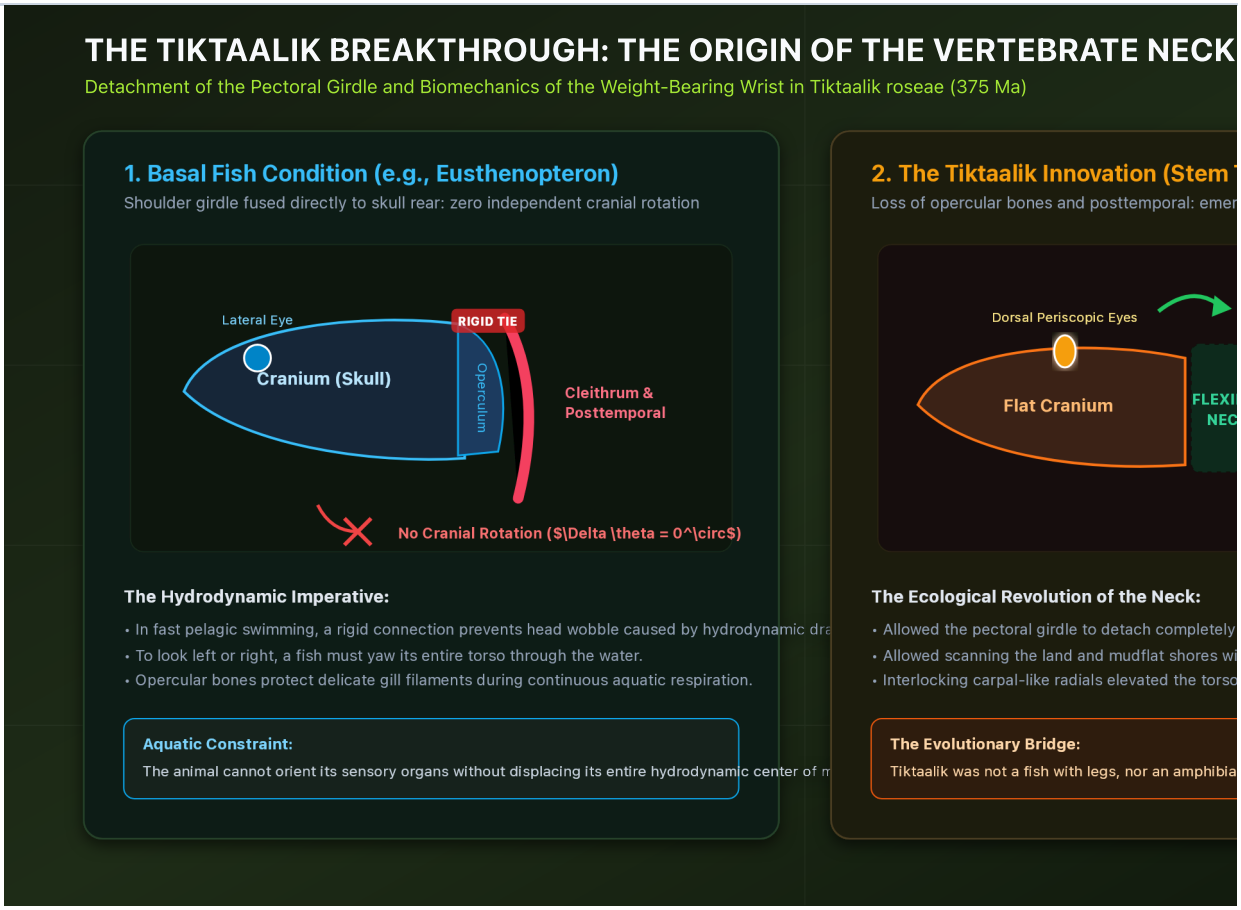


Figure 9.2: The Mechanical Inventions of Tiktaalik roseae. Left: The ancestral fish condition where the pectoral girdle (cleithrum/posttemporal) is rigidly locked to the skull, forbidding independent head movement. Right: The Tiktaalik breakthrough—loss of opercular and posttemporal bones creates a flexible neck, allowing 35° independent cranial rotation, paired with dorsally placed eyes and a push-up capable flexing wrist.

The Detachment of the Pectoral Girdle: The Origin of the Neck

In all swimming fishes, the shoulder girdle (cleithrum, supracleithrum, and posttemporal bones) is solidly bound to the posterior margin of the skull. This rigid fusion is hydrodynamically essential for an animal swimming through dense water, preventing drag-induced head wobble. However, it imposes a crippling constraint: to look left or right, a fish must yaw its entire torso through the water.

Tiktaalik completely lost its opercular bones (the gill covers) and the posttemporal connection. For the first time in vertebrate history, the skull detached from the shoulder girdle, creating a distinct, muscular, flexible **neck**. *Tiktaalik* could rest its body flat on the mud while turning its flattened, crocodile-like head up to 35° independently in all directions to snatch prey along the waterline.

The Weight-Bearing Flexible Wrist Joint

At the end of its robust pectoral fin, *Tiktaalik* evolved a transverse mobile hinge joint composed of distinct proto-carpal radials (homologues of our radiale, intermedium, and ulnare). These bones possessed smooth articular facets that allowed the distal fin to flex dorsally by more than 90°.

This allowed *Tiktaalik* to place its palms flat against the substrate and perform "pectoral push-ups," hoisting its heavy chest and lungs out of stagnant water to gulp fresh air and survey the riverbanks. It did not have walking fingers yet, but it had the mechanical wrist that made fingers possible.

3. The Polydactyly Paradox: Acanthostega and Ichthyostega

For over a century, comparative anatomists believed that the five-digit hand (pentadactyly) was the ancestral, optimal archetype for tetrapods. In 1990, Jenny Clack and Michael Coates shattered this dogma with their exquisite restudy of *Acanthostega gunnari* (365 Ma) and *Ichthyostega stensioei* from the Late Devonian of East Greenland.

To the astonishment of the scientific community, the limbs of *Acanthostega* ended not in five digits, but in **eight distinct, fully formed articulated fingers** on each hand! Its close relative *Ichthyostega* had seven toes on its hind paddle, while the Russian tetrapod *Tulerpeton* possessed six digits.

This discovery established the **Polydactyly Paradox**: the earliest limbs were broadly paddle-like and hyper-digital, acting as flexible, weed-climbing rudders in choked swamp waterways. Digits evolved in water to navigate underwater vegetation, not to walk on dry land! Only later, in the Early Carboniferous, did terrestrial locomotion exert stabilizing selection on the carpus and tarsus, pruning the digit count down to the classic five-toed pattern that characterizes modern amphibians, reptiles, and mammals.

Shakil Mahmud • Research Monograph

4. Sensory Rewiring: The Middle Ear Impedance-Matching Engine

Transitioning from water to land was not merely an orthopedic challenge; it was a sensory crisis. In aquatic environments, sound waves travel with ease directly through the animal's body into the otic inner ear because the acoustic impedance of water ($Z_{\text{water}} \approx 1.5 \times 10^6\ \text{Pa} \cdot \text{s/m}$) is virtually identical to that of biological soft tissue.

In contrast, air is an extremely tenuous medium with an acoustic impedance four orders of magnitude lower:

$$Z_{\text{air}} \approx 415\ \text{Pa} \cdot \text{s/m}$$

When airborne sound waves strike the wet, dense fluid of an animal's inner ear directly, more than **99.9% of the sound energy is reflected back into the atmosphere**, rendering the animal effectively deaf to airborne sound.

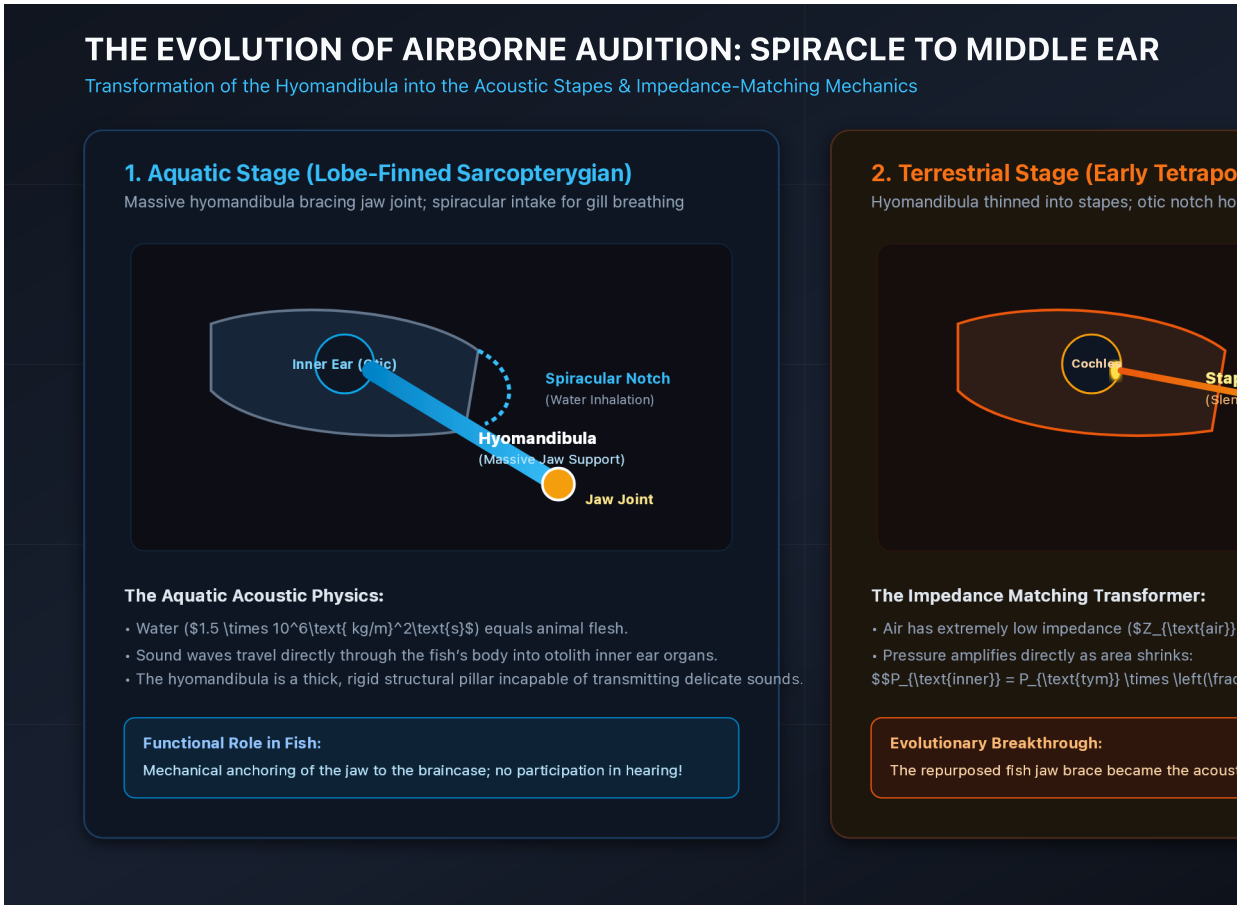


Figure 9.3: The Physics of Airborne Hearing. Left: The aquatic sarcopterygian condition where a massive, load-bearing hyomandibula anchors the jaw joint and the spiracular notch serves as a respiratory water intake. Right: The terrestrial impedance-matching transformer—the hyomandibula thins into a delicate acoustic stapes rod, coupling the large tympanic eardrum to the tiny oval window to amplify airborne sound pressures by 20–30×.

Evolution solved this physical barrier through an extraordinary structural repurposing:

- **The Otic Notch & Tympanum:** The ancestral spiracular notch at the posterolateral corner of the fish skull broadened into a deep cavity called the **otic notch**. Across this opening, evolution stretched a thin, taut, highly compliant membrane: the **tympanic membrane (eardrum)**.
- **The Transformation of the Hyomandibula into the Stapes:** Because the tetrapod lower jaw was now braced directly against the braincase, the massive, pillar-like **hyomandibula** was freed from its ancient structural duty. It shrank dramatically in thickness, converted into a slender, delicate bone rod—the **stapes (columella)**—and braced itself between the inner ear's fluid-filled oval window (*fenestra ovalis*) and the eardrum.

The stapes acted as a mechanical **impedance-matching transformer**. By collecting airborne acoustic energy across the relatively large surface area of the eardrum (A_{tym}) and concentrating it onto the tiny footplate of the stapes ($A_{\text{footplate}}$), it generated an enormous mechanical pressure amplification:

$$P_{\text{inner}} = P_{\text{tym}} \times \left(\frac{A_{\text{tym}}}{A_{\text{footplate}}}\right) \approx 20\text{–}30\times \text{ amplification}$$

This pressure multiplier overcame the water-air impedance barrier, forcefully driving the lymph fluid of the inner ear cochlea and allowing our terrestrial ancestors to hear the whispers of wind, the rustle of vegetation, and the mating calls of the Carboniferous world.

Citation: Mahmud, S. (2026). "The Water-to-Land Transition — The Anatomy of Sarcopterygian Tetrapodomorphs." In The Evolutionary Odyssey, Part 9. https://shakilmahmud.com/evolutionary-odyssey-part-9-the-water-to-land-transition/

Shakil Mahmud • Research Monograph

SHAKIL MAHMUD RESEARCH MONOGRAPHS • PART X

The Carboniferous Amphibian World & The Cleidoic Amniotic Breakthrough

The Carboniferous Amphibian World & The Cleidoic Amniotic Breakthrough

1,395 words • November 1, 2026 • Permanent URI

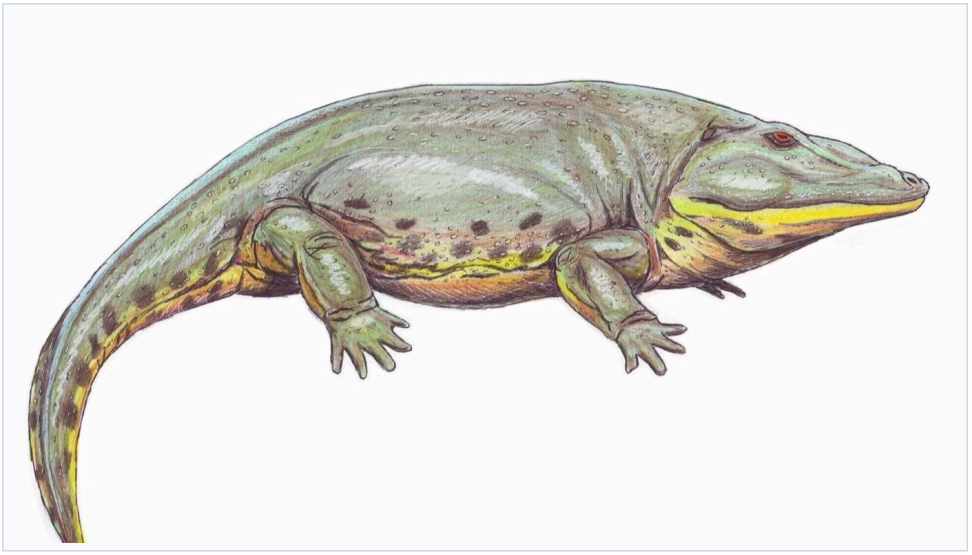


Plate X: *Figure: A Late Carboniferous coal swamp forest (~310 Ma), showing the robust temnospondyl amphibian Eryops megacephalus prowling the swamp margin beneath towering Lepidodendron clubmoss trees and giant Meganeura insects.*

Three hundred and twenty million years ago, the continents were swathed in an endless, suffocatingly dense emerald canopy: the great coal swamp forests of the Carboniferous Period. Towering forty-metre lycopsid scale trees sucked gigatons of carbon from the atmosphere, driving atmospheric oxygen to an astonishing 35%—an all-time planetary high. Under this hyperoxic sky, giant predatory griffinflies with the wingspan of hawks darted between trees, while two-metre millipedes crashed through the undergrowth. Yet for all their terrestrial dominance, vertebrates remained tethered to water by a reproductive ball-and-chain: the delicate, jelly-coated amphibian egg. The breaking of this chain through the invention of the **cleidoic amniotic egg** would permanently divorce vertebrates from the water and spark the deep evolutionary duel between synapsids and diapsids.

1. The Giant Carboniferous Ecosystem: Hyperoxia & Tracheal Diffusion

The Carboniferous Period (359\text{–}299\text{ Ma}) witnessed the most extreme atmospheric perturbation in Phanerozoic history. Vast swamp forests dominated by giant clubmosses (*Lepidodendron*, *Sigillaria*) and horsetails (*Calamites*) evolved thick trunks reinforced by **lignin**—a recalcitrant, cross-linked aromatic polymer. At this point in evolutionary history, white-rot fungi (Basidiomycota) equipped with lignin peroxidase enzymes had not yet evolved to digest this woody tissue. As trees died, they fell into stagnant, acidic, oxygen-starved peat bogs, escaping decomposition and burying immense reservoirs of organic carbon as coal seams.

Because photosynthesis releases molecular oxygen ($6CO_2 + 6H_2O \rightarrow C_6H_{12}O_6 + 6O_2$) and decomposition was blocked, atmospheric oxygen surged from a Devonian baseline of 21% to an extraordinary peak of 35%, elevating total atmospheric surface pressure by more than 35%.

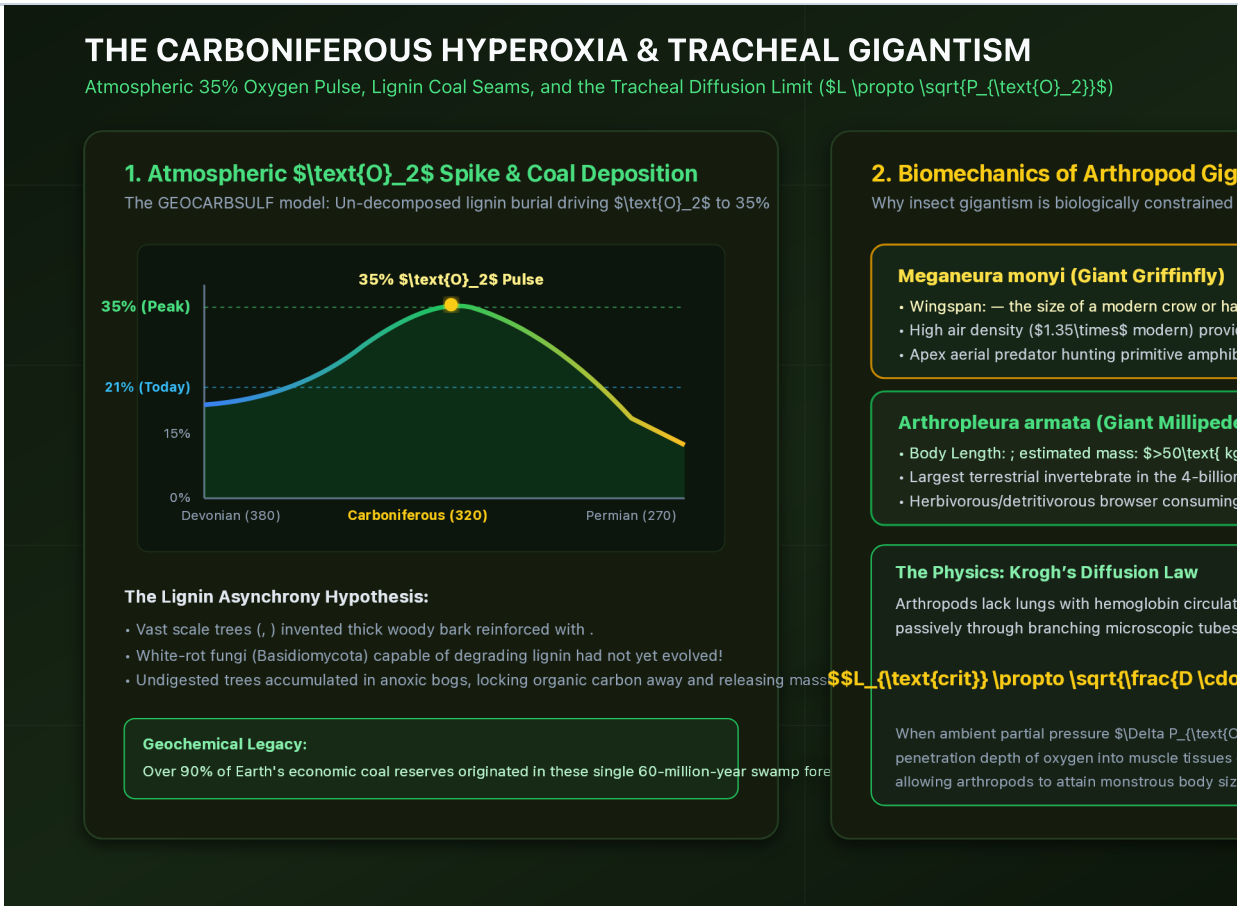


Figure 10.1: Geochemical Hyperoxia and Arthropod Gigantism. Left: Atmospheric oxygen timeline peaking at 35% during the Late Carboniferous, driven by the global burial of undigested lignin coal beds. Right: Biomechanics of tracheal diffusion—Krogh's Law demonstrates how elevated oxygen partial pressure relaxed the diffusion length barrier, enabling Meganeura (75 cm wingspan) and Arthropleura (2.6 m length) to achieve monstrous terrestrial sizes.

This atmospheric hyperoxia had a profound biophysical consequence for terrestrial arthropods. Unlike vertebrates, which circulate oxygen using a closed vascular system with hemoglobin, insects and myriapods rely on **tracheal respiration**—an invaginated network of branching micro-tubes that delivers oxygen directly to cells via passive gaseous diffusion.

Under August Krogh's classical diffusion model, the maximum penetration depth (L_{crit}) of oxygen through a tissue cylinder of radius R is governed by:

$$L_{\text{crit}} \propto \sqrt{\frac{D \cdot \Delta P_{\text{O}_2}}{R}}$$

Where D is the gas diffusion coefficient and ΔP_{O_2} is the ambient partial pressure of oxygen. In modern air ($\text{O}_2 = 21\%$), diffusion becomes lethally inefficient beyond a body diameter of a few centimeters.

With oxygen boosted to 35%, the partial pressure increased by 67%, allowing oxygen to diffuse deeper into muscle tissues without suffocation. Arthropods grew to monstrous, nightmare proportions:

- *Meganeura monyi:* A predatory griffinfly with a wingspan of $\mathbf{75\ cm\ (2.5\ feet)}$ and large compound eyes, capable of powered aerial hunting in dense air that provided 35% greater aerodynamic lift.
- *Arthropleura armata:* A heavily armored millipede reaching $\mathbf{2.6\ metres\ (8.5\ feet)}$ in length and weighing over $50\ \text{kg}$—the largest terrestrial invertebrate in Earth history.

2. The Cleidoic Amniotic Breakthrough: Packaging the Pond

While arthropods and giant labyrinthodont temnospondyl amphibians dominated the wetlands, vertebrates faced an inescapable ecological barrier. The eggs of amphibians (anamniotes) are naked, gelatinous globes permeable to water. If laid on dry land, the sun rapidly evaporates their moisture, killing the embryo. Furthermore, the developing amphibian embryo excretes soluble, highly toxic **ammonia (NH_3)**, which requires continuous immersion in surrounding water to dilute and wash away.

Consequently, amphibians were chained to the water's edge. They could hunt on land, but they were forced to return to wetlands to reproduce, and their offspring had to endure a perilous free-swimming larval (tadpole) phase.

Shakil Mahmud • Research Monograph

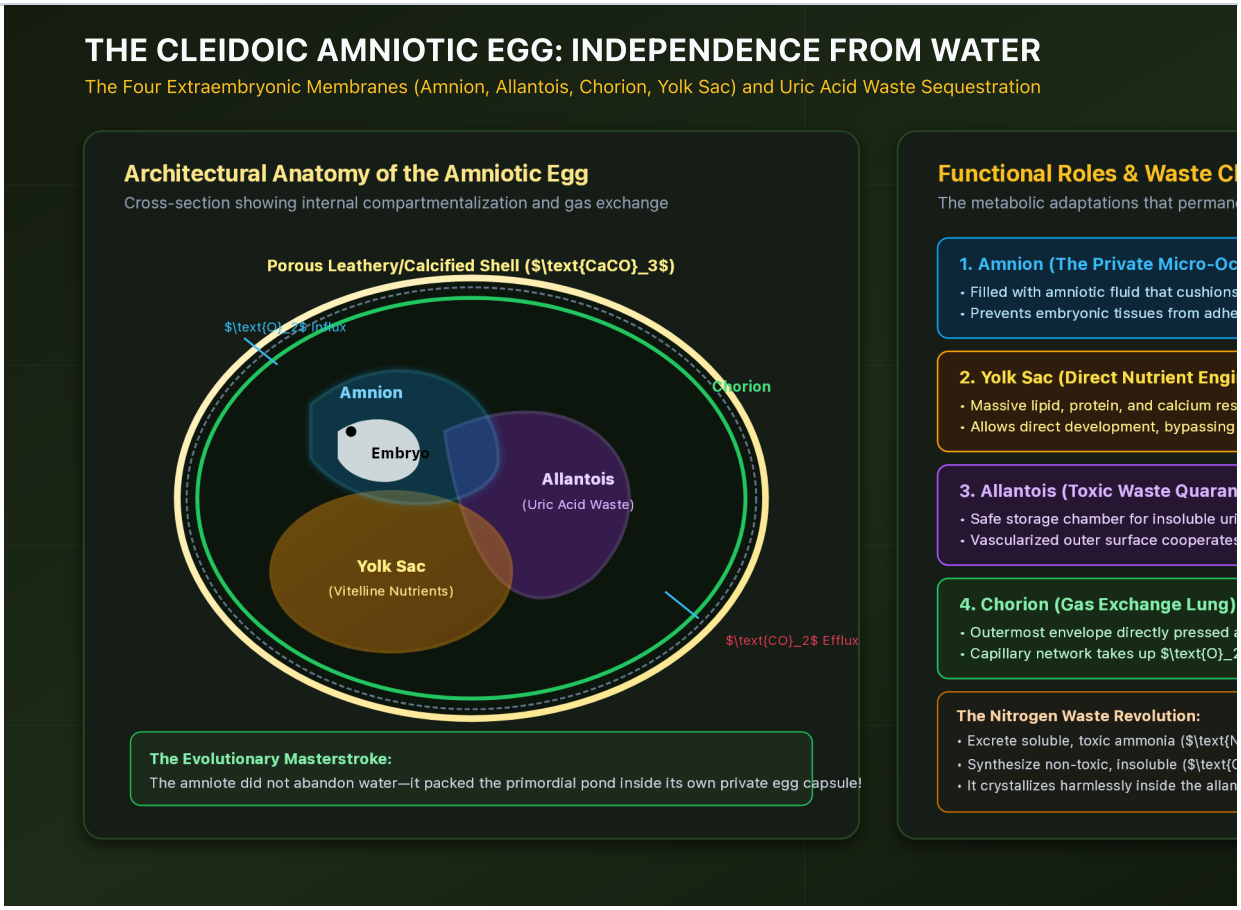


Figure 10.2: The Architectural Anatomy of the Amniotic Egg. A detailed cross-section illustrating the four defining extraembryonic membranes: (1) The Amnion, enclosing the embryo in private aquatic fluid; (2) The Yolk Sac, supplying concentrated vitelline nutrients; (3) The Allantois, sequestering insoluble uric acid waste; (4) The Chorion, conducting respiratory gas exchange across the porous shell.

In the Late Carboniferous (≈ 315 Ma), stem tetrapods achieved one of the greatest adaptive breakthroughs in evolutionary history: the **cleidoic (closed) amniotic egg**. Instead of escaping the water, the amniote did something vastly more ingenious: *it packaged the ancient primordial pond inside a waterproof capsule* through four specialized extraembryonic membranes:

1. **The Amnion:** A thin, transparent fluid-filled membrane directly enclosing the embryo. The amniotic fluid maintains a saline, buoyant micro-environment that cushions the developing tissues against gravity and physical shock, keeping the embryo suspended in an internal sea.
2. **The Yolk Sac:** An extensively vascularized diverticulum containing energy-dense lipids, proteins, and minerals. Unlike small amphibian eggs that rely on larval grazing, the massive yolk provides full sustenance until the embryo hatches as a fully formed, miniature terrestrial adult.
3. **The Allantois:** A vascularized sac growing from the hindgut. It serves as an isolated containment vault for metabolic waste, and its outer vascular network participates in gas exchange.
4. **The Chorion:** The outermost protective envelope encompassing the entire embryonic apparatus. Placed in direct contact with the inner surface of the shell, its dense capillary beds absorb oxygen and exhaust carbon dioxide through microscopic pores in the shell.

The Biochemical Revolution: Uric Acid vs. Ammonia

The amniotic egg could not have functioned without a complete overhaul of nitrogen metabolism. Ammonia excretion would have poisoned the embryo within days inside a sealed shell. Amniotes evolved the biochemical machinery to convert nitrogen waste into **Uric Acid ($C_5H_4N_4O_3$)**.

Uric acid is practically non-toxic and insoluble in water. It precipitates out of solution as harmless white crystals, sequestered safely inside the allantois until hatching with virtually zero water loss. With this biochemical triumph and a porous, calcium carbonate ($CaCO_3$) shell, amniotes severed all reproductive ties to the water. They were free to march inland, colonize high plateaus, and conquer deserts.

3. The Grand Amniote Split: Synapsids vs. Diapsids

Almost immediately upon inventing the amniotic egg, the basal amniotes bifurcated into two rival evolutionary empires. This monumental division is recorded not in the limbs or scales, but in the architectural engineering of the skull roof behind the eye sockets: **temporal fenestration**.

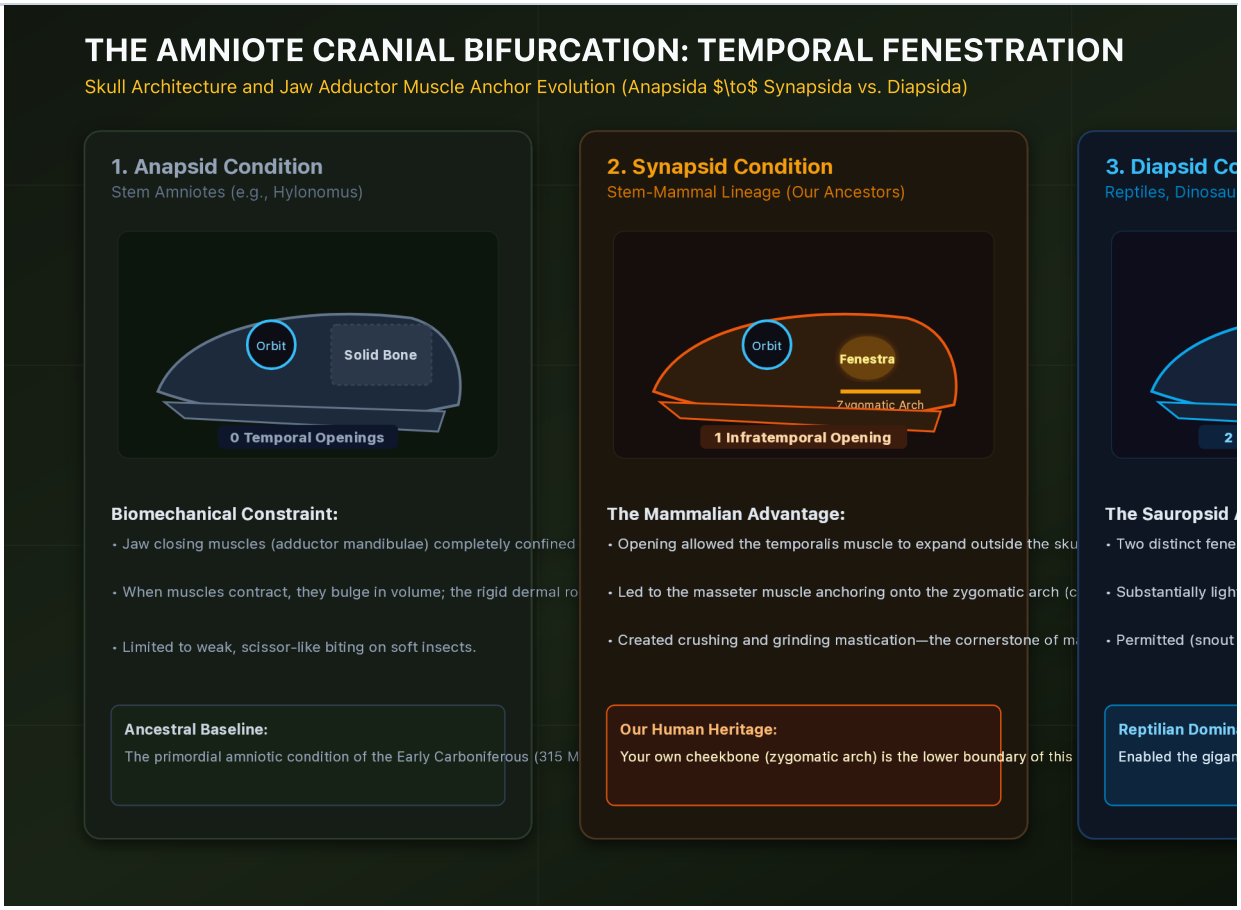


Figure 10.3: The Cranial Divergence of Amniota. Comparative profiles of the three temporal architectures: (1) Anapsid—solid dermal roof restricting jaw muscle expansion (stem amniotes); (2) Synapsid—single lower infratemporal fenestra bounded by the zygomatic arch (mammalian ancestors); (3) Diapsid—dual supratemporal and infratemporal openings enabling lightweight kinesis (reptiles, dinosaurs, and birds).

1. The Anapsid Condition (Solid Roof)

Represented by the earliest known amniote, *Hylonomus lyelli* (found fossilized inside hollow lycopod tree stumps in Nova Scotia, 315 Ma). Anapsids possessed a completely solid dermal skull roof behind the orbit, inherited directly from primitive amphibians. The jaw-closing adductor muscles were boxed inside this rigid bone cylinder; when muscles contract, they must bulge in volume, meaning anapsid bite force was fundamentally constrained by the internal volume of the braincase.

2. The Synapsid Lineage: Our Ancestral Clan

In the Late Carboniferous, one branch of amniotes opened a **single lower temporal fenestra** on each side of the skull, bounded by the postorbital, squamosal, and jugal bones. This was **Class Synapsida**—the stem-mammal dynasty.

This single opening was a biomechanical triumph. It allowed the *temporalis* muscle to expand outward and anchor directly onto the dorsal edges of the braincase, while the lower bony margin evolved into the **zygomatic arch (cheekbone)**, providing an anchor for the newly evolved *masseter* muscle. For the first time, vertebrates could execute complex grinding, shearing, and crushing chewing motions—the evolutionary prerequisite for mammalian endothermy and metabolic power.

3. The Diapsid Lineage: The Sauropsid Empire

The second great branch, **Class Diapsida** (represented by basal forms like *Petrolacosaurus*), evolved **two temporal openings**: an upper (supratemporal) and lower (infratemporal) fenestra separated by a horizontal postorbital-squamosal bone strut.

This dual-window design drastically lightened the skull while preserving tensile strength, providing multiple complex attachment angles for jaw muscles. In later Mesozoic radiations, this architecture enabled **cranial kinesis**—the ability to flex and tilt skull bones independently—which fueled the terrifying predatory bite of theropod dinosaurs and the acrobatic beak dexterity of modern birds.

As the Carboniferous drew to a close, a global cooling trend began drying up the equatorial coal swamps. The amphibians, shackled to their drying pools, began a catastrophic decline. The future of Earth now belonged entirely to the amniotes—and in the arid, challenging Permian world that lay ahead, it was our synapsid ancestors who struck first.

Citation: Mahmud, S. (2026). "The Carboniferous Amphibian World & The Cleidoic Amniotic Breakthrough." In The Evolutionary Odyssey, Part 10. https://shakilmahmud.com/evolutionary-odyssey-part-10-the-carboniferous-amphibian-world-and-amniotic-egg/

Shakil Mahmud • Research Monograph

SHAKIL MAHMUD RESEARCH MONOGRAPHS • PART XI

The Synapsid Hegemony & The Permian-Triassic Great Dying

The Synapsid Hegemony & The Permian-Triassic Great Dying

1,411 words • November 1, 2026 • Permanent URI

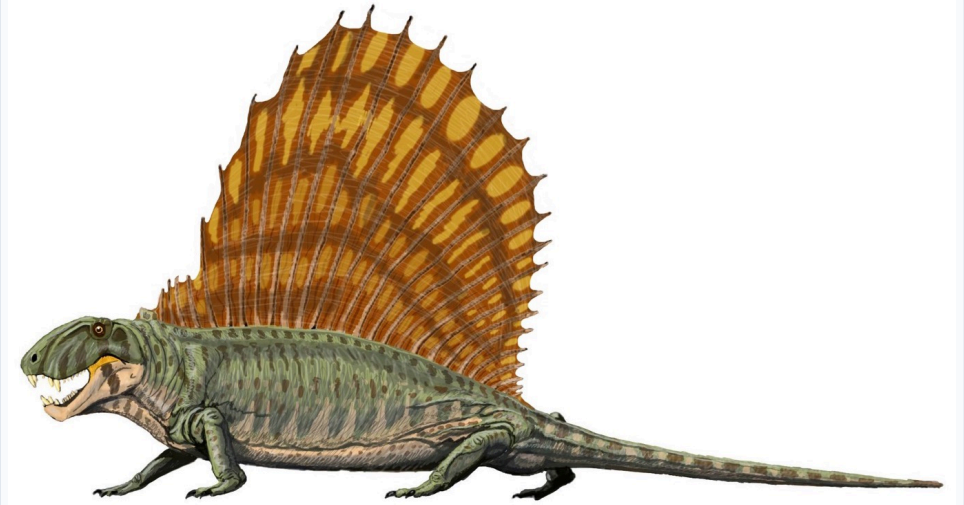


Plate XI: *Figure: The stem-mammal synapsid Dimetrodon grandis (~275 Ma) basking on a semi-arid Permian floodplain, displaying its highly vascularized thermoregulatory dorsal sail and differentiated heterodont dentition.*

Two hundred and ninety million years ago, long before the first dinosaur laid a claw upon the supercontinent of Pangaea, the continents were ruled by an extraordinary dynasty of stem-mammals: the Synapsida. From sail-backed pelycosaurs like *Dimetrodon* harnessing solar energy on ancient floodplains, to saber-toothed gorgonopsians and fur-covered cynodonts inventing heterodont chewing, our direct ancestors achieved unquestioned terrestrial hegemony. But at the boundary between the Permian and Triassic periods (**251.9 Ma**), the planet entered its darkest hour: the Siberian Traps super-volcanic catastrophe. In a geological heartbeat, 96% of all marine species and 70% of terrestrial vertebrates were obliterated in the worst mass extinction in planetary history: The Great Dying.

1. Solar Thermal Engineering: The Dorsal Sail of Dimetrodon

In popular culture, *Dimetrodon* is frequently misidentified as a dinosaur. In reality, it went extinct forty million years before the earliest dinosaur appeared, and cladistically, it is more closely related to you and me than to any reptile. *Dimetrodon* belongs to the Pelycosauria, the earliest grade of stem-mammals (Synapsida).

The most striking morphological feature of *Dimetrodon limbatus* is its towering dorsal sail, supported by neural spine elongations of up to **1.5 metres** projecting from its dorsal vertebrae. For decades, paleontologists debated whether the sail served as a sexual display ornament, a defensive barrier against predators, or an aerodynamic wind-sail. In 1973, biophysicists C. D. Bramwell and P. B. Fellgett provided the definitive thermodynamic explanation: the sail was a high-performance **solar heat exchanger**.

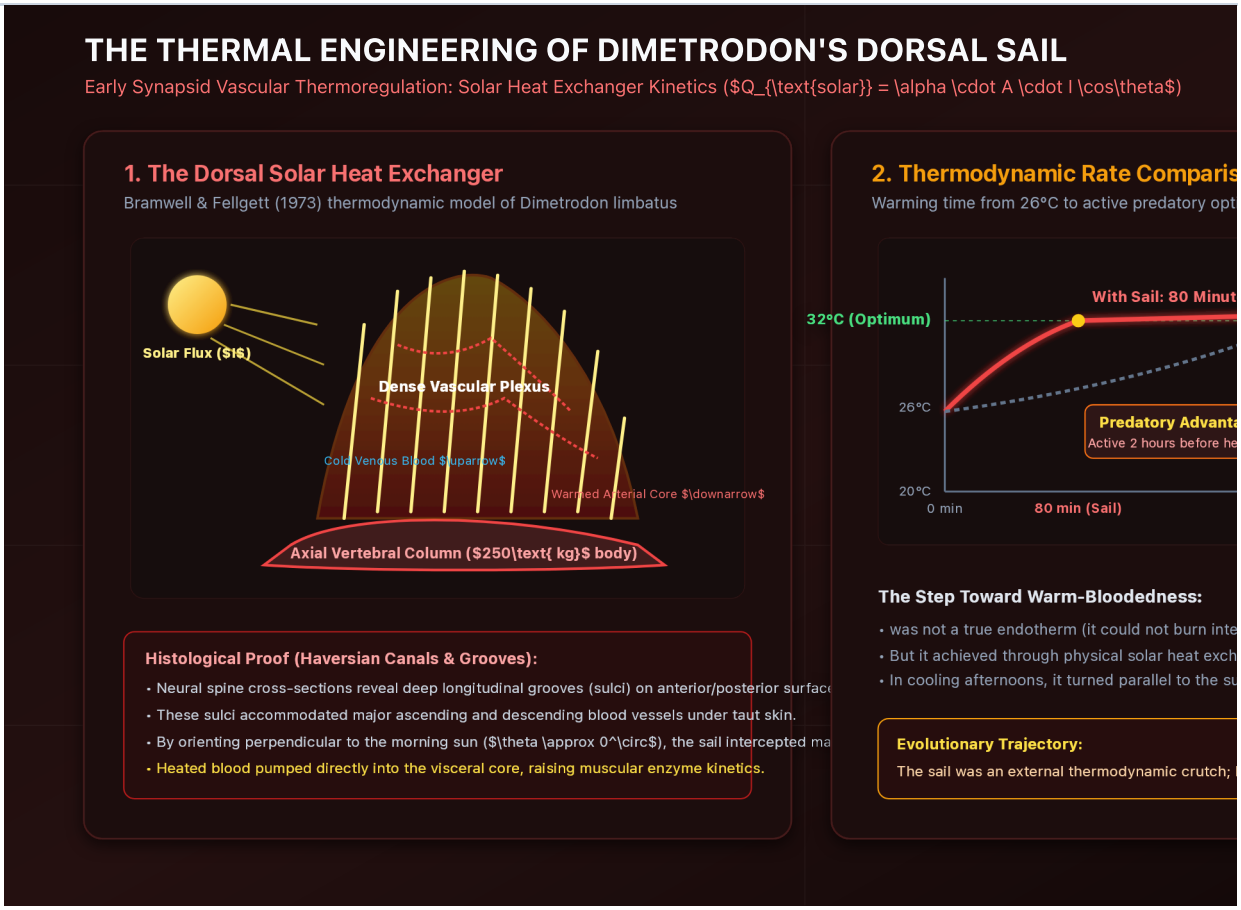


Figure 11.1: The Solar Thermal Machine of Dimetrodon. Left: Anatomical reconstruction of the dorsal sail showing neural spines channeled by longitudinal vascular sulci carrying arterial blood. Right: Thermodynamic warming curve—Dimetrodon warmed its 250 kg body to active predatory temperature (32°C) in just 80 minutes, gaining a decisive 125-minute morning advantage over sail-less ectotherms.

Histological thin-sections of the neural spines reveal deep longitudinal sulci (grooves) running parallel to the bone axis. These grooves housed major ascending arteries and descending veins, which fed into an extensive sub-epidermal vascular capillary network woven throughout the taught skin webbing.

The solar heat absorbed by the sail is governed by the radiative transfer equation:

$$Q_{\text{solar}} = \alpha \cdot A_{\text{sail}} \cdot I_{\text{sun}} \cdot \cos\theta$$

Where α is the absorptivity of the skin, A_{sail} is the surface area of the sail ($\approx 1.2\text{–}1.5\text{ m}^2$), I_{sun} is solar irradiance, and θ is the angle of incidence between the sun and the sail plane.

By orienting its body broadside to the rising morning sun ($\theta \approx 0^\circ$), a $\mathbf{250\text{-kg}}$ *Dimetrodon* heated its core blood from a dawn temperature of $\mathbf{26^\circ C}$ to its optimal metabolic hunting temperature of $\mathbf{32^\circ C}$ in just **80 minutes**. A sail-less ectothermic animal of equivalent mass required over **205 minutes** to reach the same temperature.

This thermodynamic advantage granted *Dimetrodon* a lethal two-hour window every morning during which it was fully warm, agile, and enzymatically primed, while its herbivorous prey (like the lumbering captorhinid *Cotylorhynchus*) remained sluggish, stiff, and physiologically immobilized by the morning chill.

2. The Therapsid Metamorphosis: Heterodonty & The Secondary Palate

By the Middle Permian ($\mathbf{270\text{ Ma}}$), the pelycosaurs were superseded by a vastly more sophisticated synapsid clade: the **Therapsids** ("beast-faces"), which later yielded the **Cynodonts**—the direct precursors to true mammals.

While basal amniotes possessed homodont dentition (uniform, conical peg teeth that could only seize prey), therapsids revolutionized oral biomechanics by inventing **heterodonty**—the anatomical specialization of distinct tooth categories across the jaw:

Shakil Mahmud • Research Monograph

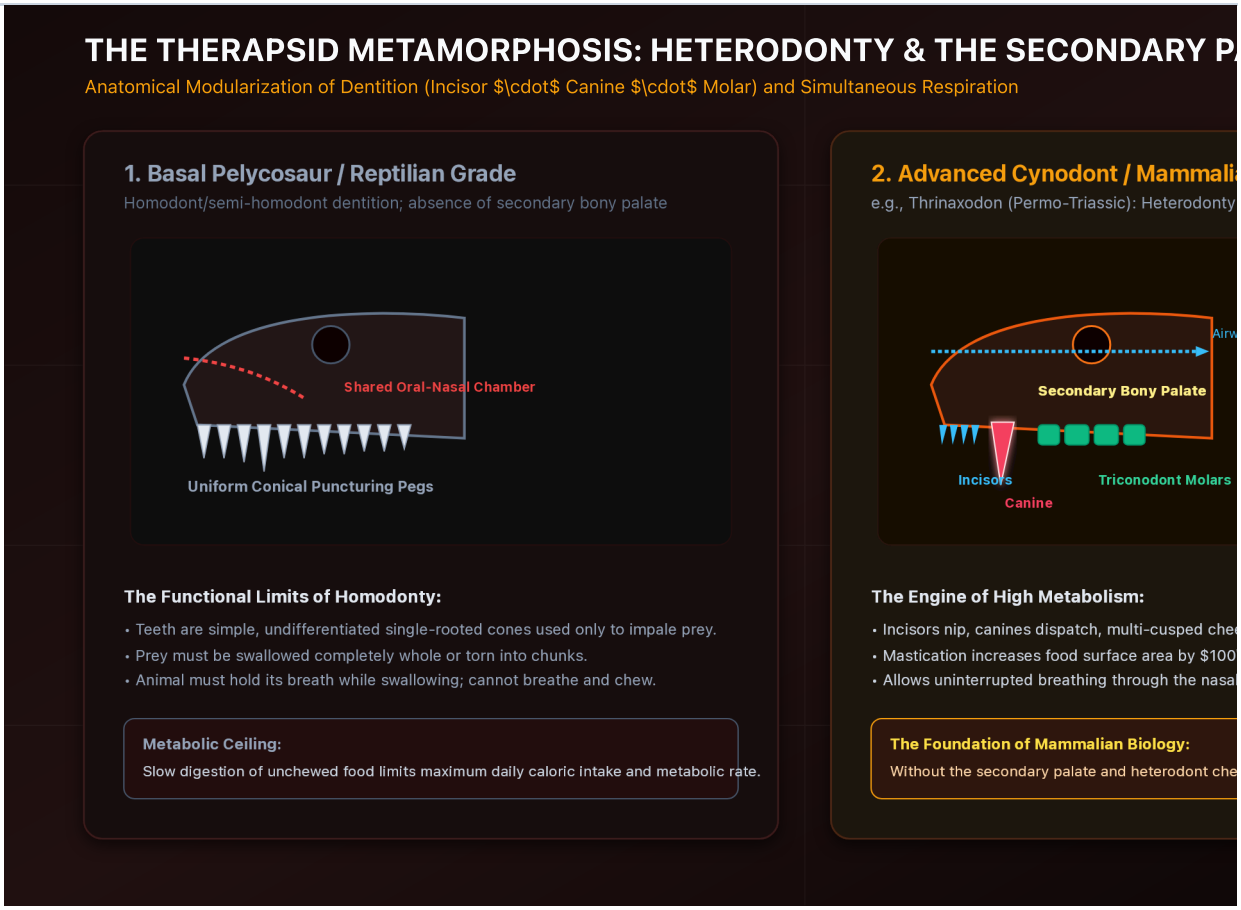


Figure 11.2: The Evolutionary Assembly of Mammalian Chewing. Left: Basal pelycosaur condition with undifferentiated conical teeth and a shared oral-nasal cavity. Right: Advanced cynodont (Thrinaxodon) displaying modular heterodonty (incisors, saber fangs, triconodont molars) and the secondary bony palate enabling continuous respiration while masticating.

- **Incisors:** Anterior, chisel-like teeth anchored in the premaxilla, specialized for grasping, nipping, and stripping meat from bone.
- **Canines:** Elongated, laterally compressed saber fangs anchored deep within the maxilla, designed to puncture vital cervical arteries and deliver swift kills. In apex gorgonopsians like *Inostrancevia*, canines reached 15 cm in length.
- **Postcanines (Premolars & Molars):** Complex cheek teeth equipped with multiple cusps (triconodont architecture) and distinct shearing facets. Instead of swallowing food in massive, unchewed chunks, therapsids chewed their food into fine pulp.

The Secondary Bony Palate: Chewing Without Suffocating

Masticating food introduces a lethal physiological conflict: if the mouth is full of food undergoing mechanical chewing, how does the animal breathe?

Reptiles and amphibians possess a primary palate; their nasal openings empty directly into the front of the oral cavity. Consequently, they must hold their breath while swallowing. Advanced cynodonts (such as *Thrinaxodon liorhinus*) solved this by extending horizontal plates from the maxilla and palatine bones to form the **secondary bony palate**.

The secondary palate created a permanent, rigid horizontal floor that completely isolated the respiratory nasal passage from the lower oral cavity. Air entered the external nares, flowed along the dorsal passage, and entered the trachea at the back of the pharynx—entirely uninterrupted by food processing in the mouth. This single innovation allowed continuous, high-volume pulmonary gas exchange during prolonged mastication—laying the anatomical foundation for warm-blooded endothermy!

3. The Siberian Traps & The Permian-Triassic Great Dying

By 255 million years ago, synapsids were at the peak of their evolutionary dominion. Then, at 251.9 Ma, planetary geology unleashed an apocalypse from which the biosphere barely recovered.

Beneath the northern continent of Siberia, a colossal mantle plume tore through the Earth's crust, erupting more than **3 to 5 million cubic kilometers of basaltic lava**—an area larger than the continental United States covered in liquid rock two kilometers deep: the **Siberian Traps**.

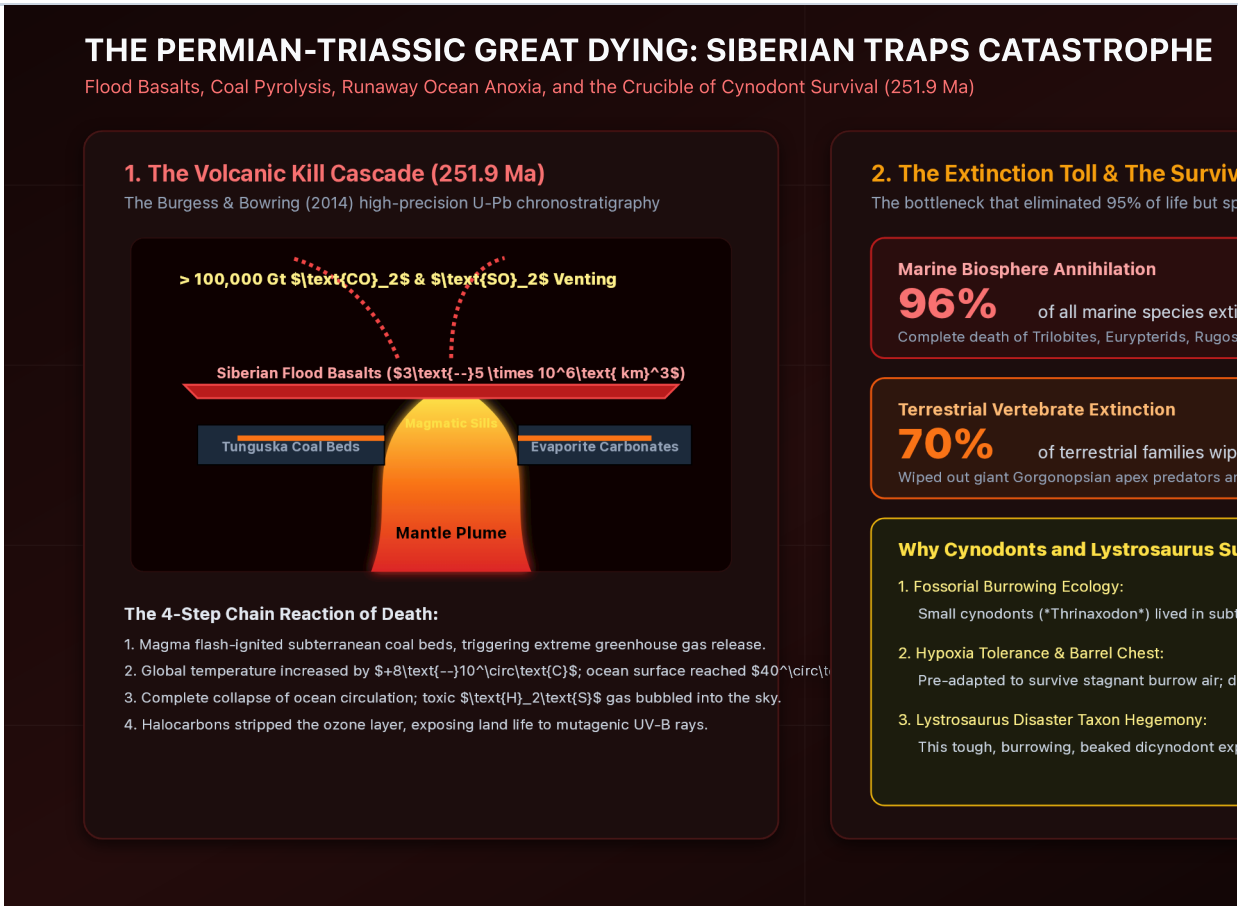


Figure 11.3: The Permian-Triassic Kill Cascade. Left: Mantle plume erupting flood basalts while sills flash-pyrolyze the Tunguska coal beds, injecting over 100,000 Gt of greenhouse and toxic gasses into the stratosphere. Right: Extinction toll metrics (96% marine, 70% terrestrial families lost) and the survival mechanics of burrowing cynodonts and the disaster taxon Lystrosaurus.

The Pyrolysis of Tunguska Coal Beds

The basaltic magma alone was not the primary killer. The fatal trigger was where the magma intruded. As the basalt rose, massive underground volcanic sills intersected the giant, organic-rich **Tunguska Basin coal deposits**, oil shales, and thick evaporite beds. The intense heat flash-pyrolyzed these subterranean fuel beds, turning Siberia into an unimaginably vast volcanic gasification engine.

More than **100,000 Gigatons of carbon dioxide (CO_2)**, methane (CH_4), and sulfur dioxide (SO_2) were blasted into the stratosphere within a geological pulse of less than 60,000 years (Burgess & Bowring, 2014):

1. **Super-Greenhouse Thermal Spike:** Atmospheric CO_2 soared past $3,000$ ppm. Global average temperatures spiked by $+8\text{–}10^\circ\text{C}$. Equatorial ocean surface temperatures surpassed 40°C (104°F)—approaching the thermal coagulation limit for complex proteins!
2. **Ocean Acidification & Anoxia:** The oceans absorbed immense volumes of CO_2, forming carbonic acid (H_2CO_3) that plummeted ocean pH. Because warm water holds vastly less dissolved oxygen, oceanic thermohaline circulation collapsed into total stagnant anoxia.
3. **Euxinia and Hydrogen Sulfide Eruptions:** With oxygen depleted, anaerobic sulfate-reducing bacteria bloomed in the deep abyss, producing immense clouds of toxic **hydrogen sulfide (H_2S)** gas. The ocean turned purple, and monstrous bubbles of H_2S erupted into the atmosphere, poisoning coastal land communities and reacting with the ozone layer to strip away Earth's UV-B protection.

4. The Crucible of Survival: Cynodonts and Lystrosaurus

The toll of The Great Dying was catastrophic. **96% of all marine species** were wiped out forever: the trilobites, eurypterids, rugose corals, and blastoids vanished completely. On land, **70% of all vertebrate families** were extinguished, wiping out the mighty gorgonopsians and pareiasaurs.

Yet, in the smoking ash-fields of the earliest Triassic (251 Ma), our synapsid lineage did not entirely perish. Two groups of stem-mammals miraculously passed through the extinction filter:

- **The Fossorial Cynodonts:** Small cynodonts like *Thrinaxodon* and *Galesaurus* had evolved semi-fossorial burrowing habits. In their underground tunnels, they were insulated from blistering surface temperatures, acid rain, and toxic atmospheric gasses. Their barrel-shaped rib cages and early diaphragmatic breathing pre-adapted them to survive in the chronically low-oxygen, high-CO_2 air of subterranean burrows.
- **The Hegemony of Lystrosaurus:** The dicynodont *Lystrosaurus*, a tough, pig-sized herbivore with a horny beak and digging tusks, survived the crucible and underwent the most astonishing demographic explosion in geological history. With all competing predators and large herbivores dead, *Lystrosaurus* multiplied until it accounted for an

Shakil Mahmud • Research Monograph

unbelievable **95% of all terrestrial vertebrate individuals** on Earth—a single genus dominating an entire planet!

Our ancestors had survived the greatest biological bottleneck in planetary history. But in the barren, overheated Triassic world that emerged from the ashes, a new and agile rival lineage was rising to challenge the battered synapsids for the crown of the continents: the Archosaurs.

Citation: Mahmud, S. (2026). "The Synapsid Hegemony & The Permian-Triassic Great Dying." In The Evolutionary Odyssey, Part 11. https://shakilmahmud.com/evolutionary-odyssey-part-11-the-synapsid-hegemony-and-permian-extinction/

SHAKIL MAHMUD RESEARCH MONOGRAPHS • PART XII

The Archosaur Empire — Dinosaurs, Pterosaurs, and the Avian Transition

The Archosaur Empire — Dinosaurs, Pterosaurs, and the Avian Transition

1,468 words • November 1, 2026 • Permanent URI



Plate XII: *Figure: A feathered dromaeosaurid dinosaur (Velociraptor / Deinonychus) in a Late Cretaceous woodland, showcasing true avian pennaceous plumage on wings and tail, binocular amber eyes, and lethal sickle claws.*

For over one hundred and sixty million years—from the recovery of the Triassic to the cataclysmic impact at the end of the Cretaceous—the Mesozoic Era belonged to a singular, magnificent clade of diapsid reptiles: the Archosauria ("ruling reptiles"). While popular imagination celebrates dinosaurs for their towering stature, razor-sharp fangs, and armored crests, the true biological engine of their supremacy lay hidden deep within their thoracic cavities: an astonishing, unidirectional flow-through respiratory system of pulmonary air sacs. This respiratory super-engine enabled sauropods to engineer 70-tonne cantilever skeletons, drove theropod dinosaurs across continents, and ultimately transformed feathers from primitive thermal fuzz into the aerodynamic marvel of avian powered flight.

1. The Respiratory Super-Engine: Unidirectional Air-Sac Ventilation

In the aftermath of the Permian-Triassic extinction, the atmospheric concentration of molecular oxygen plummeted from a Carboniferous high of 30% down to a suffocatingly low **12\text{–}15\%**—equivalent to standing at the summit of the Himalayas today. In this oxygen-starved world, our synapsid ancestors were crippled by their ancestral **tidal respiratory system**. In mammalian lungs, air travels in and out along the same dead-end alveolar passages, meaning newly inhaled air is constantly contaminated by stale, carbon-dioxide-rich residual air, capping oxygen extraction efficiency at barely 25%.

Archosaurs conquered this physiological crisis by inventing a continuous, **unidirectional flow-through respiratory circuit** powered by non-vascularized air sacs acting as bellows:

Shakil Mahmud • Research Monograph

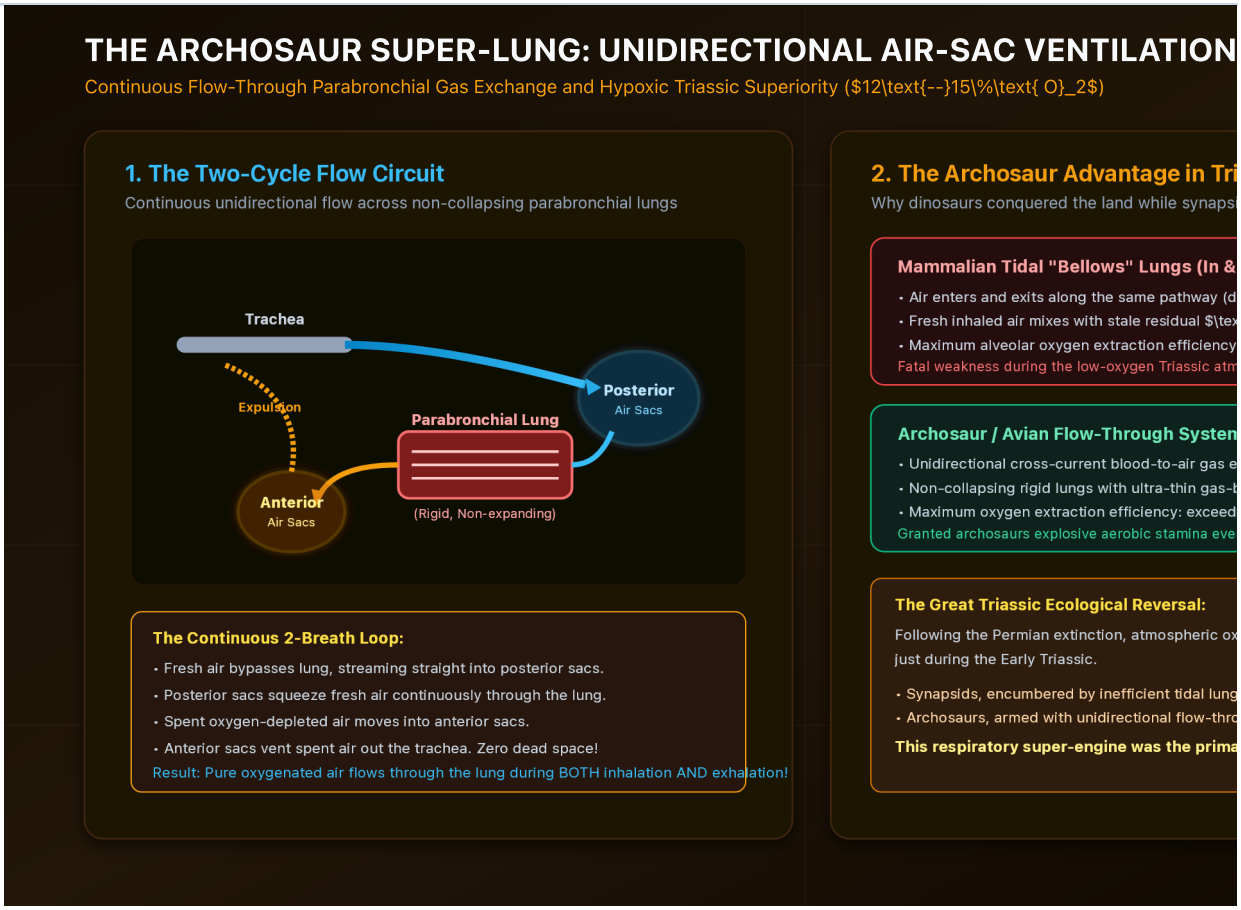


Figure 12.1: The Archosaur Respiratory Super-Engine. Left: The continuous two-cycle circuit showing how fresh air streams into posterior air sacs (Breath 1 Inhale), flows unidirectionally across non-collapsing parabronchial lungs during both breaths, collects in anterior sacs, and vents cleanly out the trachea. Right: The geochemical and physiological comparison demonstrating why archosaurs outcompeted synapsids during the low-oxygen Triassic bottleneck (12% O_2).

The system operates across a coordinated **two-breath cycle**:

1. **Breath 1 (Inhalation):** Inhaled air bypasses the lung tissue entirely, streaming directly through the primary bronchus into the compliant **posterior air sacs** (abdominal and caudal thoracic sacs).
2. **Breath 1 (Exhalation):** The posterior sacs contract, forcing a continuous stream of pure, oxygen-rich air forward through the rigid, non-expanding **parabronchial lung**. Here, blood capillaries cross the parabronchi in a counter-current or cross-current geometry, driving oxygen diffusion with maximum efficiency.
3. **Breath 2 (Inhalation):** As the next volume of fresh air enters the posterior sacs, the spent, oxygen-depleted air in the lung is pulled forward into the **anterior air sacs** (clavicular and cranial thoracic sacs).
4. **Breath 2 (Exhalation):** The anterior sacs contract, venting the spent air directly out through the trachea into the atmosphere.

Because fresh air flows unidirectionally through the parabronchi during *both inhalation and exhalation*, there is zero residual volume dead space. Oxygen extraction efficiency exceeds 60%. This single physiological breakthrough gave dinosaurs an explosive aerobic advantage over synapsids, driving stem-mammals into the nocturnal shadows while archosaurs exploded into terrestrial and aerial dominance.

2. Sauropod Gigantism: Postcranial Skeletal Pneumatization (PSP)

Armed with this respiratory system, the Saurischian branch of dinosaurs evolved the largest terrestrial animals ever to walk the Earth: the long-necked **Sauropods** (such as *Argentinosaurus*, *Brachiosaurus*, and *Patagotitan*), reaching lengths of over 35 metres and body masses exceeding 70 metric tons.

Under the square-cube law of biomechanics, scaling up an animal isometrically creates a structural crisis: body mass scales with volume ($M \propto L^3$), whereas the weight-bearing cross-sectional area of bones scales only with area ($A \propto L^2$). If an elephant were scaled to the size of an *Argentinosaurus*, its solid bones would be so heavy its skeleton would crush under its own dead weight. How did sauropods build 12-metre cantilever necks without structural collapse?

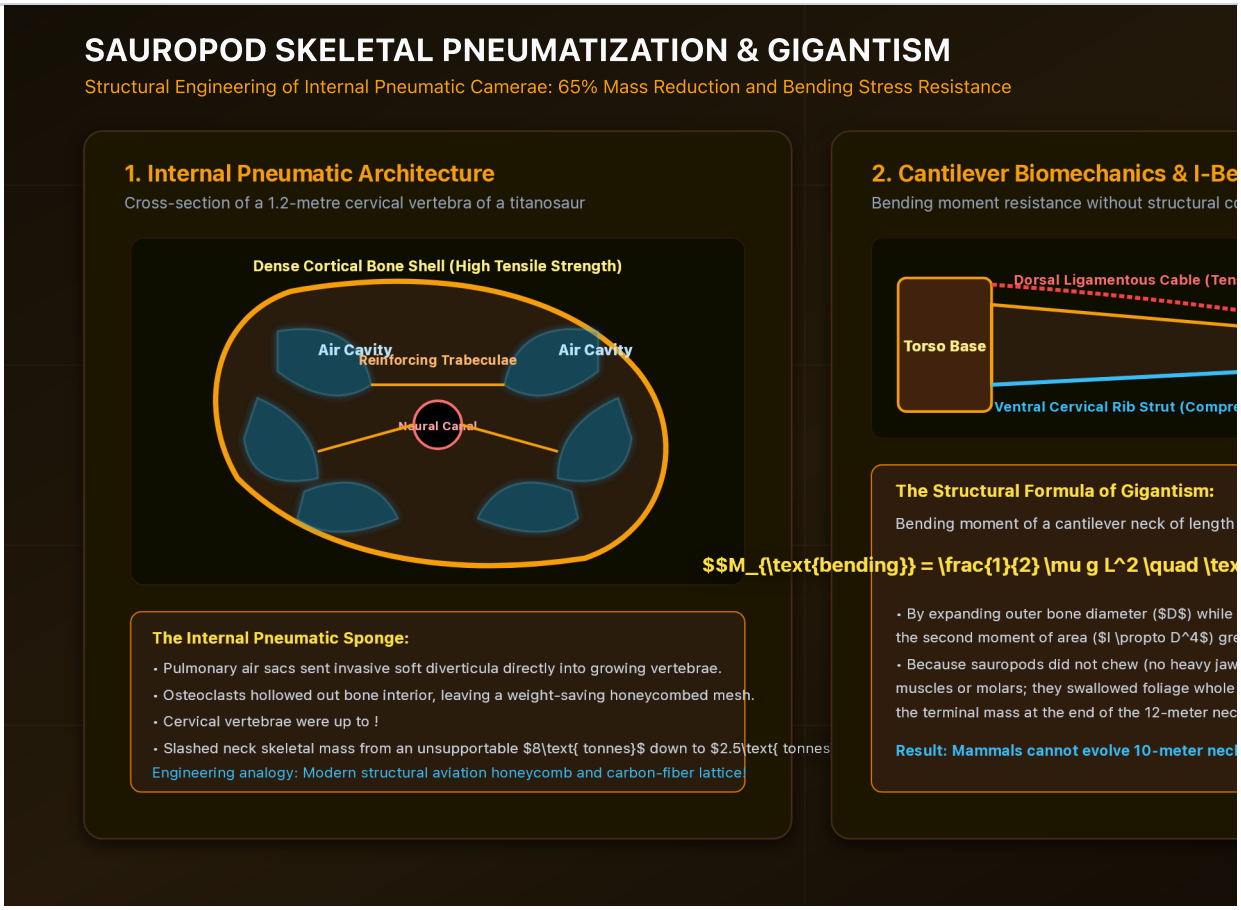


Figure 12.2: Structural Engineering of Sauropod Gigantism. Left: Vertebral cross-section showing extensive internal pneumatic camerae (hollow air chambers) surrounded by a thin, dense cortical bone shell and reinforcing trabeculae struts, slashing mass by 65%. Right: Cantilever biomechanics illustrating the bending moment formula and the critical role of a tiny, chewing-free head.

The secret lay in **Postcranial Skeletal Pneumatization (PSP)**. Soft-tissue diverticula from the cervical and thoracic pulmonary air sacs actively infiltrated the growing vertebrae, excavating deep hollow cavities known as **pneumatic camerae** and **camellae**:

- CT scans reveal that the interior of sauropod vertebrae was up to **65\text{–}70\% air by volume**, structured as a delicate, honeycombed lattice of paper-thin bony trabeculae.
- The exterior was reinforced by a dense, seamless cortical bone shell. In mechanical engineering, this mimics an optimized hollow tubular beam or an aviation honeycomb composite panel.
- By concentrating the solid bone mass at the outer perimeter (increasing the external diameter D), the second moment of area ($I \propto D^4$) expanded exponentially, conferring massive resistance against bending moments ($M = \sigma \cdot Z$) while slashing skeletal weight by more than half!

Furthermore, sauropods possessed another crucial exaptation: **they did not chew**. Because they lacked heavy molars and massive masseter jaw muscles, their skulls remained minuscule (<100\text{ kg}). A tiny head at the end of a lightweight, air-filled cantilever neck enabled sauropods to sweep a vast vertical and horizontal feeding envelope without taking a single step—a super-efficient grazing factory unmatched by any mammal.

3. Theropod Miniaturization & The Evolution of Feathers

While sauropods pursued gigantism, the bipedal, carnivorous **Theropod** lineage took the opposite evolutionary path: progressive miniaturization. Beginning with basal coelurosaurs and progressing through maniraptorans, dromaeosaurs, and troodontids, theropod body sizes shrank over fifty million years, refining skeletal traits that would eventually take to the sky.

Central to this transition was the origin of **feathers**. In 2002, evolutionary ornithologist Richard Prum proposed the groundbreaking developmental and phylogenetic model of feather evolution, which was spectacularly corroborated by the feathered dinosaur fossils of Liaoning, China:

Shakil Mahmud • Research Monograph

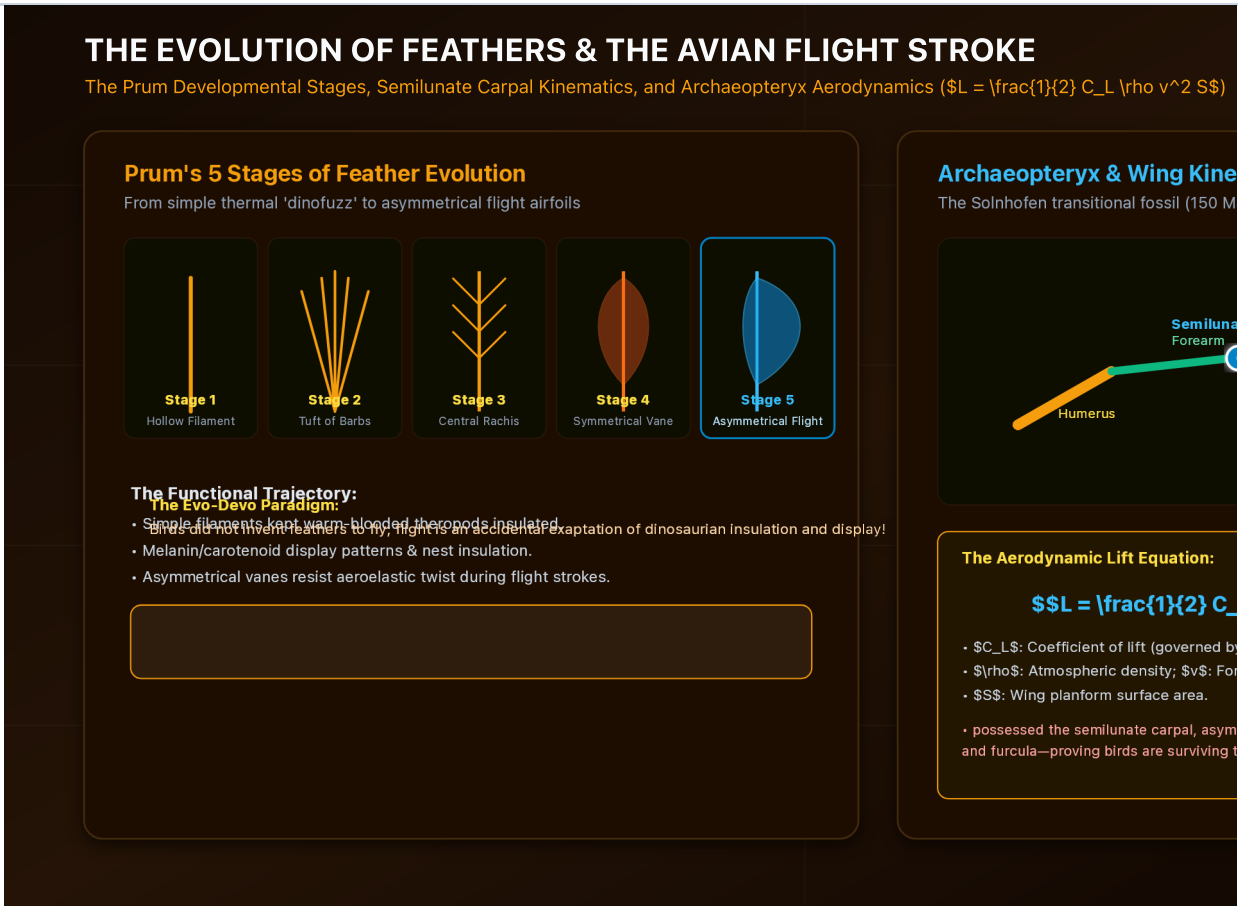


Figure 12.3: From Dinofuzz to Avian Flight. Left: Prum's five evolutionary stages: Stage 1 hollow filament (Sinosauropteryx), Stage 2 barb tuft, Stage 3 central rachis, Stage 4 symmetrical closed display vane (Caudipteryx), and Stage 5 asymmetrical aerodynamic flight airfoil. Right: Wing stroke kinematics showing the swiveling semilunate carpal wrist joint of Archaeopteryx and the aerodynamic lift equation.

1. **Stage 1 (Hollow Filament):** Unbranched cylindrical tubular follicles ("dinofuzz") found in compsognathids like *Sinosauropteryx*. Its function was strictly **thermal insulation** for high-metabolic theropods.
2. **Stage 2 (Tuft of Barbs):** Multiple unbranched barbs emerging from a single follicle collar base, forming down-like plumulaceous coats.
3. **Stage 3 (Helical Central Rachis):** Fusion of barbs into a central shaft (rachis) with open lateral barbs (e.g., *Beipiaosaurus*).
4. **Stage 4 (Symmetrical Pennaceous Vane):** Barbs evolved microscopic barbules equipped with hooklets (hamuli) that zipped adjacent barbs into a planar, wind-resistant vane. In dinosaurs like *Caudipteryx* and *Oviraptor*, these feathers bore colorful melanin bands used for **sexual display, intimidation, and brooding eggs**.
5. **Stage 5 (Asymmetrical Flight Airfoil):** The central rachis shifted off-center, making the leading vane much narrower and stiffer than the trailing vane ($w_{\text{lead}} < w_{\text{trail}}$). Under aerodynamic load, this asymmetry prevents the feather from twisting upward, creating an effective lifting surface.

> ***The Evolutionary Truth:*** *Dinosaurs did not invent feathers to fly. Feathers evolved as thermal down jackets and vibrant display banners over one hundred million years before the first bird ever flapped into the Mesozoic sky!*

4. Archaeopteryx & The Birth of Avian Flight

In 1861—barely two years after Charles Darwin published *On the Origin of Species*—quarrymen in the Late Jurassic Solnhofen limestone of Bavaria, Germany, split open a slab of lithographic stone to reveal the ultimate transitional fossil: *Archaeopteryx lithographica* (150 Ma).

Archaeopteryx was an anatomical marvel perfectly poised between non-avian theropod dinosaurs and crown birds:

- **Dinosaurian Features:** Sharp predatory teeth set in sockets, three free fingers with curved claws, a flat sternum lacking a deep keel, and a long, bony reptilian tail supported by 23 free caudal vertebrae.
- **Avian Features:** A fused wishbone (**furcula**) that functioned as an elastic spring during flapping, perching feet with a reversed hallux, and fully developed, asymmetrical Stage 5 flight feathers arranged on its wings in primary and secondary flight suites.

Crucially, *Archaeopteryx* and its dromaeosaurid cousins inherited a unique wrist bone from their predatory raptor ancestors: the **semilunate carpal**. Originally evolved in terrestrial hunters to execute a lightning-fast, two-handed grasping strike at prey, this half-moon-shaped bone permitted extreme lateral swiveling of the wrist. When feathered theropods extended this swiveling strike into the air, it became the mechanical basis for the **aerodynamic downstroke and folding upstroke** of avian flight!

According to the classical aerodynamic lift equation:

$$L = \frac{1}{2} C_L \rho v^2 S$$

Where C_L is the lift coefficient, ρ is atmospheric density, v is forward flight speed, and S is wing planform area. With cambered asymmetrical feathers creating pressure differentials and the semilunate carpal driving the stroke, theropods crossed the boundary into true, powered aerodynamic flight.

The dinosaur empire had conquered the land and the sky. But sixty-six million years ago, a six-mile-wide mountain of rock and nickel-iron was hurtling toward the Yucatán Peninsula. The Mesozoic paradise was about to come to a sudden, apocalyptic end—and in the nuclear winter that followed, it was the small, shivering mammals living in the shadows that would inherit the Earth.

Citation: Mahmud, S. (2026). "The Archosaur Empire — Dinosaurs, Pterosaurs, and the Avian Transition." In The Evolutionary Odyssey, Part 12. https://shakilmahmud.com/evolutionary-odyssey-part-12-the-archosaur-and-dinosaur-empire/

Shakil Mahmud • Research Monograph

SHAKIL MAHMUD RESEARCH MONOGRAPHS • PART XIII

The Nocturnal Mammalian Bottleneck & The K-Pg Asteroid Crucible

The Nocturnal Mammalian Bottleneck & The K-Pg Asteroid Crucible

1,484 words • November 1, 2026 • Permanent URI



Plate XIII: *Figure: Dawn of the Cenozoic (~66 Ma): the tiny nocturnal proto-primate Purgatorius and archaic mammals forage among post-impact fungal blooms and charred ferns in the atmospheric aftermath of the Chicxulub asteroid impact.*

For one hundred and fifty million years—an incomprehensible stretch of time spanning the entire Jurassic and Cretaceous periods—our mammalian ancestors lived under a biological state of siege. With dinosaurs monopolizing every diurnal ecological niche across the continents, mammals were exiled into the dark, freezing shadows of the night. Yet this prolonged exile was not an evolutionary dead end; it was the crucible that forged the defining architecture of mammalian biology. Known as the **Nocturnal Bottleneck**, this era forced mammals to sacrifice reptilian daytime color vision in exchange for an unprecedented expansion of the auditory and olfactory neocortex, the evolution of tactile whiskers, endothermic fur, and lactation. When a 10-kilometer asteroid struck Chicxulub 66 million years ago, this nocturnal survival toolkit allowed shivering burrowing mammals to outlive the dinosaur titans.

1. The Reichert-Gaupp Transformation: From Jaw Bones to Middle Ear Ossicles

One of the most astonishing homological transformations in vertebrate morphology is the evolutionary migration of the lower jaw hinge into the acoustic middle ear. Formulated originally through comparative embryology by Karl Bogislaus Reichert in 1837 and Ernst Gaupp in 1913, the **Reichert-Gaupp Theory** revealed that mammals did not evolve their three-ossicle middle ear from scratch—they dismantled their ancestors' lower jaw to build it.

In all reptiles, amphibians, and basal synapsids, the lower jaw is a composite structure constructed of up to seven distinct bones. The primary mechanical hinge connecting the lower jaw to the skull is formed by the **Articular bone** (at the posterior tip of the mandible) articulating with the **Quadrate bone** (anchored to the braincase). Only a single auditory bone existed in the ear: the slender *stapes*.

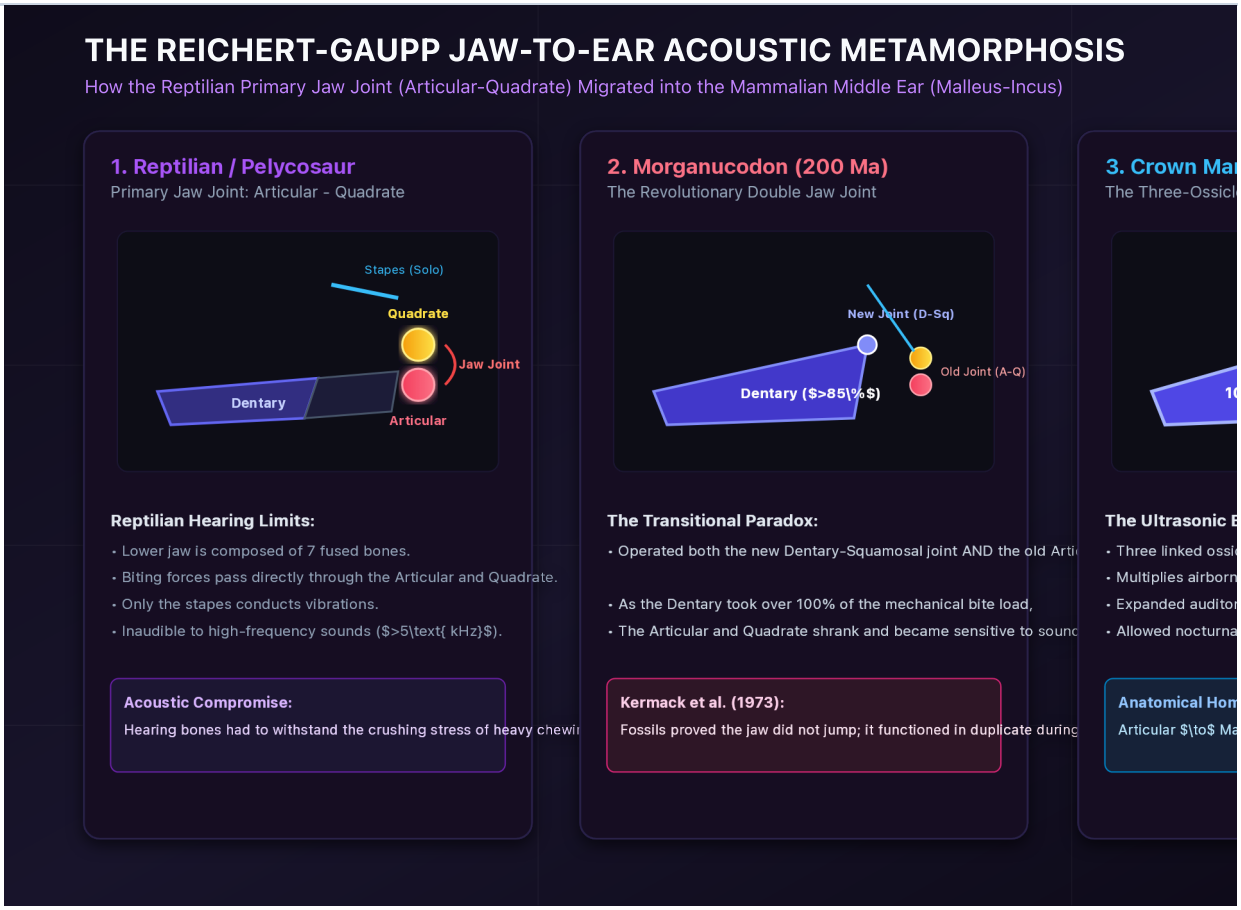


Figure 13.1: The Reichert-Gaupp Acoustic Metamorphosis. Stage 1: The ancestral reptilian condition where the primary jaw hinge is formed by the Articular and Quadrate bones. Stage 2: The transitional cynodont Morganucodon (200 Ma) operating a revolutionary double jaw joint (Dentary-Squamosal and Articular-Quadrate simultaneously). Stage 3: The crown mammalian condition where the dentary forms 100% of the mandible, freeing the Articular (Malleus) and Quadrate (Incus) to join the Stapes as a sensitive three-ossicle auditory lever.

This anatomical configuration imposed a severe functional conflict: the bones responsible for transmitting delicate sound waves were the very same bones bearing the crushing mechanical stresses of chewing. In the Late Triassic, stem-mammals like *Morganucodon* (200 Ma) solved this through a breathtaking evolutionary stepping stone: **The Double Jaw Joint**.

As the tooth-bearing **Dentary bone** enlarged to encompass over 85% of the mandible, it sprouted a backward-reaching condyle that articulated directly with the squamosal bone of the skull—forming our modern **temporomandibular joint (TMJ)**. For millions of years, *Morganucodon* chewed using both the new Dentary-Squamosal joint AND the ancient Articular-Quadrate joint simultaneously!

Once the robust Dentary-Squamosal joint bore 100% of the mechanical bite load, the ancient hinge bones decoupled completely from the feeding apparatus. They shrank dramatically, decoupled from the mandible, and migrated into the petrosal cavity of the skull:

- The **Articular** transformed into the **Malleus (Hammer)**.
- The **Quadrate** transformed into the **Incus (Anvil)**.
- The **Angular** transformed into the delicate **Ectotympanic ring** holding the eardrum.

Joined with the ancestral **Stapes (Stirrup)**, these three articulated ossicles formed an exquisite mechanical impedance-matching lever system. By converting low-force, high-amplitude eardrum vibrations into high-force, low-amplitude cochlear fluid pulses, mammals expanded their auditory bandwidth into the **ultrasonic realm (>100\text{ kHz})**—allowing them to hear the fluttering wings and rustling footsteps of insects in pitch-black night.

2. Neurosensory Remodeling: Whiskers, Neocortex, and Dichromacy

Living exclusively in the nocturnal realm for over 150 million years exerted severe, opposing selective pressures on the mammalian genome and nervous system—a phenomenon formally known as the **Nocturnal Bottleneck Hypothesis** (Heesy & Hall, 2010):

Shakil Mahmud • Research Monograph

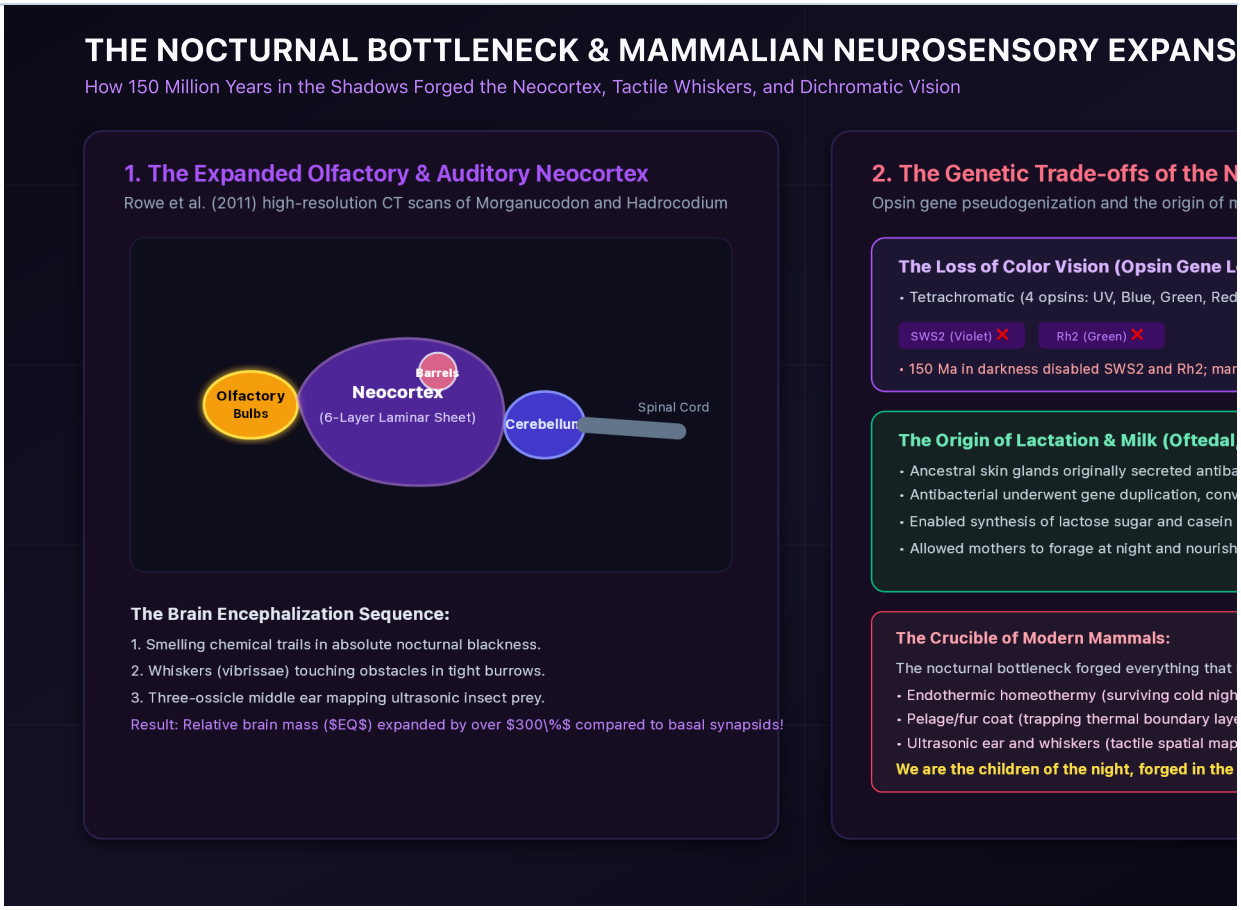


Figure 13.2: The Neurosensory Rewiring of the Mammalian Brain. Left: High-resolution endocranial reconstruction showing the massive expansion of the olfactory bulbs and the six-layered neocortex, including the specialized somatosensory barrel cortex. Right: The genetic trade-off—loss of SWS2 and Rh2 opsin genes reducing mammals to dichromatic vision, compensated by the evolutionary origin of lactation from antimicrobial lysozyme.

The Genetic Sacrifice: Loss of Color Vision

Ancestral amniotes were tetrachromats, possessing four distinct retinal cone opsin pigments: ultraviolet/violet ($SWS1$), blue ($SWS2$), green ($Rh2$), and red (LWS). In the pitch blackness of the Mesozoic night, color vision was useless; photons were scarce, favoring high-sensitivity rod photoreceptors over color cones.

Through neutral genetic drift and loss of purifying selection, mammals lost two entire opsin genes: $SWS2$ and $Rh2$ became non-functional pseudogenes. All ancestral placental and marsupial mammals were reduced to **dichromatic vision** (effectively red-green colorblind)—a visual handicap that persists in nearly all non-primate mammals today (dogs, cats, horses, and deer see the world in muted blues and yellows).

The Sensory Compensation: The 6-Layered Neocortex

To navigate the darkness, mammals reallocated neural real estate to smell and touch. High-resolution CT scans of early Jurassic stem-mammals like *Hadrocodium wui* reveal that their relative brain-to-body mass ratio (Encephalization Quotient, EQ) tripled compared to therapsids:

1. **Giant Olfactory Bulbs:** Mammalian olfactory receptors exploded to over 1,000 distinct genes, creating an exquisite chemical mapping system capable of tracking scent plumes in the dark.
2. **Vibrissae and the Barrel Cortex:** Mammals evolved specialized tactile sensory hairs—**whiskers (vibrissae)**—around the snout, richly innervated by the trigeminal nerve. In the primary somatosensory cortex, each individual whisker was mapped to an anatomically discrete cylinder of neurons known as a **cortical barrel**, creating a high-resolution, three-dimensional tactile image of tight subterranean burrows.
3. **The Origin of Lactation:** In 2002, Olav Oftedal demonstrated that ancestral skin glands originally secreted antibacterial moisture containing **lysozyme** over permeable eggshells. Through gene duplication, lysozyme mutated into **α-lactalbumin**, triggering the biochemical synthesis of lactose sugar and casein proteins: true nutritional milk! Lactation allowed mammalian mothers to forage in cold night air and return to nurse altricial offspring safely hidden within underground burrows.

3. The Chicxulub Cataclysm: The 66-Million-Year-Old Crucible

Sixty-six million years ago, the Mesozoic world came to an abrupt, violent termination. A carbonaceous asteroid measuring **10 to 15 kilometers in diameter** slammed into the shallow carbonate and sulfate platforms of the Yucatán Peninsula at a velocity of $20\ \text{km/s}$ ($45,000\ \text{mph}$): the **Chicxulub Impact**.

The impact dissipated an unfathomable 10^8 **megatons of TNT** of kinetic energy—equivalent to one hundred million Hiroshima atomic bombs detonating simultaneously. It excavated a transient crater 100 kilometers wide and 30 kilometers deep, vaporizing thousands of cubic kilometers of gypsum evaporites ($CaSO_4$) and injecting over 500 Gigatons of sulfur aerosols and 10,000 Gigatons of soot into the upper stratosphere.

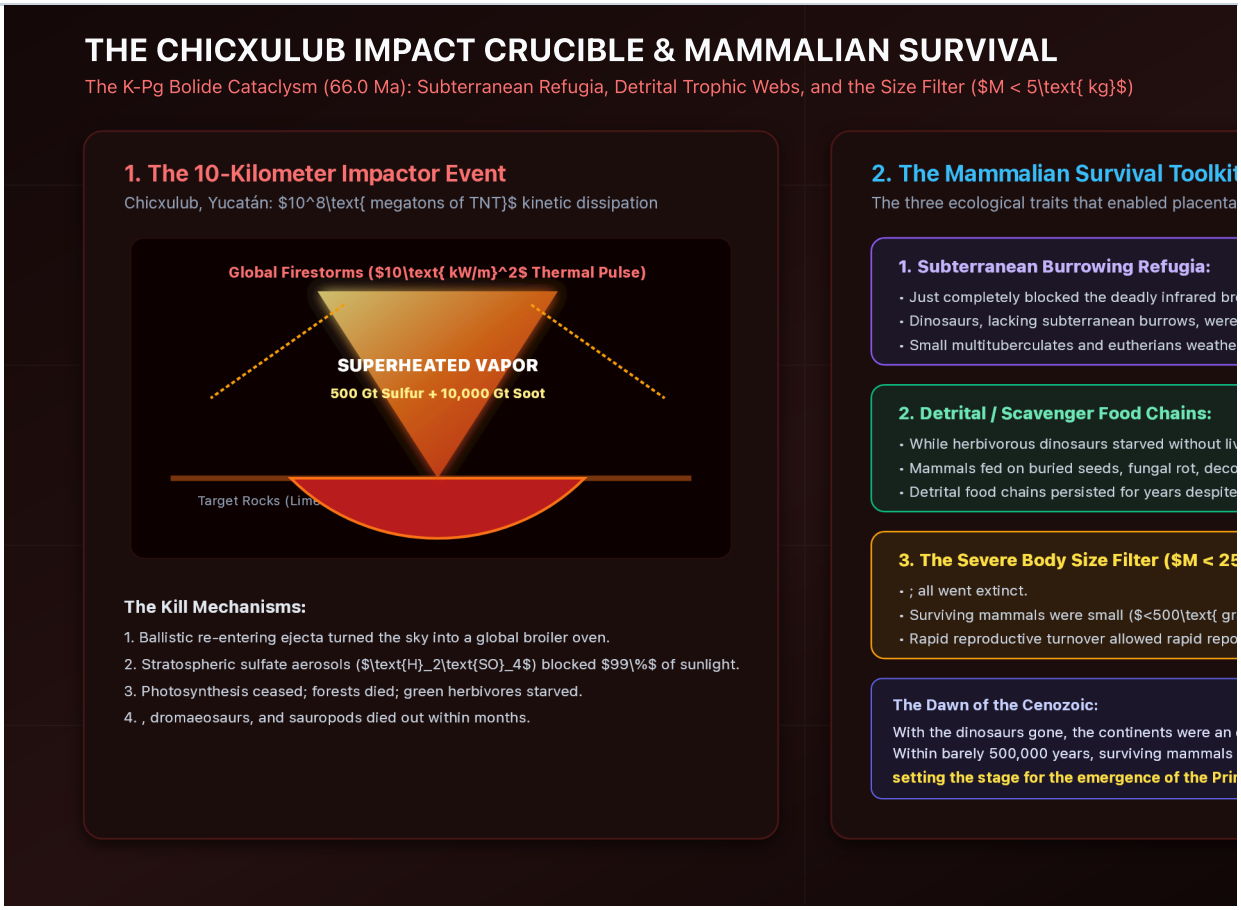


Figure 13.3: The K-Pg Bolide Cataclysm and the Survival Filter. Left: Kinetic impact schematic showing the Chicxulub crater excavation, stratospheric sulfur/soot injection, and the global 10 kW/m² infrared thermal broiling pulse. Right: The three defining traits of the mammalian survival toolkit—subterranean burrowing insulation, detrital trophic feeding, and the strict body mass filter (M < 25\text{ kg}).

The Thermal Broiler and the Long Nuclear Winter

The extinction unfolded in two lethal temporal phases:

- **The Thermal Pulse (Hours 1 to 4):** Billions of tons of sub-orbital ejecta spherules re-entered Earth's atmosphere, frictionally heating the upper air to incandescent temperatures (>1,000^\circ\text{C}). The sky glowed red-hot, delivering a global infrared thermal radiation pulse of $10\ \text{kW}/\text{m}^2$—baking Earth's surface like a broiler oven and igniting spontaneous global wildfires.
- **The Impact Winter (Years 1 to 10):** Sunlight was extinguished by stratospheric soot and sulfuric acid aerosols. Surface solar irradiance dropped by over 95%. Global temperatures plummeted by 10\text{–}15^\circ\text{C}, halting terrestrial and marine photosynthesis and collapsing the primary producers that anchored dinosaurian food webs.

4. Why Mammals Survived While Dinosaurs Died

The K-Pg boundary was not a random culling; it was an uncompromising **ecological and biophysical filter**. Every single non-avian dinosaur species on Earth perished. Why did our mammalian ancestors survive?

1. **The Subterranean Thermal Buffer:** Soil is an extraordinary thermal insulator. Theoretical modeling proves that a soil depth of just 10 to 20 centimeters completely shielded subterranean burrowers from the lethal four-hour infrared broiling pulse. Surface-dwelling dinosaurs had nowhere to hide and were incinerated alive; mammals were safely sleeping underground.
2. **Detrital Trophic Independence:** When photosynthesis collapsed, herbivorous dinosaurs (like *Triceratops* and *Edmontosaurus*) that required hundreds of kilograms of fresh green vegetation daily starved within weeks, dragging apex predators like *Tyrannosaurus rex* down with them. Mammals, by contrast, were generalist **detritivores and scavengers**. They fed on buried seed caches, fungal rot, decaying wood, and soil insects—a food web that thrived in the dark for years.
3. **The Severe Body Size Filter (M < 25\text{ kg}):** Paleontological census demonstrates that **100% of non-marine terrestrial animals exceeding 25 kg went extinct**. The surviving mammals were tiny (<500\text{ grams}), with minimal absolute caloric requirements and rapid reproductive turnover rates.

When the stratospheric soot finally settled and sunlight pierced the ash clouds of the early Paleocene, the mighty dinosaur empire was gone forever. Emerging from their subterranean burrows into an empty world of endless opportunity, the stage was set for our humble ancestors to embark on the most explosive evolutionary radiation in mammalian history—a radiation that would lead directly to the emergence of the Primates.

Shakil Mahmud • Research Monograph

Citation: Mahmud, S. (2026). "The Nocturnal Mammalian Bottleneck & The K-Pg Asteroid Crucible." In The Evolutionary Odyssey, Part 13. https://shakilmahmud.com/evolutionary-odyssey-part-13-the-nocturnal-mammalian-bottleneck-and-k-pg-impact/

SHAKIL MAHMUD RESEARCH MONOGRAPHS • PART XIV

The Paleogene Mammalian Explosion & Primate Origins

The Paleogene Mammalian Explosion & Primate Origins

1,520 words • November 1, 2026 • Permanent URI



Plate XIV: *Figure: Early primate evolution in the Eocene Thermal Maximum canopy (~50 Ma): an adapiform primate resembling Darwinius masillae (Ida) leaping between branches with grasping opposable hands, flat nails, and stereoscopic eyes.*

Sixty-six million years ago, the catastrophic Chicxulub asteroid impact erased the non-avian dinosaurs and cleared the continental ecological canvas. Into this profound vacuum stepped the surviving nocturnal mammals. Within a geological blink of ten million years during the Paleocene and early Eocene epochs (66\text{–}50\text{ Ma}), mammals underwent one of the most breathtaking adaptive radiations in Earth history. Among these pioneering placental lineages emerged our direct order: the **Primates**. Abandoning the dark forest floor, stem primates ascended into the sunlit, three-dimensional labyrinth of the dense subtropical rainforest canopy. There, intense selective pressures forged the definitive biological toolkit of humanity: grasping hands with opposable digits and flat nails, forward-facing stereoscopic eyes with postorbital protection, high-resolution color processing, and a dramatically expanded cognitive neocortex.

1. Conquering the Canopy: Competing Hypotheses of Primate Origins

What specific ecological crucible transformed a generalized insectivorous ground mammal into a specialized arboreal primate? For over a century, evolutionary biologists and biological anthropologists have debated three premier evolutionary models:

1. **The Arboreal Hypothesis (Smith & Wood Jones, 1912–1916):** Grafton Elliot Smith and Frederic Wood Jones proposed that the defining primate traits evolved primarily as generalized adaptations for life in the trees. Navigating precarious branches required grasping hands and feet rather than claws, while three-dimensional movement favored binocular vision and depth perception over olfaction.
2. **The Visual Predation Hypothesis (Matt Cartmill, 1974):** Cartmill pointed out that many non-primate arboreal mammals (such as squirrels and tree shrews) thrive in canopies using sharp claws and lateral eyes. Instead, Cartmill argued that primates evolved convergent features with terrestrial ambush predators like cats and owls: forward-facing binocular eyes with wide visual overlap and stereoscopic depth perception evolved specifically to hunt nocturnal insects in the fine-branch terminal canopy, using grasping paws to snatch prey silently.
3. **The Angiosperm Co-evolution Hypothesis (Robert Sussman, 1991):** Sussman observed that the radiation of modern primates in the early Eocene coincided precisely with the explosive evolutionary radiation of modern fruiting and flowering trees (angiosperms). Primates evolved their grasping extremities, sensitive friction-ridge tactile pads, and color vision not to hunt swift insects, but to harvest terminal-branch fruits, seeds, and nectar in the dense, tangled outer canopy.

Shakil Mahmud • Research Monograph

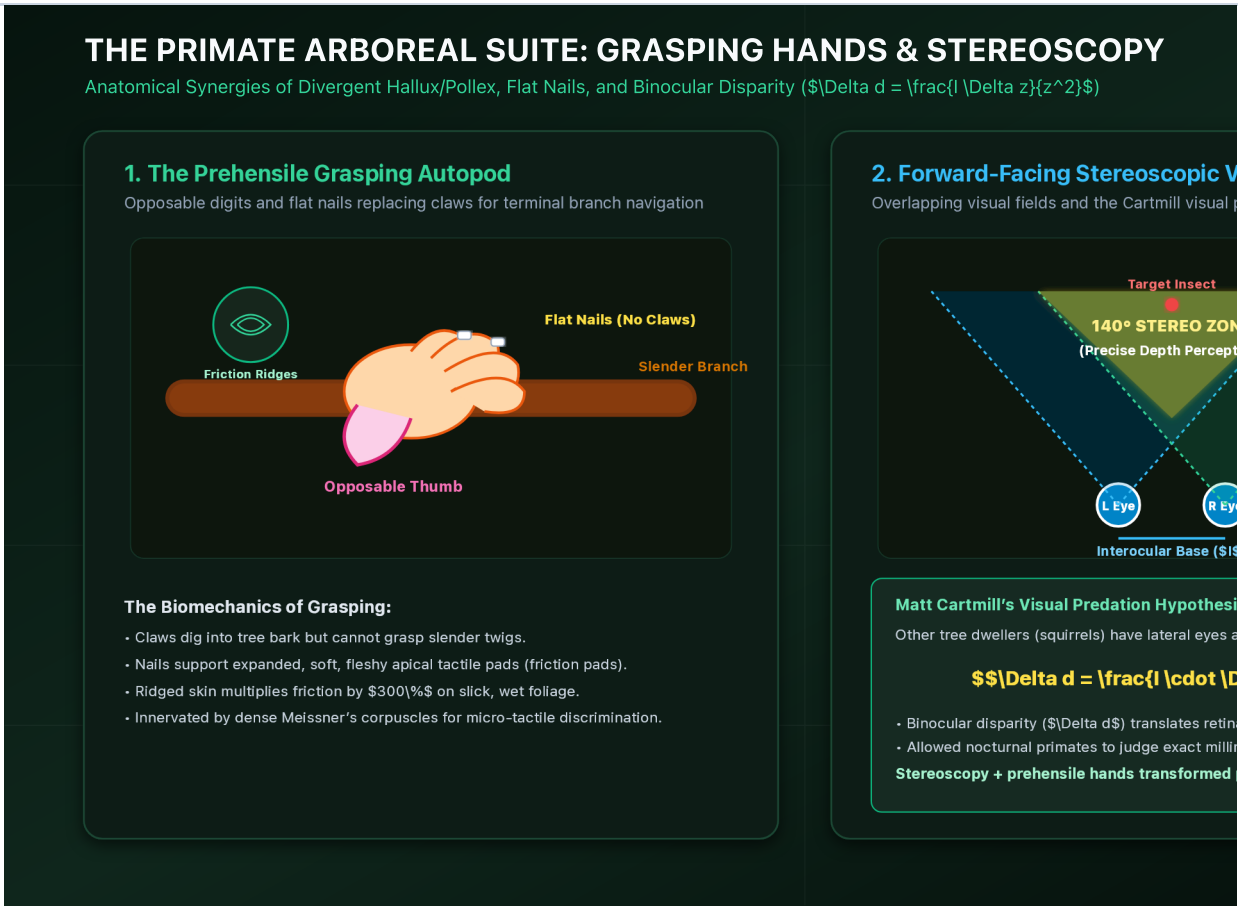


Figure 14.1: The Primate Morphological Breakthrough. Left: Comparison between ancestral clawed quadrupedal paws and the specialized primate autopod featuring an opposable hallux/pollex, flattened nails, and tactile friction ridges. Center: Optic convergence from lateral panoramic vision (typical of prey) to forward-facing stereoscopic binocular vision with postorbital bar stabilization. Right: The synthetic ecological synthesis harmonizing Cartmill's visual predation with Sussman's angiosperm frugivory.

Today, paleontologists embrace a **Synthetic Model**: basal plesiadapiforms and stem euprimates first adapted to fine-branch feeding on fruits, flowers, and exudates (as Sussman proposed), which pre-adapted the autopod for precision grasping. Once in the terminal canopy, visual predation on insects (as Cartmill proposed) drove optical convergence, the origin of the postorbital bar, and the expansion of the visual cortex.

The Anatomy of the Grasping Autopod

Unlike claws, which rely on mechanical piercing into bark, primate hands and feet evolved **opposable first digits** (the *pollex* in the hand, the *hallux* in the foot). The ungual phalanges broadened and flattened, replacing curved keratinous claws with **flat nails**. This exposed sensitive apical skin cushions richly invested with Meissner's corpuscles and papillary friction ridges (**dermatoglyphics**, or fingerprints), providing exquisite tactile feedback and non-slip friction against slick wet branches.

2. Adapoids vs. Omomyids: The Great Eocene Primate Schism

At the base of the Eocene epoch (56 Ma), true primates—known as **Euprimates** ("primates of modern aspect")—burst into the fossil record across North America, Europe, and Asia. From their inception, Euprimates were bifurcated into two dominant evolutionary super-families, representing the ancestral roots of the two major suborders living today:

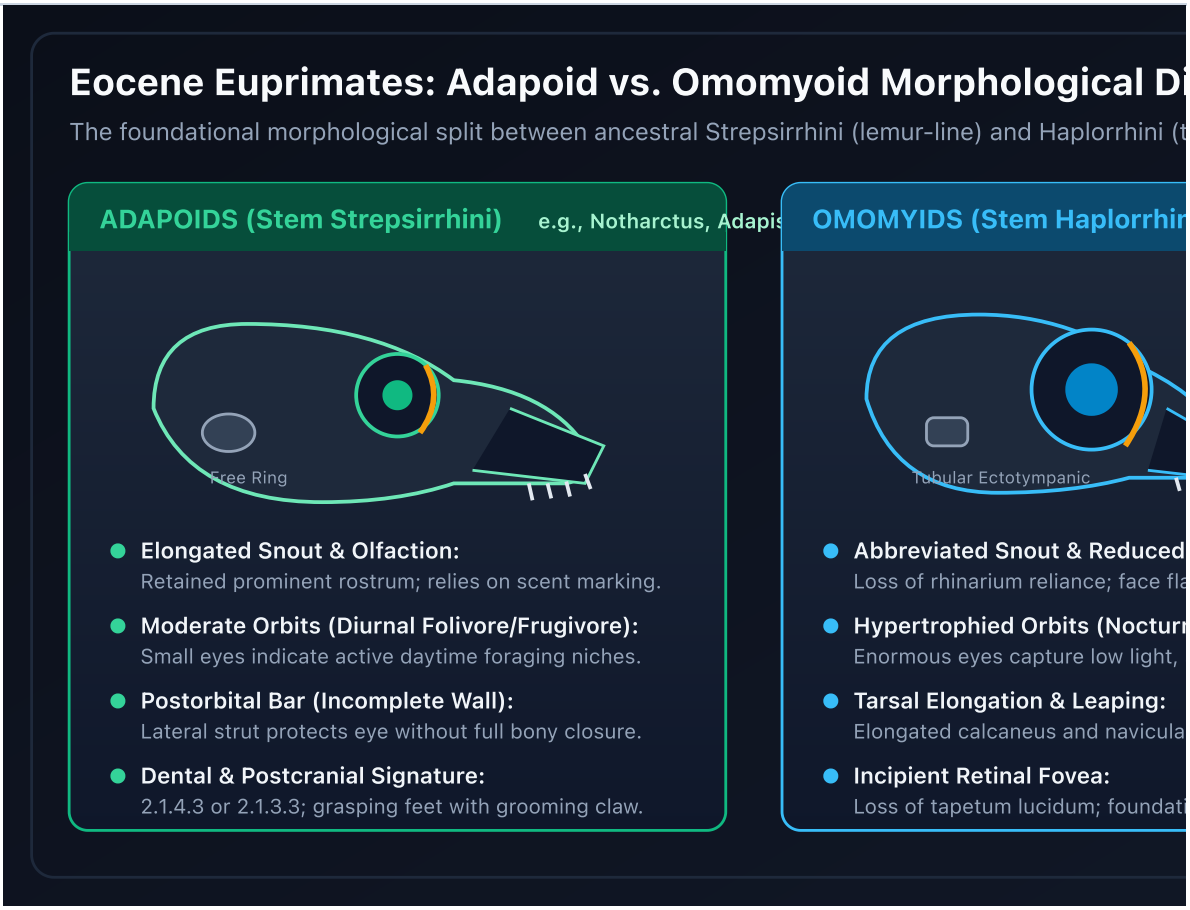


Figure 14.2: The Great Eocene Morphological Divergence. Adapoids (e.g., Notharctus, Adapis, Darwinius) represented the stem Strepsirrhines, retaining elongated rostra, smaller orbits adapted for diurnal folivory/frugivory, and ring-like ectotympanics. Omomyids (e.g., Teilhardina, Necrolemur) represented stem Haplorrhines, featuring abbreviated snouts, hypertrophied nocturnal orbits, and tubular ectotympanic bony ear canals.

1. Adapoids (Superfamily Adapoidea — Stem Strepsirrhini)

Adapoids (such as *Notharctus* in North America, *Adapis* in Europe, and the exquisitely preserved German fossil *Darwinius masillae* nicknamed "Ida") were medium-bodied arboreal primates (weighing 1\text{–}8\text{ kg}):

- **Cranial & Sensory Architecture:** Retained relatively long, pointed rostra and functional nasal turbinates, reflecting continued reliance on olfactory communication and scent marking. Their eye sockets were of moderate size, proving they were primarily **diurnal** (day-active).
- **Dentition:** Retained four premolars ($2.1.4.3$) or three ($2.1.3.3$), with shearing crests on molar cusps optimized for masticating fibrous leaves (folivory) and hard seeds.
- **Postcranial Locomotion:** Possessed long, powerful hindlimbs, grasping halluces, and mobile vertebral columns suited for quadrupedal branch running and climbing. Adapoids represent the stem clade of modern **Strepsirrhines** (the lemurs of Madagascar and lorises of Africa and Asia).

2. Omomyids (Superfamily Omomyoidea — Stem Haplorrhini)

Contemporaneous with the adapoids were the omomyids (such as *Teilhardina*, *Necrolemur*, and *Tetonius*), which were diminutive creatures typically weighing under 500 grams:

- **Cranial & Sensory Architecture:** Exhibited drastically shortened snouts and flat faces, signaling a marked reduction in olfactory apparatus in favor of vision. Their orbits were **hypertrophied (enormously enlarged)**, indicating an obligate **nocturnal** lifestyle hunting insects and small invertebrates.
- **Acoustic & Cranial Synapomorphies:** Developed a tubular ossified ectotympanic ear canal extending laterally from the auditory bulla, and postorbital plates beginning to close off the back of the eye socket—fundamental anatomical hallmarks of modern **Haplorrhines**.
- **Saltatory Locomotion:** The calcaneus and navicular bones in the ankle were significantly elongated, forming a powerful anatomical lever for vertical clinging and explosive leaping through the understory canopy—traits preserved today in their living relatives, the tarsiers, and foundational to the anthropoid monkeys and apes.

3. The PETM Hyperthermal Spike and Circumpolar Primate Radiation

How did euprimates suddenly appear simultaneously across Asia, Europe, and North America at exactly 56 million years ago? The answer lies in one of the most extreme, abrupt global climate shocks in Earth history: the **Paleocene-Eocene Thermal Maximum (PETM)**.

Shakil Mahmud • Research Monograph

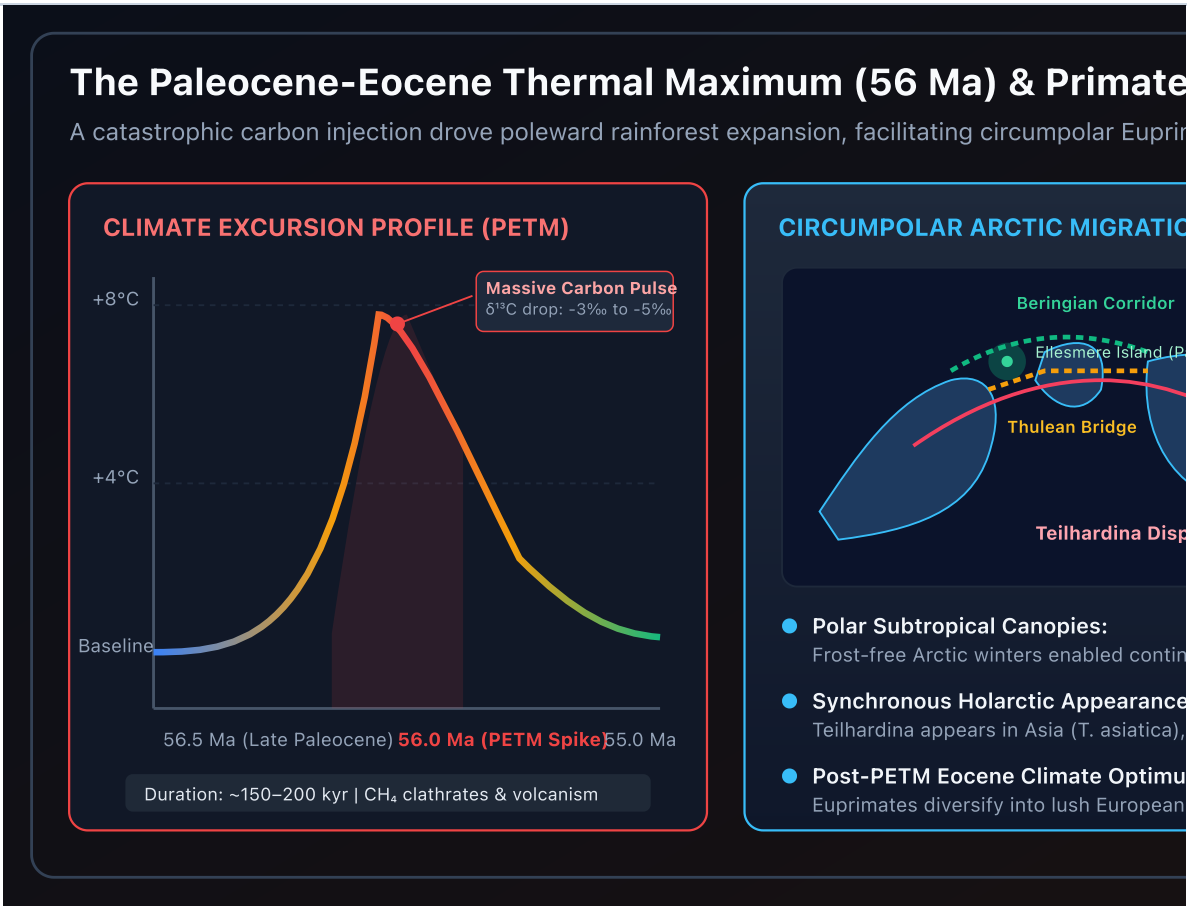


Figure 14.3: The PETM Hyperthermal Driver of Primate Dispersal. Left: The paleoclimate geochemical spike at 56 Ma showing a catastrophic negative carbon isotope excursion (CIE, $\delta^{13}C$ drop of -3‰ to -5‰) driving global surface temperatures upward by +5°C to +8°C within ~20,000 years. Right: Arctic circumpolar migration corridors (Beringia and Thulean land bridges) cloaked in frost-free subtropical palm and dawn-redwood forests at 75°N latitude, enabling Teilhardina to radiate across all northern continents in under 25,000 years.

The Geochemical Mechanism of the PETM

At approximately $56.0\ \text{Ma}$, a massive, rapid injection of light carbon (amounting to an estimated 4,500\text{–}6,000\text{ Gigatons of Carbon}, comparable to burning all modern human fossil fuel reserves) flooded the global oceans and atmosphere. Triggered by intense North Atlantic Igneous Province (NAIP) volcanism baking organic-rich sediments, paired with runaway destabilization of seafloor methane clathrates (CH_4), atmospheric pCO_2 surged beyond $1,500\ \text{ppm}$.

The resulting global greenhouse anomaly raised global temperatures by 5\text{–}8^\circ\text{C} in less than 20,000 years. Tropical and subtropical temperatures expanded relentlessly toward the poles. At 75°N latitude—in modern frozen archipelagos like Ellesmere Island and Spitsbergen—paleobotanists find fossilized *swamp cypresses, palm trees, and crocodilian reptiles*. There were no polar ice sheets; the Arctic Ocean was a warm, brackish, frost-free inland sea.

The High-Latitude Canopy Highway

Because the high Arctic was cloaked in dense, continuous subtropical rainforest, the high-latitude continental bridges connecting Asia, North America, and Europe (the **Beringian Land Bridge** across the Pacific and the **Thulean / De Geer Bridges** across the North Atlantic) transformed into lush arboreal corridors. Basal euprimates, incapable of surviving freezing winter temperatures, were able to migrate across the top of the globe without ever descending from the tree canopy.

Paleontologist Philip Gingerich and his colleagues discovered that the basal omomyid *Teilhardina* dispersed across Asia (*T. asiatica*), Europe (*T. belgica*), and North America (*T. brandti*) in less than $25,000\ \text{years}$—a stunningly rapid intercontinental radiation fueled entirely by the PETM thermal corridor. The warming created the golden age of early primates, populating the northern hemisphere with vibrant arboreal lineages.

4. Encephalization and the Foundations of Anthropoidea

The transition from basal plesiadapiforms to crown Euprimates was not merely a locomotor and sensory adaptation; it was an intellectual revolution. Relative brain size—measured by the **Encephalization Quotient** (EQ)—expanded dramatically beyond any contemporary mammalian baseline.

Life in the high canopy demanded complex cognitive processing:

- **3D Spatial Mapping:** Leaping through fine branches required calculating landing vectors, branch elasticity, and spatial trajectories in real time, driving the expansion of the parietal cortex and cerebellar coordination circuits.

- **Episodic Foraging Memory:** Angiosperm trees produce fruit asynchronously across vast forest expanses. Primates that could remember which trees were ripening, where they were located, and the fastest arboreal pathways between them gained a decisive caloric advantage, stimulating temporal lobe and hippocampal expansion.
- **The Visual Cortex Explosion:** The primary visual cortex ($V1$) expanded to occupy the entire posterior pole of the occipital lobes. New associative visual areas ($V2, V3, V4, MT$) evolved to decode color contrast, fine texture, and high-speed motion parallax.

By the late Eocene and early Oligocene (36\text{–}34\text{ Ma}), as global climates cooled and the grand Eocene forests contracted, these arboreal, large-brained, visually acute euprimates laid the morphological foundation for the next monumental chapter in our family history: the rise of the **Anthropoidea**—the true higher primates, monkeys, and apes.

Citation: Mahmud, S. (2026). "The Paleogene Mammalian Explosion & Primate Origins." In The Evolutionary Odyssey, Part 14. https://shakilmahmud.com/evolutionary-odyssey-part-14-the-paleogene-mammalian-explosion/

Shakil Mahmud • Research Monograph

SHAKIL MAHMUD RESEARCH MONOGRAPHS • PART XV

The Catarrhine Split, Trichromatic Vision & The Miocene Ape Radiations

The Catarrhine Split, Trichromatic Vision & The Miocene Ape Radiations

1,580 words • November 1, 2026 • Permanent URI



Plate XV: *Figure: Early hominoid ape Proconsul africanus (~18 Ma) moving through the lush Miocene canopy of East Africa, illustrating the evolutionary loss of the external tail, pronograde quadrupedy, and Y-5 molar morphology.*

Thirty-four million years ago, at the Eocene-Oligocene transition, global temperatures plummeted, transforming the lush polar rainforests of the Eocene into ice sheets. In this cooling, seasonal world, the surviving anthropoid primates in Africa and Arabia underwent a decisive evolutionary bifurcation: the divergence of the **Platyrrhini** (flat-nosed New World monkeys, who rafted across a narrower Atlantic Ocean to South America) from our direct ancestral lineage, the **Catarrhini** (downward-facing nosed Old World monkeys and apes). Over the next twenty million years, Catarrhines achieved profound biological milestones: a genomic duplication that restored full trichromatic color vision, an ancient transposable element insertion that deleted the external tail, and an explosive Miocene adaptive radiation that forged the orthograde, suspensory body plan shared by all apes and humans.

1. The Opsin Gene Duplication: Reclaiming the Trichromatic World

As explored in Part 13, stem mammals sacrificed two color opsin genes ($SWS2$ and $Rh2$) during their 150-million-year Mesozoic nocturnal exile, reducing ancestral placental mammals to dichromatic vision (red-green colorblindness). For tens of millions of years, early primates navigated the canopy using only short-wavelength ($SWS1$, blue, ~420 nm) and long-wavelength (LWS, green-yellow, ~540 nm) photoreceptors.

Approximately 35\text{–}30\text{ Ma}, in the ancestral catarrhine lineage inhabiting the Fayum Depression of Egypt, an unequal homologous crossing-over event altered primate vision forever. The LWS opsin locus on the X chromosome underwent a **tandem gene duplication**, creating two adjacent, nearly identical opsin genes:

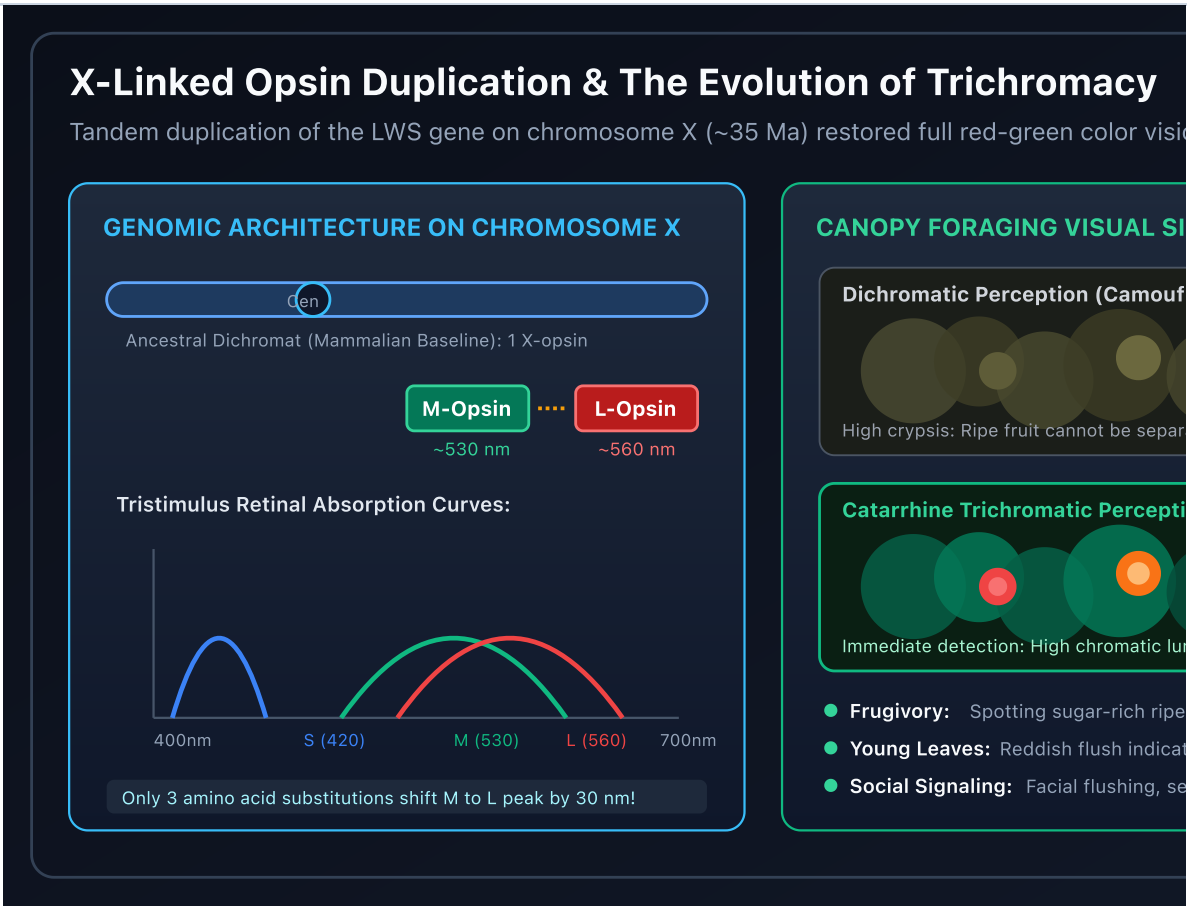


Figure 15.1: The Genomic Restoration of Trichromatic Vision. Left: Tandem duplication on the X chromosome creating the distinct M-opsin (~530 nm) and L-opsin (~560 nm) genes, driven by only three key amino acid substitutions (the 'five-sites rule'). Right: Visual ecological simulation showing the dramatic contrast difference —dichromatic camouflage versus trichromatic target pop-out, revolutionizing fruit foraging and leaf discrimination.

The Five-Sites Rule and Spectral Tuning

Following duplication, the two tandem genes accumulated subtle point mutations. Groundbreaking genetic work by Jeremy Nathans and Gerald Jacobs demonstrated that just **three to five critical amino acid substitutions** (at positions 180, 277, 285, 308, and 309 inside the retinal-binding transmembrane pocket) shifted the peak absorption wavelength (λ_{max}) of one duplicated opsin by $30\ \text{nm}$:

- The ancestral-derived **M-Opsin (Medium-Wavelength Sensitive)** retained peak sensitivity at $\lambda_{max} \approx 530\ \text{nm}$ (Green).
- The newly diverged **L-Opsin (Long-Wavelength Sensitive)** shifted peak sensitivity to $\lambda_{max} \approx 560\ \text{nm}$ (Red).

Working in conjunction with the autosomal short-wavelength opsin (**S-Opsin**, on Chromosome 7, $\lambda_{max} \approx 420\ \text{nm}$), Catarrhine primates regained **routine trichromacy**. Unlike New World Platyrrhines (where trichromacy is polymorphic and mostly restricted to heterozygous females), every single male and female Old World monkey, ape, and human inherited two distinct X-linked opsin genes.

The Triple Selective Engine

1. **Frugivory (The Ripe Fruit Hypothesis):** Ripe figs and fruits reflect wavelengths >580\text{ nm}. To a dichromat, red fruits blend seamlessly into green foliage. To a trichromat, red fruit triggers instant chromatic luminance "pop-out" across hundred-meter distances.
2. **Folivory (The Young Leaf Hypothesis):** In seasonal tropical forests, mature leaves are saturated with indigestible cellulose and toxic tannins. Young, nutrient-rich leaves flush crimson and orange with protective anthocyanins. Trichromacy allowed Catarrhines to pinpoint high-protein edible leaves at a glance.
3. **Socio-Sexual Signaling:** Trichromacy facilitated naked facial skin and sexual swellings that flush with oxygenated hemoglobin (e.g., baboon chests, human blushing), transforming color into a high-fidelity social communication channel.

2. The Genetic Mystery of Tail Loss: The TBXT Alu Insertion

For roughly 40 million years of primate history, every known fossil primate possessed a functional external tail. In tree-dwelling monkeys, the tail is an active biomechanical rudder, providing dynamic angular momentum balance during high-speed arboreal running and leaping. Yet by **25 million years ago**, in the common ancestor of all apes and humans (the superfamily **Hominoidea**), the external tail vanished entirely, reduced to an internal vestigial fused structure: the **coccyx**.

For decades, the genetic catalyst of this dramatic macroevolutionary transition remained a profound riddle. In February 2024, a landmark study published in *Nature* by Bo Xia, Jef Boeke, Itai Yanai, and their team uncovered the exact genomic smoking gun:

Shakil Mahmud • Research Monograph

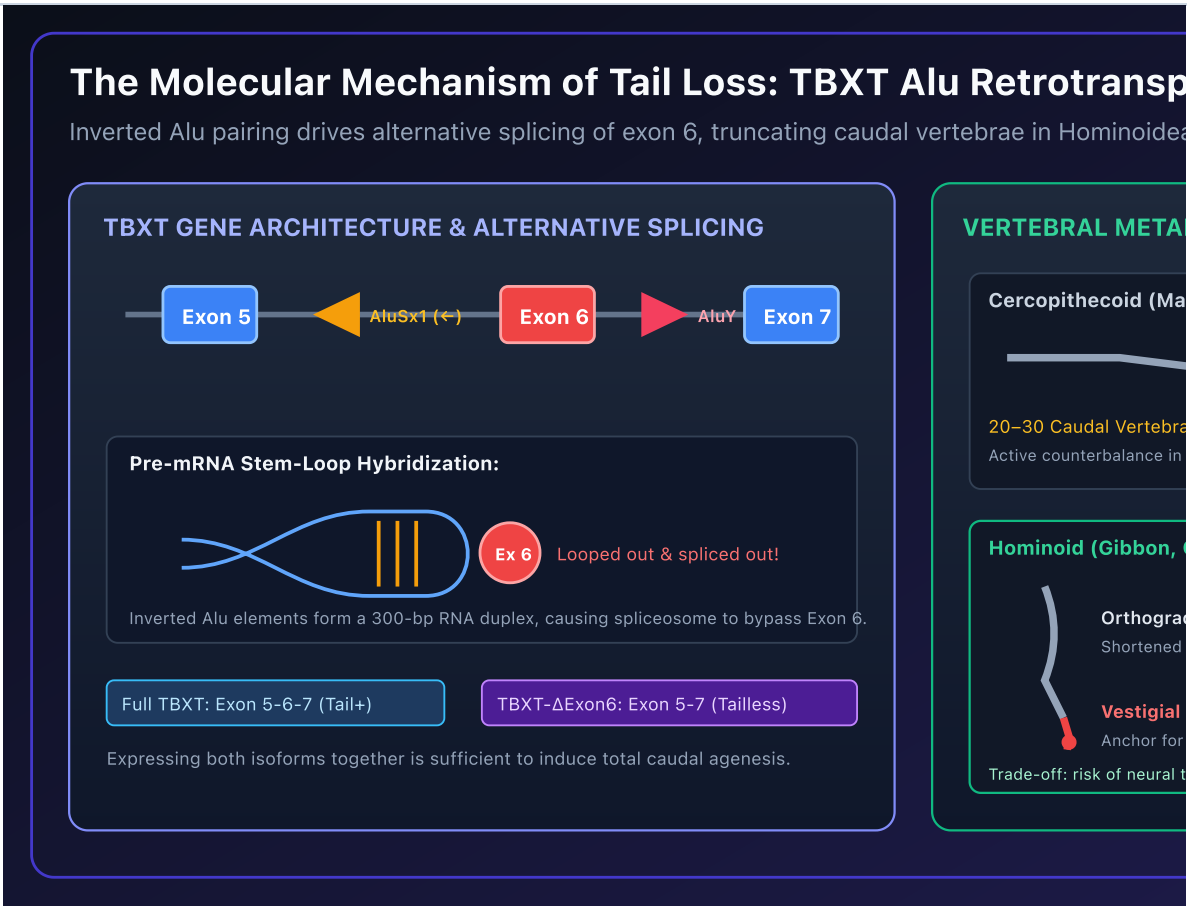


Figure 15.2: The Molecular Mechanism of Ape Tail Loss. Left: Insertion of an ape-specific AluY retrotransposon into intron 6 of the TBXT gene forms a 300-base-pair inverted RNA stem-loop with the ancestral AluSx1 element in intron 5, causing the spliceosome to skip Exon 6. Right: Biomechanical consequence—the transition from a flexible 25-vertebrae monkey caudal counterweight to a rigid, fused coccyx supporting an orthograde pelvic floor.

The Jumping Gene Mechanism

The *TBXT* gene (formerly known as *Brachyury* or *T*) encodes an ancient T-box transcription factor essential for embryonic notochord and caudal vertebral specification. The researchers discovered that approximately 25 Ma, an **Alu mobile genetic element (AluY)** hopped into *intron 6* of the *TBXT* gene in a stem hominoid.

Crucially, an older primate Alu element (**AluSx1**) was already present in *intron 5*—oriented in the reverse (inverted) direction. When the pre-mRNA was transcribed:

- The two complementary Alu RNA sequences paired up, forming a tight, 300-base-pair double-stranded RNA stem-loop.
- This hairpin loop physically pinched out **Exon 6**, concealing its splice donor and acceptor sites from the cellular spliceosome.
- As a consequence, hominoid cells began producing two distinct splicing isoforms: the full-length transcript and a truncated isoform lacking exon 6 ($TBXT^{\Delta exon6}$).

When the researchers inserted this identical Alu element into genetically engineered mice, the mice were born completely tailless! The simultaneous expression of both isoforms disrupts caudal somite elongation just enough to terminate tail growth while leaving normal spinal cord development intact.

The Biomechanical Trade-Off

Why did natural selection preserve tail loss? In an upright, climbing ape, a dangling tail offered minimal counterbalance while increasing body mass and drag. Taillessness enabled the evolution of a reinforced, muscular **pelvic floor (the levator ani complex)**, capable of supporting visceral organ weight during orthograde (vertical) posture. However, this evolutionary leap came at a cost: the authors noted that mice expressing $TBXT^{\Delta exon6}$ exhibited increased susceptibility to **neural tube defects** (spina bifida)—an evolutionary scar preserved in human medical epidemiology to this day.

3. The Miocene Ape Paradise: Orthogrady and the Y-5 Molar Pattern

During the Miocene epoch (23\text{–}5.3\text{ Ma}), the world experienced the true **Golden Age of Apes**. While today only five genera of hominoids survive (gibbons, orangutans, gorillas, chimpanzees, and humans), the Miocene Old World was teeming with ape diversity: over **40 extinct genera and 100 species** flourished across Africa, Europe, and Asia.

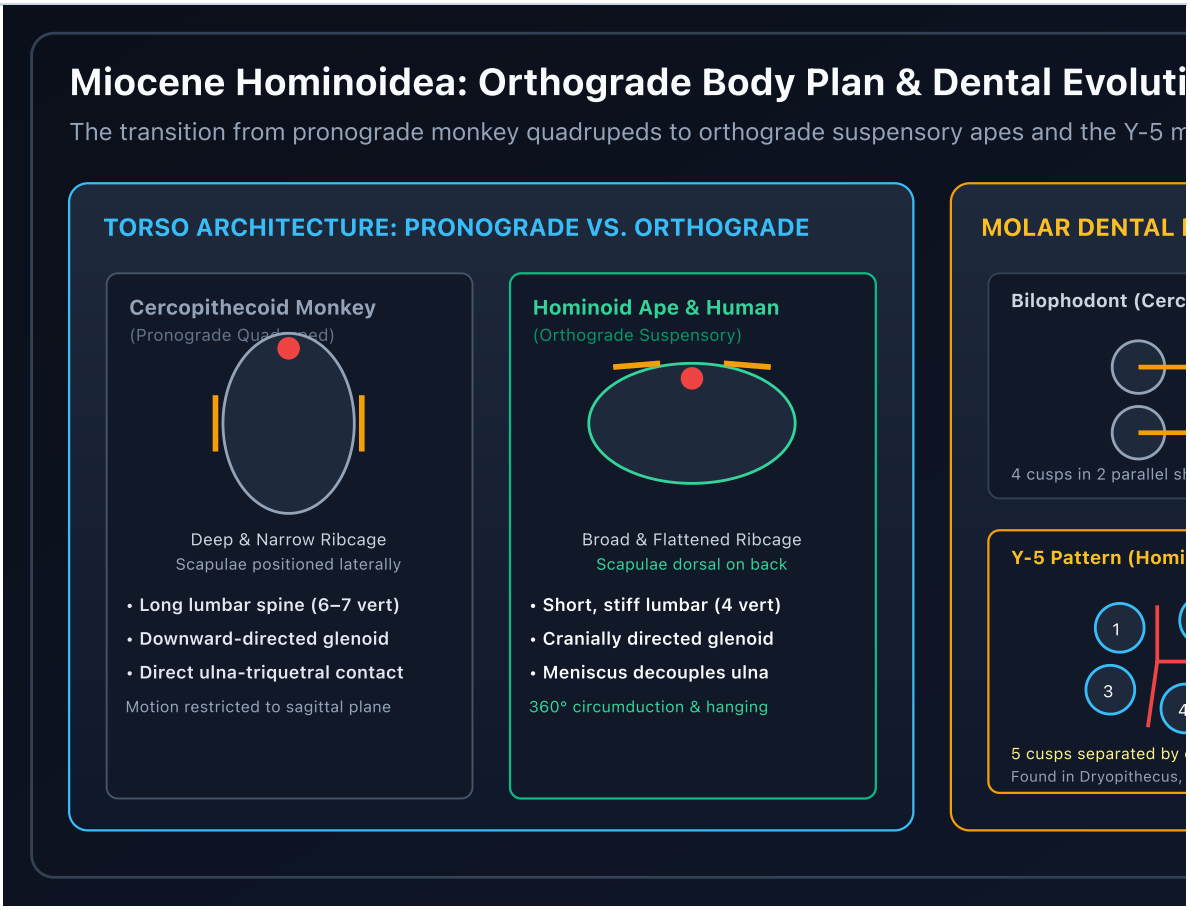


Figure 15.3: The Miocene Hominoidea Morphological Revolution. Left: Cross-sectional and skeletal comparison between pronograde cercopithecoid monkeys (narrow deep ribcage, lateral scapulae, long flexible lumbar spine) and orthograde hominoids (broad shallow ribcage, dorsal scapulae, short stiff lumbar spine, and flexible wrist meniscus). Right: Dental phylogeny contrasting monkey bilophodont molars with the diagnostic hominoid Y-5 molar cusp architecture.

The Orthograde Biomechanical Revolution

Basal Miocene apes like *Proconsul* (20 Ma) in Kenya still walked along the tops of branches on all fours (pronograde arboreal quadrupedalism). But as the early Miocene progressed into the middle and late Miocene, taxa such as *Morotopithecus*, *Pierolapithecus*, *Dryopithecus*, and *Hispanopithecus* dismantled the monkey quadrupedal body plan, constructing the **orthograde (upright) suspensory Bauplan**:

1. **Broad, Shallow Ribcage:** Monkeys have a laterally compressed, deep ribcage that keeps limbs directly beneath the body for galloping. Apes widened the thorax dorsoventrally, moving the center of gravity backward toward the vertebral column.
2. **Dorsal Scapulae and Cranial Glenoid Fossa:** The shoulder blades migrated from the sides of the chest onto the back (dorsal surface). The shoulder socket (glenoid fossa) angled upward, granting the arm a full 360° range of motion and enabling below-branch arm hanging (brachiation and clambering).
3. **Decoupled Ulnar Wrist Meniscus:** In monkeys, the ulna articulates directly with the triquetral bone of the wrist, locking the hand in a stable walking posture. In hominoids, the ulna retreated, replaced by a fibrocartilaginous meniscus disc. This granted the ape wrist extraordinary degrees of adduction, abduction, and rotation.
4. **Shortened Lumbar Spine:** Monkeys have 6 to 7 flexible lumbar vertebrae for bounding. Apes reduced their lumbar vertebrae to 4 or 5, stiffening the lower back to resist mechanical buckling during upright climbing.

The Dental Signature: The Y-5 Molar Pattern

In the fossil record, where postcranial skeletons are often lost to time, paleontologists diagnose hominoids through dental morphology. While Old World Cercopithecoid monkeys evolved **bilophodont molars** (four cusps connected in two parallel shearing ridges, specialized for masticating tough leaves), all hominoids retain the ancestral **Y-5 Molar Pattern**:

- The lower molar possesses **five distinct cusps** (protoconid, metaconid, hypoconid, entoconid, and hypoconulid).
- The valleys between cusps 2 and 3 form an unmistakable **"Y"-shaped groove system**.

From 12-million-year-old *Dryopithecus* in Europe to *Sivapithecus* in Pakistan, to modern chimpanzees and the teeth in your own lower jaw, the Y-5 molar remains an indelible morphological signature of our Miocene ape ancestry.

4. The Late Miocene Bottleneck: The African Stage is Set

Between 10 and 6 million years ago, the Miocene paradise ended. Continental drift closed the Tethys Seaway, the Tibetan Plateau surged upward, and the East African Rift system began to tear eastern Africa apart. Global climates grew colder and drier.

Shakil Mahmud • Research Monograph

The vast subtropical forests of Europe and Asia withered into open temperate woodlands. The magnificent Eurasian apes—*Dryopithecus*, *Ouranopithecus*, *Lufengpithecus*, and the giant 3-meter-tall *Gigantopithecus*—faced catastrophic extinctions. In Africa, the unbroken equatorial rainforest fractured into a mosaic of gallery forests, open woodlands, and savanna grasslands.

Trapped in this changing African mosaic, a small, resilient population of orthograde, tailless, large-brained, trichromatic apes stood at the threshold of a new ecological frontier. As the trees grew further apart, walking between them became a matter of life and death. The stage was set for the Great Ape Split and the emergence of habitual bipedalism.

Citation: Mahmud, S. (2026). "The Catarrhine Split, Trichromatic Vision & The Miocene Ape Radiations." In The Evolutionary Odyssey, Part 15. https://shakilmahmud.com/evolutionary-odyssey-part-15-the-catarrhine-split-and-miocene-apes/

SHAKIL MAHMUD RESEARCH MONOGRAPHS • PART XVI

The Great Ape Split & The Biomechanics of Habitual Bipedalism

The Great Ape Split & The Biomechanics of Habitual Bipedalism

1,633 words • November 1, 2026 • Permanent URI



Plate XVI: *Figure: The dawn of habitual bipedalism: early hominin Ardipithecus ramidus ('Ardi', ~4.4 Ma) walking upright across an ancient Ethiopian woodland mosaic while retaining grasping big toes for climbing.*

Between seven and eight million years ago, in the volatile tectonic cradle of equatorial Africa, our evolutionary journey crossed its ultimate Rubicon: the divergence of the human clade (tribe **Hominini**) from our closest living evolutionary cousins, the chimpanzees and bonobos (genus **Pan**). While our genomes remain 98.77% identical at the single-nucleotide level, this speciation event initiated a morphological transformation unprecedented in mammalian history: the adoption of **obligate habitual bipedalism**. Abandoning knuckle-walking and four-limbed arboreal scurrying, our earliest ancestors stood upright upon two feet—a biomechanical revolution that reconstructed the pelvis, realigned the lower limb musculature, and permanently emancipated the forelimbs to manipulate the material world.

1. The Pan-Homo Divergence & The Molecular Clock

In 1871, Charles Darwin famously prophesied in *The Descent of Man* that because African gorillas and chimpanzees are anatomically closest to humans, Africa was the most probable cradle of human origins. A century later, molecular biology vindicated Darwin beyond his wildest dreams. By comparing homologous protein and DNA sequences, Allan Wilson and Vincent Sarich calibrated the **Hominoid Molecular Clock**, proving that humans and African apes did not diverge thirty million years ago (as paleoanthropologists had long assumed), but in the very late Miocene ($7\text{–}8\text{ Ma}$):

Shakil Mahmud • Research Monograph

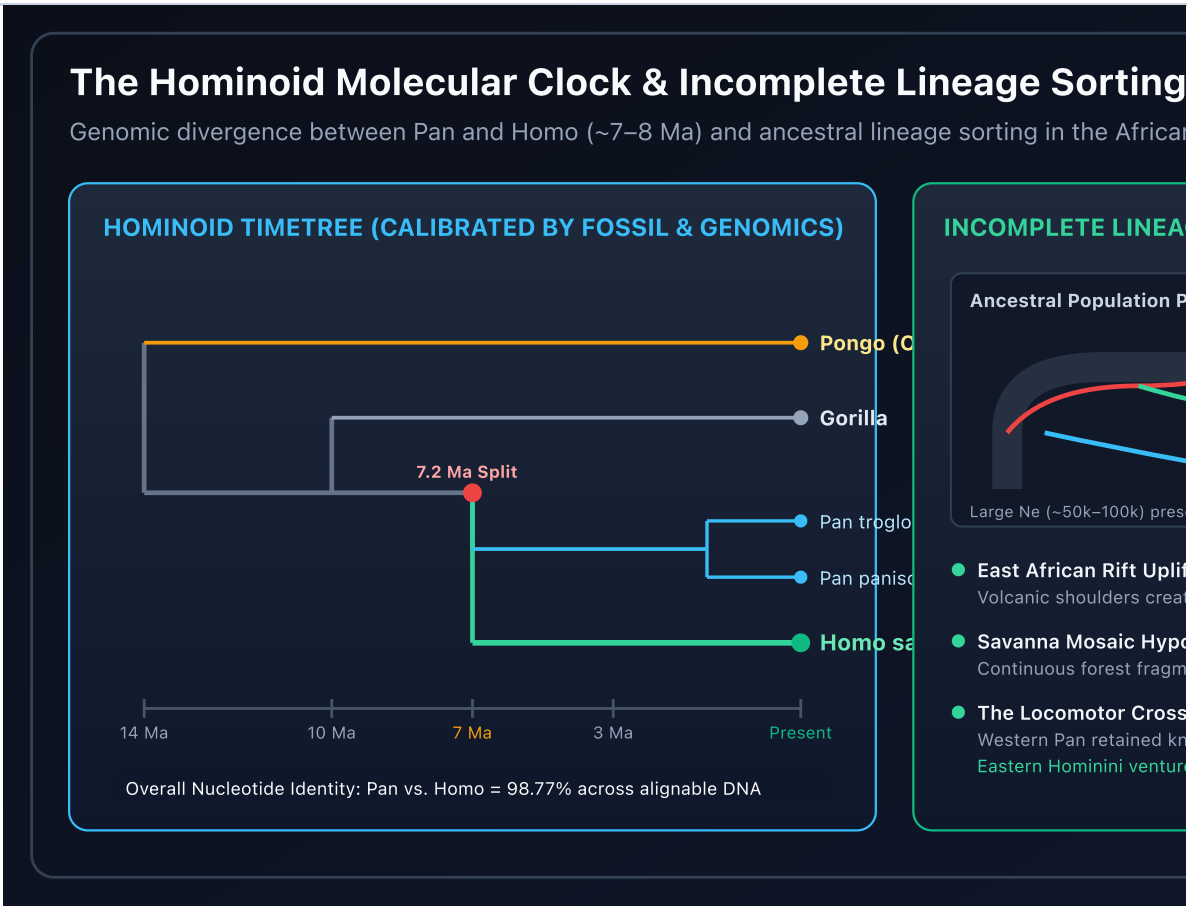


Figure 16.1: The Hominoid Molecular Clock & Incomplete Lineage Sorting. Left: Calibrated molecular timetree showing the divergence of Orangutans (~14 Ma), Gorillas (~10 Ma), and the Pan-Homo split (~7.2 Ma), followed by the chimpanzee-bonobo split (~1.8 Ma). Right: Incomplete Lineage Sorting (ILS) illustrating how ancestral genetic polymorphisms cause ~1.5% of human gene trees to cluster closer to gorillas than to chimpanzees despite an overall 98.77% Pan-Homo genome identity.

Incomplete Lineage Sorting (ILS)

Modern whole-genome sequencing has revealed a fascinating nuance of our ancestry: while the species tree clearly unites humans and chimpanzees as sister taxa, approximately **1.5% of our individual gene trees cluster humans closer to gorillas than to chimpanzees**! This phenomenon, known as **Incomplete Lineage Sorting (ILS)**, occurs because the ancestral hominine population prior to the gorilla and chimpanzee splits was genetically vast ($N_e \approx 50{,}000–100{,}000$ individuals). Polymorphic ancestral alleles failed to coalesce prior to subsequent speciation nodes, preserving discordant gene phylogenies in our chromosomes today.

The Tectonic Engine: East African Aridification

What triggered this fateful split? Tectonic geophysicists point to the formation of the **East African Rift System**. Between 10 and 6 Ma, tectonic mantle plumes domed and fractured the African continental crust, elevating the western and eastern rift shoulders thousands of meters into the sky. These towering mountain chains created a devastating rain shadow: while moist Atlantic winds continued to nourish dense rainforests in the Congo Basin (where ancestral *Pan* evolved), eastern Africa grew progressively cooler, more seasonal, and arid.

The continuous rainforest fractured into a mosaic of closed gallery woodlands, seasonal scrub, and open savannas. In this fragmented landscape, ancestral hominins faced a life-or-death caloric challenge: finding sufficient food required traversing increasingly wide open terrestrial gaps between scattered groves of trees.

2. The Biomechanical Engine of Habitual Bipedalism

Walking upright on two hindlimbs is an exceptionally rare, mechanically perilous mode of locomotion. Birds achieve it horizontally with a stabilizing counterbalancing tail; only humans among living mammals balance an upright, vertical trunk directly over extended hindlimbs. Yet bipedalism proved to be a metabolic miracle:

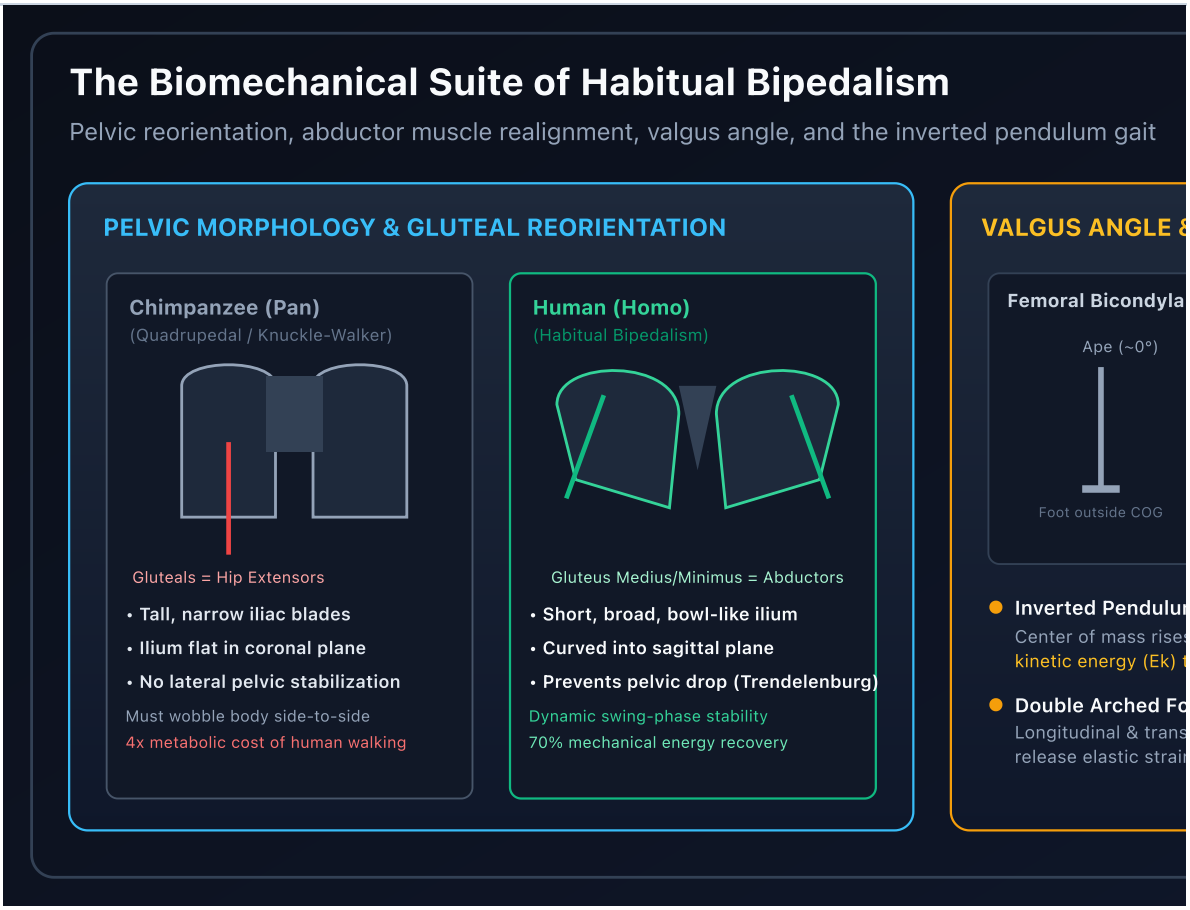


Figure 16.2: The Biomechanical Suite of Habitual Bipedalism. Left: Comparative pelvic morphology between chimpanzees (tall, flat, coronal ilium acting as hip extensors) and humans (short, broad, basin-shaped ilium curved into the sagittal plane, converting gluteus medius/minimus into lateral abductors to prevent Trendelenburg pelvic drop). Right: The femoral bicondylar (valgus) angle aligning the knee and foot directly beneath the body's center of mass, enabling the high-efficiency inverted pendulum gait.

The Inverted Pendulum Gait

Human bipedal walking operates on the physical principle of an **Inverted Pendulum**. During the stance phase of every step, the center of mass (COM) vaults over a rigid stance leg like an inverted pendulum. At the crest of the vault, forward kinetic energy (E_k) is converted into gravitational potential energy (E_p); as the body falls forward into the next step, potential energy is converted back into kinetic energy.

Biomechanical studies by Herman Pontzer and David Raichlen revealed that this mechanical exchange achieves $\sim 70\%$ **energy recovery efficiency**. In contrast, chimpanzee knuckle-walking requires continuous muscular effort with zero inverted-pendulum energy exchange, burning **four times more calories per kilometer** than a walking human! In an aridifying African landscape where food was dispersed, bipedalism provided our ancestors with a four-fold expansion of their foraging range on the same caloric intake.

The Pelvic Revolution and Gluteal Reorientation

Achieving this efficient gait required reconstructing the ancestral pelvis from the ground up:

- **Coronal to Sagittal Curvature:** In quadrupeds and chimpanzees, the iliac blades are tall, flat, and positioned in the coronal (frontal) plane along the back. In humans, the iliac blades shortened, broadened, and twisted forward into the **sagittal plane**, forming a bowl-shaped pelvic basin that cradles the abdominal viscera.
- **The Lesser Gluteal Transformation:** In chimpanzees, the *gluteus medius* and *gluteus minimus* muscles attach behind the hip joint, acting purely as **hip extensors** (propelling the leg backward). In humans, because the ilium curves around the hip, these muscles insert onto the greater trochanter of the femur laterally, transforming into powerful **hip abductors**.
- **Preventing Trendelenburg Collapse:** During bipedal walking, when one foot swings forward, gravity pulls the unsupported pelvis downward. In humans, the stance-leg gluteus medius contracts vigorously, pulling down on the ilium and locking the pelvis level. Without this adaptation (as seen in clinical Trendelenburg gait), a biped topples sideways at every step.

The Bicondylar (Valgus) Angle

In apes, the femur drops straight down from the hip joint at a 0° angle. Consequently, when an ape stands on one foot, its foot is placed wide of its center of mass, requiring an awkward, energy-wasting side-to-side waddle. Humans evolved a distinct **bicondylar (valgus) angle of $9\text{\&\#8211;}10^\circ$**: the femoral shaft slants inward toward the knee, bringing the knees and feet directly beneath the body's center of mass, eliminating lateral sway entirely.

Shakil Mahmud • Research Monograph

3. The Fossil Pioneers: Sahelanthropus, Orrorin, and Ardipithecus

For decades, skeptics argued that bipedalism could not have originated prior to four million years ago. But between 2000 and 2009, paleontologists unearthed three monumental Late Miocene and Early Pliocene fossil hominins that pushed the origin of our lineage back past seven million years:

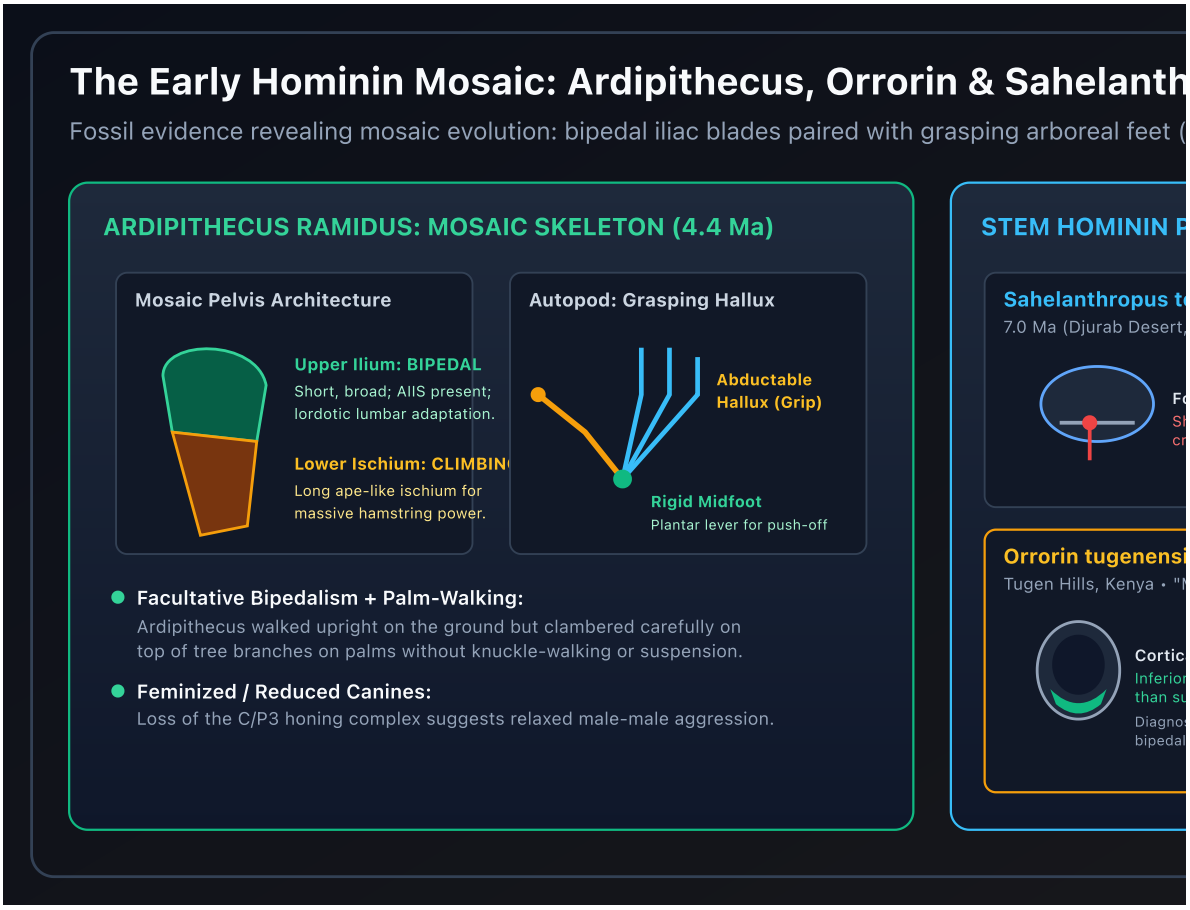


Figure 16.3: The Mosaic Anatomy of Stem Hominins. Left: The partial skeleton of Ardipithecus ramidus (ARA-VP-6/500, 'Ardi', 4.4 Ma) exhibiting a revolutionary anatomical mosaic—a bipedally adapted upper ilium paired with a primitive ape-like lower ischium and an opposable, grasping big toe (hallux) featuring a rigid midfoot lever. Right: Diagnostic bipedal hallmarks in Sahelanthropus (anterior foramen magnum, 7.0 Ma) and Orrorin (asymmetric femoral neck cortical thickness, 6.0 Ma).

1. Sahelanthropus tchadensis (7.0 Ma, Chad)

Discovered in 2001 by Michel Brunet in the Toros-Menalla desert of Chad, the fossil cranium **TM 266-01-060 ("Toumaï")** is the oldest known putative hominin. While possessing a chimp-sized brain ($360\text{–}370\text{ cm}^3$), Toumaï exhibits two astonishing derived hominin features:

1. The **foramen magnum** (the great hole where the spinal cord exits the skull) is positioned forward toward the center of the cranial base and angled horizontally downward, proving the head was balanced atop a vertical, bipedal cervical spine rather than projecting horizontally as in quadrupedal apes.
2. The canine teeth are significantly reduced and blunt, lacking the self-sharpening **C/P3 honing complex** of apes—indicating relaxed male-male sexual competition.

2. Orrorin tugenensis (6.0 Ma, Kenya)

Discovered in 2000 by Brigitte Senut and Martin Pickford in the Lukeino Formation of Kenya, "Millennium Man" is represented by fragmentary postcrania, including proximal femora (BAR 1002'00). High-resolution CT scans revealed that the **femoral neck cortical bone distribution** is distinctly human: the cortical bone along the inferior margin of the neck is over **three times thicker** than the superior margin. This asymmetric thickening is a direct biomechanical adaptation to resist the compressive bending stresses generated by habitual bipedal ground reaction forces.

3. Ardipithecus ramidus (4.4 Ma, Ethiopia) — The "Ardi" Revelation

In 2009, Tim White, Owen Lovejoy, Berhane Asfaw, and their team published the comprehensive analysis of **ARA-VP-6/500 ("Ardi")**, a female skeleton preserved in the volcanic ash of Aramis, Ethiopia. Ardi revealed the true ancestral morphotype of our lineage: **Mosaic Evolution** in its purest form:

- **The Mosaic Pelvis:** The upper ilium was broad and short with an anterior inferior iliac spine (AIIS), positioning the abductors for bipedal walking. Yet the lower ischium remained long and robust, preserving the deep attachment for massive arboreal climbing hamstrings.
- **The Grasping Foot with a Bipedal Lever:** Ardi possessed a fully **divergent, abductable big toe (hallux)** that stuck out at a right angle like a chimpanzee's, allowing her to grasp branches securely. However, the four lateral metatarsals and tarsal bones (especially the *os peroneum*) were stiffened into a rigid plantar plate, enabling her to push off the ground bipedally without collapsing the midfoot.

4. The Death of the Savanna Hypothesis

For nearly a century, textbook anthropology taught that bipedalism was invented when our ancestors stepped out of the forests onto vast, grassy African plains (the classical "Savanna Hypothesis"). The discovery of *Ardipithecus* obliterated this myth.

Paleobotanical analysis of fossil seeds, phytoliths, and thousands of fossil mammals excavated alongside Ardi revealed that Aramis was not an open savanna at all—it was a **closed, dense, subtropical woodland** populated by colobine monkeys, tragelaphin bovids (kudus), and hackberry trees. *Ardipithecus* did not evolve bipedalism on the open savanna; she was a facultative biped who walked upright along broad tree limbs and foraged on the woodland floor.

Bipedalism did not begin as an adaptation for running across grasslands. It began in the trees and woodlands as a slow, deliberate foraging adaptation—freeing hands to carry fruit, offspring, and tools. When the climate dried even further in the Pliocene, this woodland bipedal toolkit would undergo its next great leap forward in the savanna mosaic with the emergence of the **Australopithecines**.

Citation: Mahmud, S. (2026). "The Great Ape Split & The Biomechanics of Habitual Bipedalism." In The Evolutionary Odyssey, Part 16. https://shakilmahmud.com/evolutionary-odyssey-part-16-the-great-ape-split-and-bipedalism/

Shakil Mahmud • Research Monograph

SHAKIL MAHMUD RESEARCH MONOGRAPHS • PART XVII

Australopithecus, The Laetoli Tracks & Robust Paranthropus

Australopithecus, The Laetoli Tracks & Robust Paranthropus

1,560 words • November 1, 2026 • Permanent URI



Plate XVII: *Figure: Forensic life reconstruction of Australopithecus afarensis ('Lucy', ~3.2 Ma), depicting obligate terrestrial bipedal walking across the volcanic ash plains of East Africa as immortalized at Laetoli.*

Between four and two million years ago, the African continent became a dynamic crucible of hominin experimentation. The stem hominins of the late Miocene yielded to a prolific, highly successful radiation: the **Australopithecines** (genus *Australopithecus*, meaning "southern ape"). Possessing human-like upright posture below the neck while retaining chimpanzee-sized brains above, these gracile hominins perfected habitual terrestrial walking. In the volcanic ash of Tanzania, they left an indelible 27-meter trail of barefoot tracks that humanized deep time. Yet as African climates intensified their cyclical aridity during the Plio-Pleistocene transition, hominins split into two starkly divergent evolutionary pathways: the hyper-specialized chewing machine of robust **Paranthropus**, and the flexible, tool-crafting lineage of early **Homo**.

1. Lucy (A.L. 288-1) and the Gracile Australopithecine Architecture

On November 24, 1974, in the scorching Afar badlands of Hadar, Ethiopia, paleoanthropologist Donald Johanson and graduate student Tom Gray spotted a small right proximal ulna eroding from a dry gully. Over the subsequent weeks, their team excavated **A.L. 288-1**, universally known to the world as **"Lucy"** (after the Beatles' song *Lucy in the Sky with Diamonds*). Preserving roughly 40% of an entire individual skeleton dated to 3.2 million years ago, Lucy became the defining icon of *Australopithecus afarensis*:

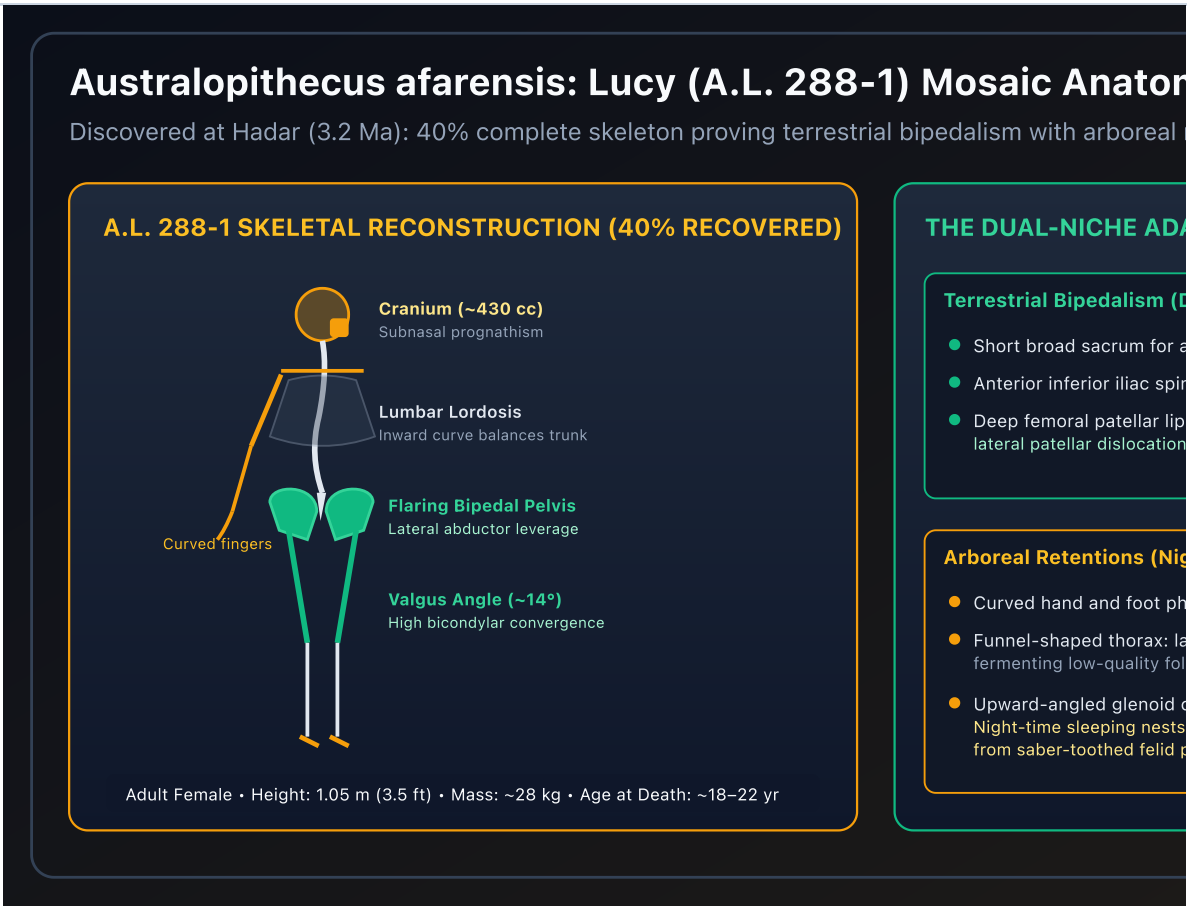


Figure 17.1: The Anatomy of Lucy (A.L. 288-1, 3.2 Ma). Left: Skeletal recovery schematic showing Lucy's adult female morphology (height: 1.05 m, mass: ~28 kg, cranial capacity: ~430 cc) featuring an extensively remodeled, flaring bipedal pelvis, lumbar lordosis, and marked femoral valgus convergence (~14°). Right: The dual-niche adaptation—efficient daytime terrestrial bipedalism combined with curved phalanges and an upward-angled shoulder socket for nocturnal safety in arboreal sleeping nests.

The Terrestrial Bipedal Anatomy

Lucy definitively demonstrated that bipedal locomotion preceded the expansion of the human brain by millions of years:

- **The Bipedal Pelvic Basin:** Lucy's iliac blades are short, broad, and flared laterally, providing an expanded lever arm for the lesser gluteal muscles (*gluteus medius* and *minimus*). This granted her dynamic lateral hip stabilization during the single-limb support phase of walking.
- **Lumbar Lordosis:** Lucy's spine possessed an inward curvature (lordosis) in the lower lumbar vertebrae, shifting her torso's center of gravity backward over the sacral platform and acetabular hip joints.
- **The Bicondylar Angle ($\approx 14^\circ$):** Lucy's femurs sloped inward from hip to knee at an acute angle of approximately 14°—even greater than the modern human average ($9\text{\&\#8211;}10^\circ$) due to her wide pelvic flare and short femoral length. Her knees converged directly beneath her body's midline, eliminating the energetic penalty of side-to-side waddling.

The Dual-Niche Hypothesis: Arboreal Retentions

Despite her terrestrial locomotion, Lucy was not a replica of a modern human. Her anatomy revealed unmistakable arboreal retentions: her manual and pedal phalanges (finger and toe bones) were noticeably curved, her forearms were relatively long compared to her hindlimbs, and her shoulder socket (glenoid cavity) was angled cranially (upward).

Most anthropologists embrace the **Dual-Niche Hypothesis**: *Australopithecus afarensis* was an obligate biped on the ground during the day, foraging across savanna woodlands. But at night, vulnerable to terrifying Plio-Pleistocene predators—such as saber-toothed cats (*Homotherium* and *Megantereon*) and giant hyenas (*Pachycrocuta*)—Lucy climbed into the trees to construct woven sleeping nests, exactly as modern chimpanzees do today.

2. The Laetoli Footprint Trail: Walking Through Deep Time

While fossil bones can be subjected to biomechanical debate, fossilized footprints provide an incontrovertible snapshot of dynamic behavior. In 1978, at Laetoli in northern Tanzania, a team led by Mary Leakey made one of the most sublime discoveries in the history of science: the **Laetoli Footprint Trail (Site G)**.

Shakil Mahmud • Research Monograph

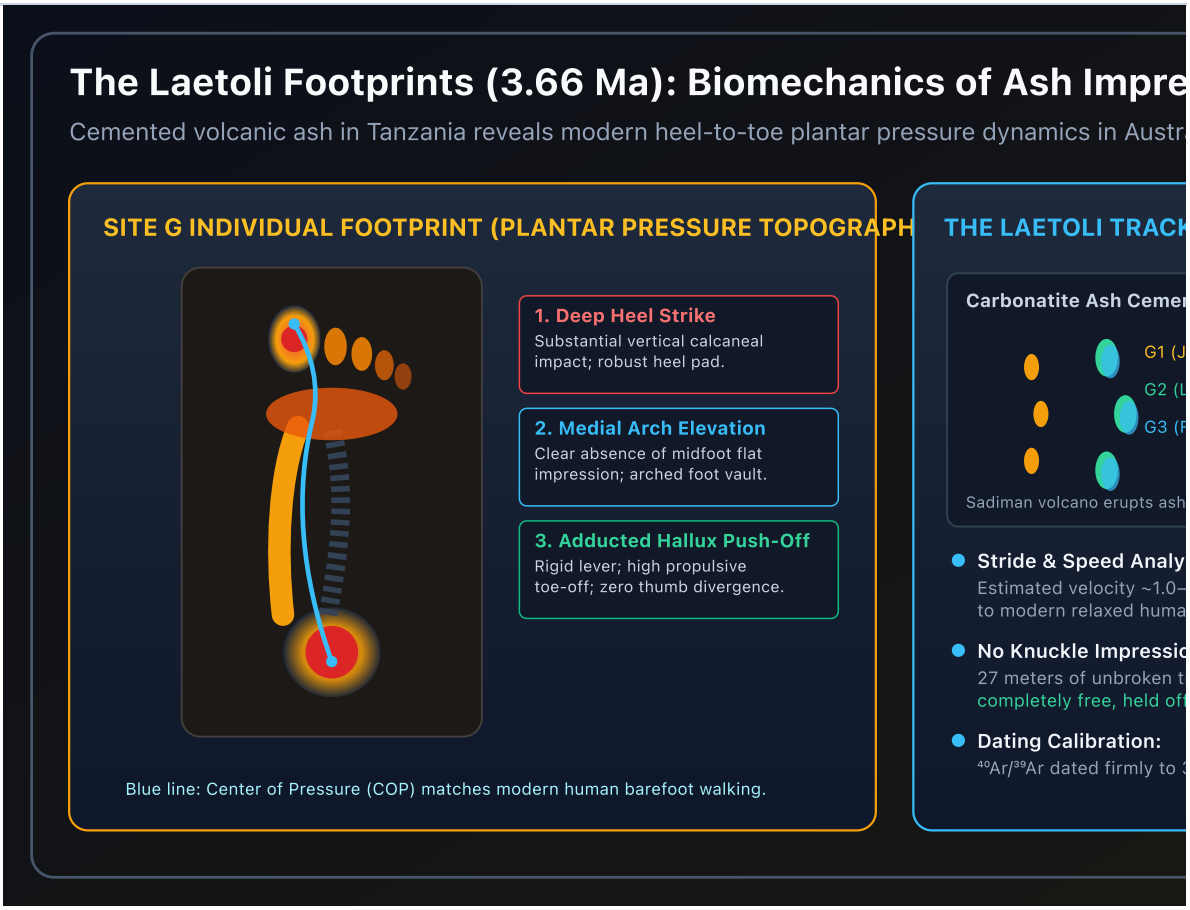


Figure 17.2: The Laetoli Footprints (3.66 Ma). Left: High-resolution plantar pressure topography of an individual footprint showing the deep calcaneal heel strike, a clearly elevated medial longitudinal arch, weight transfer along the lateral foot bridge, and a powerful toe-off from the fully adducted (in-line) big toe (hallux). Right: The 27-meter trackway context where three individuals (G1, G2, and G3 stepping into G2's tracks) walked together across damp carbonatite volcanic ash from Mount Sadiman.

A Snapshot in Volcanic Ash

Approximately **3.66 million years ago**, the nearby Sadiman volcano erupted, dusting the landscape with a fine blanket of carbonatite ash. A gentle rainfall moistened the ash layer, creating a consistency akin to wet cement. Before it set, three hominins—designated G1 (a smaller juvenile or female), G2 (a larger adult male), and G3 (a third individual walking directly behind G2, deliberately stepping into G2's footprints)—walked together for over **27 meters** across the open landscape. Subsequent ash falls sealed and preserved their barefoot impressions for eternity.

Plantar Pressure Dynamics

State-of-the-art 3D laser surface scanning and experimental pedobarographic trials by Robin Crompton, Matthew Bennett, and David Raichlen analyzed the depth contours of the Laetoli tracks:

1. **Distinct Heel Strike:** The posterior margin of the calcaneal impression is deeply depressed and rounded, proving the hominin made initial ground contact with a heavily cushioned heel strike.
2. **The Medial Longitudinal Arch:** Unlike chimpanzee footprints—which produce a uniform, flat-footed depression across the entire midfoot—the Laetoli prints display a conspicuous absence of deep impression under the medial instep, proving the presence of an elevated longitudinal arch supported by the plantar aponeurosis.
3. **Non-Divergent Adducted Hallux:** Unlike *Ardipithecus* (whose big toe diverged at 45°), the Laetoli big toe was fully **adducted (0\text{–}5^\circ divergence)**, perfectly aligned parallel with the lateral toes.
4. **The Terminal Hallux Push-Off:** The deepest impression in the anterior footprint is situated directly beneath the ball of the hallux, proving that *Australopithecus afarensis* completed its stride cycle with an energetic toe push-off, matching the center-of-pressure trajectory of modern barefoot human walking.

3. The Heavy Masticatory Machine: Paranthropus and Megadontia

As the Pliocene gave way to the Pleistocene around **2.6 Ma**, tectonic activity and Milankovitch orbital cycles drove African climates toward colder, drier, and more unpredictable regimes. The lush woodland mosaic contracted rapidly, replaced by expansive C_4 savanna grasslands dominated by tough, abrasive grasses, sedges, and hard-shelled nuts.

Faced with this caloric crisis, one branch of the australopithecine lineage opted for extreme anatomical specialization: the **Robust Australopithecines (genus *Paranthropus*)**. Exemplified by *Paranthropus boisei* in East Africa (discovered by Mary Leakey at Olduvai Gorge in 1959, cataloged as **OH 5 / "Nutcracker Man"**) and *Paranthropus robustus* in South Africa, this clade constructed the most powerful grinding apparatus in hominin history:

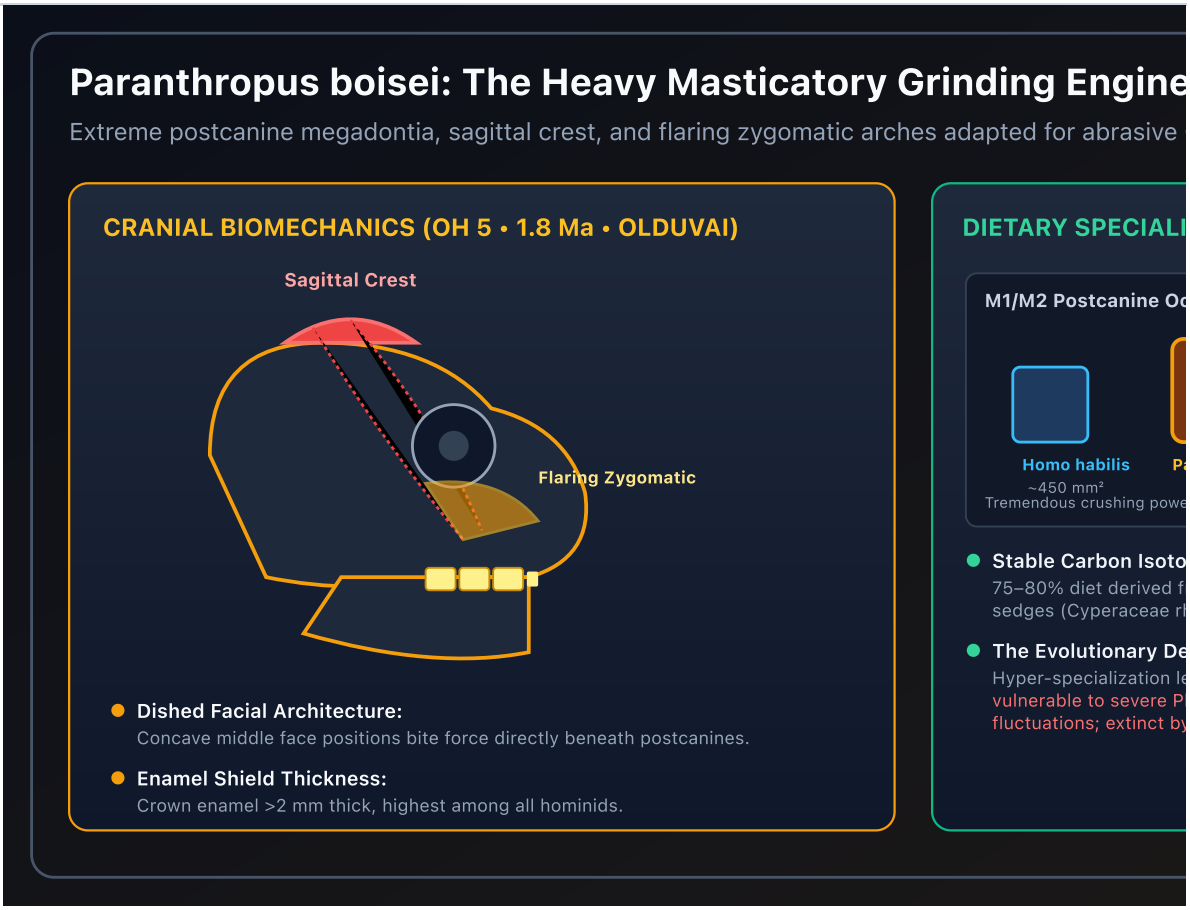


Figure 17.3: The Heavy Masticatory Engine of Paranthropus boisei (OH 5). Left: Cranial biomechanics showing the towering sagittal crest anchoring massive temporalis muscle fibers, gigantic flaring zygomatic arches providing wide muscle pass-through, and a dished, concave facial profile. Right: Molar occlusal surface area comparison—postcanine cheek teeth four times larger than modern humans with >2 mm enamel caps, adapted to grind abrasive C4 sedges and tubers.

The Biomechanics of the Crushing Engine

The cranial architecture of *Paranthropus boisei* was an engineering marvel devoted entirely to generating catastrophic bite forces:

- **The Sagittal Crest:** To anchor the gargantuan *temporalis* chewing muscles, the parietal bones fused along the skull's dorsal midline to form a towering, blade-like bone crest. In modern humans and gracile hominins, the temporalis muscle terminates low on the side of the cranium; in *Paranthropus*, it swept all the way to the top of the skull and met its counterpart.
- **Flaring Zygomatic Arches:** The cheekbones (zygomatics) bowed outward laterally and advanced forward, creating a vast sub-zygomatic temporal fossa to allow the massive masseter and temporalis muscle bellies to pass down to the lower jaw without constriction.
- **Dished Facial Profile:** The nasal bones and maxilla were set back into a concave, dish-like facial profile, positioning the chewing muscles directly over the molar teeth for maximum mechanical bite leverage.
- **Postcanine Megadontia:** While the front incisors and canines were diminutive and spatula-like, the premolars and molars were gargantuan—measuring up to **four times the surface area of modern human molars** (earning them the title of *megadont*). The molar crowns were armored with enamel caps exceeding **2 mm in thickness**, the thickest enamel of any known primate.

The Isotopic Surprise: What Did Nutcracker Man Actually Eat?

For decades, anthropologists believed that *Paranthropus* used its nutcracker teeth exclusively to crack hard-shelled nuts and seeds. But in 2011, geochemist Thure Cerling and paleoanthropologist Matt Sponheimer performed stable carbon isotope analysis ($\delta^{13}C$) on the enamel of dozens of *Paranthropus boisei* teeth. The result astonished the scientific community:

Between **75% and 80% of their lifetime diet consisted of C_4 plants**—not tree nuts (which are C_3), but tropical grasses and sedges (specifically the tough, fibrous, silica-rich underground storage organs, rhizomes, and corms of wetland sedges like *Cyperus papyrus*). *Paranthropus* had not evolved giant teeth to crack nuts; it had evolved a biological millstone to crush mountain upon mountain of gritty, low-nutrient fibrous tubers!

4. The Fork in the Evolutionary Road

By two million years ago, the African landscape was populated by two radically contrasting hominin cousins living side by side in the same river valleys of Olduvai and Turkana:

1. **The Specialist Strategy (Paranthropus):** Bet its evolutionary future on high-volume, low-quality vegetation, relying on massive teeth and jaws to grind through the dry season.

Shakil Mahmud • Research Monograph

2. **The Generalist Strategy (Early Homo):** Kept its cheek teeth small, reduced its gut, enlarged its brain, and outsourced food processing outside the body by chipping stones into razor-sharp cutting flakes.

When the Pleistocene climate entered its most severe glacial cycles around **1.2 million years ago**, seasonal wetlands dried up, and *Paranthropus* found its hyper-specialized C_4 sedge niches destroyed. Unable to adapt, the robust hominins vanished forever into extinction. Meanwhile, the generalist, tool-using branch survived and flourished, inaugurating the glorious, perilous dawn of the genus **Homo**.

Citation: Mahmud, S. (2026). "Australopithecus, The Laetoli Tracks & Robust Paranthropus." In The Evolutionary Odyssey, Part 17. https://shakilmahmud.com/evolutionary-odyssey-part-17-australopithecus-and-paranthropus/

SHAKIL MAHMUD RESEARCH MONOGRAPHS • PART XVIII

The Dawn of Genus Homo & Oldowan Lithic Technology

The Dawn of Genus Homo & Oldowan Lithic Technology

1,616 words • November 1, 2026 • Permanent URI



Plate XVIII: *Figure: Homo habilis ('The Handy Man', ~1.9 Ma), the earliest human species to engineer stone tools, exhibiting expanded cranial capacity (~650 cc) and the manual dexterity required to knap Oldowan choppers.*

Two million eight hundred thousand years ago, during a period of intense global cooling and African aridification, our evolutionary lineage crossed the most momentous threshold in the history of life on Earth: the emergence of our own genus, **Homo**. Faced with the collapse of tropical forest resources, early members of *Homo* did not develop giant chewing teeth like their cousins *Paranthropus*. Instead, they invented an entirely new evolutionary strategy: **Lithic Technology**. By understanding the fracture physics of stone, they outsourced biological digestion outside their bodies. Armed with razor-sharp Oldowan stone flakes, they breached an uncontested ecological goldmine—the calorie-dense, fatty bone marrow sealed inside the limb bones of megafaunal carcasses. This nutritional bonanza unlocked the metabolic energy necessary to fuel the greatest neurological expansion in mammalian history.

1. The Earliest Homo and Craniodental Transformation

In 2013, Ethiopian researcher Chalachew Seyoum discovered a fossilized left mandibular fragment in the Ledi-Geraru badlands of Afar, Ethiopia. Cataloged as **LD 350-1** and securely dated to **2.80\text{–}2.75\text{ million years ago}**, this jawbone pushed the origin of the genus *Homo* back by nearly half a million years. Combining primitive australopithecine-like anterior symphyseal contours with derived, slender *Homo*-like molars and a uniform mandibular corpus, LD 350-1 represents the morphological dawn of our genus.

By 2.0\text{–}1.8\text{ Ma}, at Olduvai Gorge in Tanzania and Koobi Fora in Kenya, early *Homo* had diversified into two classic lineages:

- **Homo habilis ("Handy Man"):** First named by Louis Leakey, Phillip Tobias, and John Napier in 1964 from holotype **OH 7** (a juvenile parietals and hand skeleton) and beautifully preserved cranium **KNM-ER 1813**. Brain size jumped from the australopithecine average of $\sim 430\ \text{cm}^3$ to **510\text{–}650\text{ cm}^3**. Cheeks teeth shrank, and the dental arcade adopted a parabolic curve.
- **Homo rudolfensis:** Exemplified by the grand, flat-faced cranium **KNM-ER 1470** (1.9 Ma), possessing an impressive brain capacity of **750\text{–}775\text{ cm}^3**.

Shakil Mahmud • Research Monograph

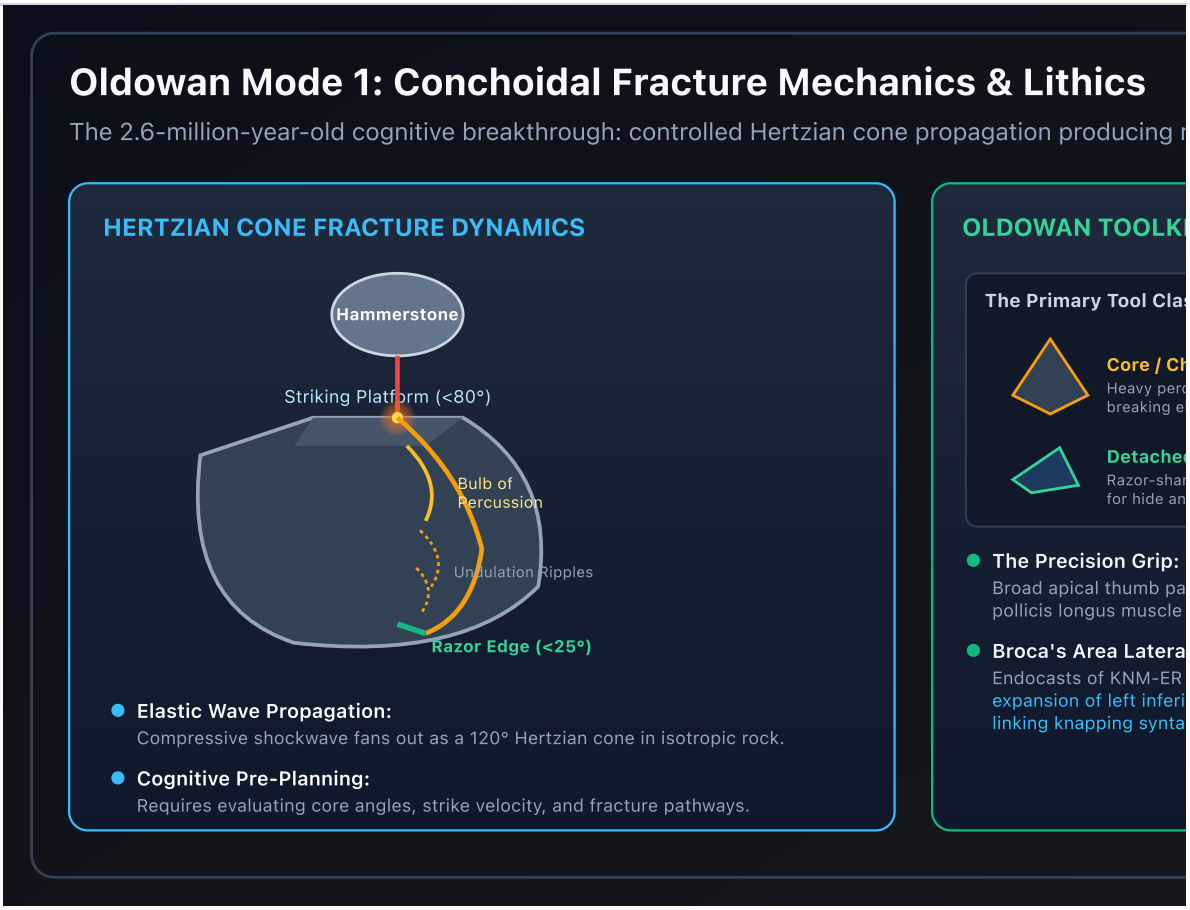


Figure 18.1: Oldowan Mode 1 Conchoidal Fracture Physics. Left: The physics of stone knapping showing the hammerstone striking the core platform at an acute angle (<80°), propagating an elastic compressive shockwave (Hertzian cone) that produces a detached flake with a bulb of percussion, eraillure scar, and razor-sharp slicing margin. Right: Oldowan toolkit taxonomy (cores/choppers vs. flakes) and the neurological lateralization of Broca's area in early Homo.

The Neurological Hardware: Broca's Cap and Precision Grip

Endocranial casts (endocasts) of *Homo habilis* (such as KNM-ER 1470 and OH 7) reveal an unprecedented structural innovation: an asymmetrical bulge in the left inferior frontal convolution corresponding to **Broca's Cap (Brodmann Areas 44 and 45)**. While modern human language was still hundreds of thousands of years away, Broca's area is neuroanatomically linked to **hierarchical sequential motor planning**—the precise mental syntax required to strike a stone core at the exact velocity, angle, and trajectory to detach a predictable flake.

Simultaneously, the hand evolved a **true Precision Grip (Three-Jaw Chuck)**: the apical thumb tuft broadened, the thumb lengthened relative to the fingers, and the insertion of the *flexor pollicis longus* muscle deepened, allowing early *Homo* to hold a spherical hammerstone securely against heavy rebound shocks.

2. Oldowan Mode 1: The Physics of Conchoidal Fracture

Discovered at Gona, Ethiopia (2.6 Ma) and famously documented by Mary Leakey in Bed I of Olduvai Gorge, the **Oldowan Industrial Complex (Mode 1)** represents humanity's inaugural technological horizon. While early scholars dismissed Oldowan tools as crude, modern lithic replication experiments by Nicholas Toth and Kathy Schick proved that knapping a successful Oldowan flake requires sophisticated mechanical comprehension:

The Mechanics of the Hertzian Cone

Oldowan hominins did not smash stones together haphazardly. They specifically selected hard, cryptocrystalline, isotropic rocks—such as volcanic basalt, chert, and quartzite—which lack natural cleavage planes:

1. **Striking Platform Geometry:** The knapper selects a cobble core with an acute exterior platform angle of **less than** 80°. Striking a platform at >90^\circ merely crushes the stone without initiating fracture.
2. **Hertzian Cone Initiation:** When the dense spherical hammerstone strikes the platform millimeters from the edge at high velocity, it creates localized Hertzian compressive stress. A high-energy elastic shockwave radiates downward through the rock matrix at an angle of roughly 120°.
3. **The Anatomy of a Flake:** As the fracture splits away from the core, it leaves unmistakable morphological signatures:
    - **Point of Percussion:** The exact microscopic impact epicenter.
    - **Bulb of Percussion:** A smooth, convex swelling formed by the expanding shockwave front.
    - **Concentric Undulations (Ripples):** Fine wave-front rings radiating outward like ripples on a pond.

- **The Razor Cutting Edge:** A microscopic edge bevel angle of $15\text{\–}25^\circ$—sharper than a modern surgical steel scalpel!

For decades, museum exhibits highlighted the heavy cobble "choppers" (the cores left behind). But use-wear analysis proved that the cores were often mere byproduct discards; the real prize was the **detached razor-sharp micro-flakes**, which provided early hominins with artificial carnivore teeth!

3. Faunal Taphonomy: Bone Marrow and the Scavenging Niche

Why did early *Homo* invent stone tools? The answer lies in the fossil bones preserved in the ancient riverbanks of East Africa. Paleoanthropologists studying **taphonomy** (the science of how organisms decay and fossilize) unlocked the secret of the Oldowan diet:

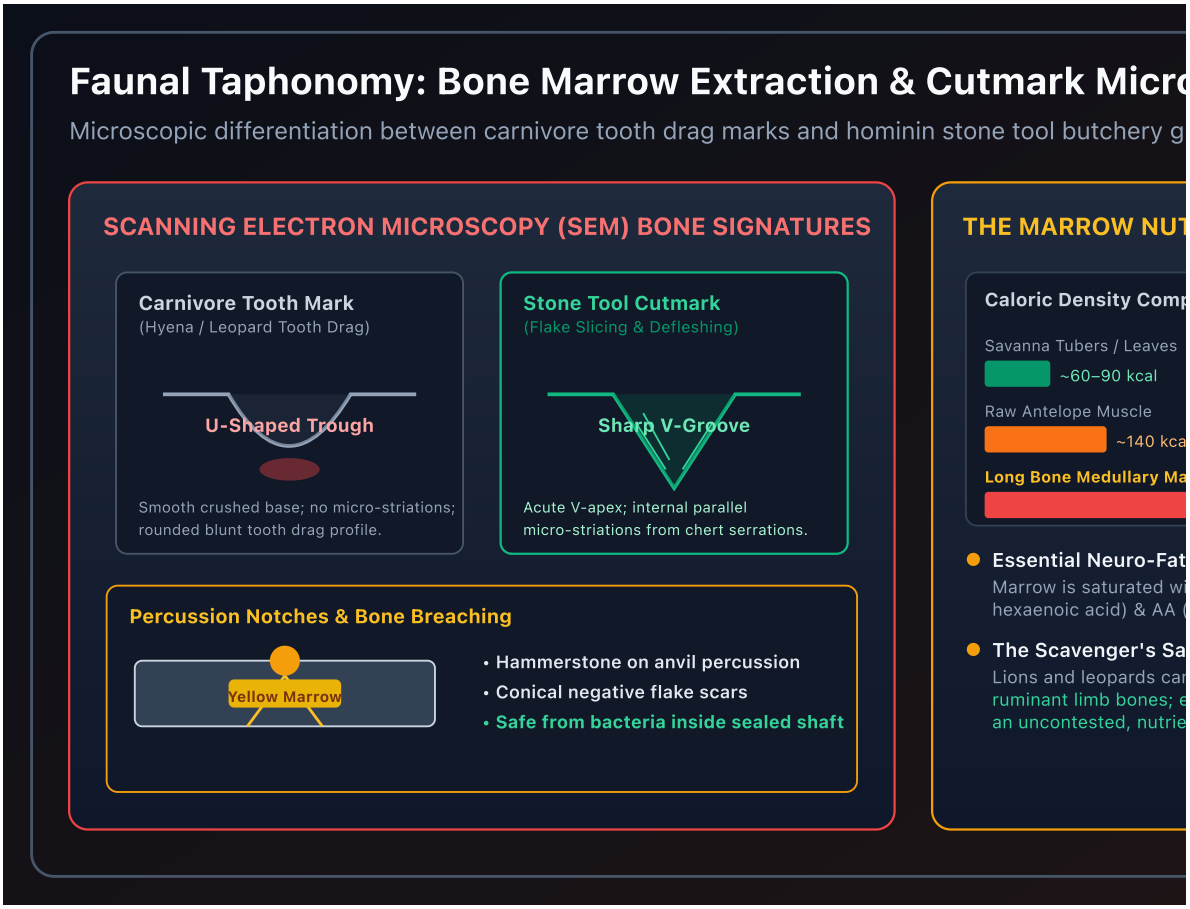


Figure 18.2: Faunal Taphonomy and Bone Marrow Extraction. Left: Scanning Electron Microscopy (SEM) diagnostic signatures comparing smooth, U-shaped carnivore tooth pits with acute, V-shaped stone tool cutmarks containing parallel internal micro-striations. Center: Percussion notches produced by hammerstone-on-anvil smashing to breach shaft medullary cavities. Right: Caloric density comparison showing bone marrow (>750 kcal/100g) delivering neuro-essential fatty acids (DHA and AA) to fuel brain expansion.

Scanning Electron Microscopy (SEM) Signatures

Under high-magnification scanning electron microscopy, taphonomists Pat Shipman, Richard Potts, and Henry Bunn established rigorous criteria to distinguish carnivore predation from human butchery:

- **Carnivore Tooth Scores:** When a hyena or leopard drags its conical canine across bone, it crushes the bone cells, producing a shallow, broad **U-shaped groove** with a rounded, smooth floor.
- **Stone Tool Cutmarks:** When an Oldowan hominin uses a sharp chert flake to slice tendons or strip periosteum, the microscopic jagged serrations of the stone carve a deep, acute **V-shaped notch** characterized by distinct, fine, parallel micro-striations lining the groove walls.
- **Percussion Impact Flakes & Notches:** When a hominin places a dense ungulate femur on a stone anvil and strikes it with a hammerstone, it produces semi-circular **percussion notches**, negative impact flakes, and radiating butterfly fracture patterns—telltale proof of deliberate bone smashing.

The Lipid Goldmine: Yellow Bone Marrow

In the dangerous African savanna, early *Homo* did not need to hunt giant buffalo or elephants directly. Saber-toothed felids (such as *Homotherium* and *Megantereon*) were hyper-carnivorous apex predators that ate soft viscera and fresh meat before abandoning the carcass. Hyenas lacked the massive jaw crushing power to crack the dense cortical shafts of adult elephant, rhinoceros, or giant giraffe long bones.

Shakil Mahmud • Research Monograph

The interior medullary cavities of these limb bones remained a sealed, sterile biological safe. By utilizing hammerstones and anvils, early *Homo* became the premier **marrow specialist** of the Pleistocene. Long bone marrow delivers an astounding **>750\text{ kcal per }100\text{ grams}**, composed of nearly 100% digestible lipids, oleic acid, and crucial long-chain polyunsaturated fatty acids: **Docosahexaenoic Acid (DHA)** and **Arachidonic Acid (AA)**—the irreplaceable molecular building blocks of neural cell membranes and synapses.

4. The Expensive Tissue Hypothesis: Gut vs. Brain

How did early *Homo* afford the energetic cost of expanding its brain? In 1995, Leslie Aiello and Peter Wheeler formulated one of the most celebrated paradigms in human evolutionary biology: **The Expensive Tissue Hypothesis**.

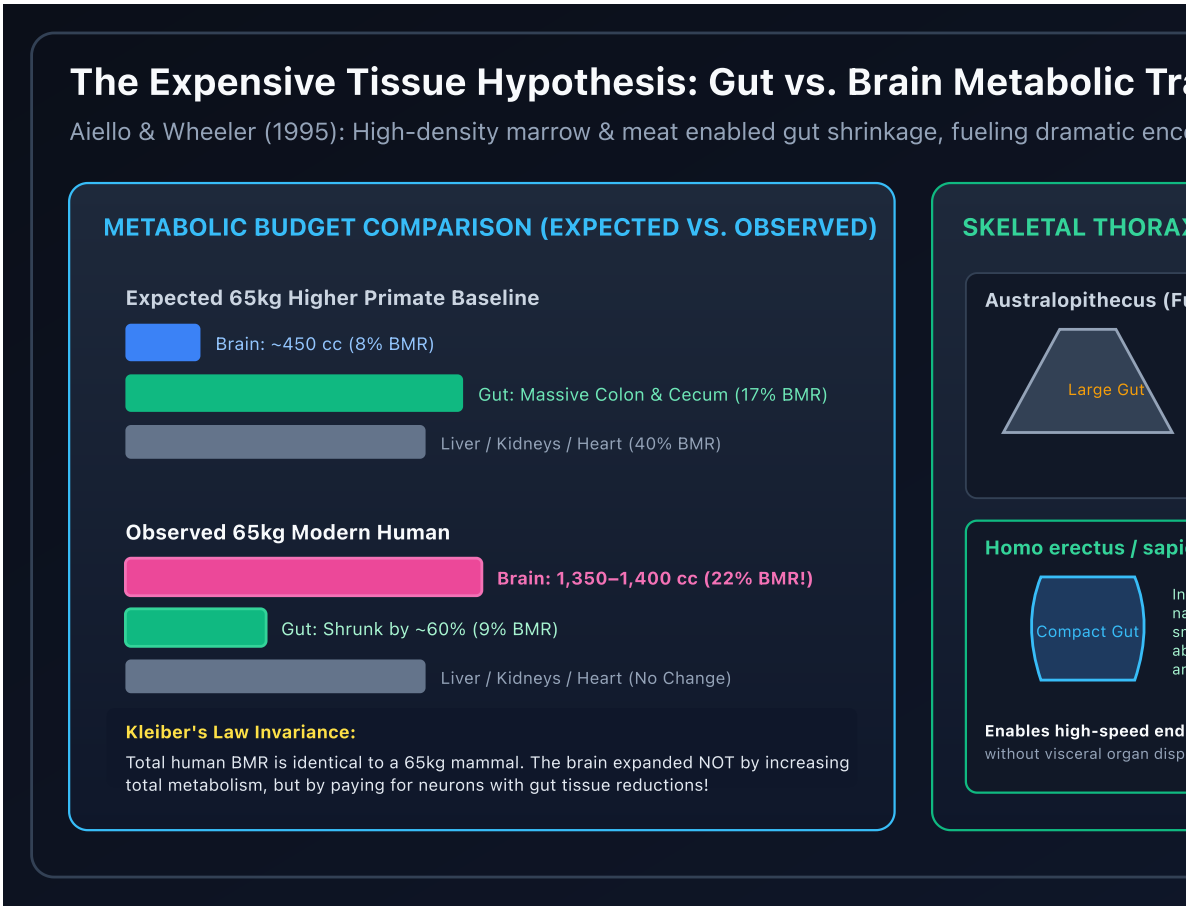


Figure 18.3: The Expensive Tissue Hypothesis (Aiello & Wheeler, 1995). Left: Metabolic budget comparison showing that while human brain tissue expanded to consume 22% of basal metabolic rate (BMR), our total metabolic rate remained constrained by Kleiber's Law; the metabolic deficit was paid for by shrinking the gastrointestinal tract by ~60%. Right: Skeletal transformation from the wide, funnel-shaped ape ribcage (housing a massive fermenting cecum) to the slender, narrow-waisted barrel ribcage of Homo.

The Metabolic Conundrum

The human brain is an extraordinarily gluttonous organ. In an adult human, the brain represents merely **2% of total body weight**, yet it consumes between **20% and 25% of total resting basal metabolic rate (BMR)**! Gram for gram, neural tissue consumes more than twenty times the energy of skeletal muscle.

According to **Kleiber's Law** ($BMR \propto M^{0.75}$), the total basal metabolic rate of a mammal is strictly governed by its overall body mass. Measurements of human metabolism confirm that our resting metabolic rate is exactly what would be predicted for a standard 65\text{–}70\text{ kg} mammal. We do not have a super-charged metabolic engine. How, then, did our ancestors pay for a 750 cc brain without starving?

The Gut-Brain Trade-Off

Aiello and Wheeler examined the five metabolically "expensive tissues" in the mammalian body: the heart, kidneys, liver, brain, and gastrointestinal (GI) tract. Heart and kidney sizes are fixed by circulatory and filtration physics. The liver is tied to detoxification.

The only organ capable of dynamic evolutionary downsizing was the **Gastrointestinal Tract**:

- **The Australopithecine Ape Gut:** Herbivorous primates consume voluminous, low-nutrient, fibrous plant leaves and stems. Digesting this material requires a massive, fermenting cecum and an elongated colon filled with symbiotic bacteria. This enormous visceral organ package required a wide, flaring, **funnel-shaped ribcage** and a broad pelvis.

- **The Genus Homo Revolution:** By using Oldowan stone flakes to process carcasses and extract calorie-dense bone marrow, early *Homo* replaced voluminous, fibrous plant matter with concentrated, easily digestible animal fats and proteins. The digestive tract shrank by $\sim 60\%$! The bulky colon retreated, and the small intestine expanded to rapidly absorb fats.

The metabolic energy saved by drastically reducing gut tissue was rechanneled directly into the expanding neocortex. This visceral remodeling is dramatically visible in the fossil record: the clumsy, funnel-shaped ribcage of *Australopithecus* transformed into the narrow, cylindrical **barrel-shaped ribcage and slender waist** of *Homo*. The stage was set for our lineage to walk out of Africa and conquer the globe.

Citation: Mahmud, S. (2026). "The Dawn of Genus Homo & Oldowan Lithic Technology." In The Evolutionary Odyssey, Part 18. https://shakilmahmud.com/evolutionary-odyssey-part-18-the-dawn-of-genus-homo-and-lithic-technology/

Shakil Mahmud • Research Monograph

SHAKIL MAHMUD RESEARCH MONOGRAPHS • PART XIX

Homo erectus, Fire & The Global Diaspora

Homo erectus, Fire & The Global Diaspora

2,136 words • November 1, 2026 • Permanent URI



Plate XIX: *Figure: A scientifically grounded reconstruction of Homo erectus in the East African savanna (~1.6 Ma), showcasing obligate bipedal endurance-running anatomy, controlled hearth fire, and an Acheulean bifacial handaxe.*

One million nine hundred thousand years ago, the African continent produced a biological and behavioral titan: **Homo erectus** (often termed *Homo ergaster* in its early African phase). Leaving behind the small-bodied, ape-like proportions of their ancestors, *Homo erectus* evolved tall, slender, modern human postcranial skeletons engineered for long-distance **Endurance Running**. Coupled with the loss of insulating body fur and an explosive proliferation of eccrine sweat glands, they became nature's ultimate daytime persistence hunters. In their hands, stone tool technology leapt from opportunistic Oldowan flakes to mathematically symmetrical **Acheulean handaxes**. Most crucially, by taming the primordial power of **fire**, they predigested their food, ignited the nocturnal campfire culture, and became the first hominin species to march out of Africa and settle across the entire breadth of the Old World—from the Republic of Georgia to the volcanic islands of Java and the glacial caves of northern China.

1. Turkana Boy (KNM-WT 15000) & The Endurance Running Hypothesis

In August 1984, legendary fossil hunter Kamoya Kimeu spotted a tiny scrap of dark cranial bone on the banks of the Nariokotome River near Lake Turkana, Kenya. Over five field seasons, Alan Walker and Richard Leakey excavated **KNM-WT 15000**, universally celebrated as **"Turkana Boy"**. Dated to 1.6 million years ago, this is the most complete early hominin skeleton ever unearthed (preserving over 80% of all bones):

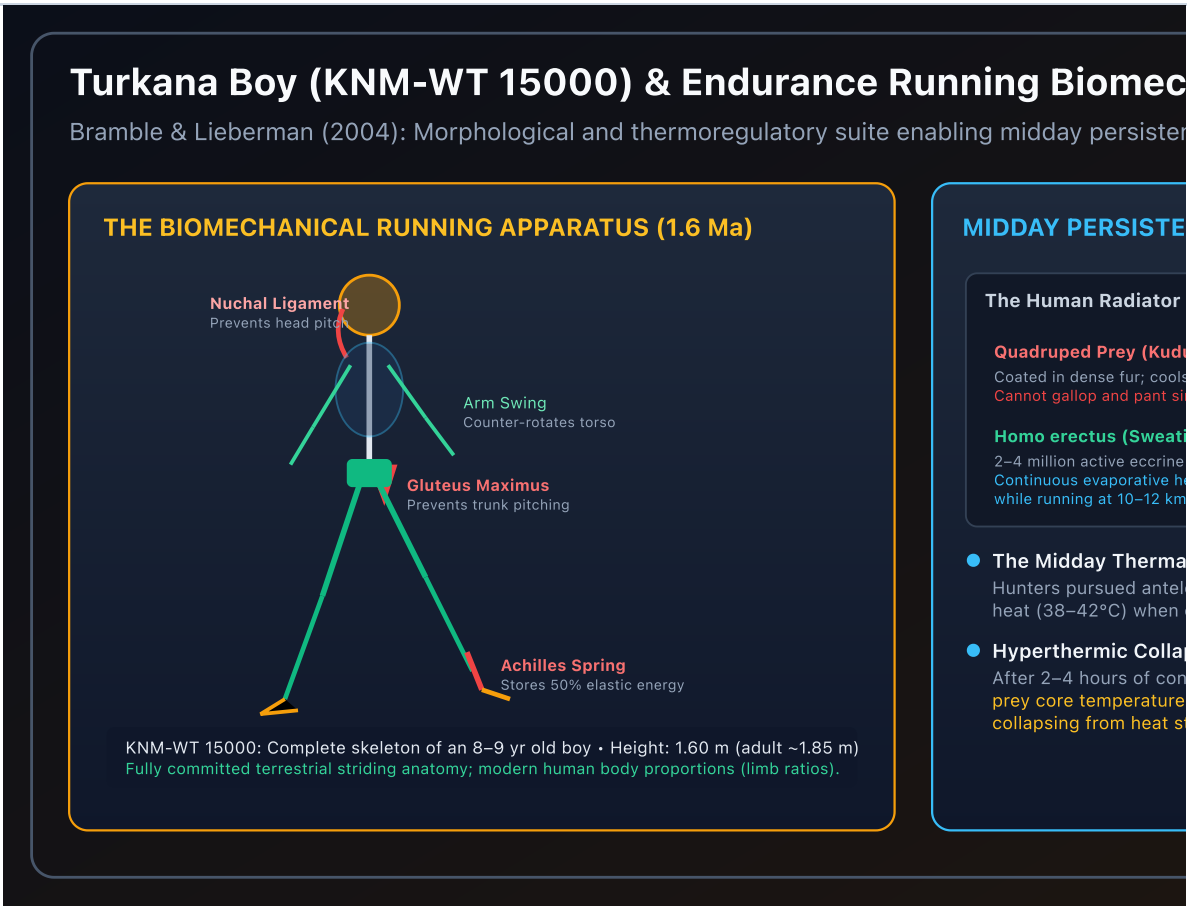


Figure 19.1: The Endurance Running Architecture of Turkana Boy (KNM-WT 15000, 1.6 Ma). Left: Skeletal running complex showing the nuchal ligament stabilizing cranial pitch, a decoupled shoulder girdle and narrow waist allowing counter-rotating arm swing, an expanded gluteus maximus preventing trunk collapse at heel strike, and long elastic Achilles tendons storing ~50% strain energy. Right: Thermoregulatory evaporative cooling—millions of eccrine sweat glands enabling midday persistence hunting under 40°C heat while quadrupeds collapse from hyperthermia.

A Modern Human Body Plan

Turkana Boy was an adolescent male approximately 8 to 9 years old at death, yet he already stood $1.60\ \text{m}$ ($5\ \text{ft}\ 3\ \text{in}$) tall and would have matured to an imposing $1.85\ \text{m}$ ($6\ \text{ft}\ 1\ \text{in}$) and $68\ \text{kg}$. His brain capacity was roughly $880\text{–}900\ \text{cm}^3$—more than double that of an australopithecine. Most remarkably, his limb proportions were completely modern: long, slender legs, shortened forearms, and a narrow, cylindrical barrel-shaped ribcage.

The Bramble & Lieberman Endurance Running Complex

Why did *Homo erectus* evolve such long legs and narrow waists? In 2004, Dennis Bramble and Daniel Lieberman published a seminal paper in *Nature* demonstrating that humans are exceptional endurance runners. While quadrupeds can easily outsprint humans over short distances ($100\text{–}400\ \text{meters}$), humans can outrun almost every mammal on Earth over marathon distances ($10\text{–}40\ \text{kilometers}$) in hot weather:

- **The Nuchal Ligament:** Quadrupedal apes lack a functional nuchal ligament because their heads are supported horizontally by dorsal neck muscles. Humans and *Homo erectus* evolved a distinct median ridge on the occipital bone where a thick, elastic nuchal ligament anchors the head, preventing the heavy cranium from pitching violently forward with each running bounce.
- **Thoracic Counter-Rotation:** Quadrupedal apes have shoulders locked close to the ribcage. In *Homo erectus*, the shoulder girdle decoupled from the skull, and the narrow waist separated the ribcage from the pelvis. When the right leg strides forward, the left arm swings forward, allowing the torso to twist in the opposite direction. This counter-rotates the body's angular momentum without wasting energy.
- **The Gluteus Maximus:** In humans, the *gluteus maximus* is hypertrophied into the largest muscle in the body. Electromyographic studies prove that the gluteus maximus is virtually inactive during ordinary walking on level ground; it fires vigorously only during running, where it acts as a colossal tensile brake preventing the upright trunk from pitching forward at the moment of foot impact!
- **The Achilles Tendon Spring:** *Homo erectus* lengthened the Achilles tendon, creating a biological spring capable of absorbing and returning over 50% of elastic strain energy with each bounce.

The Human Radiator: Eccrine Sweating & Fur Loss

Running generates staggering amounts of internal metabolic heat ($>1{,}000\ \text{Watts}$). Quadrupedal mammals (such as zebras, antelopes, and cheetahs) are cloaked in fur and can dissipate heat only through respiratory panting. However, an animal cannot gallop and pant at the same time, because galloping mechanically compresses the lungs in a 1:1 stride-to-breath ratio. If forced to gallop continuously in hot weather, a quadruped cannot breathe fast enough to shed heat, and its core body temperature climbs precipitously toward fatal heat stroke ($>42\text{–}43^\circ\text{C}$).

Shakil Mahmud • Research Monograph

Homo erectus evolved the ultimate physiological countermeasure: **loss of body hair (naked skin)** combined with a spectacular multiplication of **eccrine sweat glands (2\text{–}4\text{ million active glands})**. By secreting a thin film of watery sweat across naked skin, humans exploit the immense latent heat of vaporization of water ($2,260\ \text{kJ/kg}$). This permitted **Persistence Hunting**: hunting parties tracked antelopes during the blazing midday heat (38\text{–}42^\circ\text{C})—when lions and leopards slept in the shade—relentlessly chasing their prey at a steady trot until the animal collapsed from hyperthermic heat exhaustion, unable to stand.

2. The Mastery of Fire & The Cooking Hypothesis

While stone tools provided sharp teeth outside the body, the control of fire provided an artificial external digestive system. In 2009, Harvard biological anthropologist Richard Wrangham published *Catching Fire: How Cooking Made Us Human*, arguing that the adoption of cooked food was the primary catalyst for the dramatic evolutionary expansion of *Homo erectus*:

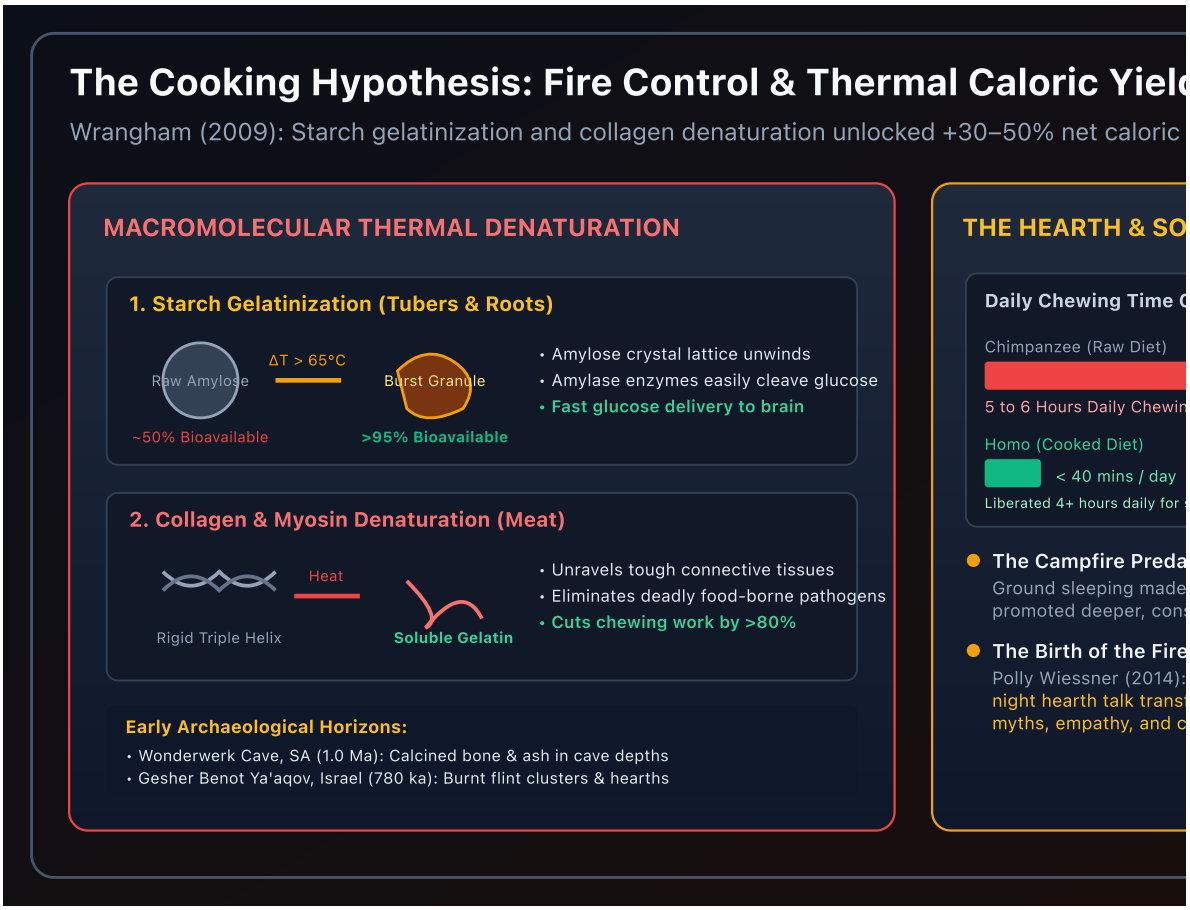


Figure 19.2: The Cooking Hypothesis & Thermal Caloric Yield. Left: The biochemistry of thermal processing—starch gelatinization uncoiling crystalline amylose lattices (boosting bioavailability from 50% to >95%) and collagen denaturation converting tough connective tissue into soluble gelatin. Right: The social and anatomical revolution—daily chewing time collapsing from 5–6 hours to under 40 minutes, and nocturnal campfires establishing the first predator-free storytelling hearths.

The Biochemistry of Cooking

Cooking is not merely a culinary preference; it is a profound chemical transformation that dramatically increases net energy yield:

1. **Starch Gelatinization:** Underground storage organs (tubers, corms, and rhizomes) contain tightly wound, semi-crystalline granules of amylose and amylopectin. In raw starch, human salivary and pancreatic amylase enzymes can only digest roughly 50% of the carbohydrates; the rest passes unabsorbed into the colon. Heating starch in water above 65°C causes the crystalline granules to absorb water, swell, and burst—uncoiling the glucan chains and boosting enzymatic glucose absorption to **over** 95%!
2. **Protein Denaturation:** Heat uncoils the rigid triple-helix structure of animal collagen and tenderizes muscle fibers (actin and myosin), converting tough gristle into soluble, easily digestible gelatin. Furthermore, heat neutralizes plant toxins (cyanogenic glucosides, lectins, and protease inhibitors) and kills lethal food-borne pathogens.
3. **The Energetic Dividend:** Wrangham and Rachel Carmody demonstrated through metabolic feeding experiments that cooking increases the net caloric gain from food by 30% **to** 50%, while simultaneously slashing the energetic cost of digestion by more than half.

The Archaeological Horizons of Fire

Detecting ash and microscopic charcoal in deep time is notoriously challenging, but multiple ancient sites confirm early fire use:

- **Wonderwerk Cave, South Africa (1.0 Ma):** Michael Chazan, Francesco Berna, and their team identified micro-charcoal and calcined (burned) bone fragments deep within the cave interior—30 meters from the entrance—precluding natural wildfire origin.

- **Swartkrans, South Africa (1.0 Ma):** C.K. Brain recovered over 270 burned animal bones heated to temperatures above 400°C.
- **Gesher Benot Ya'aqov, Israel (780 ka):** Naama Goren-Inbar documented discrete, spatial clusters of burnt flint artifacts and wood alongside Acheulean bifaces, proving systematic, repetitive hearth management.

The Social Hearth and the Sleep Revolution

The consequences of fire extended far beyond nutrition. Living great apes spend **5\text{–}6\text{ hours every single day}** aggressively chewing tough raw vegetation. Cooking collapsed human chewing time to **less than 40 minutes per day**! This liberated over four hours of daylight every day for tool crafting, social networking, and child rearing.

Furthermore, nocturnal campfires built a glowing defensive perimeter against lions, leopards, and hyenas. For the first time in hominin history, our ancestors could safely abandon the trees and sleep together on the ground. This enabled longer, deeper periods of **consolidated REM sleep**, which neuroscientists identify as essential for memory consolidation, creative cognitive processing, and emotional regulation. Around the flickering light of the evening hearth, human social communication transformed: as Polly Wiessner demonstrated in 2014, while daytime conversation focuses on economic logistics, nighttime hearthside talk transforms into storytelling, mythology, empathy, and collective cultural bonding.

3. Acheulean Mode 2: The Mental Template of the Handaxe

Around 1.76 million years ago, at Kokiselei near Lake Turkana, Kenya, stone knapping underwent its second great technological leap: the birth of the **Acheulean Industrial Complex (Mode 2)**, named after the French site of Saint-Acheul.

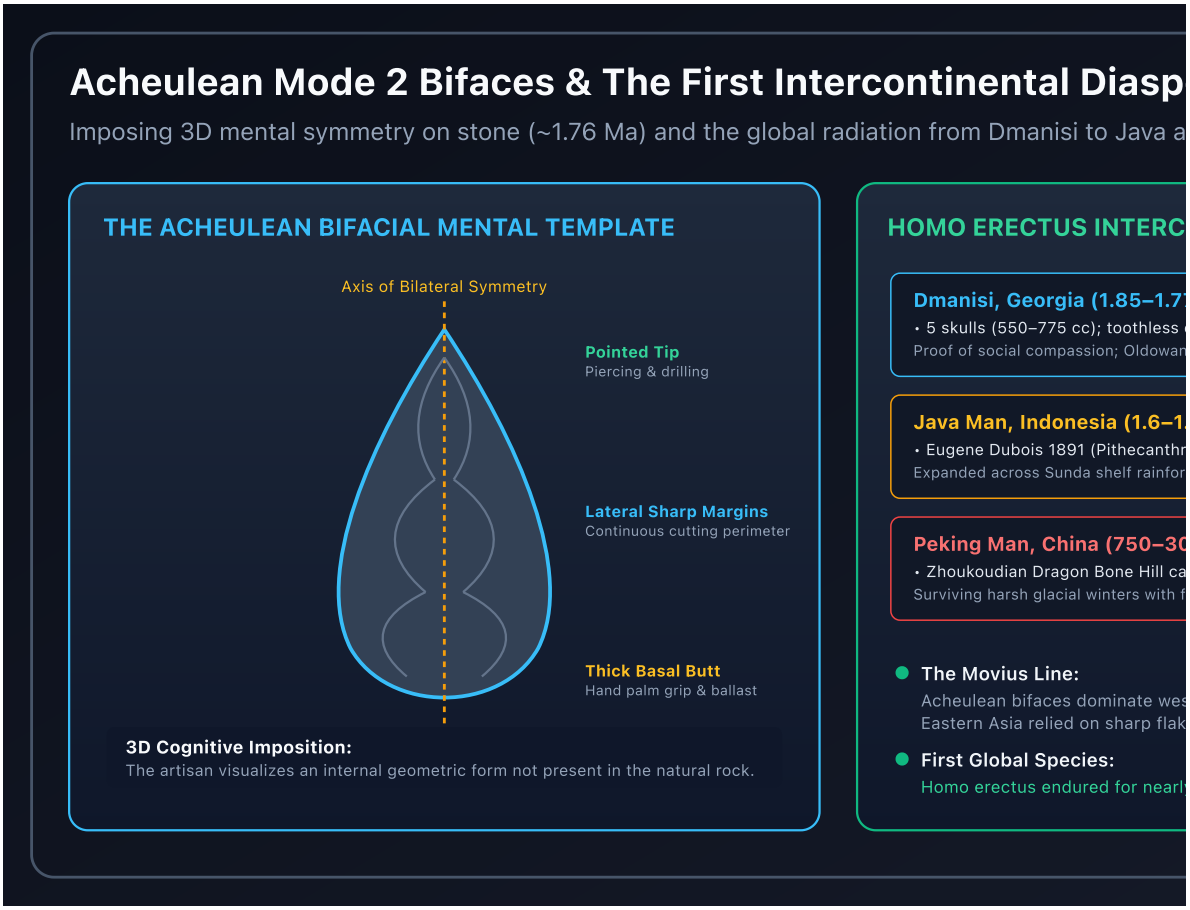


Figure 19.3: Acheulean Mode 2 Symmetry & The Intercontinental Diaspora. Left: Symmetrical teardrop biface geometry showing the imposition of a 3D cognitive mental template on raw stone, featuring bilateral symmetry, sharp perimeter slicing margins, and a heavy basal butt. Right: The grand diaspora routes of Homo erectus —from Dmanisi (1.8 Ma) to Java (1.6 Ma) and Zhoukoudian (750 ka), bounded by the biogeographical Movius Line.

The Geometry of Bilateral Symmetry

Unlike Oldowan Mode 1 choppers (which were produced simply by flaking an edge opportunistically), the Acheulean **Biface (Handaxe / Cleaver)** represents a profound cognitive milestone: **The Imposition of a Mental Template**:

1. **Bifacial Flaking:** The knapper works both sides of a large cobble or giant flake, detaching dozens of thinning flakes to create a continuous sharp perimeter edge.
2. **Bilateral and Bifacial Symmetry:** The handaxe conforms to a strict, elegant geometric shape—typically an elongated teardrop, oval, or amygdaloid form. If sliced down the middle, the left and right halves are precise mirror images. Many handaxes from Africa, Europe, and India adhere closely to the classical **Golden Ratio ($\Phi \approx 1.618$)**.
3. **The Multi-Tool of the Pleistocene:** The Acheulean handaxe was the ultimate Swiss Army knife: the sharp pointed tip was used for piercing and digging, the lateral knife-like edges for slicing through elephant hides and dismembering joints, and the heavy rounded basal butt for cracking nuts and crushing bones.

Shakil Mahmud • Research Monograph

For more than **one and a half million years**—the longest enduring technological tradition in human history—the Acheulean handaxe remained the standard gear of our lineage, passed down through observational learning across thousands of generations.

4. The Grand Diaspora: Conquering the Old World

Powered by high-calorie cooked meat, endurance running, and Acheulean technology, *Homo erectus* broke free from the African cradle. The fossil record documents a stunning inter-continental diaspora across the Old World:

1. Dmanisi, Georgia (1.85\text{–}1.77\text{ Ma})

Perched beneath the ruins of a medieval fortress in the southern Caucasus mountains, David Lordkipanidze and his international team excavated five complete hominin skulls (D2700, D3444, and the magnificent **Skull 5 / D4500**). These Georgian hominins—sometimes classified as *Homo erectus georgicus*—were small-bodied (1.45\text{–}1.50\text{ m}) with modest brains (550\text{–}775\text{ cm}^{3}), proving that hominins did not require giant 1,000 cc brains to migrate out of Africa.

Crucially, skull **D3444** belonged to an elderly individual whose teeth had all fallen out years prior to death; the jawbone alveoli had completely resorbed. This individual could not chew raw meat or tough roots; they survived for years only because the social band collectively chewed or cooked soft food for them—the earliest documented evidence of **social compassion and elder care** in the fossil record.

2. Java Man, Indonesia (1.6\text{–}1.0\text{ Ma})

In 1891, Dutch anatomist Eugène Dubois discovered a thick cranial vault with prominent browridges and a modern femur along the Solo River at Trinil, Java, naming it *Pithecanthropus erectus* ("erect ape-man"). Subsequent discoveries at Sangiran and Mojokerto revealed that *Homo erectus* had expanded across the exposed Sunda continental shelf into Southeast Asian subtropical rainforests nearly two million years ago!

3. Peking Man at Zhoukoudian, China (750\text{–}300\text{ ka})

In the 1920s and 30s, Davidson Black and Franz Weidenreich unearthed fossils representing over 40 individuals in Dragon Bone Hill cave at Zhoukoudian, near Beijing. Peking Man possessed a large brain (1,000\text{–}1,225\text{ cm}^{3}), robust supraorbital tori (browridges), and thick cranial bones. Zhoukoudian proved that *Homo erectus* was capable of surviving the bitterly cold, freezing winters of northern China, relying on cave shelters, animal skins, and hearth fires.

The Movius Line

In 1948, Harvard archaeologist Hallam Movius noticed a profound geographic boundary across the Old World: while Acheulean bifacial handaxes dominated Africa, Europe, and the Indian subcontinent, they were virtually absent east of the Bay of Bengal. In China and Southeast Asia, hominins utilized simple core and flake toolkits. Known as the **Movius Line**, this dichotomy is explained by ecological adaptation: in the lush tropical forests of East and Southeast Asia, *Homo erectus* almost certainly utilized the extraordinary versatility of **bamboo**—a material far lighter, sharper, and more rapidly renewable than stone, whose organic fibers decay without leaving a trace in the lithic record.

For nearly two million years, *Homo erectus* reigned as the master of the Pleistocene world. But as the glacial cycles deepened in the late Middle Pleistocene, regional populations began to diverge, laying the groundwork for the most complex, enigmatic chapter in our odyssey: the archaic mosaic of Neanderthals, Denisovans, and modern *Homo sapiens*.

Citation: Mahmud, S. (2026). "Homo erectus, Fire & The Global Diaspora." In The Evolutionary Odyssey, Part 19. https://shakilmahmud.com/evolutionary-odyssey-part-19-homo-erectus-fire-and-global-expansion/

SHAKIL MAHMUD RESEARCH MONOGRAPHS • PART XX

The Archaic Mosaic & The Dawn of Modern Humanity

The Archaic Mosaic & The Dawn of Modern Humanity

2,061 words • November 1, 2026 • Permanent URI



Plate XX: *Figure: Upper Paleolithic cave paintings of horses, aurochs, and rhinos from Chauvet Cave (~36,000 BP), symbolizing the cognitive revolution, symbolic language, and the dawn of modern human artistic consciousness.*

Three hundred thousand years ago, the African continent became the nursery of our own species: **Homo sapiens**. Yet contrary to the simplistic storybook myth of a single isolated "Garden of Eden", our anatomical and genetic origin was a pan-African mosaic—a continent-wide web of semi-isolated populations periodically connecting across fluctuating green Sahara corridors. Furthermore, for the vast majority of our existence, we were not alone. Fifty thousand years ago, our planet was a multi-species Tolkien-esque world inhabited simultaneously by at least five distinct hominins: *Homo sapiens*, cold-adapted *Neanderthals* in Eurasia, enigmatic *Denisovans* in Siberia and Tibet, diminutive island "Hobbits" (*Homo floresiensis*) in Indonesia, and *Homo luzonensis* in the Philippines. Through ancient DNA sequencing, we now know that our ancestors did not simply replace these archaic cousins—they loved them, interbred with them, and absorbed their adaptive genes. As the last surviving hominin standing, humanity sparked a **Symbolic Revolution** that transformed biological evolution into runaway cultural evolution, culminating in a species that now deciphers the four-billion-year epic of its own cosmic origins.

1. The Late Pleistocene Archaic Mosaic: A Multi-Species World

For decades, paleoanthropologists debated two polarized models: the strict *Recent African Origin* model (proposing modern humans arose suddenly in a single East African valley ~150 ka) versus the classical *Multiregional Evolution* model. In 2017, a team led by Jean-Jacques Hublin stunned the scientific world by redating the fossil site of **Jebel Irhoud** in Morocco. Thermoluminescence dating of heated flints established that anatomically early *Homo sapiens* lived in northwestern Africa $315,000$ years ago—pushing the dawn of our species back by over $100,000$ years!

Shakil Mahmud • Research Monograph

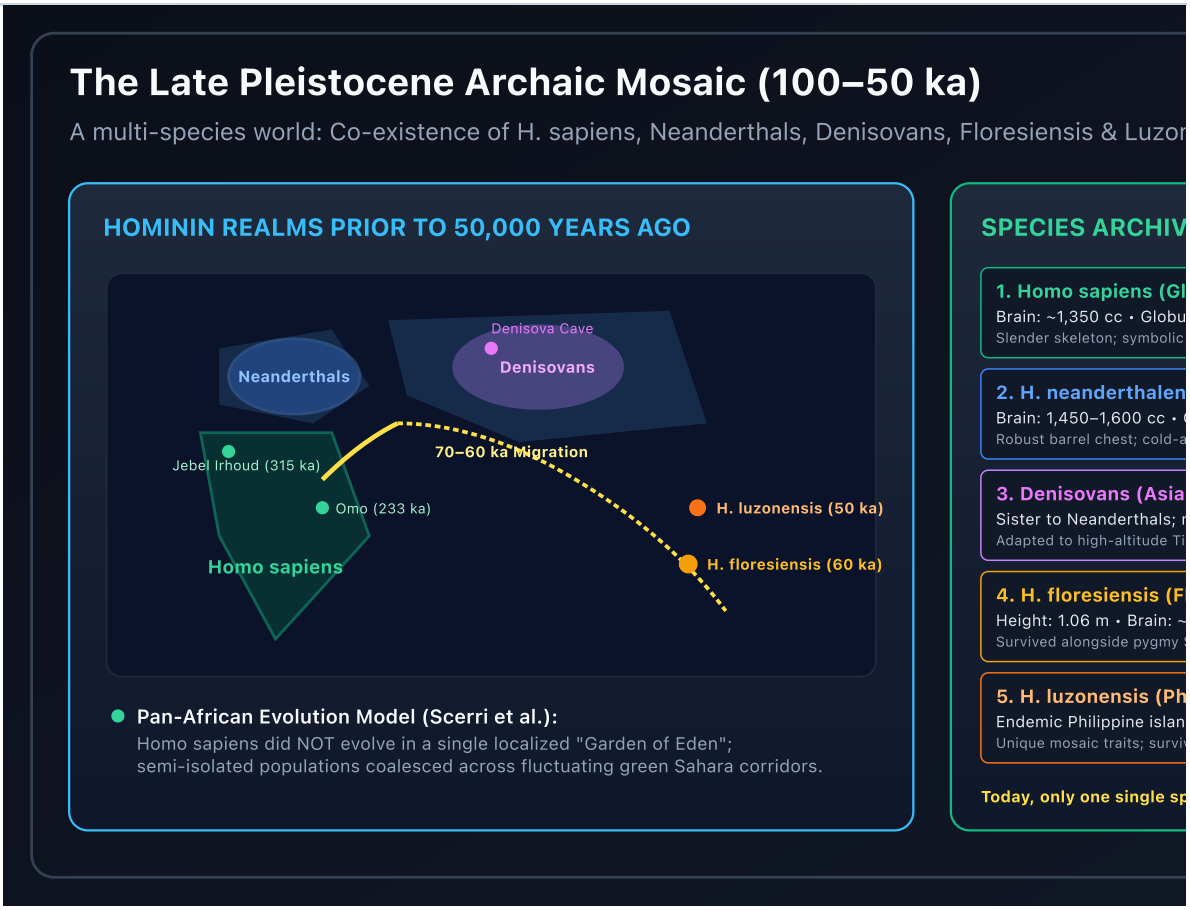


Figure 20.1: The Late Pleistocene Archaic Mosaic (100–50 ka). Left: Geographic distribution of hominin realms prior to the global expansion of Homo sapiens—showing the Neanderthal range across Europe and western Asia, Denisovans across Siberia and high-altitude Tibet, the pan-African cradle of Homo sapiens, and isolated island species (Homo floresiensis and Homo luzonensis). Right: Cranial and morphological matrix comparing the five contemporary hominin species that shared planet Earth 70,000 years ago.

The Pan-African Evolution Model

Synthesizing fossil discoveries from Jebel Irhoud (315 ka, Morocco), Omo Kibish (233 ka, Ethiopia), Florisbad (260 ka, South Africa), and Herto (160 ka, Ethiopia), Eleanor Scerri and colleagues formulated the **Pan-African Multiregional Evolution Model**. Early *Homo sapiens* populations were geographically structured across the vast African landmass. During wet "Green Sahara" pluvial episodes, rivers and lakes connected North, East, and Southern Africa, allowing migrating bands to exchange genes and lithic innovations. During arid phases, populations retreated into isolated environmental refugia, developing unique morphological traits. Our species did not evolve from a single tribe; it emerged from the dynamic, continent-wide coalescence of a shifting ecological metapopulation.

The Five Hominin Species of the Late Pleistocene

As recently as $60,000$ years ago, an alien visitor arriving on planet Earth would have encountered a vibrant diversity of human species:

1. **Homo sapiens:** Characterized by a globular neurocranium, a flat face retracted beneath the frontal lobes, an average brain capacity of $\sim 1,350\ \text{cm}^3$, and a distinct, protruding bony mental trigon (the **true chin**).
2. **Homo neanderthalensis:** Flourishing across Europe and Western Asia. Possessing a larger cranial capacity ($1,450\text{–}1,600\ \text{cm}^3$) housed in a long, low skull with an occipital bun, sweeping browridges, and no chin. Cold-adapted with broad, barrel-shaped chests and thick, stocky limbs conforming to Allen's and Bergmann's ecogeographical rules.
3. **Denisovans:** Identified from a fingertip bone and massive molars in Denisova Cave, Siberia, and a jawbone from the Baishiya Karst Cave in Tibet. Genetically a sister lineage to Neanderthals, adapted to high-altitude cold environments.
4. **Homo floresiensis ("The Hobbit"):** Discovered in Liang Bua cave on the Indonesian island of Flores. Standing only $1.06\ \text{m}$ ($3\ \text{ft}\ 6\ \text{in}$) tall with an australopithecine-sized brain of $\sim 420\ \text{cm}^3$, this species evolved extreme insular dwarfism to survive on an isolated island alongside pygmy *Stegodon* elephants until $\sim 60,000$ years ago.
5. **Homo luzonensis:** Discovered in Callao Cave, Luzon, Philippines ($50\text{–}67\ \text{ka}$), exhibiting a unique mosaic of primitive, curved australopithecine-like phalanges and derived small molars.

2. Paleogenomics: Ancient DNA and the ABBA-BABA Proof

For more than a century, anthropologists debated whether migrating modern humans violently exterminated archaic populations or peacefully interbred with them. The answer came from the revolutionary science of **Paleogenomics**, spearheaded by Swedish geneticist **Svante Pääbo** at the Max Planck Institute for Evolutionary Anthropology (honored with the **2022 Nobel Prize in Physiology or Medicine**).

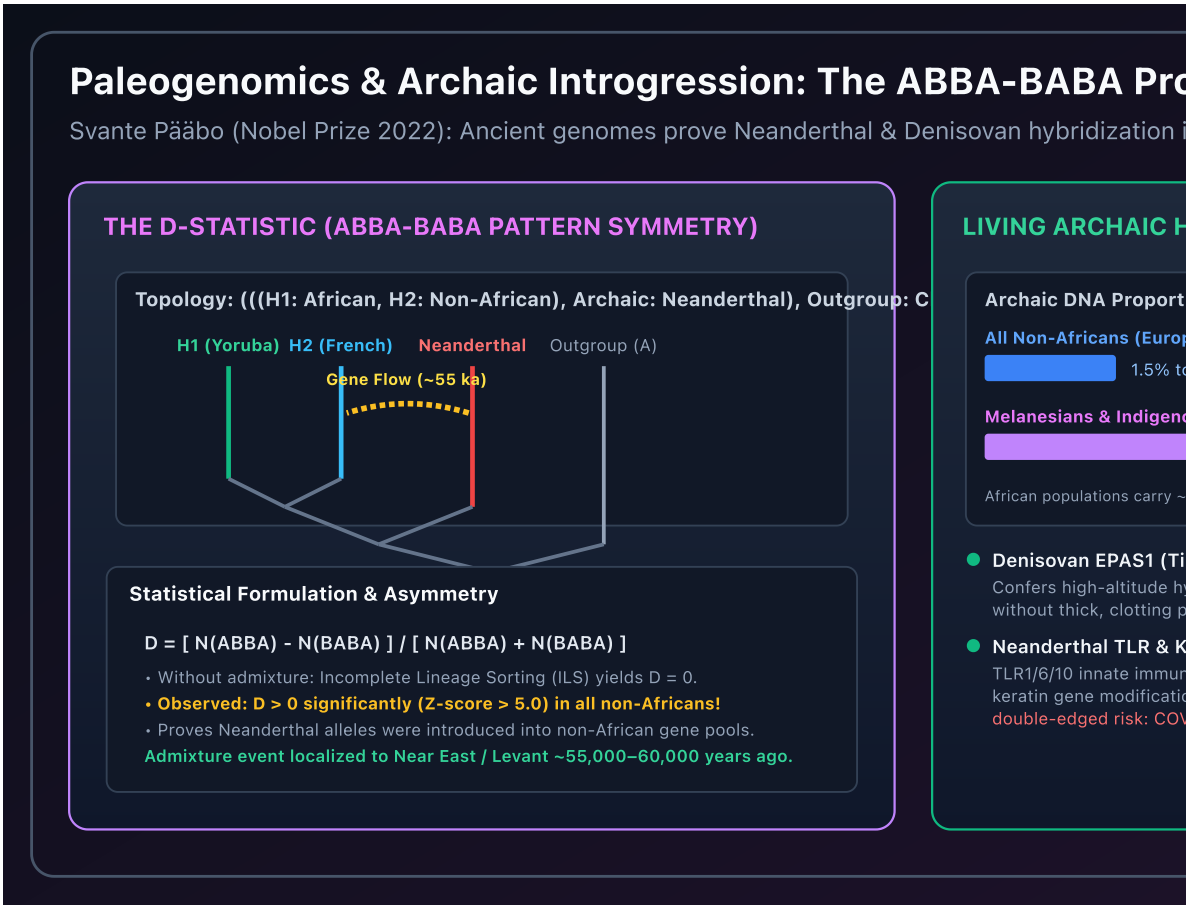


Figure 20.2: Paleogenomics & Archaic Introgression. Left: The ABBA-BABA D-statistic test analyzing discordant single-nucleotide polymorphisms across four taxa (((H1: African, H2: Non-African), Archaic), Outgroup). Because D > 0 significantly in all non-Africans, archaic hybridization is proven beyond doubt. Right: Living archaic genomic heritage—1.5–2.5% Neanderthal DNA in all Eurasians, up to 4–6% Denisovan DNA in Melanesians, and adaptive introgression of the EPAS1 high-altitude hypoxia gene in Tibetans.

The D-Statistic: The Mathematical Proof of Admixture

In 2010, Pääbo's consortium published the first draft sequence of the Neanderthal genome extracted from 40,000-year-old bones from Vindija Cave, Croatia. To test for gene flow, population geneticist Richard Green developed the D**-Statistic (the ABBA-BABA Test)**:

Consider four genome sequences aligned at orthologous nucleotide sites: an African modern human (H_1), a non-African modern human (H_2), a Neanderthal (A), and a chimpanzee outgroup (O). Let 'A' denote the ancestral allele (shared with the chimpanzee) and 'B' denote the derived mutation:

- An **ABBA site** occurs when the African carries the ancestral allele (A), while both the non-African and the Neanderthal share the derived mutation (B): $[A, B, B, A]$.
- A **BABA site** occurs when the non-African carries the ancestral allele (A), while the African and the Neanderthal share the derived mutation (B): $[B, A, B, A]$.

Under a null hypothesis of strict species divergence without gene flow, stochastic Incomplete Lineage Sorting (ILS) predicts that the number of ABBA sites must equal the number of BABA sites: $N(\text{ABBA}) \approx N(\text{BABA})$, yielding a D-statistic of zero:

$$D = \frac{N(\text{ABBA}) – N(\text{BABA})}{N(\text{ABBA}) + N(\text{BABA})} = 0$$

When Pääbo's team ran the calculation across billions of base pairs, the result was staggering: in every non-African human on Earth (French, Han Chinese, Papuan), $N(\text{ABBA})$ **significantly exceeded** $N(\text{BABA})$, generating a highly positive D-statistic with a statistical significance exceeding Z > 5.0! This proved mathematically that Neanderthals interbred with modern humans. The primary admixture event occurred between $\mathbf{55,000}$ **and** $\mathbf{60,000}$ **years ago** in the Near East or Levant, just as our ancestors first expanded out of Africa.

The Living Archaic Heritage: Adaptive Introgression

We are not pure-blooded; we are walking mosaics of archaic genomes:

Shakil Mahmud • Research Monograph

- **Neanderthal Legacy (1.5\text{–}2.5\%):** Present in all non-African human genomes. Archaic alleles conferred essential immune adaptations to survive Eurasian pathogens: *TLR1, TLR6, and TLR10* (Toll-like receptors), as well as keratin genes (*BNC2*) that toughened skin against cold climates. However, archaic alleles also carry legacy vulnerabilities, including an archaic haplotype on Chromosome 3 linked to increased risk of respiratory failure from COVID-19.
- **Denisovan Legacy (4\text{–}6\%):** Extensively preserved in Indigenous Australians, Papuans, and Melanesians. In 2014, Rasmus Nielsen discovered that modern high-altitude Tibetans inherited a miraculous Denisovan genetic gift: an archaic variant of the **EPAS1** transcription factor. While standard human alleles cause the blood to thicken dangerously with excess red blood cells at elevations >4,000\text{ meters}, the Denisovan *EPAS1* variant prevents chronic mountain sickness, enabling Tibetans to thrive in the low-oxygen heights of the Himalayas.

3. The Upper Paleolithic Symbolic Revolution

By 45,000 years ago, as Neanderthals and Denisovans retreated toward extinction, modern humans ignited a cognitive and cultural explosion across Eurasia and Africa: **The Upper Paleolithic Symbolic Revolution**.

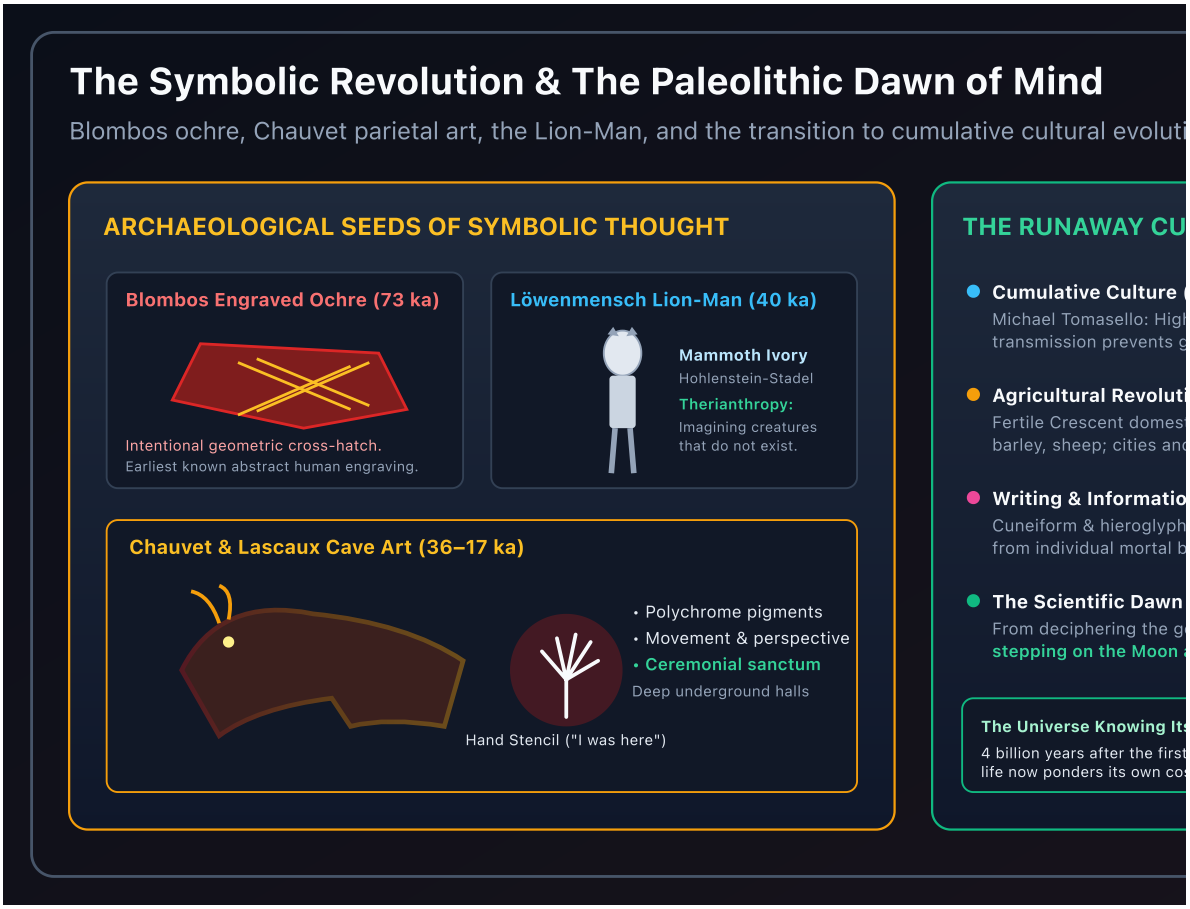


Figure 20.3: The Symbolic Revolution & Cumulative Culture. Left: Archaeological milestones of symbolic cognition—geometric engraved ochre at Blombos Cave (73 ka), the Löwenmensch ivory Lion-Man figurine representing metaphysical therianthropy (40 ka), and parietal cave paintings at Chauvet/Lascaux featuring polychrome pigments and negative hand stencils. Right: The runaway cultural engine—the ratchet effect driving the transition from foraging bands to agriculture, writing, science, and the Anthropocene.

The Materialization of the Human Mind

What sets modern humans apart from every other creature that has ever lived is our capacity for **Symbolic Thought**—the ability to assign arbitrary, shared conceptual meaning to an external material object:

1. **Abstract Geometry (Blombos Cave, South Africa, 73 ka):** Christopher Henshilwood excavated chunks of red ochre engraved with meticulous, deliberate cross-hatched diamond patterns, alongside perforated marine tick-shell beads (*Nassarius kraussianus*) worn as personal identity jewelry.
2. **Therianthropy & Myth (The Löwenmensch, Germany, 40 ka):** Carved from mammoth ivory found in Hohlenstein-Stadel cave, the "Lion-Man" depicts an upright human body topped with the head of a cave lion. This sculpture represents a momentous cognitive threshold: the capacity to conceptualize, visualize, and sculpt an imaginary entity that does not exist in the physical world—the birth of religious imagination, mythology, and art.
3. **Parietal Cave Sanctuaries (Chauvet & Lascaux, France, 36\text{–}17\text{ ka}):** Deep within pitch-black subterranean limestone chambers, Upper Paleolithic artists used charcoal, red hematite, and yellow goethite to render dynamic, shaded herds of running horses, fighting woolly rhinos, and charging steppe bison. Alongside these animal masterpieces are haunting **negative hand stencils**: an artist placed their open hand against the rock and blew a cloud of liquid pigment through a hollow bone pipe, leaving a permanent personal signature across deep time: *"I am here. I was here."*

4. **Music and Harmonics (Hohle Fels, Germany, 40 ka):** The discovery of delicate flutes carved from the radius bones of griffon vultures with meticulously spaced finger holes proves that complex musical harmony and melodic expression are as old as our species.

4. The Cumulative Cultural Horizon: The Grand Epilogue

With the symbolic revolution, the primary driver of human adaptation shifted forever. For 3.8 billion years, life adapted to its environment through the slow, blind, generational filtering of biological natural selection. But in *Homo sapiens*, a new evolutionary engine emerged: **Cumulative Cultural Evolution (The Ratchet Effect)**.

As cognitive psychologist Michael Tomasello demonstrated, human culture possesses a unique "ratchet": once a useful innovation is invented (a bone sewing needle, a bow and arrow, a herbal medicine), high-fidelity social learning, language, and shared intentionality prevent it from slipping backward. The next generation does not reinvent the wheel; it starts where the previous generation left off.

From Savannas to the Stars

In a geological heartbeat of twelve thousand years—a mere fraction of one percent of our evolutionary history—the cultural ratchet accelerated with staggering exponential speed:

- **The Agricultural Revolution (12\text{–}10\text{ ka}):** In the Fertile Crescent, Yangtze River, and Mesoamerica, humans domesticated wheat, rice, corn, and livestock. Nomadic hunting bands settled into permanent villages, sparking the emergence of cities, architecture, and division of labor.
- **External Information Storage (5 ka):** In ancient Sumer and Egypt, the invention of cuneiform and hieroglyphic writing decoupled human knowledge from individual mortal brains. Ideas could now be transmitted across thousands of miles and thousands of years without loss of fidelity.
- **The Scientific Revolution & Modernity (500\text{ yr — Present}):** The institutionalization of the empirical scientific method unlocked the fundamental laws of thermodynamics, electromagnetism, and quantum mechanics. We built telescopes that gaze back to the cosmic dawn, mapped the three-billion-base-pair human genome, and stepped foot on the lunar surface.

The 4-Billion-Year Epic: The Universe Knowing Itself

Four billion years ago, in the scalding, pitch-black hydrothermal crevices of an Archean ocean, simple alkaline fluids bubbled through catalytic iron-sulfur chambers, giving birth to the first fragile, replicating molecular chains. Through four billion years of planetary catastrophe—the Great Oxygenation Event, Snowball Earth glaciations, the Cambrian explosion, the conquest of land, the Permian Great Dying, the meteoritic vaporization of the dinosaurs, and the arid crucible of the African rift—that continuous unbroken chain of replicating DNA never snapped.

Today, that epic journey resides inside you. The water flowing in your veins carries the salinity of the primordial ocean. The mitochondria powering your cells are the living descendants of alphaproteobacteria engulfed two billion years ago. The calcium phosphate minerals in your bones were forged by Ordovician jawless fish. The middle ear bones vibrating to the sounds of this world are the transformed jaw joints of Permian synapsids. And the brain contemplating these words is the direct beneficiary of the nocturnal mammalian neocortex, the primate visual canopy, and the Oldowan stone-knapper's spark.

As Carl Sagan once poetically observed: *"We are a way for the cosmos to know itself."* Four billion years after the spark of abiogenesis, the epic of evolution has produced a conscious, compassionate, inquisitive species capable of looking back across the abyss of deep time, marveling at the odyssey that brought us here, and taking conscious stewardship of our living planetary home.

Citation: Mahmud, S. (2026). "The Archaic Mosaic & The Dawn of Modern Humanity." In The Evolutionary Odyssey, Part 20. https://shakilmahmud.com/evolutionary-odyssey-part-20-the-archaic-mosaic-and-modern-humanity/

Shakil Mahmud • Research Monograph

PRIMARY SOURCES & SCHOLARLY REFERENCES

Consolidated Bibliography

The formulations, historical contexts, and conceptual developments presented throughout this monograph draw upon the following primary treatises, foundational papers, and critical editions:

Darwin, Charles (1859). *On the Origin of Species by Means of Natural Selection*. John Murray, London.

Dawkins, Richard (1976). *The Selfish Gene*. Oxford University Press.

Lane, Nick (2015). *The Vital Question: Energy, Evolution, and the Origins of Complex Life*. W. W. Norton & Company.

Gould, Stephen Jay (1989). *Wonderful Life: The Burgess Shale and the Nature of History*. W. W. Norton & Company.

BIOGRAPHICAL NOTE

About the Author

❖

Shakil Mahmud

Independent Scholar, Writer & Systems Architect

Shakil Mahmud is an independent scholar, author, and software systems architect. His research interests span the foundations of theoretical physics, the history and philosophy of mathematics, evolutionary biology, macroeconomic history, and the architecture of neural computing. His work synthesizes deep historical rigor with accessible first-principles exposition. His complete published archives and monographs are maintained at **shakilmahmud.com**.

COLOPHON

Typeset in EB Garamond (English) and Kohinoor Bangla / Noto Serif Bengali (Bengali).
Mathematical typesetting generated with Donald Knuth's TeX algorithms and KaTeX.
Published digitally as a monolithic research monograph by Shakil Mahmud Editorial Series.
Dhaka & Singapore • 2026 • https://shakilmahmud.com